STUDYING THE ROLE OF INTEGRIN

$\alpha V\beta 6$ IN PANCREATIC CANCER

SABARINATH S VALLATH

A THESIS SUBMITTED FOR THE DEGREE OF
DOCTOR OF PHILOSOPHY
UNIVERSITY OF LONDON

JANUARY 2013

Declaration

The work presented in this thesis was done by the author, Sabarinath Sashikumar Vallath, at the Centre for Tumour Biology, Barts Cancer Institute, Barts and the London School of Medicine and Dentistry, Queen Mary University of London. All collaborators and external sources have been properly acknowledged.

This work was funded by Pancreatic Cancer Research Fund (PCRF), the first Howard-Kerr scholarship and the ORSAS scholarship from Queen Mary University of London.

Sabarinath Sashikumar Vallath

Acknowledgements

I am extremely grateful to Prof. Ian Hart for giving me the opportunity to work at the Centre for Tumour Biology, Barts Cancer Institute. You have been a pillar of support for me over the past seven years and I am proud to have started my career in your laboratory under your expert guidance. Thank you for all your help, constructive feedback throughout and most importantly for teaching me the principles of good science.

I cannot thank enough my supervisor, Dr. John Marshall, without whom I couldn't have done this. Working for you in the "Beta6 group" shaped my career and it has been a fantastic experience over the past seven years! Thank you for your enthusiasm, unwavering support, patience and belief in me from day one. Our inspiring discussions at 'Costa' and the 'front Sutton' will be sorely missed! I am truly grateful for all that you have done for me and I hope to stay in touch with you even after my PhD.

A special thank you to Mr. Hemant Kocher, my second supervisor, who welcomed me to his group and guided me throughout my PhD. Your knowledge and expertise helped me immensely and I will miss our fun conferences together!

There are far too many people to thank individually at the Barts Cancer Institute but I will attempt to. A big thanks to all past and present members of the "Beta6 group". It was an absolute joy to work with all of you. Will miss our 'wine and cheese' weekly group meetings. Thank you Linda (Hammond) for your constant support and help with everything right from the beginning. Thanks to Hagen and Julie (ATS service) for all your help. Thanks to George (Elia) for providing me tissue sections on demand in extremely short notice. Thanks to Louise (Reynolds) for all her help in the lab. I have had many a great time with Bernardo, Fieke, Rita, Silvia, Antonio, Monika, Abasi and Ami both in and outside the lab. Thanks to Katrina Sweeney and Katrina Pirlo for all your help and friendship both at work and otherwise. I will miss our coffee/tea breaks and night outs!

Special mention must go to Mike, Monica, Sally and Colan, for their friendship. You guys have always been there for me and I count you as very good friends. I wouldn't have been able to go through many a days when experiments just did not work, without your constant support and encouragement. Of course, the countless

coffee/lunch breaks and the “one quick drink” after work definitely helped! Mike, you have been extremely helpful throughout my time in the laboratory. I have learnt a lot from you and I am very grateful for all your help.

To Lynsey, I have to say, thank you for everything. I am glad you were there with me to share the joys and sorrows in our lives as PhD students at the Institute. I hope you know how much it meant to me. You made going to work more fun and I enjoyed our PhD days! I also have to mention our serious scientific discussions after work over “two bottles and the all important extra glass!” Here is to many more years of fun together!

I would like to thank my great-aunt, my cousin and her family in London for their support and belief in me. Last but never the least, my parents, my sister and my grandparents, without whom none of this would have been possible. No words can describe my gratitude and I would like to thank them for always being there for me, for supporting me and trusting my decisions in life.

Abstract

Pancreatic cancer is often referred to as the “silent killer“ due to the asymptomatic nature of the disease in the early stages and the extremely poor prognosis overall. The average one-year survival rate for PDAC patients is 24% (American Cancer Society, facts and figures, 2010), decreasing to 5%-6% over 5 years (WHO report, Pancreatic cancer, 2010). Only 20% of patients are suitable for surgical resection at the time of diagnosis and treatment options available to PDAC patients have not improved significantly over the past few decades. Thus novel therapeutic approaches are essential to treat this disease. Our experimental, clinical and pre-clinical data suggest integrin αvβ6 may be a suitable target.

Bioinformatics studies using the Pancreatic Expression Database revealed that the β6 gene (ITGB6) was highly up regulated in pancreatic ductal carcinoma (PDAC) compared with normal pancreas. Further analysis carried out showed that there was a significant correlation between *ITGB6* expression at the mRNA level and survival in a cohort of 292 PDAC patients. Immunohistochemistry analysis on two separate patient cohorts (n=118 and n=147) showed that normal pancreas lacked αvβ6 expression whereas 91% of PDAC tissues expressed αvβ6 at the protein level. There was no significant correlation between αvβ6 expression and survival at the protein level in both cohorts of patients tested.

Flow cytometry and Western blotting analyses on a panel of PDAC cell lines confirmed expression of αvβ6 in PDAC cell lines. This study investigated the functional role of αvβ6 in PDAC cell lines. Antibody mediated function blockade of αvβ6 significantly inhibited proliferation in a dose dependent manner, specifically in αvβ6 positive PDAC cell lines. A significant reduction in migration and invasion was also observed in a panel of αvβ6 positive PDAC cell lines when treated with an αvβ6 function-blocking antibody. αvβ6 targeted antibody mediated therapy in combination with gemcitabine significantly inhibited tumour growth in a physiologically relevant pre-clinical subcutaneous xenograft model of PDAC.

These data reaffirms that αvβ6 is a potential novel therapeutic target and an αvβ6 specific function-blocking antibody can be used as a novel agent to treat pancreatic adenocarcinoma patients.

Abbreviations

3-D	Three dimensional
ATRA	All Trans Retinoic Acid
BM	Basement Membrane
BSA	Bovine Serum Albumin
CAF	Cancer Associated Fibroblasts
CAV9	Coxsackie Virus 9
CdK	Cyclin Dependent Kinase
CO_2	Carbon dioxide
COX2	Cyclooxygenase-2
DAB	3-3'-diaminobenzidine
DAPI	4',6-diamidino-2-phenylindole
DMEM	Dulbecco's Modified Eagle's Medium
DMSO	Dimethyl sulphoxide
DNA	Deoxy Ribo Nucleic Acid
DPC4	Deleted in Pancreatic Cancer 4
ECL	Enhanced Chemiluminescence
ECM	Extracellular Matrix
EDTA	Ethylene Diamino Tetra acetic acid
EGF	Epidermal Growth Factor
EGFR	Epidermal Growth Factor Receptor
EMT	Epithelial to Mesenchymal Transition
ERK	Extra cellular signal Related Kinase
ETK	Epithelial and Endothelial Tyrosine Kinase
FAK	Focal Adhesion Kinase
FCS	Foetal Calf Serum
FGF	Fibroblast Growth Factor
FMDV	Foot and Mouth Disease
GFAP	Glial Fibrillary Acid Protein
GI	Gastrointestinal
Grb2	Growth factor receptor bound protein 2
H&E	Haematoxylin and Eosin
HER2	Human Epidermal Growth Factor Receptor 2
HGF	Hepatocyte Growth Factor
HRP	Horse Radish Peroxidase
hTERT	Human Telomerase Reverse Transcriptase

IL	Interleukin
IP	Intra-Peritoneal
IPMN	Intra ductal Papillary Mucinous Neoplasms
Kda	Kilo Dalton
LAP	Latency Associated Peptide
LIBS	Ligand Induced Binding Site
MAPK	Mitogen Activated Protein Kinase
MCN	Mucinous Cystic Neoplasm
MFI	Mean Fluorescent Intensity
MLCK	Myosin Light Chain Kinase
Min	Minutes
MMP	Matrix Metalloproteinases
MTT	(3-(4,5-Dimethylthiazol-2-yl)-2,5-diphenyltetrazolium bromide)
NT	Non Targeting
OD	Optical Density
OSCC	Oral Squamous Carcinoma
PaCa	Pancreatic Cancer
PAK	P21- Activated Kinase
PanIN	Pancreatic Intraepithelial Neoplasia
PARP	Poly (ADP-ribose) Polymerase
PBS	Phosphate Buffered Saline
PCR	Polymerase Chain Reaction
PDAC	Pancreatic Ductal adenocarcinoma
PDGF	Platelet Derived Growth Factor
Pdx1	Pancreas duodenum homeobox 1
PSC	Pancreatic Stellate Cell
qPCR	Quantitative PCR
RGD	Arginine-Glycine-Aspartic Acid
RNA	Ribo Nucleic Acid
RTK	Receptor Tyrosine Kinase
SDS-PAGE	Sodium Dodecyl sulphate Poly Acrylamide Gel Electrophoresis
SD	Standard Deviation
SEM	Standard Error of Mean
shRNA	Short Hairpin RNA
siRNA	Small Interference RNA
SMA	Smooth Muscle Actin

SSC	Side Scatter
STAT3	Signal Transducer and Activator of Transcription 3
TBS	Tris Buffered Saline
TGFβ	Transforming Growth Factor beta
TN-C	Tenascin C
TNFα	Tumour Necrosis Factor alpha
UV	Ultra Violet
uPA/uPAR	Urokinase Type Plasminogen/Receptor
VCAM1	Vascular Cell Adhesion Molecule 1
VEGF/R	Vascular Endothelial Growth Factor/Receptor
VWF	Von Willebrand factor

CONTENTS

LIST OF FIGURES

LIST OF TABLES

INTRODUCTION

1. Introduction

1.1 Cancer

Cancer is a name given to a broad collection of almost 200 different diseases. It is usually characterised by uncontrolled growth of cells in a specific area of the body. The cells that become “cancerous” harbour molecular changes within their genomes, also known as mutations, which are passed onto the next generation of cells when they divide [1]. Cellular proliferation in normal tissue is a carefully controlled process regulated by signalling pathways that enable the entry and progression of cells through the cell cycle, with multiple check-points, including tumour suppressor genes (e.g. p53 gene, retinoblastoma (Rb) gene), to ensure any abnormal cells (mutated) are not allowed to replicate and forced to undergo apoptosis (programmed cell death) [2]. Mutation of key genes means cancer cells can deregulate these pathways and are able to form a mass of tissue commonly referred to as a tumour. In many cancers, this abnormal mass of tissue has the ability to grow at a very rapid rate and invade into the surrounding extra cellular matrix (ECM). These malignant cancer cells have the ability to up regulate the production of various matrix-remodelling enzymes, such as matrix metalloproteases (MMPs), which favour invasion into the surrounding stroma. Thus, cancer arising from one specific part of the body can invade to other parts of the body through the vasculo-lymphatic network and grow at a distant site; this process is referred to as metastasis. Cancer cells can also secrete factors that modify (activate) the local stromal cells, which in turn can secrete growth factors that are essential for the growth/survival of cancer cells (paracrine effect). This cross talk between the tumour cells and the surrounding stromal cells plays an important role in the progression of cancer, especially in pancreatic cancer, where sometimes up to 70%-80% of the tumour is composed of the stroma [3].

Detection and diagnosis of cancer at an early stage is extremely crucial for better prognosis. Current chemotherapy remains fairly ineffective in curing patients that already possess metastatic disease. Thus, in many cancers, early diagnosis and treatment leads to a significant improvement in the clinical outcome. Targeting cancer cells specifically is yet another major challenge, as many of the current chemotherapeutic drugs available to patients in the clinic are generic and do not delineate between normal and cancer cells. Rather, they often target replication non-specifically; a characteristic frequently manifested by non-transformed cells. There are several studies focusing on targeting integrins, a molecule expressed on the cell surface of most cells, that integrate the extracellular matrix to the cytoplasm, to treat

cancer [4]. Finding the ideal target to image and treat cancer is critical in order to manage this disease. This study will focus on one such integrin, $\alpha v\beta 6$, which is epithelial cell specific, expressed by many solid cancers and completely absent in the normal adult tissue in humans [5].

Despite better strategies to prevent cancer related deaths through introduction of screening programmes and improving therapeutic interventions, this figure is expected to rise over the next decade or so and one in three people in developed countries will develop cancer before the age of 75 (Cancer Research UK, 2012). Cancer is a leading cause of death worldwide and in 2009 alone, 320,500 people were diagnosed with cancer (excluding non-melanoma skin cancer) in the United Kingdom (UK) (Cancer Research UK, 2012). A direct comparison between cancer incidence in 1979-1981 and 2007-2009, shows that there has been a 25% increase in cancer in the UK, 14% for men and 32% for women (Cancer Research UK, 2012). Even though there are so many different types of cancers, only some of them, such as breast, lung, bowel and prostate account for over half of the new cases that are diagnosed (Cancer Research UK, 2012). In 2006, it was estimated that about 1.2 million people in the UK were alive having received a diagnosis of cancer [6]. Metastasis of cancer cells is often recognised as the most frequent cause of death in patients with cancer. The diagnosis of malignancy usually involves clinical examinations including blood test, biopsy, histology and, in recent years, advanced contrast imaging.

According to the national cancer statistics (Cancer Research UK, 2012), lung cancer accounts for the largest number of cancer related deaths but breast cancer remains the cancer that has the greatest incidence rates. Pancreatic ductal adenocarcinoma (PDAC), sometimes referred to as pancreatic cancer, has a relatively low incidence rate compared with many other cancers. Despite the low incidence rates, mortality rates are very high, and it is 5th in the list of 20 most common cancer related deaths in people in the UK. It is worth mentioning that the incidence rates of pancreatic cancer almost mirror the mortality rates, with five-year survival rates of PDAC patients ranging between 5%-6% from the time of diagnosis, making this one of the deadliest cancers. The 20 most common death rates from cancer are shown in Figure 1.

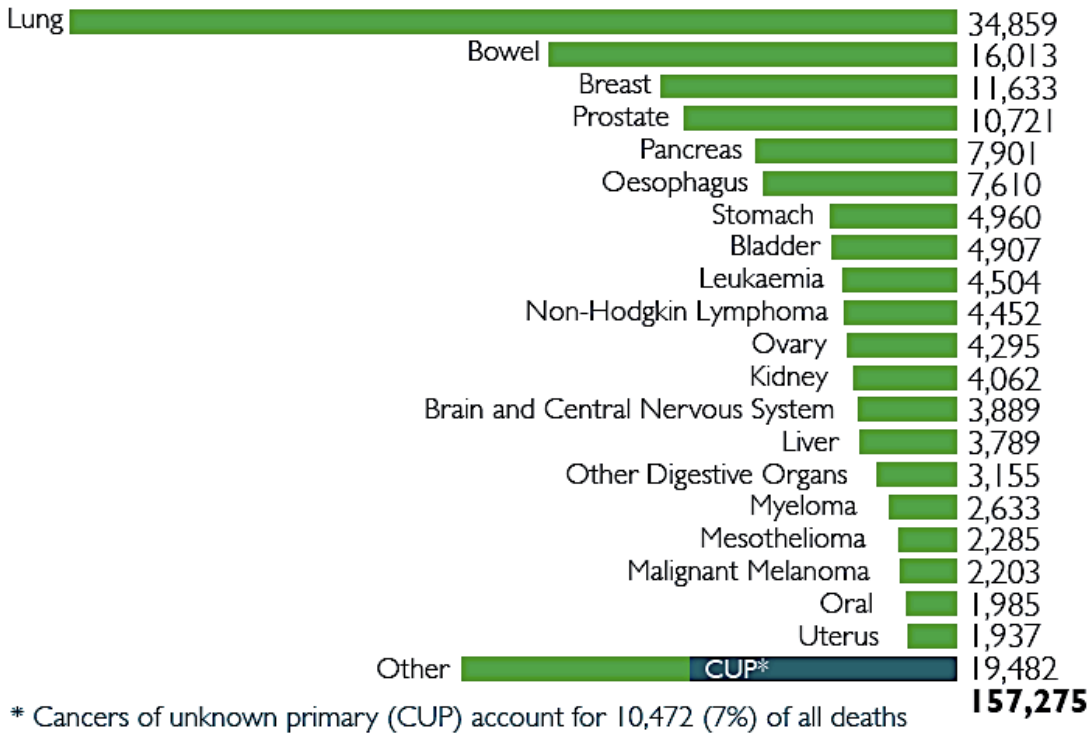

Figure 1: Cancer related mortality in the UK in 2010. ***Modified from Cancer Research UK, 2012. http://info.cancerresearchuk.org/cancerstats.***

This study will focus on Pancreatic ductal adenocarcinoma (PDAC) or pancreatic cancer [7]. Incidence rates are relatively low (8364 in 2010, Cancer Research UK, 2012) compared to other cancers (Breast cancer – 48,788 in 2010, lung cancer - 41,428 in 2010, Cancer Research UK, 2012) but mortality rates are extremely high (7901 in 2010, Cancer Research UK, 2012) and are usually very similar to the incidence rates. Research conducted to date has improved the understanding of the molecular biology of this disease as well as staging and diagnosis. This disease is usually not detected at an early stage and treatment options available to patients have not improved significantly over the last two decades. This study will be aiming to understand the functional role of integrin $\alpha v\beta 6$ in PDAC and its use as a potential novel therapeutic target to treat pancreatic cancer.

1.2 Pancreas

1.2.1 Structure and function

The pancreas is a dual function organ located in the upper abdomen behind the stomach. It is divided into three parts: the head, the body, and the tail. In humans it is approximately 18cm long and 4cm wide (Figure 3). The pancreas is both an exocrine and an endocrine gland with two major physiological roles: it aids digestion by producing pancreatic juice comprising various digestive enzymes (exocrine function) and regulates glucose metabolism by producing the hormones insulin and glucagon (endocrine function) [8].

The exocrine pancreas comprises small glands formed by pyramidal-shaped acinar cells (acini), which drain into small ducts, composed of cuboidal epithelium, which gradually become tall columnar mucus-secreting epithelial cells, in the larger ducts. These ducts ultimately drain via the main pancreatic duct into the duodenum and together form the pancreatic ductal system (Figure 2). The acinar cells contain zymogen granules in the apical areas and the basilar cytoplasm is basophilic. It produces an alkaline “juice” containing various pro-enzymes such as trypsinogen, lipase, amylase, pro-elastase within membrane bound zymogen granules, which are secreted into the pancreatic ductal system upon stimulation. The alkaline nature of the pancreatic juice is due to a high concentration of bicarbonate ions and the pancreatic juice is essential for digestion of acidic food, proteins and vitamins [8].

Scattered throughout the exocrine pancreas are clusters of endocrine cells called islets of Langerhans, which constitute about 1%-2% of the pancreas (Figure 2). They are round, highly vascularised and comprised of four different cell types [9]. The α cells secrete glucagon (resulting in an increase of glucose in the blood), β cells secrete insulin (decreases glucose in the blood), δ cells secrete somatostatin, (which regulates the function of α and β cells) and PP cells (pancreatic polypeptide secreting cells), which secrete pancreatic polypeptide, which helps in regulating the secretory function of both exocrine (pancreatic digestive enzymes) and endocrine pancreas (hormones) [8].

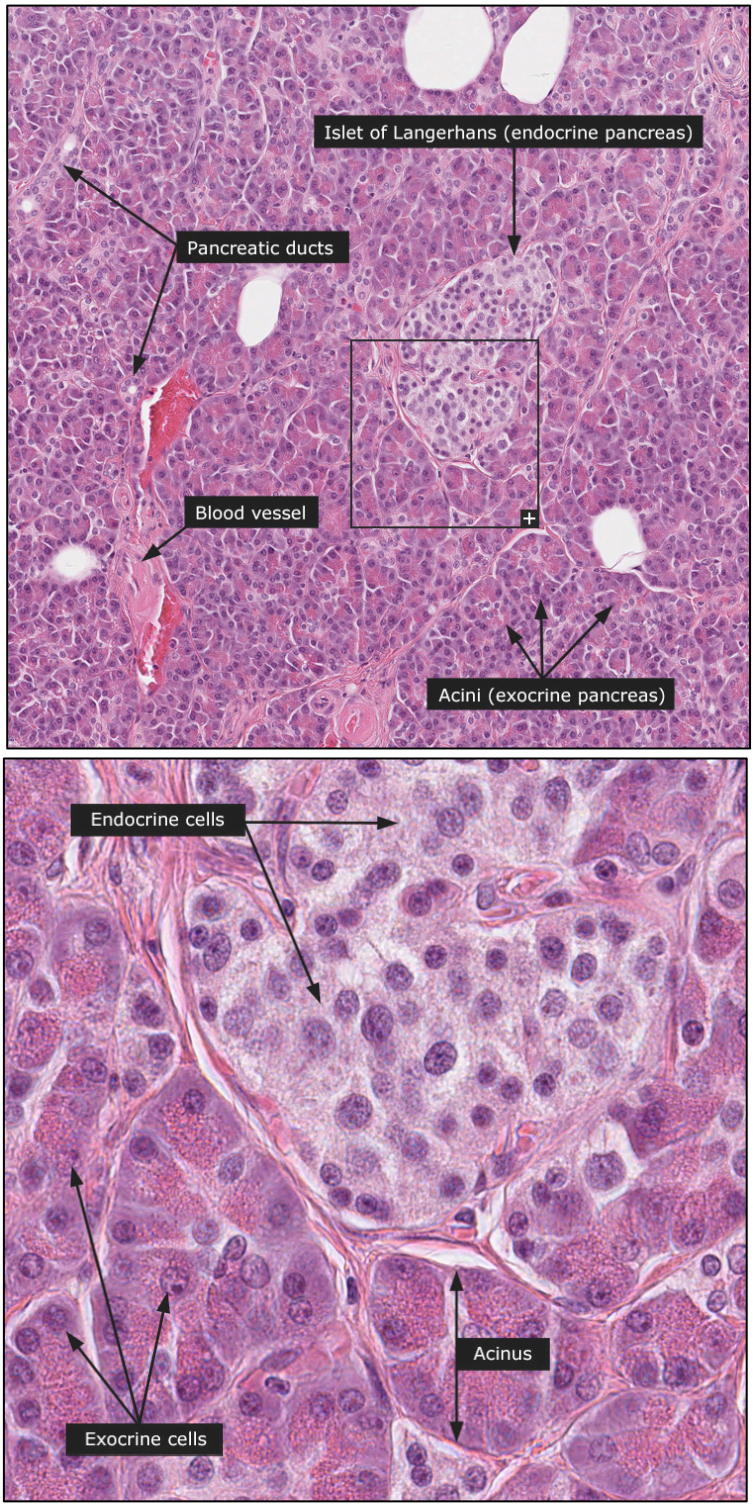

Figure 2: H&E picture of the normal pancreas showing pancreatic ducts, blood vessel, acini (exocrine pancreas) and the Islets of Langerhans (endocrine) cells (top). Higher magnification H&E image (inset black square in top picture) of normal pancreas showing the endocrine islet cells and the exocrine acinar cells that form the acinus.

Image reference:
http://www.proteinatlas.org/dictionary/normal/pancreas/detail+1.

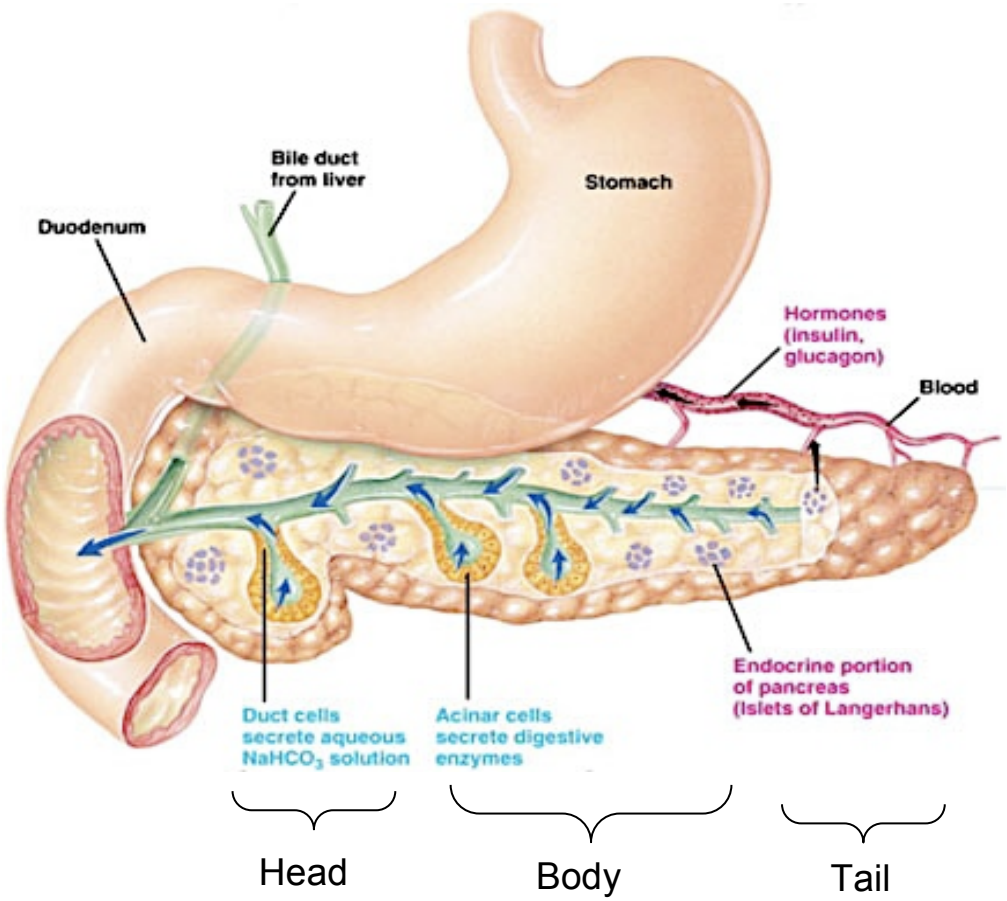

Figure 3: Location of the pancreas in the human body. The location of the pancreas in the human body is illustrated in the cartoon.

Image reference: location of pancreas in human body modified from University of Colorado at Boulder, (*http://bodymindspiritintegration.com/wpcontent/uploads/2010/01/pancreas.jpg*).

1.3 Classification of pancreatic neoplasms

Neoplasms of the pancreas are classified on the basis of cellular differentiation of the three main epithelial cell types (epithelial cells that line the pancreatic duct, acinar and endocrine cells) and also on the tumour type (solid, cystic or intra-ductal) [10]. In most cases, the term pancreatic cancer refers to pancreatic adenocarcinoma (PDAC), which represents >80% of pancreatic neoplasms. This cellular classification may not reflect the true origin of the PDACs. There are reports showing PDAC to be derived from either the ductal epithelium or the centro-acinar (cells present at the junction between acinus and duct) epithelium [11]. Some studies have linked the development of PDAC with cancer stem cells, which are defined as cells within a tumour that can self-renew and drive tumour progression. Recent studies have shown the existence of cancer stem cells in solid tumours including colon, breast and pancreas, which could also give rise to carcinomas [9, 12, 13].

Cancer stem cells have been identified in immunocompromised murine models of pancreatic cancer on the basis of expression of various cell surface markers including CD44, CD24 and epithelial surface antigen (ESA) and also by their ability to initiate tumours [14]. These cells were shown to be more resistant to the routinely used chemotherapeutic drug in the clinic, gemcitabine [15]. These cells also demonstrated an increased migratory and invasive potential [16]. However the origin of these pancreas stem cells still remains largely unknown with no clear study implicating their presence in the normal pancreas. Genetic changes in the progenitor cell population or lineage-committed cells that may have re-acquired stem cell characteristics may be an explanation [15]. However *KRAS* mutations in adult acinar or endocrine lineages only result in tumour formation in the presence of inflammation [17], suggesting that genetic changes in certain cell populations are not solely responsible for the development of pancreatic cancer. Recent advances in transgenic studies using mouse models are starting to help widen our understanding of the cellular origin of pancreatic cancer. This will be discussed in detail in section 1.9.6.

1.4 Pancreatic cancer

Due to the high mortality rate and its asymptomatic nature, pancreatic cancer, is often referred to as a 'silent killer'. It is the fourth leading cause of cancer-related death in the UK and five-year survival rates are less than 6% and have not improved over the last 40 years [18]. Surgery seldom is curative, as the tumour usually has metastasised by the time of diagnosis. Therapeutic options to target pancreatic cancer are limited to chemotherapy and surgery, the latter being suitable for only about 20% of patients who are diagnosed. In the UK, 5-year survival rates have improved marginally for patients with localised resectable disease.

The head of the pancreas accounts for nearly 65% of PDACs that are diagnosed, 15 % occur in the body, 10% occur in the tail and the remaining 10% are multi focal. The cancer usually breaches the basement membrane and invades into the surrounding normal tissue, including nerves and lymphatics. Perineural and lympho-vascular invasion are observed in about 40% - 75% of primary lesions, which are usually less than 2 centimetres, indicative of the aggressive nature of the cancer. Most patients that are diagnosed present with distant metastasis, usually in the liver and peritoneal cavity [19].

1.5 Epidemiology

People diagnosed with pancreatic cancer usually have a poor prognosis. There are a variety of factors that contribute to this poor prognosis such as the complete absence of a specific symptom, which in turn leads to the late presentation of the disease. 8,085 new cases of pancreatic cancer were diagnosed in the UK in 2008 (Table 1). (Cancer Research UK, 2012). The lifetime risk of developing pancreatic cancer is 1 in 79 for women and 1 in 77 for men (Figure 4) (Cancer Research UK, 2012).

Number of new cases, crude and European age-standardised (AS) incidence rates per 100,000 population in the UK.

Male		Incidence in UK
	Cases	4001
	Crude Rate	13.3
	AS Rate	10.5
	AS Rate - 95% LCL*	10.2
	AS Rate - 95% UCL*	10.9

Female		Incidence in UK
	Cases	4008
	Crude Rate	13.1
	AS Rate	8.2
	AS Rate - 95% LCL*	8
	AS Rate - 95% UCL*	8.5

Total cases		Incidence in UK
	Cases	8,085
	Crude Rate	13.2
	AS Rate	9.3
	AS Rate - 95% LCL*	9.1
	AS Rate - 95% UCL*	9.5

***95% LCL and 95% UCL are the 95% lower and upper confidence limits around the AS rate**

Table 1: Number of new cases, crude and European age-standardised (AS) incidence rates per 100,000 people in the UK. ***Office for National Statistics. Cancer Statistics: Registrations Series MB1. Modified from Cancer research UK, 2012. http://www.statistics.gov.uk/statbase/Product.asp?vlnk=8843.***

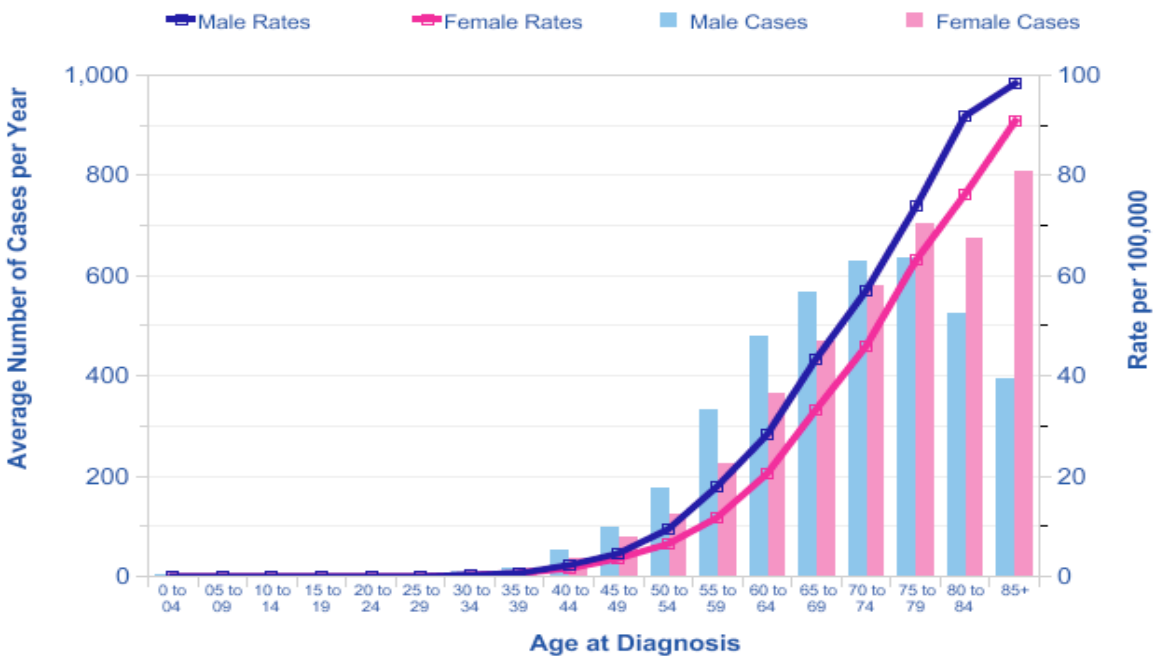

Figure 4: Average number of new cases per year and age-specific incidence rates of pancreatic cancer, UK, 2006-2008.

Office for National Statistics. Cancer Statistics: Registrations Series MB1. http://www.statistics.gov.uk/statbase/Product.asp?vlnk=8843.

Due to the late stage presentation and the aggressive nature of pancreatic cancers, surgery is possible only in a minority of patients (~20%) as the tumour usually has metastasised due to aggressive tumour behaviour and late presentation [18]. However in the cases where surgical resection is possible, together with adjuvant chemotherapy, five-year survival rates improve dramatically up to about 21% [20].

1.6 Pancreatic cancer: risks and causes

Although the precise events that result in development of pancreatic cancer are unknown, studying the biology of pancreatic cancer in large population based studies/meta analyses may provide a better understanding of the development of the disease. Pancreatic cancer is rare in people under 40, with a peak incidence in men between the age group of 70 - 80 and 75 - 85 for women [18]. Smoking, and thus presumably the carcinogens in cigarette smoke, is a major risk factor with a meta analysis of 82 studies between 1950 and 2007 showing smokers to have a 1.7 fold increased chance of developing pancreatic cancer [21] [22].

Various other factors including, a diet rich in meat and fat, obesity [23], alcohol intake [24] and people with diabetes mellitus [25] may have a slightly increased risk of developing pancreatic cancer. Long-term inflammation of the pancreas i.e. chronic pancreatitis [26] is a major factor increasing risk of pancreatic cancer. The risk of pancreatic cancer also increases in those who have a genetic predisposition. This is defined as having at least two first degree relatives with pancreatic cancer in the absence of other inherited cancer syndromes such as Peutz-Jeghers syndrome (mutation in *STK11/LKB1* gene) or Hereditary pancreatitis (mutations in *PRSS1* gene), familial atypical multiple mole melanoma (*FAMMM*) syndrome (caused by mutations in the *INK4A* gene), hereditary nonpolyposis colorectal cancer syndrome (caused by mutations in the *hMLH1* or *hMSH2* gene) [27] [28] [29]. The more first-degree relatives affected, the higher the risk, which might be due to an autosomal dominant inheritance of a rare allele. Interestingly, a mutation of *BRCA2* is found in about 20% of all familial pancreatic cancer [27] with three or more cases of pancreatic cancer.

1.7 Pathology of pancreatic cancer

1.7.1 Non-invasive pancreatic neoplasia

Research over the years has shed some light on the molecular and histological events that are associated with pancreatic carcinogenesis. Pancreatic intra epithelial neoplasia (PanIN), Mucinous Cystic Neoplasms (MCN) and intraductal papillary mucinous neoplasms (IPMN) are the three different forms of precursor non-invasive pancreatic neoplasia [30].

1.7.2 Pancreatic intra epithelial neoplasia (PanIN)

PanINs are neoplastic epithelial proliferations in the small pancreatic ducts and are usually seen as microscopic precursor lesions (<5mm). PanINs are sub-classified based on their differentiation into three grades, PanIN 1, PanIN 2, PanIN 3.

PanIN 1 is further subdivided into PanIn 1-A, characterised by lesions that are flat and cells with increased levels of mucin (arrow) (Figure 5) have basally located small oval nuclei while PanIN 1-B are papillary lesions with basal nuclei and appear to have pseudo-stratified tissue architecture (Figure 5-arrow,). They maintain cell polarity, have high levels of supra nuclear mucin with no nuclear atypia (Figure 5).

PanIN 2 lesions (Figure 5) are predominantly papillary with nuclear abnormalities. Mitotic bodies can also be observed (non luminal and not atypical) [30].

PanIN 3 lesions lose nuclear polarity, exhibit nuclear atypia and show abnormal mitosis. PanIN 3 (Figure 5) lesions have a marked similarity to Pancreatic Ductal Adenocarcinoma (PDAC) but cells do not breach the basement membrane (carcinoma in situ) [30]. Studies have reported patients with PanINs to develop invasive pancreatic cancer. When comparing the normal pancreas to PDACs, there is a progressive increase in the number and grade of PanINs [31]. Present imaging techniques available to patients cannot detect PanINs but can image larger macroscopic MCNs and IPMNs, usually larger than 1cm [32].

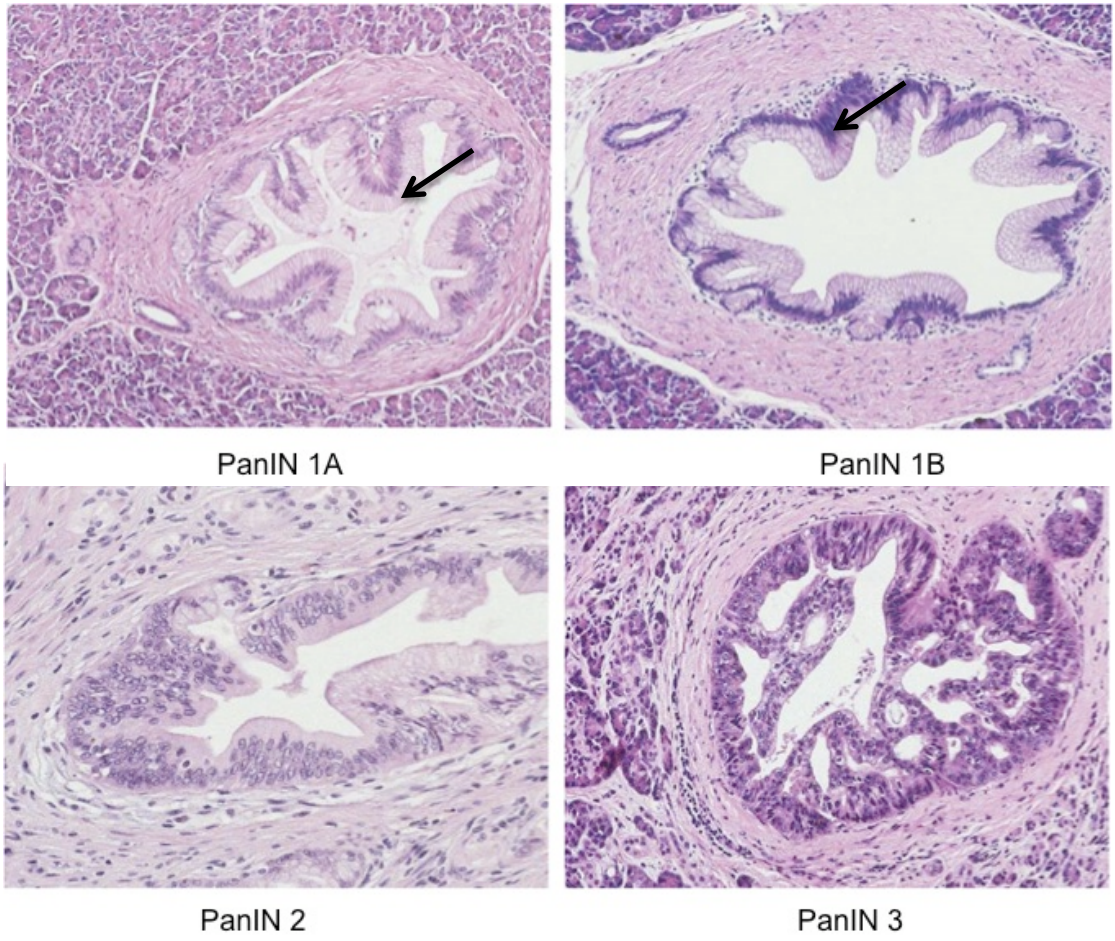

Figure 5: Histological images of haematoxylin stained human PanIN sections showing the different sub-classification. (arrow points to increased secretion of mucin). ***Figures courtesy of Mr. Hemant Kocher, Barts Cancer Institute, Queen Mary University of London.***

1.7.3 Mucinous cystic neoplasms (MCN)

With a characteristic “ovarian type” stroma, MCNs are mucin-producing epithelial neoplasms which mostly affect women [31]. Arising in the tail of the pancreas these are columnar cells with varying degrees of differentiation (Figure 6). They are sub classified into mucinous cystadenomas (uniform nuclei, no significant atypia), border line MCNs (minimal cytological and architectural atypia), MCNs with carcinoma in situ (high grade dysplasia) and invasive mucinous cystadenocarcinoma [33]. About a third of all MCNs are associated with a ductal type of adenocarcinoma of the pancreas [34].

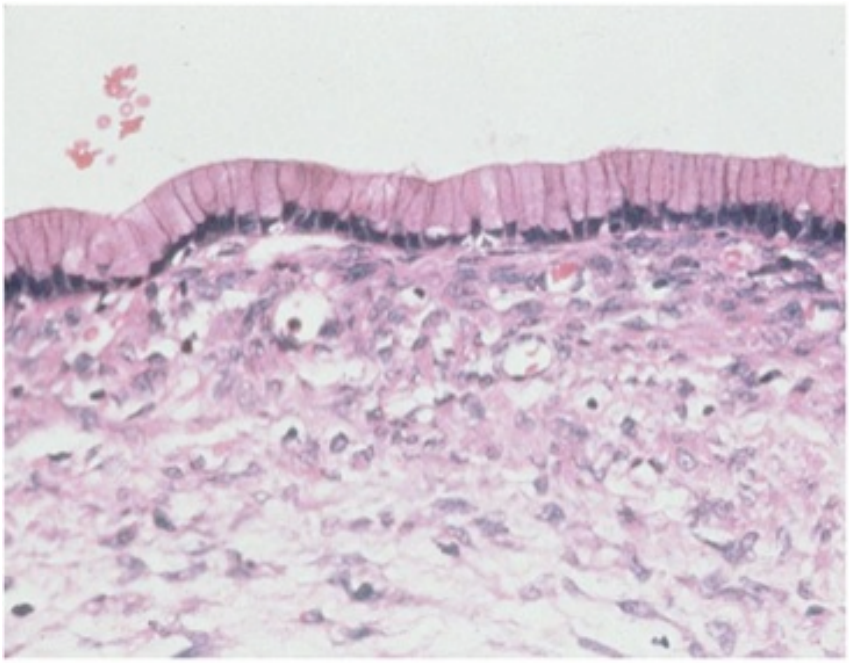

MCN

Figure 6: Haematoxylin stained section of mucinous cystic neoplasm (MCN). (10X magnification) ***Figure courtesy of Mr. Hemant Kocher, Barts Cancer Institute, Queen Mary University of London.***

1.7.4 Intraductal papillary mucinous neoplasm (IPMN)

Intraductal papillary mucinous neoplasms (IPMNs) are usually detected more easily in the head of the pancreas using magnetic resonance cholangiopancreatography, and these cells secrete the mucin MUC 2 (most PanINs express MUC 1) [35]. IPMNs are composed of columnar cells and are classified into two broad groups – those that are, and those that are not associated with invasive cancer; the latter having an excellent prognosis after surgery. IPMNs arising in the branch ducts (Figure 7) are less likely to progress to invasive carcinoma compared with main duct IPMNs [34]. Tubular/ductal invasive adenocarcinoma or the colloid or muconodular types of invasive cancer are two types of invasive cancers associated with IPMNs [30] [32] [34].

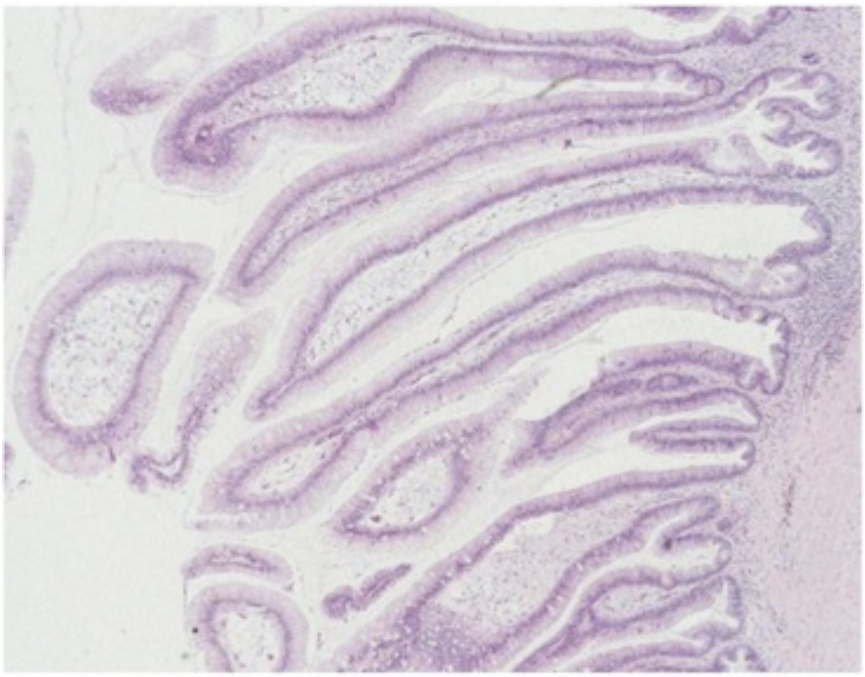

Figure 7: Haematoxylin stained section of intraductal papillary mucinous cystic neoplasm (IPMN) (5X magnification). ***Figures courtesy of Mr. Hemant Kocher, Barts Cancer Institute, Queen Mary University of London.***

All the above-mentioned precursor lesions have their own characteristic morphological features (Table 2) and genetic alterations that have an impact on the prognosis of these lesions. It has been well established now that these precursors have a tendency to progress and ultimately transform into invasive adenocarcinoma [30].

	MCN	IPMN	PanIN
Age at diagnosis	Non invasive, 55 years. Invasive, 65 years.	Non invasive, 63 years. Invasive, 68 years	Increasing with age
Gender	90% F	40% F	50% F
Location in pancreas	Tail	Head	Head
Growth within larger pancreatic ducts	No	Yes	No
Manifests clinically	Yes	Yes	No
Grossly visible	Yes	Yes	No
Mucin oozing from ampula	No	Yes	No
Ovarian type stroma	Yes	No	No
Extra-pancreatic neoplasms	No	Yes	No
Presenting symptoms	Asymptomatic or vague abdominal symptoms (Pain, anorexia)	Abdominal pain, weight loss, pancreatitis	Asymptomatic

Table 2: Features of precursor lesions of PDAC and their presenting symptoms. *Modified from Maitra et al. Adv Anat Oathol, 2005* MCN – Mucinous Cystic Neoplasm, IPMN – Intraductal Papillary Mucinous Neoplasm, PanIN – Pancreatic Intraepithelial Neoplasia, PDAC – Pancreatic Ductal Adenocarcinoma.

1.8 Progression into pancreatic ductal adenocarcinoma

PDAC is the deadliest and most frequently occurring form of pancreatic cancer among the multiple histological subtypes of this disease. With a dismal five year survival rate of <5%, there is an urgent need for a thorough understanding of the molecular changes of this disease to allow early diagnosis and therapeutic intervention.

Macroscopically the tumours appear as a white-yellow firm mass and microscopic observations show that the infiltrating glands comprise low columnar mucin-containing cells [36]. The area surrounding the cancer is highly desmoplastic and the cancer cell nuclei often show loss of polarity, pleomorphism, and prominent nucleoli [36]. More than 80% of patients with PDACs show metastasis to distant organs, the most common sites being the liver (80%), peritoneum (60%), lung, pleura (50%-70%) and adrenal gland (25%) [37]. The cancer invades the vasculature, lymphatic and perineural tissue surrounding the pancreas with approximately 80% of resected organs showing disease in the regional lymph nodes [36].

1.8.1 Genetic changes leading to PDAC

The aggressive nature of pancreatic cancer is a result of multiple heterogeneous genetic changes, which is a hallmark of pancreatic cancer. Variations in copy number, micro-satellite instability (e.g. mutations in *LMLH1*), epigenetic silencing (e.g. hyper methylation of promoter CpG islands in ppENK) are some of the common genetic abnormalities observed [38]. There are many common genetic aberrations between PanINs and PDACs, which might be an indication that PanINs could be a precursor to PDACs. Some of the genetic mutations tend to accumulate as the disease progresses from a pre-invasive neoplastic stage to an invasive and aggressive ductal adenocarcinoma [31].

The GTPase KRAS protein is part of the RAS superfamily of proteins and plays a role in many vital cellular functions including proliferation, differentiation and survival. Mutations in the *KRAS* oncogene are observed in about 90% of PDACs and these are widely believed to be an initiating event, which drives tumour progression. *KRAS* mutations occur more frequently, the more advanced the lesions are; thus PanIN 1 has about 10% - 30%, PanIN 2 has about 45% and PanIN 3 has about 85% of activating *KRAS* mutations [39]. The most common mutations observed is the point

mutation at codon 12 from GGT to GAT or GTT and more rarely from GGT into CGT [40], which results in a substitution of a single amino acid, glycine with aspartic acid (G12D), or with valine (G12V) or with alanine (G12A) with the latter more commonly observed in colorectal carcinomas [41]. These mutations often lead to a constitutively activated form of *KRAS*. Once activated, *KRAS* can activate many downstream signalling pathways including the RAF-Mitogen Activated Protein Kinase (MAPK) and the Phosphoinositide-3-Kinase (PI3K) pathway, which are shown to be involved in pancreatic cancer [42] (Figure 8).

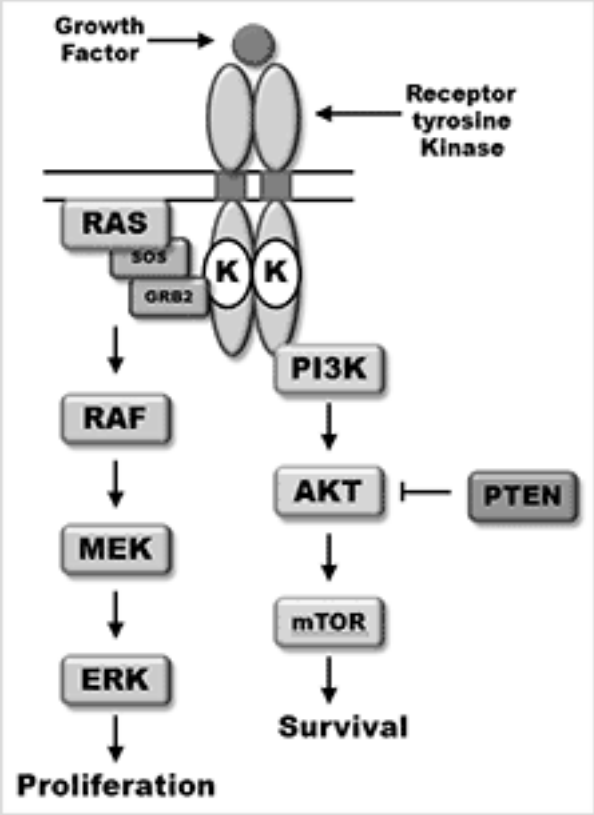

Figure 8: Down stream signalling as a result of KRAS activation either by growth factor receptor mediated activation or presence of activating mutations in the KRAS gene as described above.

In addition to mutations in KRAS about 80%-95% of PDACs also have loss of function mutations of a tumour suppressor gene, p16/CDKN2A/INK4A and these mutations are usually observed in the later stages of pancreatic cancer [35]. Tumour suppressor gene INK4A/p16 inhibits phosphorylation of the retinoblastoma (Rb) gene mediated by cyclin dependent kinases (CDK4/6) and prevents cell cycle progression at the S phase [43]. During the development of PDACs, this gene is usually mutated

through deletion or promoter methylation. Alternative reading frame (ARF/p19) is another tumour suppressor gene transcribed from an alternate reading frame of the CDKN2A (INK4A or p16) gene with distinct first exons and alternative reading frames in the shared downstream exons [44]. ARF usually inhibits tumour progression through stabilising the p53 gene by inhibiting Mdm2 mediated degradation of p53 [43]. It is not yet fully understood if loss of function mutations of ARF alone can affect p53 function in PDAC progression because both ARF and p53 deletions coexist in about 40% of human PDAC [45]. There are studies which suggest that the loss of function of ARF/p19 could simply be due to the loss of function mutations in the INK4A/p16 gene [43]. Mutations in the KRAS gene can activate the INK4A and ARF tumour suppressor genes, which in turn can induce cell death (senescence), thus acting as a defence mechanism against oncogene activation [46]. Studies on pancreatic mouse models with mutations in the KRAS gene have shown that early lesions in the pancreas (PanINs) do express INK4A but expression was lost almost completely when lesions progressed to invasive cancer [47] suggesting that activating mutations of KRAS followed by changes in growth factor signalling can lead to loss of function mutations in the INK4A and ARF genes as the lesions progress from PanINs to PDAC (Figure 9) [43].

PDAC is often comprised of profound aneuploidy and intra-tumoural heterogeneity and this has been widely attributed to the loss of function mutations of the p53 gene [43]. Almost 50%-75% of PDAC patients have missense alterations (point mutation) in the DNA-binding domain of the p53 gene (Figure 9) [48]. Similar to the other tumour suppressor genes, including *INK4A* and *ARF*, *p53* mutations are more common as the early pancreatic lesions progress to PDAC. The fact that *p53* is only mutated and not deleted in PDAC could result in a gain of function of the mutant *p53*, which could in fact promote tumour growth. In fact, mutant *p53* has been shown to play a key role in overcoming senescence (growth arrest) induced as a result of activating mutations of the *Kras* gene and promote PDAC tumour growth in a mouse model for PDAC [49]. Further studies have also revealed that mice with accumulated mutant *p53* are more prone to developing metastatic osteosarcomas and carcinomas, including PDAC, compared to *p53* null mice where no metastasis was observed [49, 50].

TGFβ belongs to a superfamily of secreted proteins and these are secreted as inactive complexes with a pro-peptide, latency-associated peptide (LAP) of TGFβ [51]. TGFβ signalling in cancer is extremely complex and there are contradictory reports published describing its functional role in cancer, both as a tumour suppressor and as a tumour promoter. Upon binding to its receptor, TGFβ downstream signalling is mainly carried out by the SMAD family of proteins (SMAD1-8). One of the signalling routes described is through the phosphorylation and activation of SMAD 2 and 3, which in turn bind to the transcription factor, SMAD4, which is translocated into the nucleus where it acts to regulate gene expression [52]. TGFβ signalling is very important in pancreatic cancer progression as about 50% of PDAC patients in the late stages have a mutational deletion of SMAD4 or DPC4 (deleted in pancreatic cancer, locus 4) a key component in the TGFβ signalling cascade, being a transcriptional regulator [53] (Figure 9). In PDAC, *SMAD4* deletions are associated with the interaction between the tumour and its microenvironment and restoring SMAD4 expression had a major impact on angiogenesis and matrix remodelling in xenograft mouse models [54]. Loss of heterozygosity (LOH) of the *SMAD4* gene in PDAC means that the epithelial growth inhibitory effects promoted by TGFβ are lost and in fact in some cases, it has been shown to provide PDAC tumour cells with a survival advantage [52].

Mutations are also observed in the DNA repair genes like *BRCA2*, Fanconi anaemia (*FANC*) gene, and the mis-match repair genes, *hMLH1* and *hMSH2* [35] [55]. Apart from PDACs, there are other tumours that arise in the pancreas including primary non-endocrine tumours, adenosquamous carcinoma, acinar cell carcinoma, giant cell carcinoma, which have been observed in recent years. These tumours are not as deadly as PDAC and most of them are treatable with good clinical outcomes [8] The exact roles of tumour suppressor genes and oncogenes implicated in these events remain unclear but continued efforts to elucidate the genetic and molecular causes will translate into better diagnostic tests and therapies.

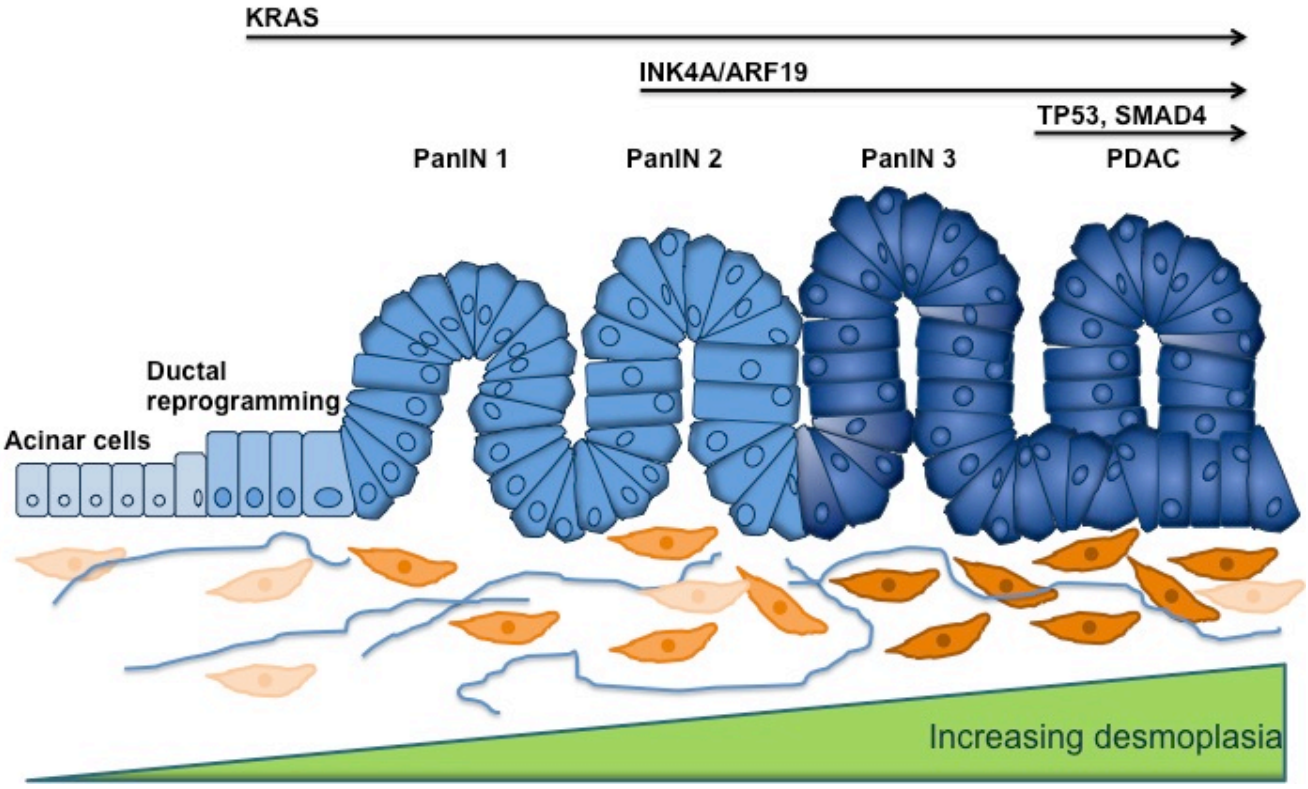

Figure 9: Genetic progression model for pancreatic cancer. Early stages of pancreatic cancer involve the shortening of telomeres and mutations in the KRAS oncogene. As the disease progresses the cells accumulate more mutations in the INK4A/ARF19 tumour suppressor gene leading to an accelerated progress into PDAC where further inactivating mutations of TP53 and SMAD4 are observed. The changes observed in the epithelial cells are accompanied by alterations in the tumour microenvironment. Figure adapted from Morris et al, 2010 [56].

1.9 Pancreatic cancer – the role of the microenvironment

There have been many studies which have examined the molecular mechanisms of carcinogenesis but it has become widely accepted that tumour progression actually is a consequence of the dynamic interaction between the transformed cancer cells and the cellular and the neighbouring non-cellular components that surround them, the stroma [57].

1.9.1 Tumour stroma

Tumour stroma is composed of a mixture of various extracellular matrix (ECM) proteins containing cellular components including fibroblasts, immune and inflammatory cells and blood vessels. Previously thought to be a passive milieu

through which cancer cells invaded, it is now evident that there is an active exchange of signals between cancer cells and the stromal environment, which influences and determines the behaviour of the tumour [57]. The cancer cells themselves can modify the stroma, often referred to as “activated” stroma, and, depending on the degree of activation, a desmoplastic (fibrotic) stroma provides a permissive milieu for tumour progression [58]. A large amount of intense fibrous or desmoplastic stroma is a characteristic feature of pancreatic cancer and it accounts for a large proportion (70% or more) of the tumour mass (Figure 10) [19].

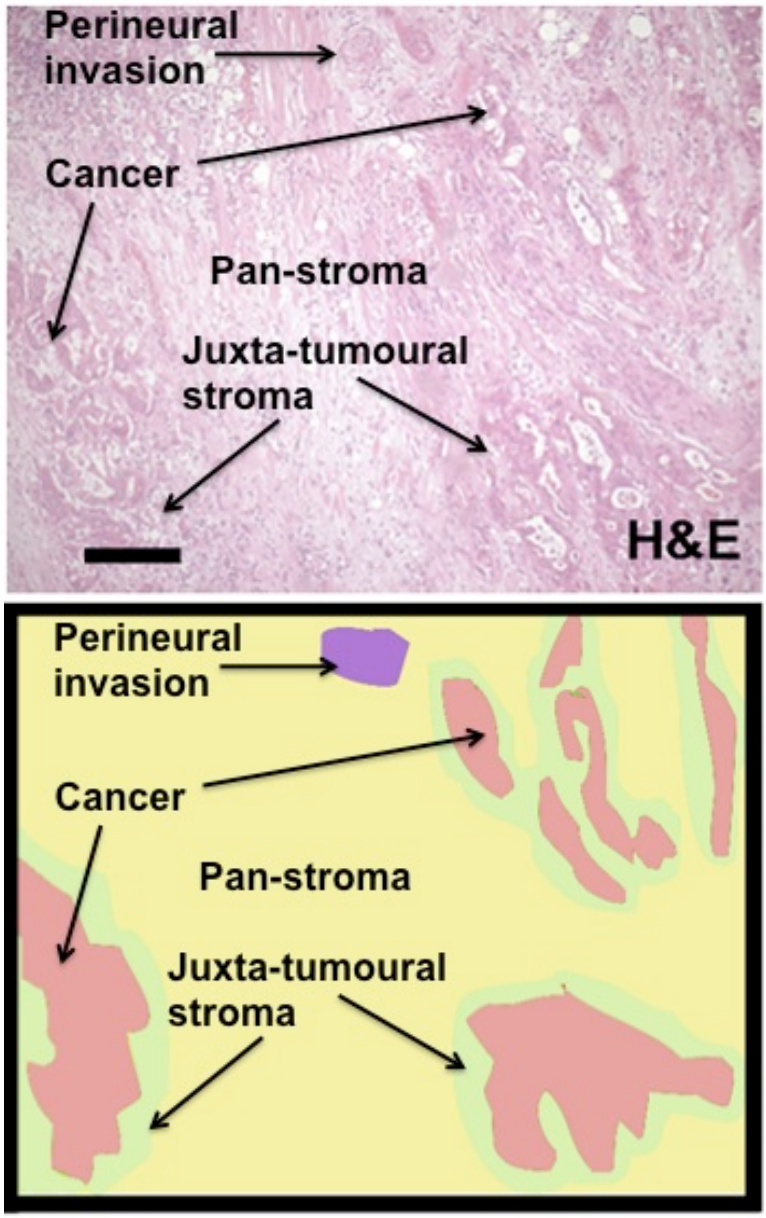

Figure 10: Histology of pancreatic cancer showing the intense stromal response. H&E section shows staining of pancreatic cancer and below is the schematic representation, which shows the area of desmoplasia in yellow. ***Figure reference:[59].***

Indirect immunofluorescence studies carried out on 12 PDACs showed that the main components that made up the stroma were collagen type 1, type 5 and fibronectin. Studies have reported a three-fold increase in the average collagen content in pancreatic cancer compared to normal pancreas [60, 61]. Even though PDAC cells can secrete various ECM proteins such as collagen, fibronectin and laminin, there is increasing evidence that myofibroblasts (activated or transformed fibroblasts) and activated pancreatic stellate cells play a major role in modifying the ECM [62]. In normal pancreas, there are stromal cells (fibroblasts and pancreatic stellate cells) which have a controlled level of proliferation and secrete growth factors required to maintain tissue homeostasis. In PDACs, where the cells breach the basement membrane in to the surrounding stroma, the stromal cells rapidly proliferate and secrete more growth factors and collagen much like a wound healing response. The difference being, in cancer, the stromal activation does not revert back into the quiescent state [62].

1.9.2 Cancer cells modify their stromal environment

Cancer cells can modify their adjacent environment directly by producing enzymes that modify stromal proteins and indirectly by activating stromal cells to modify the ECM. Thus tumour cells often secrete matrix metalloproteinases (MMPs), which are proteolytic enzymes that can degrade ECM proteins [63]. They also secrete a variety of growth factors, including epidermal growth factor (EGF) and transforming growth factor-β (TGF-β), which can act in a paracrine fashion to modify the surrounding stroma [64]. These secreted factors activate the stromal cells, which in turn start to proliferate more and secrete more growth factors, which then will aid in tumour progression.

1.9.3 Tumour associated fibroblasts

The idea of a cross-talk between cancer cells and their microenvironment was suggested as early as 1889 by Steven Paget in his “seed and soil hypothesis” [65]. According to this hypothesis, an active tumour-stroma interaction is required for the cancer cells (seeds) to metastasise into a secondary microenvironment (soil) and grow [66]. Genetic changes in epithelial cells initiate release of cytokines and growth factors, which activate the stromal fibroblasts. Once activated, these cells are often referred to as tumour-associated fibroblasts or cancer associated fibroblasts (CAFs) or myofibroblasts. Due to their mesenchymal origin, myofibroblasts have similarity

with the muscle cells, including the expression of α-smooth muscle actin (α-SMA), expression of which is used as a marker for the myofibroblastic phenotype [67]. The tumour cells secrete growth factors including TGF-β, basic fibroblast growth factor (bFGF), vascular endothelial growth factor (VEGF), which can activate the fibroblasts and in turn upregulate various growth factors such as hepatocyte growth factor (HGF), which has a paracrine effect on the tumour cells by binding to its receptor c-Met, expressed on epithelial cells and thereby leads to increased proliferation, migration, invasion and matrix remodelling. This process is cyclical and leads to the formation of a stroma, which supports tumour growth and invasive behaviour [68-70].

TGFβ is one of the most important factors that induce desmoplasia [71]. It does this principally by causing the trans-differentiation of pancreatic stellate cells and fibroblasts into the activated state, which is characterised by α-SMA expression and increased collagen secretion. In addition to this, resistance of tumour cells to growth inhibition by TGFβ is usually accompanied by an increased expression of TGF-β. In PDAC this is usually due to a mutation of the *SMAD4* gene (DPC4) allowing cells to escape the growth inhibitory function of TGF-β [68] [72]. Other growth factors, including platelet derived growth factor (PDGF) or fibroblast growth factor (FGF), also have been shown to induce myofibroblast differentiation and promote desmoplasia [73]. A study which looked into the invasive ability of pancreatic cancer cells co-cultured with pancreatic specific fibroblasts showed more invasion in the presence of fibroblasts than in their absence [74]. This could possibly be due to increased expression of HGF by the fibroblasts [74]. This study will focus on pancreatic stellate cells, the major cellular components in PDAC stroma and their role in PDAC progression.

1.9.4 Pancreatic stellate cells

With fibroblast-like morphology, pancreatic stellate cells (PSC) are localised in areas of the pancreas that have an exocrine function. These cells can be identified by accumulation of vitamin A (retinol) in intracellular fat droplets and were first identified in mouse and human pancreas in 1982 and 1990 respectively [75, 76]. Vitamin A is auto fluorescent and under ultraviolet (UV) light emits a rapidly fading blue green fluorescence, which is a characteristic feature of cells which store vitamin A. Due to their close resemblance to the hepatic stellate cells, these cells were characterised by two independent laboratories and subsequently called pancreatic stellate cells

[77, 78]. A gene-expression microarray analysis revealed that only 29 genes of the 20,000 studied were differentially expressed in pancreatic stellate cells compared with hepatic stellate cells [79]. This might suggest a common stellate precursor with a few organ specific adaptations. More recently, immunohistochemical analysis on tissues revealed the presence of stellate cells in other organs including kidney, lung and heart [80].

In normal pancreas, stellate cells are primarily located in the peri-acinar and interlobular space and constitute only about 4% of all pancreatic cells. In addition to storing vitamin A, these cells express a set of specific markers, which include glial fibrillary acidic protein (GFAP), nestin, desmin and vimentin [81] [77, 78]. Similar to the fibroblasts, pancreatic stellate cells can be activated into a myofibroblast-like phenotype. When this happens, they lose their vitamin A fat droplets and start secreting various ECM proteins including collagen type 1, fibronectin, laminin [78] [81]. They also begin to express the myofibroblastic marker, α-SMA. Co-culture of pancreatic stellate cells and cancer cells compared with cancer cells alone *in vivo* (subcutaneous xenografts or orthotopic injections in nude mice models) show that the introduction of stellate cells markedly increased the desmoplastic response observed [82-84]. Sections from tumours isolated from co-cultured *in vivo* experiments showed remarkable similarity to human pancreatic cancer and alcohol-induced chronic pancreatitis [85]. Immunohistochemical analysis of these tumours showed strong positive staining for desmin, GFAP and α-SMA in the stroma. Co-localisation of α-SMA-positive cells with mRNA encoding procollagen α1 suggests that activated pancreatic stellate cells contribute significantly to the desmoplastic reaction observed in pancreatic cancer [86].

Cancer cell proliferation and invasion increased when these transformed cells were co-cultured with pancreatic stellate cells in an orthotopic mouse model [83]. The authors of this publication also observed a significant increase in tumour incidence, growth and metastasis when a higher proportion of pancreatic stellate cells were co-injected with the cancer cells (1:5 cancer cell : stellate cell ratio). Very recently, *in vitro* observations in our laboratory showed that cancer cell invasion into a 3D matrix using the organotypic co-culture model was dependent on the number of stellate cells in the system. Maximum invasion and growth was observed at a ratio of 1:2 (cancer cell:stellate cell), (In-house data, not published).

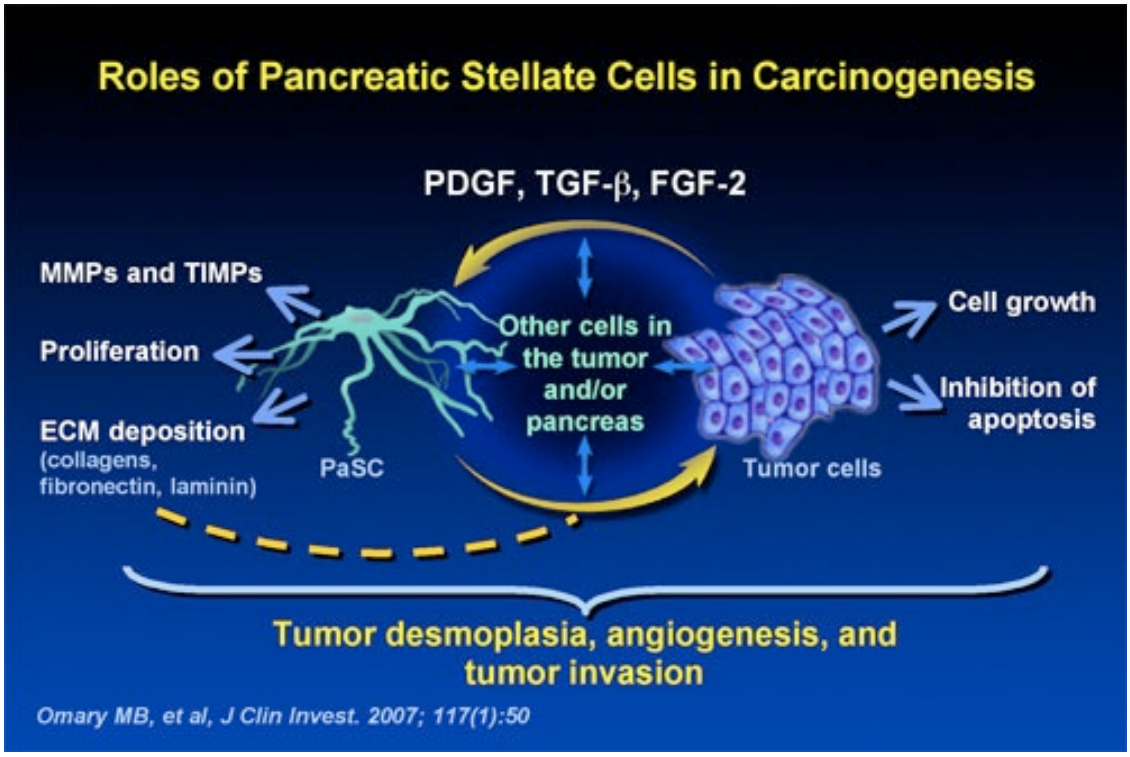

Figure 11: Pancreatic stellate cell. Various factors that are secreted by the stellate cell, which in turn have a paracrine or autocrine effect and contribute to the modulation of the ECM [81].

TGFβ plays an important role in the activation of pancreatic stellate cells via several direct and indirect mechanisms. It is one of the growth factors known to increase the migratory potential of stellate cells [87]. Activin A (member of the TGFβ family) has been shown to activate pancreatic stellate cells, thereby increasing collagen deposition and secretion of other growth factors, which in turn have an autocrine effect to keep them in an activated state [88]. Activated stellate cells also secrete factors that have a paracrine effect on the cancer cells and help in tumour progression. Cancer cells can secrete tumour necrosis factor α (TNFα), FGF2, interleukin (IL) 1, 6 and 8, all of which have been implicated in the activation of pancreatic stellate cells. Activated PSCs are known to stimulate various intra-cellular signalling pathways including the mitogen activated protein kinase pathway (MAPK), phosphatidyl inositol 3 (PI3) kinase pathway, Rho-Rho (ROCK) and TGFβ / SMAD4 pathway (Figure 11) [89].

The role of pancreatic stellate cells, both in the quiescent and activated state, is far from completely understood. There are many recent studies that show a very strong cross talk between the pancreatic cancer cells and pancreatic stellate cells. Thus increased understanding of pancreatic stellate cells is essential for studying pancreatic cancer progression.

1.9.5 Three dimensional (3D) *in vitro* models of pancreatic cancer

Over the years, *in vitro* 2D cell culture has contributed to vast amounts of data relating to various genetic, biochemical and cell biological processes. However, cells grown as a monolayer in 2D on tissue culture plates differ in their morphology, cell-cell and cell-matrix interactions compared with 3D cell cultures. 3D models are increasingly used to study cell-cell and cell-matrix interactions because they can be used as a preliminary screen to examine specific genetic, biochemical or cellular questions more easily than in complex animal models. While they cannot replace animal models, they offer a significant advantage over 2D systems because they act as physiological mimetics.

Studying cellular behaviour in 3D is extremely important to understand the various biochemical pathways that are involved in cancer progression. Tissues are very heterogeneous and contain multiple cell types, like epithelial cells, mesenchymal cells (fibroblasts, stellate cells), vascular cells (endothelial cells, pericytes), inflammatory or immune cells (macrophages, lymphocytes). Co-culturing multiple cell types *in vitro* in a single organotypic model is a very complex process but it recapitulates better the *in vivo* condition. There are very few 3D co-culture models that are established for pancreatic cancer to date. Froeling F.E et al; 2010 [59] in our laboratory adapted the organotypic co-culture model, used for studying skin cancer [90], to study pancreatic cancer. The pancreatic cancer cells were co-cultured with pancreatic stellate cells embedded in a matrix of collagen type 1 and Matrigel™ in a 1:1 ratio and grown at an air-liquid interface. These co-cultures offered a three dimensional matrix for the cancer cells to interact with the stellate cells and also provided a matrix for them to grow on and invade into. This model can be used for a variety of *in vitro* experiments and can be set up for using genetically manipulated cells (siRNA treated) or testing new therapeutic agents (antibodies or small molecule inhibitors) to target the epithelial or stromal, or both, cell types in a more physiologically relevant environment. The same co-culture model has been used to

target the pancreatic stellate cells (stromal compartment) specifically using all trans retinoic acid (ATRA). The ATRA rendered the activated stellate cells quiescent, leading to a decreased proliferation and increased apoptosis of the surrounding pancreatic cancer cells (epithelial compartment) [91]. This clearly highlights the importance of tumour-stroma cross talk and the need for these three dimensional models to study biological functions. These organotypic co-culture models provide a system, which can be manipulated to address specific questions, and serve as useful tools before using *in vivo* models.

1.9.6 *In vivo* mouse models of pancreatic cancer

In vivo mouse models for pancreatic cancer are crucial for our understanding of the complex nature of this disease. A pre-clinical animal tumour model is essential for obtaining data on development, progression, signalling pathways, mechanism of action and therapeutic efficacy of new anti-cancer agents, which are clinically relevant. Selecting the right animal tumour model, its design and use is entirely dependent on the questions to be answered and a successful pre-clinical animal tumour model should be reliable, reproducible and affordable. It should also allow the user to determine an objective and quantitative end point [92]. Various types of *in vivo* mouse models for pancreatic cancer have been developed over the years.

One such model is where immunocompromised mice are inoculated (ectopic injection), with human cancer cells alone or a combination of human cancer cells and pancreatic stellate cells, subcutaneously [82]. The main advantages of using this model are the ease of design compared with other animal models, extreme reproducibility, minimal labour, easily quantifiable data, varying treatment plans according to tumour burden and the fact that it is cheaper compared with other animal models. The major drawback is the absence of metastasis, absence of relevant host infiltrate and also the presence of an inappropriate tumour microenvironment.

Another model, widely considered to be better than the subcutaneous model, because of its physiological relevance is the orthotopic (site/organ specific) injection into immunocompromised mice [83]. The main advantage of using this model is that the cells are injected into the relevant site so there occurs an interaction between the host organ and tumour cells. This method aids both local and distant metastasis. Any therapy given, thus will be site directed to affect the specific relevant organ and

clinical situations can be recreated to a certain extent by removing the primary tumour and treating the secondary metastasis. The main disadvantage is that it is very labour intensive. Injecting into the mouse pancreas requires anaesthesia and surgery for each mouse, which can be technically difficult, and with Home Office restrictions in place, only one injection per animal can be performed, thus even the slightest mistake can result in the animal being removed from the group and culled. It is more expensive compared to the subcutaneous model because more animals are required per experiment due to complications that could arise due to the surgery and also due to a lack of a 100% uptake of tumours. Also it is more difficult to monitor tumour growth, compared with the subcutaneous tumours, although this is being overcome by use of ultrasound machines (which are expensive) [93].

Although both the above-mentioned models are an advance on the 3D *in vitro* models, there is wide spread criticism over injecting human cells into immunocompromised mice. A genetically engineered mouse model, which can give rise to spontaneous pancreatic cancer, is considered to be the gold standard model. It provides valuable insights and closely resembles the pathophysiological and molecular features of human pancreatic cancer. It also allows the user to study the early events during the development of cancer, study the genetic background of the disease, study metastatic patterns that are more relevant to human disease and might help to design strategies to prevent cancer initiation.

Like most gastrointestinal (GI) organs, the pancreas develops from the endoderm during gastrulation. Many key embryonic signalling pathways, including hedgehog signalling, notch signalling and retinoic acid signalling determine the lineage of the pancreas [94]. The development of the pancreas is controlled by transcription factors, which regulate gene expression. One of the earliest transcription factors essential for the development of pancreas is the homeodomain transcription factor pdx1 (pancreas duodenum homeobox 1). Pdx1 was initially considered to be an exocrine transcription factor but more recent studies have revealed that it is necessary for both the exocrine and endocrine differentiation [95]. Lineage tracing studies were possible in animal models using the Cre-Lox technology. This technology is currently in use for generating animal models with specific deletions (knock out) and insertions (knock in) of genes. Cre gene and lox p sites have to be introduced into mice using transgenic technology and the majority of the cre-lox strains generated can be grouped into four categories [96]. Cre expressing strains have a transgene controlled by a promoter (which can be tissue specific). Inducible

Cre expressing strains have a transgene, which becomes functional only upon the addition of an inducing agent (e.g. doxycycline, tetracycline). Lox p flanked (floxed) strains have the gene of interest flanked by lox p sites, which are recognised by the cre-recombinase and this technology is used mainly for gene deletion (knock out models). Cre reporter strains combines a marker (fluorescent or lac z) together with the lox p sites so that the recombination or alterations in gene expression can be monitored [97].

Transgenic mice with a mutation in the oncogenic *Kras*^{G12D} allele controlled by Cre-mediated recombination and driven by Pdx1 (a specific promoter) were created and the pancreata of these mice spontaneously developed tumours similar to PanINs observed in humans [98]. In the pancreas of many of these mutant mice, an intense stromal response with inflammatory cells, fibroblasts and collagen deposition was observed. When these mice were crossed with conditional knockout mice of the *Ink4a*/*Arf* locus (eliminates p16^{INK4A} and *p19*^{ARF} proteins) or mice with a single G to A nucleotide substitution in the endogenous *TP53* gene, they developed invasive and metastatic pancreatic tumours [99, 100]. *Kras*^{G12D} mice crossed with *Ink4a* knockout mice developed poorly differentiated tumours whereas *Kras*^{G12D} mice crossed with mutated *TP53* showed a higher prevalence of well or moderately differentiated adenocarcinomas [101]. The loss of tumour suppressor genes along with activated *Kras* can influence the type of lesions formed and in turn affect the differentiation state and progression of tumour. Activated *Kras* gene is essential for initiation and development of pancreatic tumours. Loss of function of tumour suppressor genes (*TP53*, *Ink4a*/*Arf*) alone did not give rise to any tumours, suggesting *Kras* mutations drive tumorigenesis as well as determining cellular differentiation [101]. It has to be mentioned that in the PdxCre;*Kras* ^{G12D} mice, which have a mutant allele of *Kras* in all three lineages (endocrine, exocrine and acinar), the only neoplastic feature that is observed are PanIN lesions and PDAC; endocrine and acinar tumours are not observed. In addition to the above-mentioned models, which are based on conditional expression under the control of Pdx1 transcription factor, there are many transgenic mouse models, which have been developed employing various promoters to drive mutagenic expression. These models are currently used to study various deregulated signalling pathways and pathogenetic changes that lead to invasive pancreatic cancer (Table 3).

Reference	Promoter	Model	Background	Tumours	Other organs
Hingorani 2003 (98)	Pdx1 or p48	Pdx1-Cre; LSL-KRAS^{G12D} p48-Cre; LSL-KRAS^{G12D}	B6/129vJae	3 stages of PanINs, 7% progression to PDAC with local spread and met to liver	Pdx-Cre mice; mucocutaneous papillomas, hyperplastic polyps of the duodenum
Aguirre 2003 (99)	Pdx1	Pdx1-Cre; LSL-KRAS^{G12D} INK4A/ARF$^{fl/fl}$	FVB/B6	PanIN and 100% progression to PDAC with met to duodenum, stomach, spleen	-
Hingorani 2005 (100)	Pdx1	Pdx1-Cre; LSL-KRAS^{G12D} LSL-TP53^{R172H}	B6/129SvJae	Rapid progression to PDAC with met to liver and lung and a high degree of genomic instability	Oesophageal papillomas and hyperplasia
Bardeesey 2006 (101)	Pdx1	Pdx1-Cre; LSL-KRAS^{G12D} ; TP53$^{fl/fl}$ with either INK4A$^{+/+}$ or INK4A$^{fl/+}$ or INK4A$^{fl/fl}$	FVB/n	Rapid progression to invasive cancer, independent of INK4A status	Lymphoma in mice with INK4A/ARF^{flox} allele
Bardeesey 2006 (101)	Pdx1 or p48	Pdx1-Cre or p48-Cre; LSL-KRAS^{G12D} ; SMAD$^{fl/fl}$	FVB/n	IPMN and invasive PDAC with increased proliferation of stromal and epithelial cells	Gastric tumours in Pdx1-Cre mice
Izeradjene 2007 (282)	Pdx1	Pdx1-Cre; ; LSL-KRAS^{G12D} ; SMAD$^{fl/+}$ or INK4A$^{fl/fl}$	BISwiss/129/ SvJae/ C57Bl/6	Pre-invasive PanIN lesions and MCNs in the body and tail of pancreas	Large gastric tumours
Guerra 2007 (283)	Rat Elastase	Elas-tTA/tetO-Cre; LSL-KRAS^{G12Vgeo}	B6/129SvJ/ FVB	KRAS^{G12V} expression during late embryonic development. At 12 months, high grade PanIN lesions in 80% mice and 50% progress to PDAC	
Habbe 2008 (284)	Rat elastase or Mist1	Elas-tTA/tetO-Cre; LSL-KRAS^{G12D} or Mist1-Cre$^{ERT2/+}$	B6/129SvJae	PanIN lesions grade I-III, acinar-ductal metaplasia. No progression to PDAC	

Reference	Promoter	Model	Background	Tumours	Other organs
Heiser 2008 (285)	p48	p48-Cre; CTNNB1$^{exon3fl/+}$	Mixed	Ductal associated lesions and large well encapsulated pancreatic tumours. No met	
Morris 2010 (56)	p48	p48-Cre; CTNNB1$^{fl/fl}$ or CTNNB1$^{fl/+}$	Mixed	Reduced acinar regeneration post caerulein treatment	

Table 3: Mouse models of pancreatic cancer. LSL – Lox-Stop-Lox, Pdx – pancreas duodenum homeobox 1, Ela – elastase, Mist1 – muscle intestine and stomach 1.

Despite the number of transgenic models that are in use to study pancreatic cancer the long latency periods involved make these models very expensive to maintain and non-amenable to rapid experimental manipulation. Orthotopic transplantation is not an ideal model to screen new anti cancer targets because it is labour intensive and is difficult to monitor tumour growth on a daily basis. Ectopic models on the other hand are easier to maintain and make a good and easier model for screening of new agents to target cancer. This study uses a new ectopic model of PDAC that addresses some of the criticisms of this model.

In this study we have identified the epithelial specific integrin, $\alpha v\beta 6$, expressed on the surface of pancreatic cancer cells. This integrin is absent in normal tissue including pancreas, making it a promising therapeutic target. Integrins and more specifically integrin $\alpha v\beta 6$ will be introduced before describing its role in PDAC cell biology in detail.

1.10 The integrin super family

Tamkun et al, first coined the term “integrin” in 1986 to describe a structurally and functionally related set of heterodimeric cell surface receptors, which “integrated” the ECM with the intra-cellular cytoskeleton [102]. Integrins belong to a superfamily of heterodimeric, transmembrane cell adhesion glycoproteins. Integrins are composed of an evolutionarily conserved series of α and β subunits, which heterodimerise to give rise to the functionally active integrin. Many studies have shown that integrins play a key role in various intra-cellular signalling pathways, which affect diverse cellular functions including differentiation, proliferation adhesion, migration and invasion [103].

In humans, there are eighteen α subunits (α1-α11; αIIb, αD, αE, αL, αM, αV, αX) and eight β (β1 - β8) subunits (Figure 12). The different α and β subunits can dimerise in various, but specific, combinations to give rise to twenty-four different functional integrins, each with distinct functions and tissue distribution. Integrins recognise various ligands and the heterodimer composition determines their ligand binding specificity [103]. Differential splicing and other post-translational modifications also give rise to integrin variants [104]. Integrins bind to specific ligands through recognition of short peptide motifs. The most common integrin binding motif is the arginine-glycine-aspartic acid (RGD) motif found in many ECM ligands including fibronectin, vitronectin, fibrinogen, Von Willebrand factor (VWF) and osteopontin [103]. Eight different integrins recognise the RGD (Arg-Gly-Asp) motif, αvβ1, αvβ3, αvβ5, αvβ6, αvβ8, α5β1, α8β1, αIIbβ3 [105]. Several integrins, α1β1, α2β1, α10β1, α11β1 bind to the different collagens present in the ECM. Integrin expression can be tissue specific, e.g. β2 integrins are expressed only in leukocytes whereas α6β4 is expressed only in epithelial cells [106]. Figure 12 shows the different α and β subunits present in humans along with the possible combinations and ligand specificities.

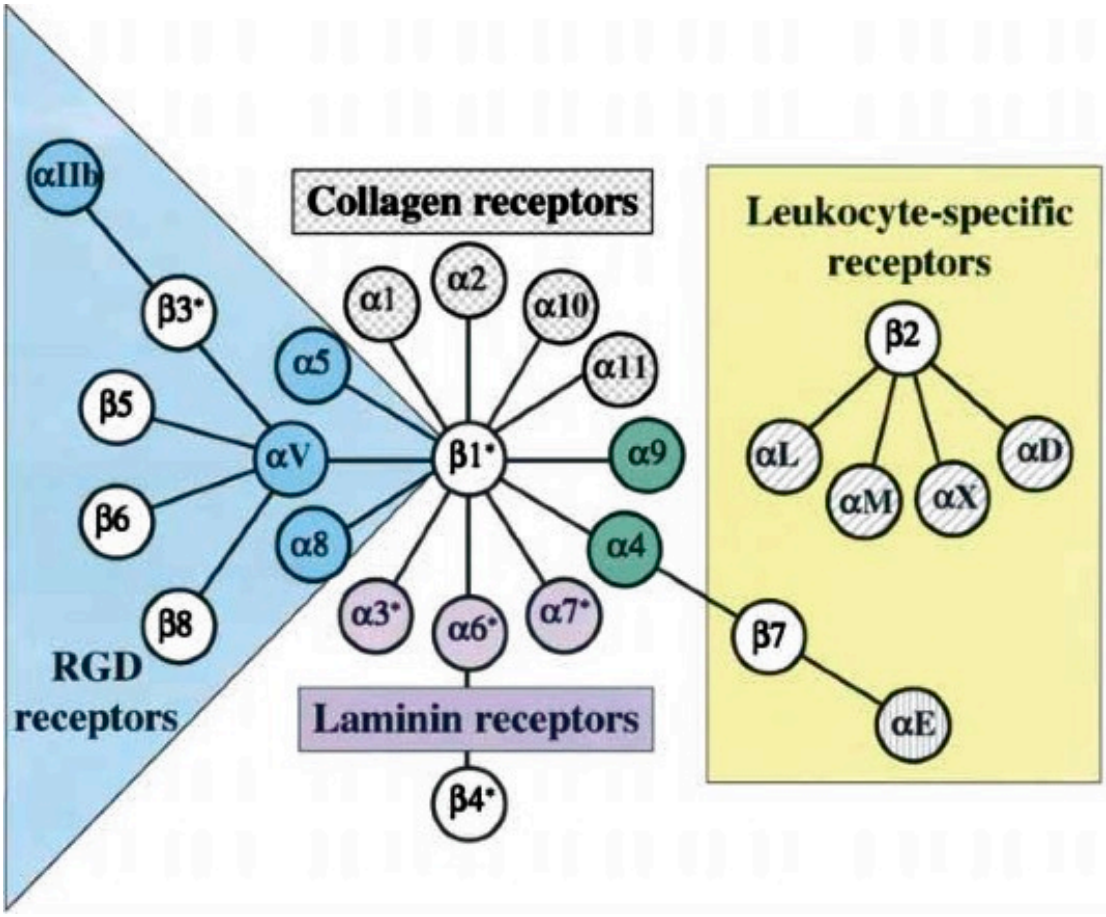

Figure 12: The integrin family with the 18α subunits and 8β subunits. The known combination of the α and β subunits are divided into RGD receptors in blue, collagen receptors in shaded grey, laminin receptors in purple and leukocyte specific receptors in yellow. α4 and α9 in green are restricted to chordates. *(Picture modified from Hynes et al, 2002)*.

1.10.1 Structure and function of integrins

The α and β subunits are membrane glycoproteins expressed on the plasma membrane with a long extra-cellular domain, a trans-membrane domain and, usually, a short cytoplasmic domain (30-50 amino acids) with the exception of β4, which has a cytoplasmic tail of over 1000 amino acids. The extracellular domain has a globular head, which binds to the target ligands whereas the cytoplasmic tail interacts with a variety of signalling and structural molecules, which will be discussed later. The α and β subunit dimerisation occurs in the extra-cellular region and this is where the ligands bind to integrins (Figure 13) [107]. Although integrins can bind to a wide variety of ligands, both ECM proteins and some cellular proteins (Table 4), their ability to do so requires that they are in the active conformation [108].

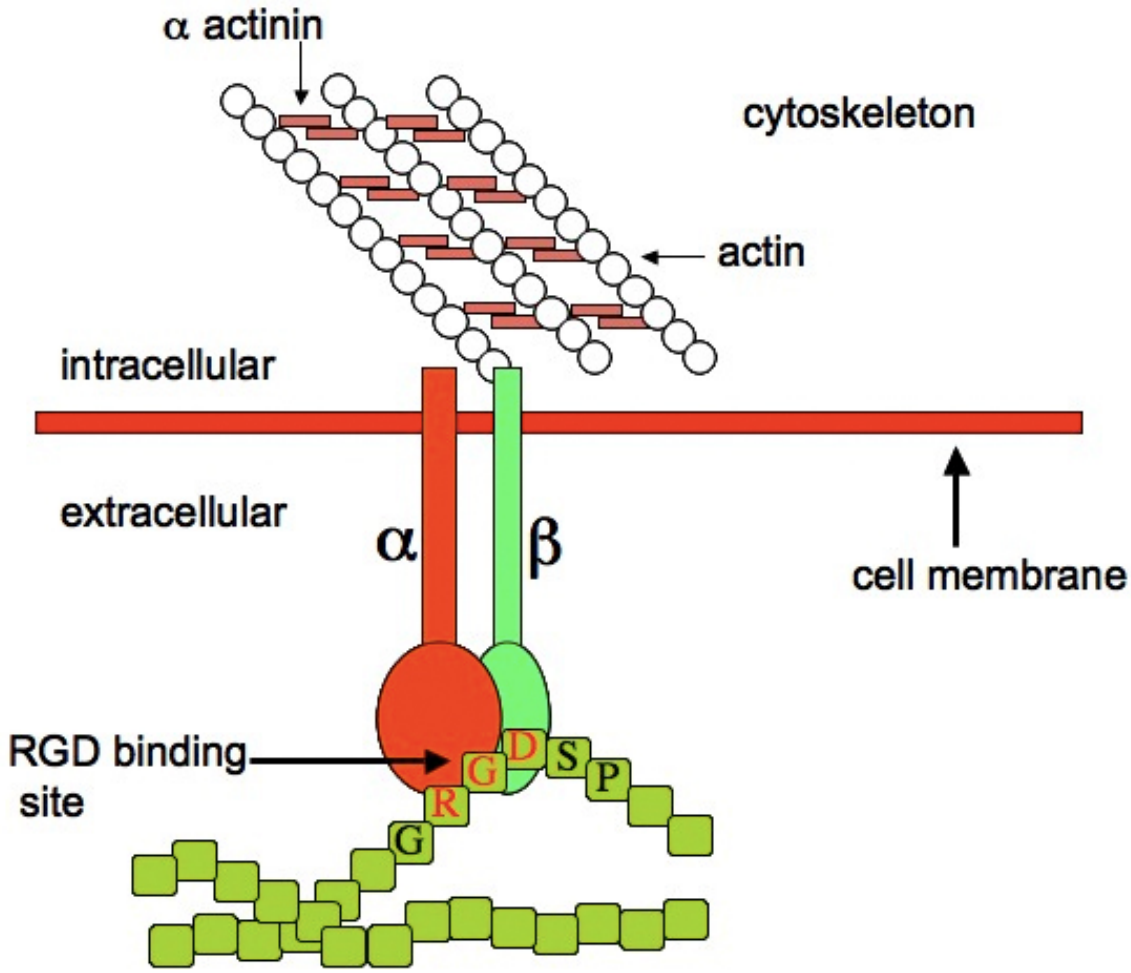

Figure 13: Schematic diagram of the general structure of integrins demonstrating that they can physically connect extracellular ligands to the intracellular architecture of cells.

It has been shown for the integrin αvβ3 that integrins can exist in different structural conformations [109]. Figure 14 A shows αvβ3 in the "bent" inactive form and upon activation, the two extra cellular "legs" are straightened resulting in the high affinity conformation with an "open" head domain (Figure 14 B) [109, 110]. Recent electron microscopic studies have shown that there is also a "closed" head domain, with the "legs" extended, which is a transitional conformation; hence this form is believed to have an "intermediate" affinity for ligands. There is compelling evidence showing that the cytoplasmic domain of the β subunit directs most downstream signalling of integrins. Cytoplasmic-tail truncation mutants of αIIb and β3 subunits transfected into CHO cells showed that only the β3 subunit cytoplasmic tail was essential for integrins to bind to focal adhesions [111]. Studies were carried out to determine the exact cytoplasmic residues that were essential for proper location of β1 integrins to the

focal adhesions [112]. A series of mutant chicken β1 cytoplasmic tail constructs with a single or double non-conservative substitution of every residue was expressed in NIH3T3 fibroblasts and their ability to locate to focal adhesions was determined [112]. Mutations in nine specific residues resulted in a reduced ability to locate to focal adhesions and comparison of sequences revealed that eight out of the nine residues were highly conserved in human β1, β2, β3, β5, β6, and β7 subunits [112]. These studies highlight the importance of the β subunit cytoplasmic tail and its role in downstream signalling.

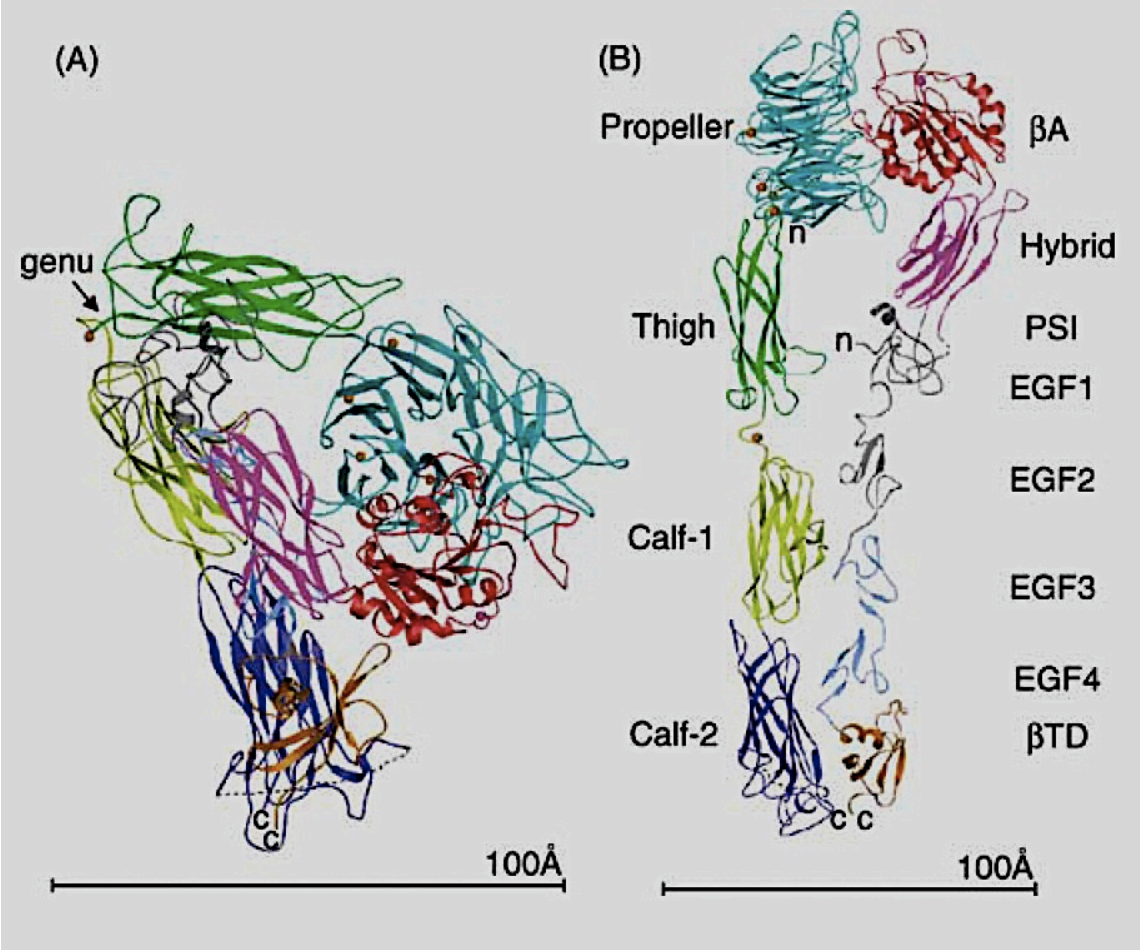

Figure 14: Schematic picture of x-ray crystal structure of αvβ3 integrin. (A) shows the inactive structure and (B) shows the active form. ***(Picture modified from Xiong, JP et al, 2001).***

The above figure shows the crystal structure of the αvβ3 extracellular region shown as a ribbon diagram (Figure 14) [109]. The inactive integrin is bent at a 'genu', or knee (arrow) in (A) compared with the active straightened model with the 12 domains individually labelled in (B). The αv subunit consists of a 7-bladed β-propeller, a 'thigh' domain and two 'calf' domains. The β3 subunit consists of a βA domain, a 'hybrid' domain, a PSI (for plexins, semaphorins and integrins) domain, four epidermal growth factor (EGF) domains and a β-tail domain (βTD). 'n' and 'c' represent N- and C-termini. Ligand binding occurs at the interface between the β-propeller (αv subunit) and the βA-domain (β3 subunit). It is believed that all integrins exhibit these stereochemical changes. As mentioned before, the cytoplasmic tail acts as a link between the ECM and the cytoplasm [113]. This is often referred to as "outside-in" signalling (to be discussed later). However, in some cases the cytoplasmic tail is able to regulate signalling proteins, which in turn have a functional effect on the behaviour of the cell. This is often referred to as "inside-out" signalling (to be discussed later). A classic example for "inside-out" signalling is the ability of the binding of the highly conserved KXGFFKR motif, in the cytoplasmic domain of the α subunit, to calreticulin (regulator of the calcium transmembrane channel influx) for stabilising the "active" conformation of the integrin which in turn is crucial for integrin-mediated cell adhesion [114, 115].

1.10.2 Ligand binding to integrins

One of the principal functions of integrins, as the name suggests, is to integrate the ECM with the intracellular cytoskeleton. This is turn initiates a variety of downstream signalling pathways which affect cell proliferation, survival, adhesion, migration [116]. Integrins normally recognise short peptide motifs in their target ligands. Arginine-Glycine-Aspartic Acid (RGD) tri-peptide was the first motif to be identified in fibronectin [117, 118]. Some integrins have the ability to recognise multiple ligands (Table 4) e.g. αvβ3 ligands include fibrinogen, laminin, thrombospondin, fibronectin, vitronectin and osteopontin. In some cases one ligand can be recognised by multiple integrins (e.g. fibronectin can be bound by αvβ1, αvβ3, αvβ6, α5β1, α4β1, α8β1) while others may be recognised by only one integrin (e.g. E-cadherin is recognised by αEβ7 [119]). Integrins also bind to cell surface ligands, thus all β2 integrins bind to immunoglobulin super family molecules including intracellular adhesion molecules (ICAM 1,2,3) [120]. Integrins also bind to some bacteria (bacterial invasin is an integrin ligand) and some viruses are internalised through binding of their cell surface

proteins to specific integrins (e.g. foot and mouth disease virus (FMDV) and coxsackie virus 9 (CAV) gain entry to cells that express αvβ6) [121]. Although some integrins recognise multiple ligands, their affinity for different ligands can vary widely. Thus the integrin αvβ6 can recognise fibronectin and the latency associated peptide (LAP) of TGFβ1 and 3 [122]. It was reported that binding to LAP was much stronger than binding to fibronectin [123]. Subsequent studies showed optimal ligands for αvβ6 have RGD at the tip of a hairpin bend in the protein followed by an adjacent α-helix. This helix forms a second binding site on the integrin, therefore increasing the affinity [124].

The α and β heterodimers cross the cell membrane with two short cytoplasmic domains. The extracellular domain of integrins binds to glycoproteins in the extracellular matrix (ECM) (through the short peptide motif e.g. RGD) and activate various downstream signalling processes (Figure 13). The signals generated can vary between different integrins, even when they bind to the same ligand e.g. both α5β1 and αvβ6 bind to fibronectin but only binding of αvβ6 to fibronectin induces squamous cell carcinomas to secrete MMP-9 [125]. The conformation of the ligand is important because that determines the exposure of its "integrin activation sequence". Based on the motifs recognised, integrins can be divided into two classes: those with an αA domain (e.g. α2), which recognises glutamic acid based motifs (e.g. the ASP-GLY-GLU-ALA (DGEA) tetrapeptide sequence is essential for the binding of α2β1 mediated adhesion to platelets [126]) and those without an αA domain (e.g. αvβ3), which recognise aspartic acid based motifs (e.g. GLY-ARG-ASP-SER-PRO (GRDSP) tetrapeptide sequence. In both cases, the motifs form a complex with a metal ion bound within the integrin, referred to as metal-ion dependent adhesion site, (MIDAS), and this is essential for ligand binding to integrins [107, 109, 121]. The responses of different cell lines from various lineages, both transformed and non-transformed, to the surrounding microenvironment can vary depending on the repertoire of integrin heterodimers expressed on their cell surfaces. Thus even within the same ECM, different cells may interact with different components of the substrate, thereby resulting in divergent biological responses.

As mentioned earlier, integrins can bind to different types of ligands present in the ECM. Table 4 below details some of the major extracellular ligands, which bind to integrins. The list also includes microorganisms, which use integrins to gain entry into the cell.

Ligand	Integrin
Adenovirus penton base protein	αvβ3, αvβ5
Bone sialoprotein	αvβ3, αvβ5
Borrelia burgdoferi	αIIβ3
Candida albicans	αMβ2
Collagens	α1β1, α2β1, α11β1, αIIbβ3
Denatured collagen	α5β1, αvβ3, αIIbβ3
Cytotactin/tenascin-C	α8β1, α9β1, αvβ3, αvβ6
Decrosin	αIIbβ3
Disintegrins	αvβ3, αIIbβ3
E Cadherin	αEβ7
Echovirus 1	α2β1
Epiligrin	α2β1
Factor X	αMβ2
Fibronectin	αvβ1, αvβ3, αvβ6, α4β1, α5β1, α8β1
Fibrinogen	α5β1, αMβ2, αvβ3, αxβ2, αIIbβ3
HIV Tat protein	αvβ3, αvβ5
iC3b	αMβ2, αxβ2
ICAM-1	αLβ2, αMβ2
ICAM-2,3,4,5	αLβ2
Invasin	α3β1, α4β1, α5β1, α6β1
Laminin	α1β1, α2β1, α3β1, α6β1, α7β1, α6β4, αvβ3
LAP-TGFβ 1, 3	αvβ6
MAdCAM-1	α4β7
Matrix metalloproteinase-2	αvβ3
Neutrophil inhibitory factor	αMβ2

Ligand	Integrin
Osteopontin	αvβ3
Plasminogen	αIIbβ3
Prothrombin	αvβ3, αIIbβ3
Sperm fertilin	α6β1
Thrombospondin	α3β1, αvβ3, αIIbβ3
VCAM-1	α4β1, α4β7
Vitronectin	αvβ1, αvβ3, αvβ5, αIIbβ3
von Willebrand factor	αvβ3, αIIbβ3

Table 4: ECM ligands and integrins to which they bind. ***Adapted from Plow, EF et. al, 2000.***

1.11 Signal transduction

Sometimes integrin activity needs to be regulated rapidly and this means there needs to be a rapid "on" "off" mechanism. E.g. αIIbβ3, expressed by platelets, has to be activated rapidly for blood clots to be formed during bleeding. αIIbβ3 recognises the H-H-L-G-G-G-A-K-Q-A-G-D-V sequence in the fibrinogen gamma chain leading to rapid platelet aggregation, which acts as a plug to prevent bleeding. In other cases, integrin signalling has to be turned off so that cells can detach (e.g. during mitosis or during physiological migration) [127]. Integrin signalling has to be extremely dynamic so that it can switch between the active and inactive states quickly. Integrins usually are in the inactive state and in this state they cannot bind to any ligands. The switch from an inactive to active form correlates with their ability to bind ligands and requires a conformational change in the integrin. The structural changes occurring were confirmed by electron microscopy in recombinant integrins treated with calcium (does not support ligand binding); treatment with this element showed more "bent structures" (inactive) whereas when treated with manganese (supports ligand binding), the integrins showed more "extended structures" (active) [128]. Ligand induced (antibody) binding site (LIBS) epitopes, which were first described in αIIbβ3 in response to ligand mimetic binding [129], are concealed epitopes exposed upon activation. Sometimes intracellular signals lead to these epitopes being exposed and

therefore they are also known as activation-dependent binding sites [128]. Several monoclonal antibodies have been characterised, which can identify and bind to these epitopes. They have been valuable in monitoring the activation of integrins during biological processes, e.g. addition of 12G10 monoclonal antibody to cells stimulated cell adhesion and spreading in an $\alpha 5\beta 1$ dependent manner [130].

Integrins are key regulators of many important cellular functions. They do this by transducing signals across the cell membrane subsequent to ligand binding. Integrins have the ability to transmit signals in both directions (bi-directional signalling). Expression of an integrin by a cell does not imply that it has a functional role. For example, αIIbβ3 is expressed by platelets but cannot bind to its ligands in the absence of platelet activators such as thrombin or collagen. If αIIbβ3 was activated at a site other than the site of tissue damage, it could lead to generalised thrombosis [131]. Therefore, regulation of integrin activation is essential for maintaining tissue homeostasis. *In vitro*, integrins can be activated using different techniques such as addition of an agonist to simulate a natural ligand [131], binding of specific antibodies to induce the "active" state, addition of manganese salts to cells [132] and also by addition of phorbol esters [133].

Once activated, integrins cluster at the cell membrane bringing them in close proximity to other integrins and signalling molecules that are associated with the cytoplasmic tail. This increased proximity allows signalling molecules to generate intracellular signals. This clustering of integrins with the cytoplasmic associated proteins occurs at adhesive structures called focal adhesions. Studies have shown that these integrin clusters specifically recruit talin and this is important for formation of focal adhesions, acting as a link between the integrin and actin cytoskeleton [134]. It has also been demonstrated that the interaction of phosphoinositol-4-5-biphosphate (PI4,5P2) with talin is crucial for clustering of integrins. PI4,5P2 reveals the integrin binding site on talin by inducing a conformational change upon its binding [135]. The focal adhesions help the cells to anchor to the surrounding ECM serving as an adhesion site and also help in the downstream signalling, which controls many cellular functions including cell spreading and cell movement (Figure 15). Normal cells, with the exception of leukocytes, require anchorage to a suitable matrix in order to survive and thus these cells are often called "anchorage dependent" [136]. Such cells usually undergo apoptosis when they do not have a suitable matrix to adhere to and this type of cell death is termed "anoikis" [137]. Integrins play a key role in controlling anchorage dependence. In many cancers, the transformed cells

overcome the integrin mediated cell death signals and continue to survive and proliferate. This is a characteristic feature of neoplastic transformation. Thus these adhesive interactions translate into cellular signals that result in processes such as proliferation, survival, migration or invasion [138].

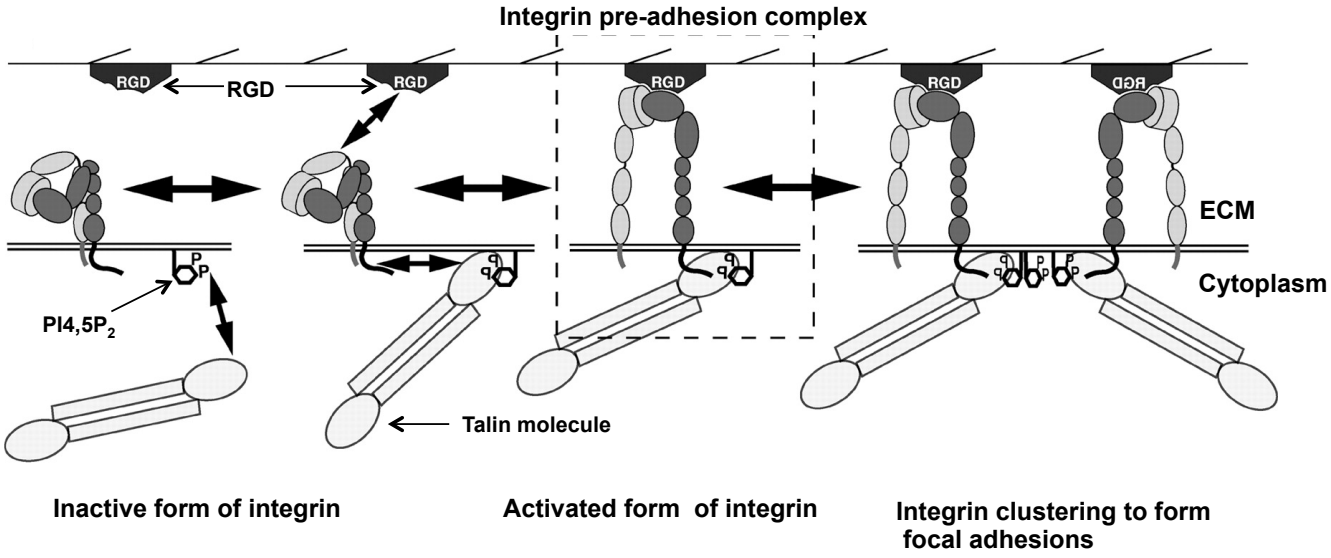

Figure 15: Schematic diagram showing integrin activation and clustering of integrins. $PI4,5P_2$ binds to talin and exposes the integrin binding site. Talin binds to the cytoplasmic tail of the integrin, thus activating it to form the pre-adhesion complex (inside-out signalling). Integrins can also bind to its ligands (RGD) in the ECM and become activated. The integrin-talin complex clusters together to form focal adhesions, which are essential for cellular functions [139].

1.11.1 Inside-out signalling of integrins

When a cell receives signals from other receptors, it can activate downstream signalling pathways. These signals can in turn interact with the cytoplasmic tail of the integrins and convert the integrin to its activated form. (e.g. c-Met binding to HGF can affect $\alpha 6\beta 4$ activity [140]). The structural changes that cause the integrin to be activated alter the way the integrin interacts with the ECM [141]. This activation is crucial to modulate the affinity of integrins towards the ECM and the cell can regulate integrin adhesiveness to its ligand (affinity modulation). Receptor clustering can also be controlled by intracellular signalling, where the cell can remodel its cytoskeletal integrin complexes or change its receptor diffusion rates, which can also regulate the ability of the integrins to bind to its ligand (avidity modulation) [142]. The adhesive ability of integrins to bind to the ECM is regulated by altering its affinity for its ligands

or its avidity (Figure 16). For example, R-RAS activation in cells can lead to increased affinity for binding to the ECM while H-RAS activation can have the opposite effect. Similarly, small GTP binding proteins Rac and Cdc42 can activate integrin clustering, thereby increasing integrin avidity [143]. Therefore, integrin activity is tightly regulated by affinity and avidity modulation through which cells control their ability to adhere, migrate or invade [144, 145].

Some studies in the past have shown that "inside-out" signalling is initiated by the disruption of the non-covalent clasp or "salt-bridge" between the membrane proximal regions of the α and β cytoplasmic tails [103]. Point mutations in these cytoplasmic tails, in either one of the α and β subunits, can lead to constitutive activation of the receptor [146]. Springer and colleagues used leukocyte specific $\alpha L\beta 2$ integrin to show that replacing the cytoplasmic transmembrane region between the tails inactivated the receptor, whereas breakage of the clasp activated the receptor [110]. The affinity and avidity modulation of integrins prevents excessive integrin-mediated signalling which, if left unchecked, could lead to profound pathological conditions. For example, constitutive activation of $\alpha IIb\beta 3$ integrins could lead to spontaneous clot formation and thrombosis. Therefore a rigorous regulation of integrin mediated signal transduction is essential for efficient functioning of the cell.

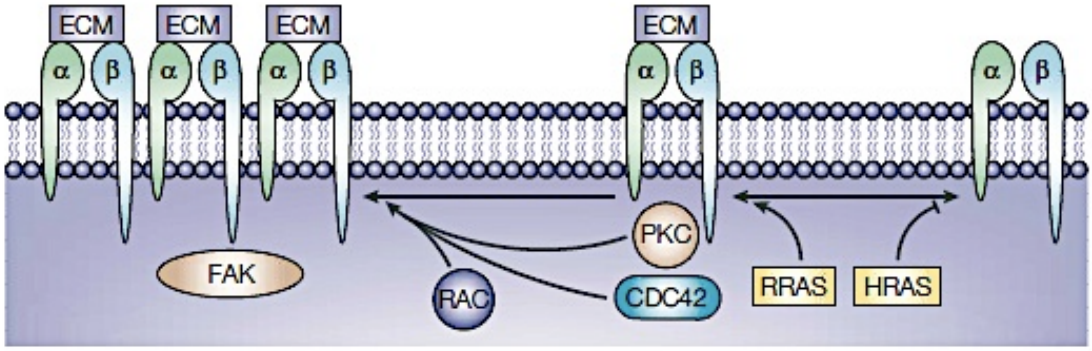

Figure 16: Schematic diagram of inside out signalling of integrins. Small GTP-binding proteins play an important role in the regulation of "inside-out" integrin signalling. There is an increase in integrin affinity for its ECM upon activation of RRAS and the converse holds true when HRAS is activated. Integrin avidity is increased as a result of enhanced clustering due to activation of RAC, CDC42 and protein kinase C (PKC), which play an important role in cell migration. ***Figure from Hood, JD et al, 2002 [143].***

1.11.2 Outside-in signalling of integrins

"Outside-in" signalling is considered to be a more 'classical' form of signal transduction and is initiated by ligand binding to the extracellular domain of the integrin (Figure 17). It can be divided into two broad categories – "direct signalling" and "collaborative signalling". When a ligand binds to an integrin resulting in clustering of integrins, and if this is the *only* extracellular stimulus, it is often referred to as direct signalling. This can activate multiple cytoplasmic tyrosine kinases including focal adhesion kinase (FAK), serine threonine kinases like mitogen activated protein kinase (MAPK), small GTPases and induce lipid metabolism [147]. When the downstream signalling pathways that are activated as a result of ligand binding to integrins are modulated by other signalling events initiated through other receptors such as receptor tyrosine kinase, it is termed as collaborative signalling [147]. For example, $\alpha 6\beta 4$ binding to laminin leads to an increased activation of human epidermal growth factor receptor 2 (HER2). Transformed epithelial cells, which express both $\alpha 6\beta 4$ and HER2, have a proliferative and invasive edge suggesting that there might be an interaction between $\alpha 6\beta 4$ and HER2 in carcinoma progression [148].

When integrins binds to a ligand in the ECM they usually activate FAK, allowing activated SRC to bind, which then phosphorylates several tyrosines on FAK. These act as docking sites for other signalling molecules. For example, growth factor receptor bound protein 2 (Grb2) can bind to Y925 tyrosine residue on FAK, recruit SOS-1 and thereby activate RAS [149]. When FAK is activated it can also promote Src-dependent phosphorylation of Shc, which in turn can drive Grb2 to activate RAS [150]. RAS can activate MEK, ERK and PI3 kinase, as a result of FAK being activated due to integrin binding to its ligand. PI3 kinase can activate Rac and activated Rac together with Cdc42 regulates numerous biochemical pathways including those regulating the actin cytoskeleton. Together with activated ERK, the signalling leads to changes in the transcriptional activity, which ultimately can lead to regulation of cellular behaviour including differentiation, survival, migration and invasion (Figure 17) [143].

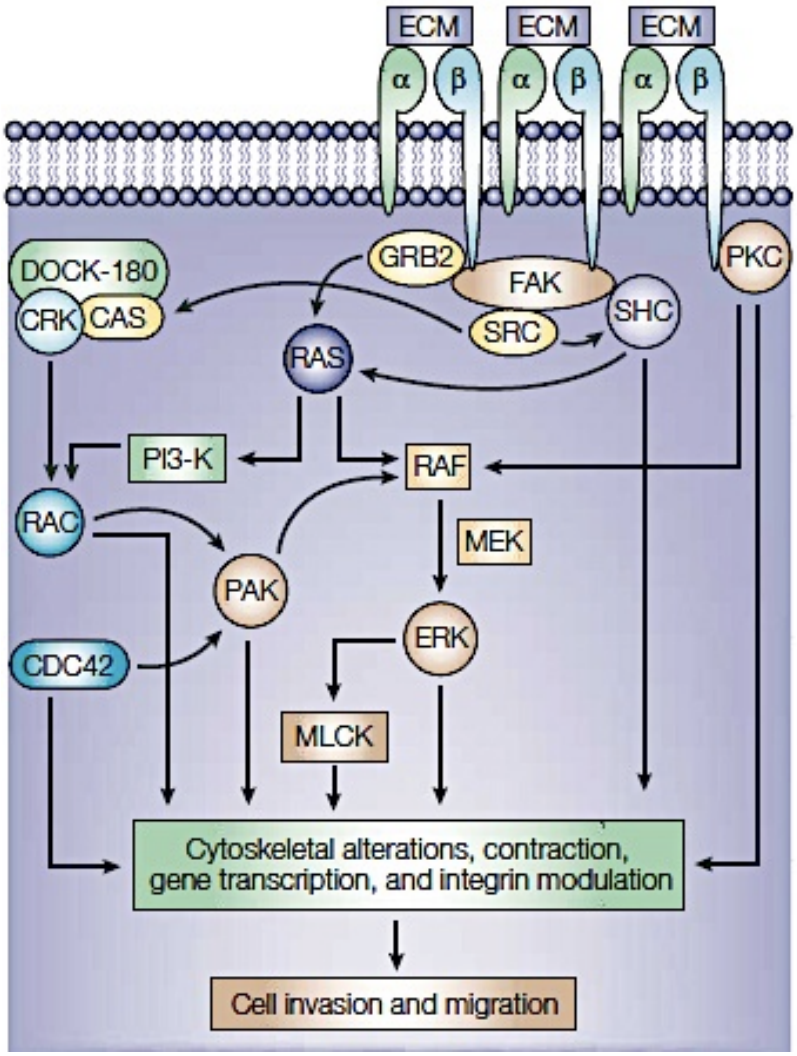

Figure 17: Schematic diagram showing outside-in integrin signalling in cells. When integrins bind to their ligand, it can phosphorylate FAK (activated), which in turn can activate growth factor receptor bound protein (GRB2). GRB2 can activate RAS. FAK can also activate RAS in a SRC dependent manner, which can then recruit mitogen activated protein kinase (MEK) and extracellular signal regulated kinase (ERK). Activation of ERK leads to transcriptional activity and also affects the myosin light chain kinase (MLCK) activity. RAS can also activate PI3K and RAF pathways. Activated SRC phosphorylates CRK associated substrate (CAS), which allows it to bind to CRK and dedicator of cytokines 180 (DOCK180). RAC can be activated as a consequence, which together with activated cdc42 can regulate various cellular functions. ***Picture from Hood, JD et al, 2002 [143].***

1.12 Integrins and cancer

Given that integrins bind cells to the ECM and can modulate cell growth, survival, migration and invasion, it would be expected that they are involved in cancer development and spread. Cancer cells often disseminate from their site of origin and move to a secondary location, a complex process known as metastasis. Thus the cells have to detach from their neighbouring cells and possibly the basement membrane, invade through a basement membrane, reorganise the ECM through which they migrate, often travel in the blood vessels or lymphatics, extravasate and proliferate once they reach the secondary site (Figure 18). For cancer cells to do this, the first step is to alter the expression or activity of their adhesion molecules, including their integrins that they express. For example, carcinoma cells reduce or lose expression of E-cadherin, thereby reducing cell-cell cohesion [151]. By up regulation of certain integrins binding to ECM ligands, cells can activate downstream signals, which will cause cancer cells to secrete proteases such as matrix metalloproteases (MMPs). For example, MMP9 secretion is up regulated by oral cancer cell ligation of the integrin $\alpha v\beta 6$ [125]. This can aid invasion through the basement membrane and the stroma.

Once cells have intravasated, they may bind to platelets via integrins [152]. This can help in their arrest in distant capillary beds and their survival. Some cancers express integrins that recognise endothelial cell markers. Thus melanomas express $\alpha 4\beta 1$, which can bind to vascular cell adhesion molecule 1 (VCAM-1) on activated endothelial cells [153]. Once the tumour cells have arrested they may grow in the capillary and eventually burst it or they may extravasate and invade into the new stroma. The integrin-mediated adhesion contributes to growth, signalling and survival of the metastatic cells.

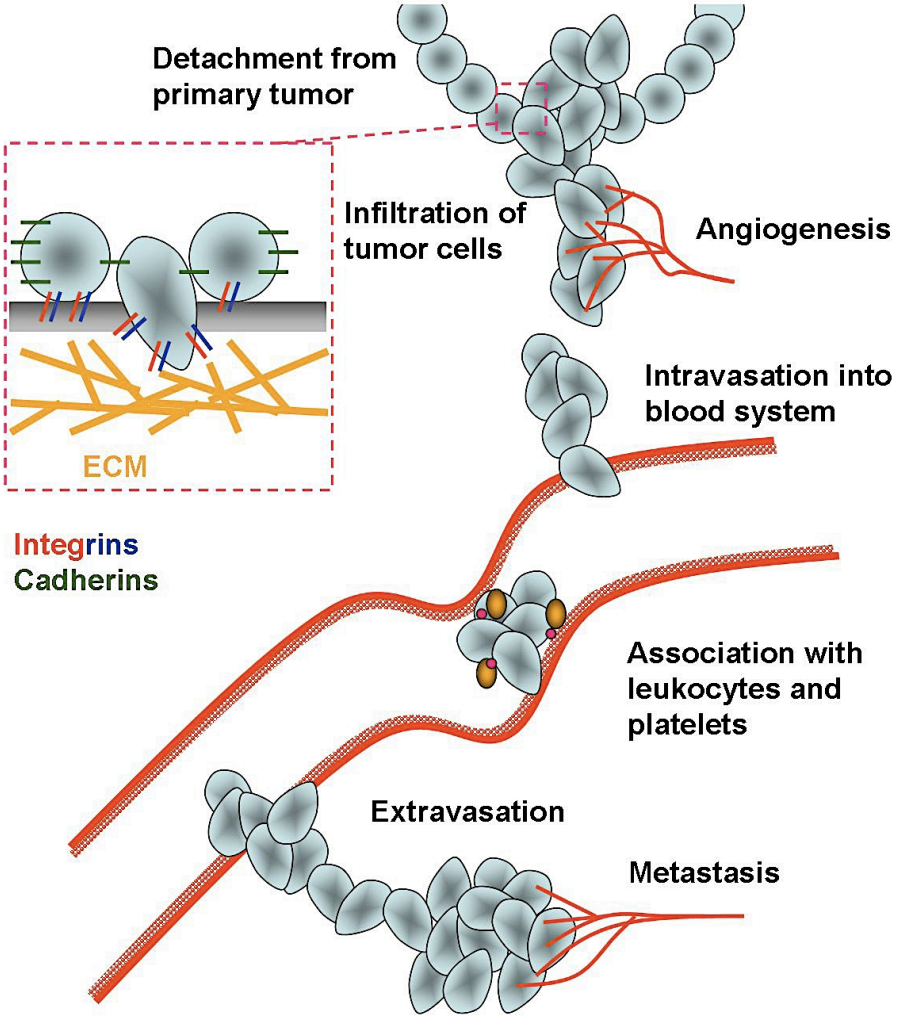

Figure 18: Metastasis of cancer cells from primary tumour to a secondary site. Integrins are involved in almost all the stages of metastasis from the detachment of the cells from the basement membrane in the primary tumour, migration/invasion of the cells through the surrounding stroma, intravasation into the vasculolymphatic system, association with leukocytes and platelets in the blood/lymph vessels, extravasation and invasion into the new ECM (secondary site). Thus integrins are crucial for the cells to be able to metastasise. *Picture taken from Michael, A and Bendas, G, 2011*.

1.12.1 Survival

Normal adherent cells are programmed to undergo anoikis, which is apoptosis caused by the absence of adhesion, in the absence of a suitable ECM to bind to. Anoikis is caspase-dependent and is tightly regulated by integrin-mediated interactions with the ECM. The first step in anoikis is the inactivation of FAK/Src signalling, leading to a “switching off” of the RAS/PI3kinase/ERK pathway, which

usually provides the cell with pro-survival signals [154]. Once anoikis sets in, there is disassembly of the focal adhesions, which destabilises the cytoskeleton, leading to the activation of Bim and Bax (pro-apoptotic factors) [154]. This is soon followed by activation of "pro-apoptotic" proteins including pro-caspase 8. This begins the caspase cascade resulting in activation of executioner caspases (caspase 3) that can lead to degradation of DNA [155].

Cancer cells have survival mechanisms to ensure they can continue to proliferate by evading anoikis [156]. Cancer cells are not dependent on adherence to the ECM for their survival. Thus cancer cells often have activating mutations in growth factor signalling pathways that remove the need for cooperative adhesion signalling from integrins. Sometimes this anchorage independence may be a result of the interactions between integrins and other receptor tyrosine kinases. For example, $\alpha 6\beta 4$ and c-Met are known to interact with each other in cancer cells to form a complex, shown by immunoprecipitation. Upon HGF stimulation, c-Met provides the additional signalling platform to activate FAK and RAS, regardless of the fact that $\alpha 6\beta 4$ was not binding to laminin [140]. This study showed that cancer cells have the ability to turn integrins from adhesive proteins to non-adhesive integrators with other receptor tyrosine kinases to promote oncogenic signalling and survival. It was also reported that the downregulation of $\alpha v\beta 5$, through upregulation of $\alpha v\beta 6$, might protect SCCs from anoikis by activating the AKT survival signalling pathway [157].

1.12.2 Proliferation

Various pathways and multiple environmental factors including interaction of the cell with the ECM regulate normal cell proliferation. Most normal cells are anchored to the ECM and this is critical for cell proliferation. Loss of adhesion usually leads to a G1 phase cell cycle arrest and cell death [158]. Cancer cells, in contrast, often proliferate at a rapid rate, as this is crucial for formation of tumours and their spread to a secondary site. This is dependent on the ability of the cancer cells to detach from the ECM and still be able to survive. Together with various growth factors, integrins use multiple cytoplasmic signalling pathways, which are highly interwoven into complex networks, to regulate cell proliferation (Figure 19). It has to be noted that integrin signalling occurs via defined points of focal contacts as opposed to stimulation of pathways through soluble factors, which affect the entire cell. Integrins bind to their ligands and can activate various receptor tyrosine kinases, which in turn activate the ERK signalling pathway at multiple points [159]. Integrins can also

activate Rac and Cdc42 both directly and indirectly thereby affecting cell proliferation [160]. Integrins can also activate the PI3 kinase pathway mediated via FAK and Cdc42 [161] and also aid in actin polymerisation and organisation. These generate tension/mechanical force, which contribute to G1 cell cycle phase progression [162]. Cyclin D1 regulation through the ERK pathway modulation by integrins is one of the methods by which integrins control cell proliferation [162].

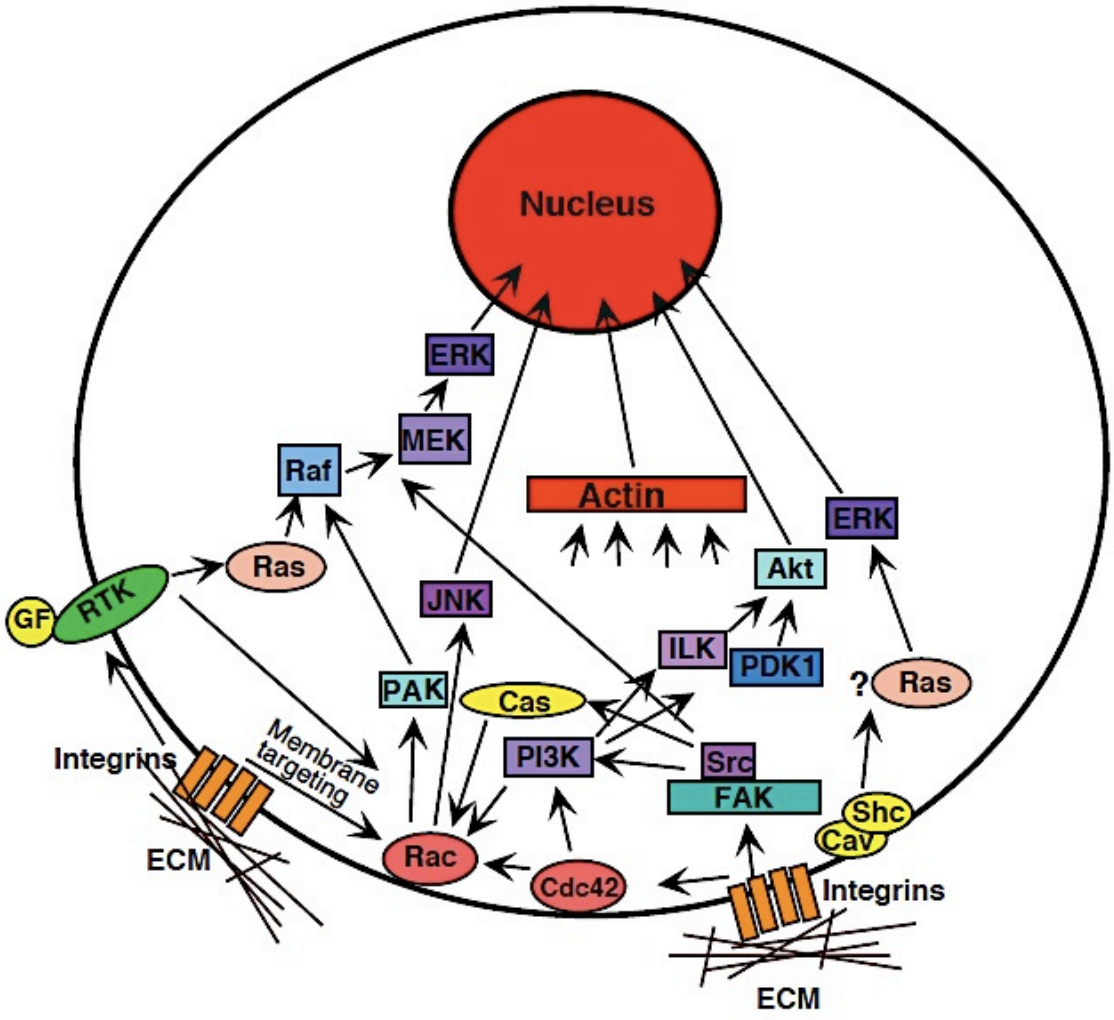

Figure 19: Role of integrins in regulating cell proliferation. Note: activation of the Raf/MEK/ERK pathways happens at the cell membrane. Shown in the cytoplasm to avoid overcrowding. Picture from Schwartz et al, 2001.

1.12.3 Migration

Migration involves the movement of cells along a gradient. In normal adults, cell migration is crucial for wound healing and maintaining immunity. However, uncontrolled migration can result in serious pathological situations like metastasis of cancer cells. Cell migration is a complex process, which occurs as a result of changes in the cytoskeleton, cell-substrate adhesion and ECM components. The Rho family of GTPases have been shown to play an important role in migration and there occurs a significant cross talk between the Rho family of GTPases and RAS. Integrins can activate RAS, which in turn can lead to the activation of Rho leading to the assembly of contractile actin myosin filaments (stress fibres) and associated focal adhesion complexes [163]. Rac, another member of the Rho family of proteins, also plays a role in the assembly of the actin filaments at the cell periphery, which aids in the formation of lamellipodia and membrane ruffles [163]. Filopodia (actin rich surface protrusions) formation has been shown to be induced by the activation of cdc42, also a member of the Rho GTPase family of proteins. Thus, the Rho family of proteins together with RAS activated by integrins plays an important role in cell migration.

Cell migration can essentially be divided into five distinct steps (Figure 20). Extension of the lamellipodia at the leading edge is often the initiating step, which is followed by formation of new focal adhesion complexes. Several integrins have been shown to play a key role at this step, e.g. $\alpha v\beta 3$ has been shown to be involved in migration and invasion of melanoma cells [164]. This is followed by secretion of proteolytic enzymes (MMPs), which modify the ECM and helps in the movement of cells through the ECM. The cell body contracts through the formation of the actin-myosin complexes (Rho-Rac-cdc42 activity) and moves forward towards a gradient (e.g. the surrounding ECM have proteins that are recognised by integrins and in turn favour migration) while the tail end of the cell is detached from the ECM, which has been shown to be regulated by a protease, calpain, which cleaves the focal complex proteins such as talin and the cytoplasmic tails of $\beta 1$ and $\beta 3$ integrins [165] [166].

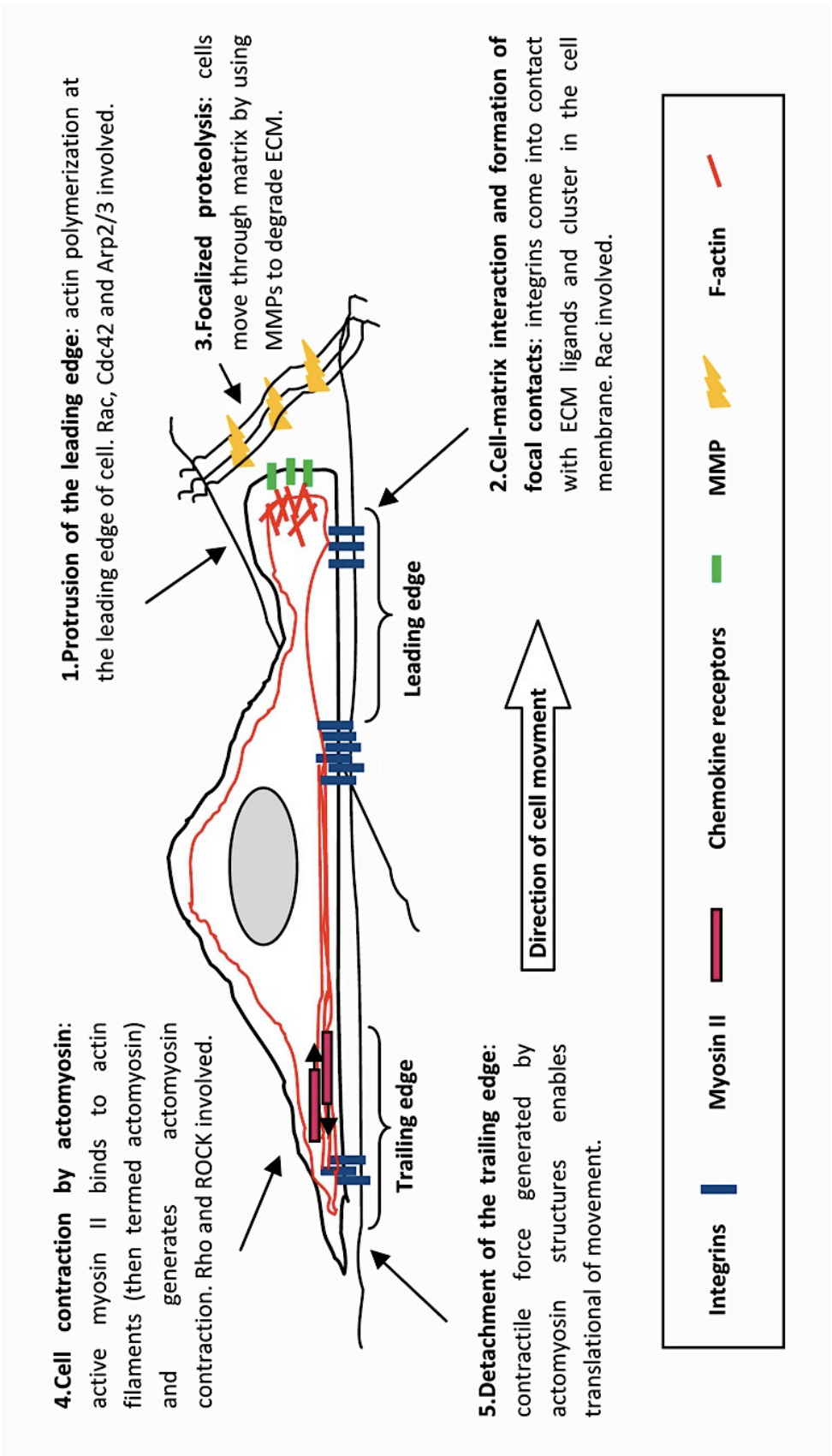

Figure 20: Schematic diagram showing cell migration. Picture modified from Parri, M et al, 2010 [166].

1.12.4 Invasion

Invasion is the migration of cells through a non cell-permeable barrier usually towards a gradient (ECM proteins, blood vessels). In order for (epithelial) cancer cells to invade, they have to detach from the primary tumour mass, breach the basement membrane and invade into the surrounding stroma (Figure 21). The basement membrane is impermeable to cells under normal physiological conditions and is composed predominantly of collagen type IV, laminins, fibronectin, nidogens and heparan sulphate proteoglycans [167]. Invasion is a multifaceted process, which involves the modulation of cell adhesion, survival and directed migration [168].

For cancer cells to invade and metastasise, they must dissolve the basement membrane, which is achieved by secretion of various proteolytic enzymes such as matrix metalloproteinases (MMPs). Type IV collagen, a predominant basement membrane protein, is a substrate for a variety of MMPs (-2, 3,7,9,12 and 19). Certain integrins have been shown to upregulate secretion or production of MMPs, in turn favouring cancer cell invasion. For example, $\alpha v\beta 6$-positive oral squamous cell carcinoma cells have been shown to invade in an MMP9-dependent manner [125]. The invasive potential of these cells is acquired through a series of changes to the intra and intercellular signalling pathways along with widespread remodelling of the ECM. Different cancers express different integrins and, in some cases, there are variations in integrin expression between subtypes of cells within the same tumour. Therefore, it is hard to judge the effect of an individual integrin because of the extreme complex nature and the sheer number of signalling pathways that are involved in cellular invasion. Looking at published data over the years, there are many studies which link a certain integrin to certain cancers. For example, $\alpha 2\beta 1$ has been linked to tumour progression and metastasis in melanoma [169], prostate [170] and gastric carcinoma [171] while the same integrin is expressed by normal breast epithelium and down regulated in breast cancer [172]. The fact that the same integrin is expressed by both normal and cancer cells shows that it has varied functions depending on the phenotype of the cell. It may have been downregulated during transformation of the breast epithelium because it supports a normal phenotype or inhibits cell growth but in transformed cells it plays an active role in tumour progression. There are several studies showing expression of a particular integrin correlating with cancer progression. For example, high expression of $\alpha v\beta 3$ in melanoma correlates with development of metastasis [173, 174].

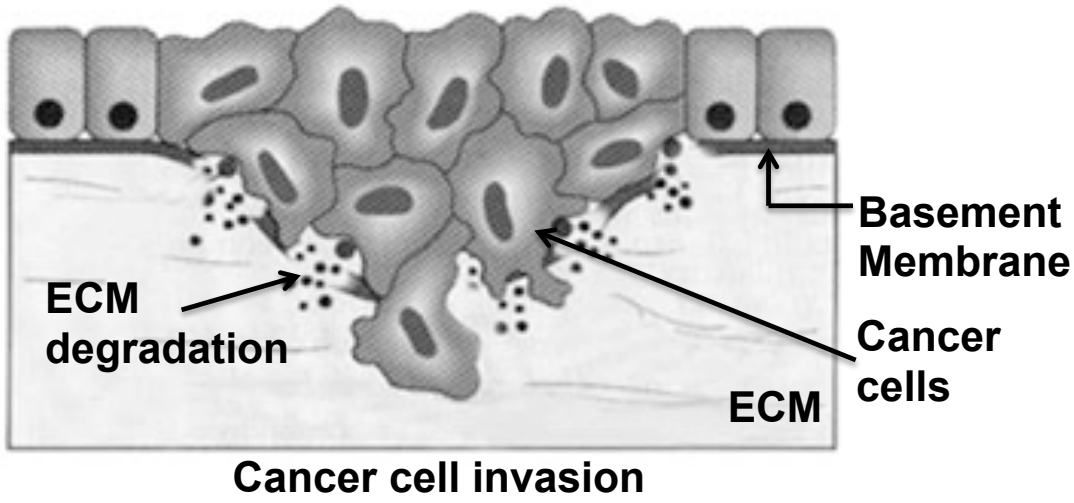

Figure 21: Schematic figure of cancer cells invading through the basement membrane into the surrounding ECM. Figure modified from Guo, W et al, 2004 [116].

1.13 Integrin αvβ6

Of the 24 different integrin heterodimers in humans, this study will focus on the epithelial specific integrin, αvβ6. This integrin is not constitutively expressed in healthy epithelia but is expressed *de novo* by many epithelia undergoing tissue remodelling processes such as wound healing, chronic inflammatory responses and carcinogenesis [175]. The αv subunit is coded at chromosome 2q31-q32. The β6 subunit dimerises only with the αv subunit as a heterodimer and is located at chromosome 2q24-q31. Under reducing conditions the β6 subunit migrates on SDS-PAGE gels at about 100-110kDa, whereas the αv subunit migrates at 130kDa [176]. As discussed later, the β6 subunit retains conserved domains that enable it to promote cytoplasmic signalling processes of αvβ6 [146, 177].

1.13.1 Transcriptional regulation of αvβ6

Not many studies have focused on transcriptional regulation of αvβ6. Ets-1 has been described as a transcription factor for the β6 gene ITGB6 and four potential Ets-1 binding sites were identified in the first 1kb of the β6 promoter in humans [173]. Gel shift assays and site-directed mutagenesis showed Ets-1 bound strongly to site one, out of the four sites identified (Figure 22).

αvβ6 is strongly expressed in wild type keratinocyte cells. Scott and colleagues showed that TNFα knock out mice had significantly lower expression of αvβ6 expression in keratinocytes, compared with the wild type mice [178]. They went on to show that addition of recombinant TNFα to the TNF knock out mice resulted in an up regulation of expression of αvβ6 in keratinocytes in a dose dependent manner. Bates et al also suggested that TGFβ works together with TNFα to up regulate expression of αvβ6 [173]. Both the above-mentioned cytokines are known to work via the Ets-1 transcription factor but this relationship with αvβ6 is yet to confirmed [125].

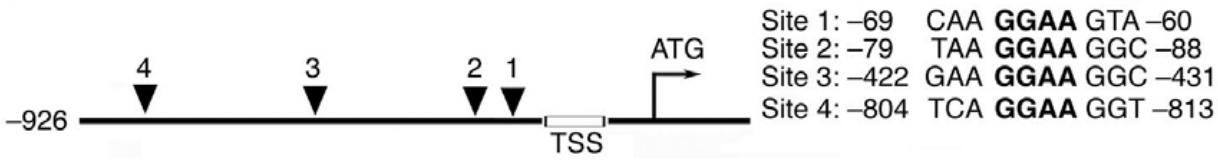

Figure 22: Schematic diagram for β6 promoter. TSS is the transcription start site and translation starts at the ATG site. Site 1-4 shows the potential Ets-1 binding site and its location. Consensus DNA binding sites, GGAA, are shown in bold. *Figure taken from Bates et al, 2005 [173].*

Another potential transcriptional regulator for β6 is STAT 3 [179]. Several STAT 3 binding sites have been discovered in the β6 promoter and these were confirmed using cross-linking immunoprecipitation assays [179]. The same authors also observed that increased expression of αvβ6 led to an increase in cell migration and anchorage-independent growth, characteristic features in cancer cells. It is also known that STAT 3 regulates expression of fibronectin and tenascin C, both of which are ligands of αvβ6 [179].

1.13.2 Ligands for αvβ6

The integrin αvβ6 is one of eight integrins that binds arginine-glycine-aspartic acid RGD motif in its target ligands. The principal ligand for αvβ6 is the pro-peptide of TGFβ-1 and TGFβ-3, called latency associated peptide (LAP). αvβ6 binds to the sequence RGDLXXI, found in LAP, but also to the closely related RGDLXXL found in the viral capsid proteins of FMDV and coxsackievirus A9 (CAV9) [51, 180]. αvβ6 also binds to fibronectin, vitronectin and tenascin-C [180]. The table below shows some of the main ligands for αvβ6 (Table 5).

Ligand	Type of protein
Fibronectin	ECM protein
Tenascin-C	ECM protein
Vitronectin	ECM protein
LAP of TGFβ-1	Cytokine
LAP of TGFβ-3	Cytokine
Foot and mouth disease virus (FMDV)	Viral capsid protein
Coxsackievirus 9 (CAV9)	Viral capsid protein

Table 5: Main ligands of αvβ6 and the type of protein

1.13.1 Sequence of the cytoplasmic tail of β6

Most integrin β subunits have three highly conserved cytoplasmic domains, cytodomains -1, -2, and -3 as shown in Figure 23. These conserved regions are involved in recruitment of integrins to focal adhesions and play an important role in integrin affinity [112]. In addition there is an unique eleven amino acid C-terminal extension (EKQKVDLSTDC) specific to β6.

Figure 23: Integrin β subunit homology in cytoplasmic tails

The cytoplasmic tail amino acid sequences of β1, β3, β6 subunits are compared using the single letter method for naming amino acids. The highly conserved (cytodomain 1, 2, 3) areas are highlighted in red and the unique C-terminal 11 amino acid extension for β6 is highlighted in green. This sequence has been reported as critical for several β6 dependent functions (Figure 23). The table below lists a few of them (Table 6).

Function	Cell type
Enhances cell proliferative capacity	Colon carcinoma
Promote PKC-dependent MMP 9 secretion	Colon carcinoma
Necessary for foot and mouth disease virus (FMDV) infection	Colon carcinoma
Essential for cell density dependent increase in beta 6 expression	Colon carcinoma
Required for decrease in urokinase receptor expression and function	Oral SCC
Required for promotion of invasion through up regulation of MMPs	Oral SCC

Table 6: Table showing reported functions of the β6 C terminal 11 amino acid tail.

1.13.2 αvβ6 signalling

There are very few studies detailing the signalling pathways associated with ligation of the αvβ6 integrin. As with many other integrin studies, recent investigations on interaction of αvβ6 with other proteins have begun to shed more light on its effects on cellular functions. As discussed below, ERK-2 and Fyn are the only two 'classical' signalling molecules, which have been shown to bind directly to αvβ6 and, as a consequence, evoke a functional response down stream.

1.13.2.1 Extracellular signal related kinases (ERK)

A sub-family of mitogen activated proteins (MAPs), called ERKs are activated by phosphorylation of their tyrosine and threonine residues through signalling cascades originating from the plasma membrane [181, 182]. ERK 1 (p44) and ERK 2 (p42) are the most widely studied members of this sub-family of MAP kinases. Ahmed and colleagues performed an in vitro assay in colon carcinoma cells, where they observed an interaction between the last 130 amino acids of ERK2 (generated from a clone) and the β6 cytoplasmic domain (presented as a biotinylated peptide) using co-immunoprecipitation from soluble lysates. They also showed that deletion of the ERK 2 binding site (RSKAKWQTGTNPLYR) on the cytoplasmic tail of the β6 subunit reduced proliferation of cells compared to the control cells, suggesting that there might be a direct interaction between these two molecules. Moreover p42/p44 signalling has been shown to be upregulated in cells expressing high levels of αvβ6 [181, 183]. These authors also showed that binding of ERK 2 to the β6 subunit increased MMP 9 secretion, which is a proteolytic enzyme thought to be necessary for tumour progression [183]. This pathway can thus regulate the malignant potential of cancer cells and appears to require the direct binding of ERK 2 to the cytoplasmic domain of β6 (Figure 24).

1.13.2.2 Src family kinase, Fyn

Integrins have been shown to interact with, and initiate signal transduction through, tyrosine kinase phosphorylation including members of the Src family kinases (SFKs) [184]. The cytoplasmic tail of the β6 subunit has been shown to interact directly with a member of the Src family kinase protein, Fyn, which becomes activated upon integrin ligation [185, 186]. Studying oral carcinoma cells, Li and colleagues performed in vitro kinase assays, which showed that ligation of β6 to fibronectin,

recruited Fyn and this activation was absent when an irrelevant substrate (i.e. substrate not recognised by β6) was used or when β6 was blocked using function blocking antibodies. They went on to show that the Fyn-β6 complex induced FAK phosphorylation which, in turn, was recognised by various FAK associated proteins. Activation of Fyn by β6 is also required for activation of another adaptor protein, Shc, which in turn activated the ERK/MAPK pathway (Figure 24) [185, 186].

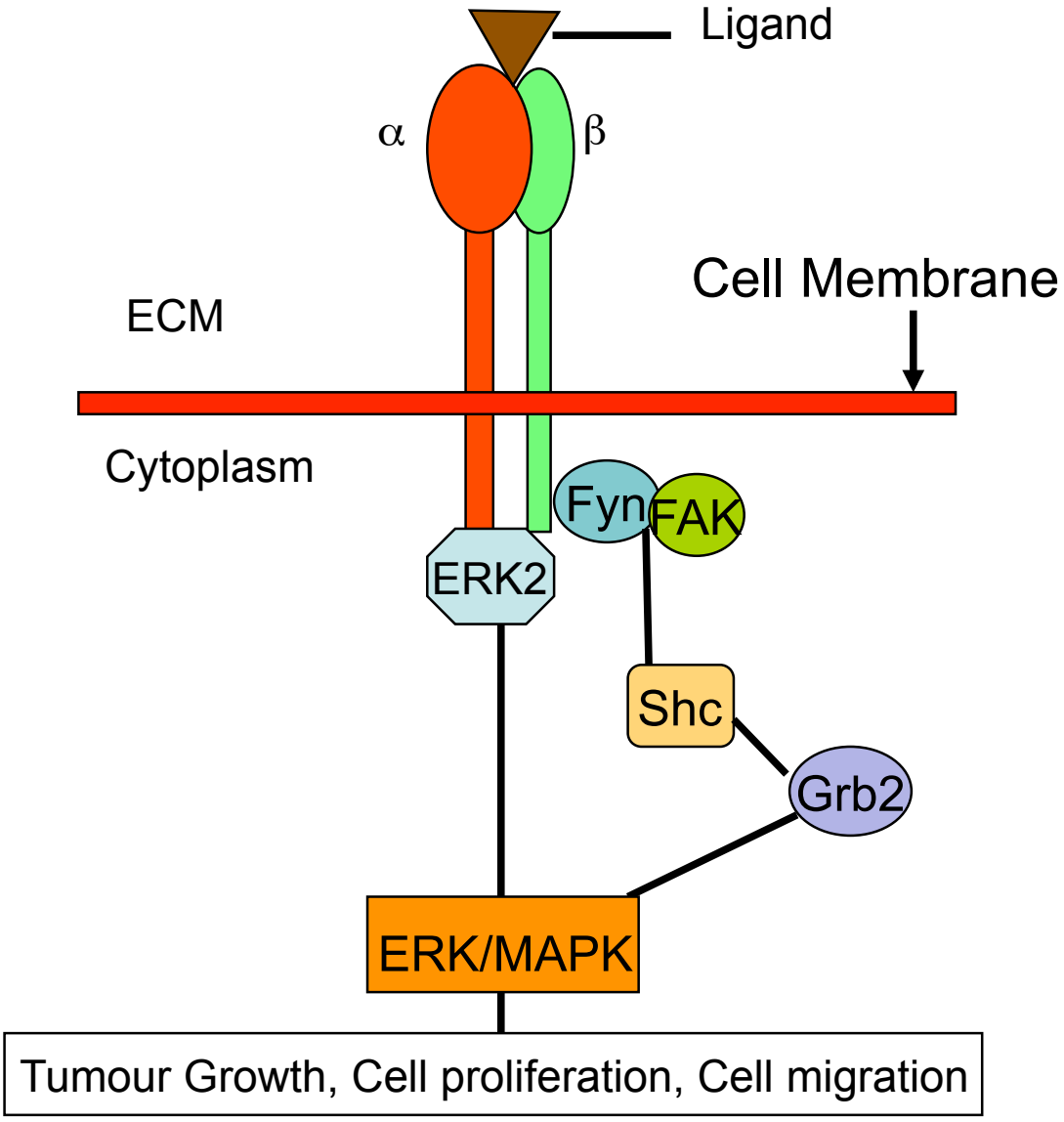

Figure 24: Schematic figure of known αvβ6 signalling pathways.

1.13.2.3 TGFβ activation and role of αvβ6

Transforming Growth Factor β belongs to a family of cytokines that regulate cellular behaviour, migration, proliferation as well as gene expression [53]. It has 3 isoforms in mammalian cells, TGF-β1, 2, 3, each encoded by distinct genes. TGF-β is expressed in the inactive pro-peptide form covalently linked with the corresponding LAP at the N-terminus from which it has to be cleaved or exposed to become biologically active. This acts as a safeguard against inadvertent activation of TGFβ, which is anchored to the ECM, where it is sequestered. Thus, the matrix acts as a reservoir from which TGF-β can rapidly be recruited. TGFβ is often referred to as the "double edged cytokine" in cancer. It has been shown to be a tumour suppressor in the early stages of cancer by suppressing cell growth [187]. However in late stages of cancer, biochemical and genetic changes alter the TGFβ signalling pathway, which promotes cell growth, thus making it a tumour promoter. TGFβ is secreted at elevated levels by cancer cells and this has been shown to activate the surrounding stromal cells, which in turn can upregulate factors that favour tumour progression [188].

Several integrins are reported to bind to LAP through recognition of the RGD motif. αvβ6 is rapidly upregulated by injury (wound healing) or inflammation [175]. While β6 knock out mice do not develop lung fibrosis, despite exaggerated lung inflammation caused by bleomycin treatment [189]. The study went on to show that αvβ6 was a ligand for TGFβ1 and, by knocking out β6 in mice, there was a localised deficiency of active TGFβ1 leading to the lack of fibrosis. They also reported that conformational changes in LAP, caused due to the binding of αvβ6, led to activation of TGFβ rather than the cleavage of LAP peptide. Colon carcinoma cell lines with a mutated β6 cytoplasmic tail were able to bind to LAP but could not interact with the actin cytoskeleton, hence transfected cells lost the ability to activate TGF-β [190]. TGF-β 1 and 3 have LAP peptides, which contain an RGD sequence, whereas TGFβ 2 does not and hence cannot be activated by αvβ6. Since activated TGFβ has a growth inhibitory effect on epithelial cells, it may seem confusing as to how αvβ6, which can activate TGF-β, can promote tumourigenesis [191]. However, studies have revealed the complex biphasic role of TGF-β in tumour biology.

Even though there is a general consensus amongst scientists that TGFβ is a tumour suppressor in early stages of cancer and a tumour promoter in late stages of cancer,

there are no verified biomarkers to accurately define when a tumour has “switched” from seeing TGFβ as a tumour suppressor to a tumour promoter. This makes it a challenge to target TGFβ therapeutically. Often cancers acquire TGFβ pathway mutations as they progress; perhaps the best known is the loss of SMAD4 (deleted in pancreatic cancer, locus 4) (DPC4) in pancreatic cancer, where over 50% of late stage PDAC patients acquire SMAD4 mutations [52]. In early tumourigenesis of breast cancer, TGFβ is capable of inhibiting cell cycle progression via G1- arrest. The anti-proliferative effects are mediated by suppression of c-Myc through mobilisation of cyclin dependent kinase inhibitors p15, p21, p27 [192].

In contrast, TGFβ is known to induce epithelial to mesenchymal transition (EMT), a process believed to be the transitional stage of non-invasive to invasive cancer [193] and is known to facilitate tumour growth indirectly by modifying the tumour microenvironment [53]. Tumour cells up regulate TGFβ secretion and this in turn can activate fibroblasts into myofibroblasts (cancer associated fibroblasts), which modify the ECM, alter angiogenesis and promote tumour growth [194, 195]. In an ongoing study of 355 patients with pancreatic cancer, either with locally advanced or metastatic disease, there was a significant correlation between levels of TGFβ in the plasma and overall survival. Overall survival of patients with high levels of TGFβ in the plasma (>19.05ng/ml) was 27.7 weeks versus 40 weeks for patients with low levels of TGFβ in the plasma (Milind JM et al, 2012, data not yet published. Data presented at ASCO 2012, poster 201). αvβ6 was found to be expressed more at the invasive front in oral squamous cell carcinomas (OSCCs) consistent with the likelihood that β6 binds to LAP of TGF-β, frees it for modulating the microenvironment, thereby promoting tumour growth [196, 197]. With its broad range of biological activities the TGF-β signalling pathway has become one of the major therapeutic targets as a strategy towards controlling cancer. Unfortunately small molecule inhibitors of TGF-β receptor I resulted in high toxicity, including increased risk of colon cancer [173]. However local blockade of TGFβ activation by blocking αvβ6 may be a therapeutically viable scenario to treat advanced cancers to negate the pro-tumourigenic effects caused by TGFβ.

1.13.3 Role of αvβ6 in wound healing

β6 mRNA is detected in human keratinocytes at the wound edge at an early stage of wound healing [175]. Detection of αvβ6 at a protein level occurs at a later stage, usually when epithelial integrity has been restored [198]. There is also a correlation of αvβ6 expression and TN-C expression leading to the suggestion that the principal functions of αvβ6 in wound healing are modulated through its interaction with this particular matrix protein [199]. α9β1 is also a ligand for TN-C and is known to induce proliferation in cells plated on TN-C. α9β1 is upregulated during early wound healing and is downregulated in the later stages, which coincides with the increased expression of αvβ6. Haapasalmi et al, 1996 suggested that the principal role of αvβ6 is not related to the initial cell migration but is more critical after the initial movement of wound keratinocytes has occurred [198, 199]. This switch between integrin expression during different stages of tumour progression has been described previously in cancers. For example, there is a reciprocal expression of αvβ5 (expressed in stratified squamous epithelia but down regulated in SCC) and αvβ6 (expressed in SCC but not in normal epithelia).

1.13.4 Expression of αvβ6 in carcinomas

Carcinogenesis has been considered a deregulated form of wound healing as both phenomena have many biological processes in common [200]. αvβ6 overexpression was first described in OSCCs but since then this integrin has been shown to be up regulated in various carcinomas including colon, stomach, lung, breast and ovary [175, 181, 190, 201, 202]. αvβ6 protein is not expressed in normal adult tissue barring very low expression in the basal layer of the hair follicle in skin and the base of the crypt in the small gut [201]. Figure 25 shows the expression of αvβ6 in carcinomas and its absence in the corresponding normal tissue.

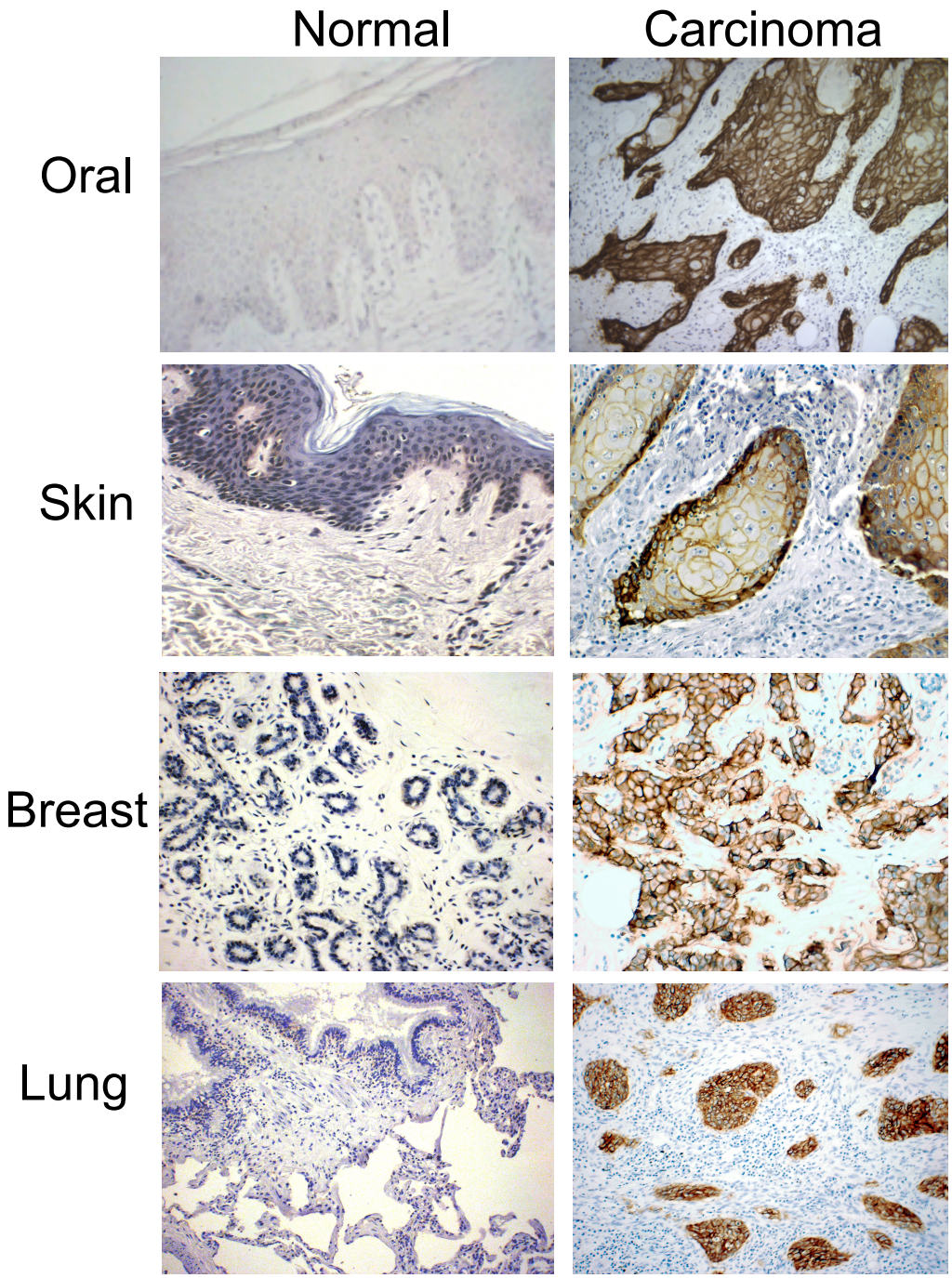

Figure 25: Expression of β6 in carcinomas. The normal tissue on the left is completely negative while the brown membranous staining on cancer tissue indicates strong up regulation of αvβ6. *Figures courtesy of Dr. John Marshall, Barts Cancer Institute, Queen Mary University of London.*

αvβ6 expression was often found to be localised to the tumour-stroma interface or the invasive front [203]. It should be noted that, in the studies above, αvβ6 expression was not detected or was very weak in the corresponding normal tissues. In oral leukoplakia patients, expression of αvβ6 meant that the progression to malignant disease had occurred, suggesting that αvβ6 expression may be useful in predicting malignant transformation of cells [201]. However about 85% of specimens of lichen planus (a mucocutaneous disease associated with a low risk of malignant change) also expressed αvβ6 suggesting that the mere expression of the integrin is not enough to drive malignant progression in some diseases [201].

Since the initial observation in OSCCs, numerous studies of different carcinomas have correlated poor prognosis with αvβ6 expression. Elayadi et al, 2007 showed that 54% of lung cancer patients significantly up regulated expression of αvβ6 in the lung epithelium out of the 311 lung cancer patients in the study. They went on to show that αvβ6 can be used a prognostic marker for non small cell lung cancer (NSCLC) with the high expressers showing lower survival rates [204]. Similarly, Hazelbag et al, 2007 reported high to moderate expression of αvβ6 in 58% of cervical cancer patients out of a total of 85 patients studied. The authors reported that patients negative for αvβ6 had a 91% 5 year survival compared with 76% for moderate expressers and dropping to 54% in the strong expressers of αvβ6. In ovarian cancer, higher levels of αvβ6 have been correlated with progression of tumour grade [181] and in gastric cancer, it has been shown to correlate with lymph node metastasis [205]. Bates et al, 2005 showed that expression of αvβ6 correlated inversely with patient survival. Median survival of colorectal cancer patients with nil or very low expression of αvβ6 was up to 16.5 years compared with 5 years for high expressers of αvβ6 [173]. These data confirm that the persistent presence of αvβ6 expression is linked strongly with the prognostic outcome for many types of cancer.

Carcinoma	Reference	No: of carcinomas	% positive tumours	Evidence	Comment
Oral Squamous Cell carcinoma	Breuss et al, 1995 (175)	30	90	ISH	Normal tissue negative
	Jones et al, 1997 (202)	17	100	IHC	
	Hamidi et al, 2000 (286)	5	80	IHC	41% expression in oral leukoplakia
	Impola et al, 2004 (288)	11	100	ISH	Expression maintained in lymph mets
	Regezi et al, 2002 (202)	40	100	IHC	Colocalised with TN-C
Colon	Bates et al, 2005 (173)	488	37	IHC	Poor prognostic marker
Pancreas	Sipos et al, 2004 (201)	34	100	IHC	Well differentiated tumours expressed more than poorly differentiated tumours
Gastric	Kawashima et al, 2003 (205)	38	47	IHC, RT-PCR	94% of positive carcinomas had LN mets
NSCLC	Smythe et al, 1995 (290)	51	50	IHC	Good prognostic marker?
Breast	Arihiro et al, 2000 (291)	90	18	IHC, WB	No grade 1 tumours beta 6 positive
Ovary	Ahmed et al, 2002 (181)	45	100	IHC	Staining correlated with grade, benign mucinous tumours are also positive
NSLC	Elayadi et al, 2007 (204)	311	54	IHC	Poor prognostic marker

Table 7: Published data for expression of αvβ6 in carcinomas. ISH – In situ hybridisation; TN-C – Tenascin-C; LN-met – lymph node metastasis; NSCLC – non small cell lung carcinoma, IHC – immunohistochemistry; WB- western blotting; RT-PCR – Real time PCR.

1.13.1 Role of αvβ6 in tumour progression

Expression of integrins by cancer cells often differs compared with their non-transformed normal counterparts. Several integrins are reported as down regulated in neoplastic tissues. For example, αvβ5 expression is reduced in melanoma [164] and oral SCC, whereas α2β1 and α3β1 are reduced in colon and breast cancer [206]. In contrast, αvβ3 is upregulated in melanoma and glioblastoma and αvβ6 is up regulated in many carcinomas (Table 7). It is perhaps worth noting that in general the down-regulated integrins are associated with more static behaviour, whereas the upregulated integrins, e.g. αvβ3 and αvβ6, are associated with proliferation, migration and invasion.

1.13.1.1 Role of αvβ6 in proliferation and survival

Very little is known about the role of αvβ6 in modulation of cell proliferation. One study has shown that αvβ6 enhances proliferative capacity of tumour cells. Thus, SW480, an αvβ6-negative colon carcinoma cell line, when transfected with the gene for wild type β6 showed a remarkable increase in proliferation in 3D culture compared with identical cells transfected with a control plasmid [190]. These authors went on to show that the proliferative enhancement specifically was due to the presence of the unique 11 amino acid sequence of the β6 cytoplasmic tail. More recently, another group identified β6 as part of a "gene signature" in lung and pancreatic cancer cells that are dependent on mutant *KRAS* for their survival [207]. They have shown that depleting β6 in these "*KRAS* dependent" cell lines leads to apoptosis proving that β6 is crucial for cell survival in certain cancer cell types [207]. In this latter study, results clearly highlight the role of αvβ6 in pancreatic cancer cell proliferation and survival (to be discussed later). This makes β6 a prime therapeutic target in cancers.

1.13.1.2 Role of αvβ6 in migration

Since αvβ6 binds to both fibronectin and vitronectin, it makes it a key player in cellular migration. Huang et al showed that β6 knock out keratinocytes migrated less readily compared to the wild type keratinocytes [208]. Transwell® migration assays performed to study haptotactic migration of oral squamous cell carcinoma cell lines showed that αvβ6 promoted migration towards fibronectin [209]. Both groups

performed proliferation assays in addition to migration assays to confirm that the difference in cell numbers observed were a true reflection of the influence of αvβ6 on cellular migration. There is also a study which reported that αvβ6 mediated Fyn activation correlated with increased migration [185].

1.13.1.3 Role of αvβ6 in invasion

Transwell® invasion assays were used to study a panel of oral squamous cell carcinoma cell lines, which express varying levels of αvβ6 [209]. Their results showed that, the higher the levels of αvβ6, the higher the levels of invasion through Matrigel™. These authors confirmed the specificity of the role of αvβ6 by using specific blocking antibodies to block the function of αvβ6 and showed a reduction in invasion compared with a control antibody [209]. In a separate study, the same authors demonstrated that malignant keratinocytes with high expression of αvβ6 up regulated secretion of type IV collagenases (pro-MMP-9 and pro-MMP-2), shown by zymographic examination [210]. They went on to show that blocking αvβ6 or αv alone significantly decreased MMP-9 activity and cell invasion. Li et al, showed that activation of the Fyn-FAK complex through αvβ6 leads to the activation of Shc and the Raf-ERK/MAPK pathways which, in turn, promoted the transcriptional activation of the *MMP-3* gene leading to increased *in vitro* proliferation of OSCC cells and increased metastasis in animal models [185]. These data, together with other published literature linking αvβ6 expression in various solid cancers to poor prognosis and dismal survival rates, suggest strongly that αvβ6 is a major driver of tumour progression.

1.14 αvβ6 in pancreatic ductal adenocarcinoma

The last decade has seen a handful of publications linking αvβ6 and pancreatic cancer. As mentioned earlier, many solid cancers express αvβ6 including PDACs. In the initial study showing αvβ6 expression in PDACs, all 34 of the PDAC cases stained for αvβ6 expression were strongly positive [201]. The authors of this study also observed that αvβ6 was expressed at higher levels in the well differentiated tumours compared to the poorly differentiated tumours. They went on to check for some of the major known ligands of αvβ6, fibronectin and tenascin-c, in the small number of PDAC cases and found no correlation between their presence in the ECM and αvβ6 expression [201]. Their findings indicated that αvβ6 positive PDAC cell

lines tend to form spheroids when cultured *in vitro*. *KRAS* is a frequently mutated oncogene occurring in about 20% of solid cancers. Most pancreatic adenocarcinomas have a mutant *KRAS* and it is a very potent tumour initiator [207]. Most of the pancreatic adenocarcinoma cell lines harbour *KRAS* mutations, the most frequent being a single nucleotide mutation at codon 12. Singh et al, 2009, established a "gene expression signature" in a panel of PDAC cell lines by dividing them into two groups based on their requirement for activated *KRAS* for cell growth *in vitro*. Gene microarray studies revealed a sub set of genes, which included *Syk*, *RON-β*, *MST1R* and integrin β6 (*ITGB6*) subunit, which were also required by cell lines dependent on activated *KRAS* for cell viability. These authors went on to show that β6 is strongly associated with a well differentiated *KRAS* driven phenotype [207]. Efforts to develop drugs to target *KRAS* have been challenging due to the difficulty in targeting a specific down stream RAS GTPase but these signature genes, including β6, could have implications as a potential therapeutic targets in pharmacologically intractable cancers like PDACs. PDACs tend to have a very high desmoplastic response compared to other cancers. In some cases, almost 70%-80% of the tumour is comprised of stroma. Since chronic expression of αvβ6 leads to chronic activation of TGFβ and thus fibrosis in lung [189] and kidney [211], it is likely that αvβ6 contributes to the desmoplasia seen in PDAC.

Very recently published data using a transgenic mouse model for PDAC show that targeting TGFβ using a blocking antibody led to an increase in tumour growth. The authors also targeted αvβ6, using a αvβ6 blocking antibody, and found that it too induced tumour progression [212]. These data may highlight that TGFβ may suppress early pancreatic cancer growth. It should be noted that the murine model used in the above mentioned study are *Kras-p53*$^{Lox+}$ (mutant *Kras* and *p53* knockout) with homozygous deletion of *Smad4* and these animals give rise to tumours from cystic precursors as opposed to tumours formed by progressing through PanINs [213]. These mice form fairly large pancreatic tumours at approximately 10 weeks, which is when most of their antibody treated animals were terminated. As mentioned, the mice were p53 null, whereas human PDAC has mutant p53. It has been shown that accumulation of mutant p53 can help overcome growth senescence and drive metastasis in another mouse model for PDAC [49]. This study highlights the extremely complex nature of the TGFβ signalling pathway and αvβ6 in PDAC progression.

1.15 Current treatment options available to PDAC patients

Treatment options for PDAC patients depend on multiple factors including stage and extent of disease (mainly two factors: distant spread, involvement of local vessels such as portal/mesenteric vein and/or celiac/superior mesenteric artery) and also the general fitness of the patient. The only potentially curable option available to patients is surgical resection of the pancreas, which is available for only about 20% of the individuals who present with the disease [7]. There are different surgical options available to these patients who can undergo surgery. The "Kausch-Whipple procedure", also known as the proximal pancreaticoduodenectomy with antrectomy, or the "Traverso-Longmire procedure" also known as the pylorus-preserving pancreaticoduodenectomy, are the most common surgical procedures used to remove tumours from the head of the pancreas, which may improve the quality of life of the patient and help increase the survival rate [214]. For tumours that arise in the body or the tail of the pancreas, a left pancreatectomy combined with a splenectomy might be appropriate [215]. Chemotherapy and radiotherapy can be used as a palliative treatment as well as in the adjuvant setting after surgical resection. Surgery can also be used for palliation, usually when endoscopic and percutaneous methods are unsuccessful in relieving biliary and/or duodenal obstruction.

Gemcitabine-based chemotherapy is the current standard treatment option available to patients with locally advanced unresectable disease or those with metastasis. This has been shown to increase overall survival rate and quality of life of patients [216]. Chemoradiation and 5-fluorouracil-based chemotherapy maybe useful in some instances. Some patients who respond well to the above combination of drugs may also be treated with a gemcitabine combination and a platinum analogue chemotherapeutic drug like oxaliplatin or cisplatin [217]. Recent data suggest that FOLFIRINOX based chemotherapy [218] as well as nab-paclitaxel chemotherapy (von Hoff, GI ASCO 2013) may give survival advantage over gemcitabine alone therapy.

For patients with metastatic disease, who account for 50%-55% of cases, there are very limited treatment possibilities and often palliation is the only option available. These patients have a very short survival rate, ranging from three to six months, depending on the tumour burden and performance status at the time of presentation [22]. Inserting a stent or a surgical bypass in the bile duct relieves any gastric obstruction and these individuals who are operated upon usually receive gemcitabine

monotherapy. If patients respond to this, they are given a combination of gemcitabine and cisplatin or oxaliplatin. Co-therapy with the EGFR inhibitor, erlotinib has been shown to improve survival rates marginally compared with gemcitabine alone [219].

1.16 Potential novel therapies

The treatment options available to pancreatic cancer patients have not shown significant improvement over the last forty years. The last major change in treatment of pancreatic cancer was in 1997, when gemcitabine in combination with fluorouracil was introduced and this regimen marginally increased survival rates and reduced associated side effects such as weight loss and pain reduction in patients who presented with advanced disease [220]. Poor prognosis of PDAC means any clinical trials where new agents are used to target the cancer, either on their own or in combination with gemcitabine, bring about only a modest improvement in survival. However, very recent data using a combination drug regimen consisting of oxaliplatin, irinotecan, fluorouracil and leucovorin (FOLFIRINOX) used in combination with gemcitabine have given a significant improvement in overall survival (11.1 months) compared with gemcitabine treatment alone (6.8 months) in PDAC patients with metastasis [218]. In recent years, scientific research is helping to understand the disease at a molecular level and there are now new agents, which are developed particularly to target specific pathways. One such drug is the EGFR inhibitor, erlotinib, which is a small molecule inhibitor that binds to the ATP binding site on the kinase domain of EGFR and thereby preventing its downstream signalling [219]. The original trial was performed in patients with advanced disease and there was a marginal but significant increase in median survival of 6.24 months compared to 5.91 months in the gemcitabine treated group alone ($p=0.03$). Since EGFR is expressed by a variety of cells in the body, there was a marked increase in toxicity and the drug has proven difficult to manage in the clinic.

Other novel therapies, which are in phase III trials for people with advanced pancreatic disease include cetuximab, a monoclonal antibody targeting EGFR used as a single agent, which so far has not shown a significant difference in overall survival (6.3 months) of PDAC patients compared with patients treated with gemcitabine alone (5.9 months) [221]. Bevacizumab (Avastin), another monoclonal antibody targeting VEGF, when used in combination with gemcitabine did not show any difference in the overall survival (5.8 months) compared with gemcitabine/placebo control group (5.9 months) in PDAC patients in a phase III

clinical trial [222]. Small molecule inhibitors of the RAS pathway (tipifarnib) MMP inhibitors and inhibitors of the gastrin pathway are some of the other novel small molecule inhibitors which are in clinical trials at the moment to treat PDAC patients [223]. Many of the above-mentioned agents showed very promising results *in vitro* and in some cases *in vivo* but did not show any promising improvements in clinical outcome. Thus, there remains an urgent need to try and develop new agents to target PDAC specifically and efficiently to improve therapy of this disease. This thesis will be focusing on studying the role of integrin $\alpha v\beta 6$ in PDAC and using it as a potential therapeutic target for the treatment of pancreatic cancer.

1.17 Aims

This study will aim to:-

Study the expression of αvβ6 in a panel of well differentiated and poorly differentiated PDAC cell lines.

Establish the functional role of αvβ6 in PDAC cell lines with particular emphasis on possible roles in proliferation, adhesion, migration and invasion, which are known key functions modulated by αvβ6 in many carcinomas.

Evaluate the expression of αvβ6 in human PDAC tissue samples and correlate expression levels of αvβ6 with available clinical follow up data.

Generate pancreatic cancer xenograft models (subcutaneous and orthotopic), which are physiologically relevant and replicate the human disease, using human PDAC cell lines expressing αvβ6.

Investigate the potential of αvβ6 as a new therapeutic target in PDAC using the novel xenograft models by giving a function-blocking antibody at physiologically relevant doses alone or in combination with gemcitabine.

MATERIALS AND METHODS

2. Materials and methods

2.1. Cell culture and cell lines

All the pancreatic cancer cell lines and stromal cell lines used in this study grew as adherent monolayers, in 100% humidified atmosphere of 8% (volume/volume) of carbon dioxide (CO_2) / air. Cell lines were tested routinely for, and found free of, *Mycoplasma* and were cultured in sterile tissue culture flasks (Corning life sciences, USA) of various sizes (T-25, T-75, T-175 cm^2 of surface area as required).

2.1.1 Pancreatic Cancer Cell lines

All cancer cell lines were grown in Roswell Park Memorial Institute (RPMI) -1640 medium or Dulbecco's Modified Eagle Media (DMEM) (PAA Laboratories, E15-842; E15-843) supplemented with 10% foetal calf serum (FCS) (Biosera) and glutamine (4mM final concentration, PAA Laboratories, M11-004).

Name	Derivation	Differentiation	Mutations	Growth Medium	Reference
AsPc1	Ascites	Poor	KRAS, p53, p16	RPMI 1640	Chen WH et al (224)
BxPC3	Primary tumour	Moderate to poor	p53	RPMI 1640	Tan MH et al (225)
Capan1	Liver met	Well	BRCA-2	RPMI 1640	Fogh J et al (226)
CFPac1	Liver met	Well	KRAS, DPC4	RPMI 1640	Schoumacher RA et al (227)
Colo357	Lymph node met	Well	-	DMEM	Morgan R et al (228)
HPAF-II	Ascites	Well	-	DMEM	Metzgar RS et al (229)
MiaPaCa2	Primary tumour	Poor	KRAS, p53	RPMI 1640	Yunis AA et al (230)
Panc04.03	Primary tumour	Well	KRAS	RPMI 1640	Jaffee EM et al (231)
Panc1	Primary tumour	Poor	KRAS, p53, p16	DMEM	Lieber M et al (232)

Table 8: List of pancreatic cancer cell lines used in this study [224-232]. The genetic identity of each cell line was confirmed by STR-profiling (short tandem repeats). ***(Mutation and differentiation status of some cell lines were not known).***

Table 8 summarises all the cell lines used in this study together with the media requirements, differentiation status (at the time of origin) and known associated mutations. The four cell lines used most regularly for *in vitro* experiments are detailed below.

CFPac1 (CRL-1918 – ATCC) [227] is a well-differentiated epithelial cell line derived from a liver metastasis from a patient with pancreatic cancer and cystic fibrosis. It possesses mutations in K-Ras (G12V), p53 and methylated INK4A, along with the most common mutation in CFTR (CFTRΔF508).

Panc04.03 (CRL-2555 – ATCC) [231] is a well differentiated epithelial cell line derived from a primary tumour from the head of the pancreas of a male patient. It harbours a K-Ras mutation (G12A).

MiaPaCa2 (CRL- 1420 – ATCC) [230] is a poorly differentiated epithelial cell line with p53 and K-Ras mutations at codon 12 (G12C), derived from tumour tissue of the pancreas obtained from a male patient.

Panc1 (CRL-1469 – ATCC) [232] is a poorly differentiated epithelial cell line derived from a primary tumour with mutated K-Ras (G12D), p53 and INK4A.

2.1.2 Pancreatic Stromal cells

Human pancreatic stellate cells (PSCs) were first isolated through the outgrowth method from fibrotic regions of the pancreas surgically resected from patients with chronic pancreatitis [78]. Another laboratory also identified pancreatic stellate cells at the same time and demonstrated that they played a crucial role in the desmoplastic response observed in pancreatic cancer [77] [86].

In our laboratory, non-tumourigenic pancreatic stellate cells were isolated using the outgrowth method from an adult male human pancreas (donation for transplantation) donated by the UK human Tissue Bank (Ethics approval; Trent MREC (05/MRE04/82). The resulting cell strain, called FS1, was verified for characteristic markers of stellate cells, such as the presence of lipid droplets in the cytoplasm, expression of GFAP, desmin, vimentin and αSMA as published previously. Stellate cell line FS1 was immortalised using ectopic human telomerase reverse transcriptase (hTERT) expression by Dr.Fiona Li and Ms. Jennifer Saddle and were

named FS1^{hTERT} or PS1 cells after confirmation of immortalised cell telomerase activity by TRAP assay and continuous passage over a period of six months without loss of phenotypic characteristics.

PS1 cells were grown in a 1:1 mixture of DMEM (PAA, E15-843) and Ham's F12 (PAA Laboratories, E15-817) supplemented with 10% FCS, glutamine (4mM final concentration) and 1µg/ml puromycin (Sigma, P9620), as a selection agent.

2.2 Routine Cell Culture

The cultures were examined daily under an inverted phase contrast microscope (Olympus IMT-2; Olympus Opticals, Welwyn Garden City), their morphology noted, (e.g. dendritic-like appearance for stellate cells). This acted as a check as to how confluent the cells were (cell density) before being passaged and re-plated at a lower density. Old medium was removed and cells were washed with phosphate buffered saline (PBS) (CR-UK services). PBS was replaced with 0.25% (w/v) trypsin/5mM EDTA (PAA Laboratories, L11-003) and flasks were placed at 37ºC for 5 – 15 minutes depending on the cell line. Once all the cells had detached (confirmed by microscopy) 5 – 10X volume of serum-containing growth medium was added to inactivate the trypsin. Cells were pipetted repeatedly to ensure a homogenous single cell suspension. A fraction of the cell suspension was then transferred to fresh flasks with fresh medium.

2.2.1 Counting Cells

A disposable haemocytometer (Fast Read102™, #BVS100H, Immune systems, UK) was used to determine cell counts. A small volume of cell suspension (10µl) was isolated from a diluted suspension and mixed thoroughly with trypan blue (0.04% final concentration) for a minimum of 2 minutes. Live cells exclude the dye and appear unstained while dead cells, which have permeabilised membranes, appear blue. The average number of cells in a square was determined.

Total cells/ml = average cell count/1mm square x dilution factor x 10^4.
Total cells = total cells/ml x original volume from which sample was removed.
% Viability = Total number of live cells (unstained) x 100 / total number cells counted.

2.2.2 Preservation of Cells

Cells detached by trypsination (trypsin/EDTA) were centrifuged (1200rpm for 3 minutes) and resuspended to 1 – 10 x 10^6 per ml of freezing medium (70% DMEM, 20% FCS, 10% DMSO) in Nunc cryotubes. Cells were cooled slowly in a freezing box (1 degree a minute) (Eprak Scotlab, Scotland) at -80°C to prevent ice crystal formation. Cells were then left at - 80°C overnight. Then cryovials were transferred to liquid nitrogen (-196°C) for long-term storage.

When required, the frozen cryovials were transferred directly to a 37°C water bath. As soon as the cells thawed out, they were diluted with 10 volumes of fresh growth medium and centrifuged (1200 rpm for 3 minutes). The pellet was re-suspended in fresh medium and immediately transferred to tissue culture flasks.

2.3 Antibodies

All antibodies used for carrying out experiments are summarised in the table below.

Antibody/ Clone	Target	Species	Supplier	Conc: for IF/IHC/WB	Conc: for Flow
5E8D9	α1	Mouse	Chemicon	NA	10μg/ml
P1E6	α2	Mouse	Chemicon	NA	10μg/ml
P1D6	α5	Mouse	Chemicon	10μg/ml	10μg/ml
62oW	β6	Rat	CRUK	10μg/ml	NA
62G2	β6	Mouse	Biogen	5μg/ml	NA
C19	β6	Goat	Santa Cruz	1:1000	NA
23C6	αvβ3	Mouse	Chemicon	10μg/ml	10μg/ml
P1F6	αvβ5	Mouse	Chemicon	10μg/ml	10μg/ml
10D5	αvβ6	Mouse	Chemicon	10μg/ml	10μg/ml
53a.2	αvβ6	Rat	CRUK	10μg/ml	10μg/ml
264RAD	αvβ6	Human	Astra Zeneca	NA	10μg/ml

Antibody/ Clone	Target	Species	Supplier	Conc: for IF/IHC/WB	Conc: for Flow
14E5	αvβ8	Mouse	Collaborator	NA	1:100
Anti-αSMA	αSMA	Mouse	Dako	1:300	NA
Anti-GFAP	GFAP	Mouse	Sigma	1:500	NA
Anti-Ki67	Ki67	Rabbit	Novocastra	1:200	NA
Anti-HSC70	HSC70	Mouse	Santa Cruz	1:5000	NA
W6/32	MHC I	Rat	CRUK	10μg/ml	NA
Negative Control	IgG	Human	Astra Zeneca	NA	10μg/ml
Negative Control	IgG	Mouse	Dako	10μg/ml	10μg/ml

Table 9: List of primary antibodies used for experiments

IF – Immunofluorescence, IHC- Immunohistochemistry, WB- Western Blot, Flow – Flow cytometry, NA – Not Applicable, HRP- Horseradish Peroxidase.

Antibody/ Species	Detects	Supplier	Conc: for IF/IHC/ WB	Conc: for Flow
Goat Alexa Fluor-488	Mouse	Invitrogen	1:500	1:250
Donkey Alexa Fluor-488	Rat	Invitrogen	1:500	1:250
Anti mouse HRP (#P0260)	Mouse	Dako	1:1000	NA
Anti goat HRP (#P0160)	Goat	Dako	1:1000	NA

Table 10: List of secondary antibodies used for experiments

IF – Immunofluorescence, IHC- Immunohistochemistry, WB- Western Blot, Flow – Flow cytometry, NA – Not Applicable, HRP- Horseradish Peroxidase.

2.4 Introduction of siRNA duplexes into cells using Oligofectamine™

Oligofectamine™ reagent (Invitrogen) is a lipid based transfection reagent, which interacts efficiently with oligonucleotides to form transfection complexes, and is used for transfecting cells. Manufacturer's instructions were followed for transfections.

Custom SMARTpool siRNA oligonucleotides targeting β6 integrin gene (ITGB6) were purchased from Dharmacon RNA technologies, USA (MQ-008012-01-0002) and were re-suspended in 1X siRNA buffer (100mM KCl, 30mM Hepes-pH 7.5, 1mM $MgCl_2$ to a 20μM stock solution) and then stored at -20°C until used.

Cancer cells were seeded into 6 well plates ($5x10^4$ cells/well) in growth media such that, after 24 hours, the cells were approximately 30%-40% confluent, which is optimal for transfection. For each 6 well plate, the following solutions were prepared. To 1188μl of Optimem™ (Invitrogen) was added 33μl of ITGB6 siRNA or control non-targeting siRNA from the 20μM stock. The final concentration of siRNA used for the transfection was 100nM. In another tube (tube 2) 79.2μl of Optimem™ was added to19.8μl of Oligofectamine™ and mixed gently. After 10 minutes at room temperature the siRNA mixture was added into tube 2, mixed gently and incubated at room temperature for 20 minutes. Meanwhile, the medium on the cells was removed and washed with fresh Optimem™ (twice) before adding 800μl of Optimem™ per well. Finally, 200μl of the transfection mixture was added to each well and the cells were incubated for 4 hours at 37°C. 500μl of medium with 30% FCS was added and left at 37°C for 48 hours before harvesting.

2.4.1 Introduction of shRNA (short hairpin RNA) into cells to knock down αvβ6

The ITGB6 shRNA targeting sequence was in a pGIPZ lentiviral vector driven by a CMV promoter (Figure 26). The vector also had a turbo-GFP as a read out to measure the levels of expression. The vector contained both puromycin and zeocin antibiotic selection for eukaryotic and prokaryotic selection respectively. HEK 293 FT cells were used to make the lentivirus, which carried the expression vector with the shRNA sequence.

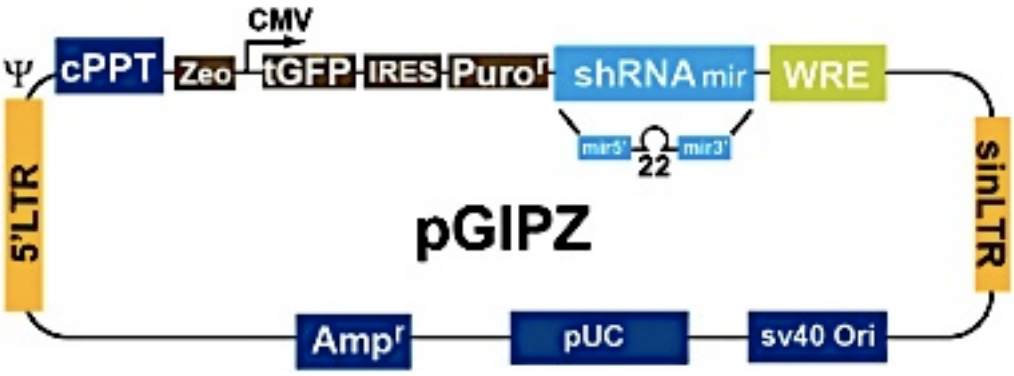

Figure 26: Schematic diagram of the vector with the shRNA sequence. (Figure from Open Biosystems ltd).

CMV Promoter - RNA Polymerase II promoter
cPPT - Central Polypurine tract, helps translocation into the nucleus of non-dividing cells
WRE - Enhances the stability and translation of transcripts
turbo GFP - Marker to track shRNAmir expression
Puro^r – Puromycin - Mammalian selectable marker
AMP^r – Ampicillin - bacterial selectable marker
5'LTR - 5' long terminal repeat
pUC ori - High copy replication and maintenance in E.coli
SIN-LTR - 3' Self inactivating long terminal repeat
RRE - Rev response element
ZEO^r - Bacterial selectable marker

The shRNA sequences to knock down ITGB6 (β6) were purchased from open biosystems (Thermo fisher, UK).

1) Hairpin sequence for V3LHS_374278 (mir-30 context sense loop antisense)
TGCTGTTGACAGTGAGCGAATGCTGAAAGATTCAATGAAATAGTGAAGCCACAG
ATGTATTTCATTGAATCTTTCAGCATCTGCCTACTGCCTCGGA
Mature Sense for V3LHS_374278
TGCTGAAAGATTCAATGAA
Mature Anti sense for V3LHS_374278
TTCATTGAATCTTTCAGCA

2) Hairpin sequence for V3LHS_374274 (mir-30 context sense loop antisense)
TGCTGTTGACAGTGAGCGAAAGCTGCTGTGTGTAAGGAAATAGTGAAGCCACA
GATGTATTTCCTTACACACAGCAGCTTGTGCCTACTGCCTCGGA
Mature Sense for V3LHS_374274
AGCTGCTGTGTGTAAGGAA
Mature Antisense for V3LHS_374274
TTCCTTACACACAGCAGCT

3) Hairpin sequence for V3LHS_374276 (mir-30 context sense loop antisense)
TGCTGTTGACAGTGAGCGCCTGGTACAAAACAACGTGTTATAGTGAAGCCACAG
ATGTATAACACGTTGTTTTGTACCAGTTGCCTACTGCCTCGGA
Mature Sense for V3LHS_374276
TGGTACAAAACAACGTGTT
Mature Antisense for V3LHS_374276
AACACGTTGTTTTGTACCA

The lentivirus containing the shRNA sequence was generated over a period of four days.

DAY1: HEK293T cells were seeded at one million cells per well 24 hours prior to transfection in a T75. (Cells should be sub-confluent at the time of transfection and numbers may need to be adjusted according to the cell line used).

DAY2: Transfection: The shRNA sequences were diluted in a total volume of 15ml with TE buffer (pH 8.0) at a final concentration of 1.5µg. 200µl of Optimem™ was added to 10µl Fugene and mixed carefully with the packaging vector and target sequences. The mixture was left at room temperature for 15 minutes and Optimem™/fugene/shRNA mix was added to the cells carefully and the plates were incubated overnight at 37°C.

DAY3: 24 hours following transfection, the medium in the plates was replaced with 8ml of fresh growth media.

DAY4-6: virus collection: The supernatants from the plates were collected on days 4, 5, 6 and stored at -80°C. Fresh growth medium was added to the plates following the collection of each supernatant.

Infection with lentivirus:

The supernatant containing the lentivirus with the shRNA targeting ITGB6 was used to knock down β6 expression in β6 positive PDAC cell lines.

DAY1: Target cells were seeded into a T25 flask, which were sub-confluent the next day.

DAY2: Infection: The growth medium was replaced with 2ml of fresh growth medium containing the shRNA encoding lentiviral particles + 2µl (1:1000) of polybrene and incubated at 37°C for 4 h following which an additional 2 ml of fresh growth medium was added and left overnight.

DAY3: 24 hours later, the medium was replaced with 4ml of fresh growth medium containing 1.25µg/µl puromycin, a selection marker for the transfected cells.

Cells were later analysed using flow cytometry for levels of GFP and αvβ6 expression.

2.5 Polymerase Chain Reaction (PCR)

2.5.1 Isolation of RNA and cDNA synthesis

A Qiagen RNA extraction kit (Qiagen#74106) was used for lysing cells to extract RNA. Cells were trypsinised, counted and re-suspended to the required concentration. Cells were pelleted and lysed using the lysis buffer (RLT buffer) provided with the kit. One volume of 70% ethanol was added to the homogenised lysate and mixed well. The suspension was then transferred to a RNEasy spin column, provided with the kit, which then was centrifuged at 8000g for 15 seconds. The flow through was discarded. The spin column membrane containing the homogenised lysates were then washed in RW1 buffer, provided with the kit, to get rid of any DNA contamination. This was followed by a wash in RPE buffer, provided with the kit, by centrifugation for 2 minutes at 8000g. The last step was to add RNAase free water to the spin column with a new collection tube and this was spun at 8000g for 1 minute to elute the RNA. The quality and quantity of RNA was measured using a NanoDrop spectrophotometer (OD 260/280 ratio > 1.80) as well as run on an agarose gel to control for contamination with genomic DNA. For detailed protocol, see manufacturer's guide (Qiagen). cDNA was synthesised from extracted RNA, using Superscript III First Strand Synthesis kit using random hexamers, according to manufacturer's instructions (Invitrogen, #18080-051).

2.5.2 Quantitative Real Time PCR

The SensiFAST™ Probe Hi-ROX One-step kit (Bioline BIO-77005) was used for first-strand c-DNA synthesis followed by real time PCR in a single tube. The kit has been optimised for use with the ABI7900HT (Invitrogen) real time instrument. Primers were designed using the primer design tool, *(http://www.ncbi.nlm.nih.gov/tools/primer-blast/)* NCBI. Care was taken to make sure that the primers had a melting temperature (T^M) of about 60°C and were intron-spanning to avoid any possible amplification from genomic DNA. The primers were used at a final concentration of 400nM. 100ng of RNA was used per 20µl reaction. The master mix was prepared following instructions provided with the kit. Cycle times were optimised, one cycle at 45°C for 10 minutes (reverse transcription), one cycle at 95°C for 2 minutes to activate polymerase and 40 cycles of 95°C for 5 seconds (denaturation) followed by 60°C for 20 seconds (annealing/extension). For each gene, the first cycle when exponential amplification could be detected, Ct values were normalised to the

endogenous expression of the house-keeping gene 18s. For detailed protocol, see manufacturer's protocol (Bioline BIO-77005).

Primer sequences used in this study were ordered from Sigma Aldrich, UK.

1) CAPG primer sequence:

Forward primer: GGGCGTCTTCTTCTCGGGGGA
Reverse primer: CCCGGGATGACTGCTGGCCTAT

2) ITGA2 primer sequence:

Forward primer: CCGAGGTGACCAGATTGGCTCC
Reverse primer: GGTGCACCTACCAAGAGCACGT

3) MMP11 primer sequence:

Forward primer: TTGCACCGCTGGAGCCAGAC
Reverse primer: TCGGATGGTGGAGACCGCGT

4) ITGB6 primer sequence:

Forward primer: CGTACAAGGTGGCTGTGCCCTG
Reverse primer: GCACACCAGGCACACTGAGGTC

5) 18S (house keeping gene) primer sequence:

Forward primer: CACGGGAAACCTCACCCGGC
Reverse primer: AACGGCCATGCACCACCACC

2.6 Immunohistochemistry (IHC)

All archived patient samples were obtained with prior Research Ethics Committee approval (East London & the City REC3 07/H0705/87). Pancreatic cancer and Ampullary cancer Tissue Microarrays (TMAs) were received from collaborators (Beatson Institute, Glasgow, UK and University of Verona, Verona, Italy) and stained for $\alpha v\beta 6$.

2.6.1 General immunohistochemistry protocol

Harvested organotypic co-cultures, organs and tumours from mice were fixed in formal saline containing 4% formaldehyde (Fisher Scientific) for 24 hours before transfer to 70% ethanol. Samples were then embedded in paraffin by the histopathology department (Barts Cancer Institute) and 5µm sections were cut. The sections were de-waxed in xylene for 5 minutes (x2) and taken through a series of graded ethanol (100%, 95%, 50% v/v in water) solutions, each twice, for 2 minutes. Endogenous peroxidase was blocked with a 0.45% solution of H_2O_2 in methanol for

15 minutes. An Immedge™ Pen (Vector laboratories) was used to delineate the specimen edge on the slide, surrounding it with a hydrophobic barrier in order to minimise the volume of reagents required to coat the sample. The slides were then subjected to antigen retrieval. This step is critical and varies for different primary antibodies. Antigen retrieval protocols used in this study are detailed below.

Heat retrieval (citrate buffer)

1.47g Tri-sodium citrate was dissolved in 500ml of distilled water and pH adjusted to 6. The slides were transferred into boiling citrate buffer and microwaved for 10mins to 12mins. Slides were allowed to cool for 30mins at room temperature in the citrate buffer before carrying on with the next step.

Pepsin retrieval

Pepsin Solution Digest all (Invitrogen 003009) was warmed to 37°C before use. The pepsin was added directly onto the sections and incubated for 5 minutes at 37°C in a humid incubator.

The sections were then washed twice in PBS for 2 minutes and then incubated for 10 minutes each at room temperature with avidin and biotin blocking solutions respectively (Vector laboratories SP-2001). After washing twice in PBS, the sections were incubated with a blocking buffer (normal horse serum, Vector ELITE ABC Kit, Vector laboratories) for 30 – 45 minutes at room temperature. Primary antibody was added to the sections at required final concentrations as specified in the data sheet and left overnight at 4°C. An isotype IgG antibody was also used as a negative control in parallel.

The following day, sections were washed in PBS and then incubated with HRP conjugated secondary antibody for 45 minutes at room temperature. The sections were then washed again and incubated with the avidin-biotin enzyme complex (ABC) Vectastain Elite ABC kit (Vector Laboratories) for 30 minutes at room temperature. Following washes, DAB (Dako, K3467) was added for about 2-5 minutes and excess DAB was washed off. Sections were counterstained with Mayer's haematoxylin (Dako, S3309) for one minute and excess stain washed away. The sections were dehydrated in reverse through the different grades of alcohol, cleared in xylene and mounted in DPX (VWR #360294H). Digital images of samples were recorded using a light microscope (Zeiss Axioplan, Welwyn, Garden City, UK).

TMA samples labelled for αvβ6 expression were scored out of four (0: negative; 1: background staining; 2: weak; 3: moderate; 4: strong), and the proportion of epithelial cells staining positively was scored out of four (1: <25%; 2: 25-50%; 3: 51-75%; 4: 76-100%). The combined score gave a score in the range of 0 to 8 and grouped as - (score = 0), + (score = 1-3), ++ (score = 4-5), or +++ (score = 6-8). Three independent observers carried out blind scoring of all samples. The scores were averaged and used to perform statistical analyses.

2.6.2 Immunofluorescence (IF)

Cells ($1x10^4$ - $1x10^5$) were plated in a 24 well plate on coverslips as a monolayer, dependent on the time of fixation. Cells were fixed with 3.7% formaldehyde for 10 minutes, permeabilised with 0.1% Triton-X 100 for 5 minutes, blocked with DMEM/0.1% BSA for 10 minutes and incubated with primary antibody for 1 hour at room temperature. Coverslips were washed three times with blocking buffer and incubated with appropriate secondary antibodies for 1 hour at room temperature (Invitrogen, alexa fluor). The nuclei were stained with 4',6-diamidino-2-phenylindole (DAPI) (1:5000 of stock at 5mg/ml) for 15 minutes at room temperature. Isotype specific immunoglobulins were used at matching concentrations as negative controls. Coverslips were mounted onto slides with Mowiol (mountant with anti-fade #AF1, Citifluor Ltd). Cells were viewed using a confocal laser-scanning microscope (LSM 510 META, Carl Zeiss, Inc., Germany) with a 63x/1.4 NA Plan-Apochromat oil immersion objective. A diode 405nm laser, 488nm argon laser and helium neon 543nm laser were used to excite DAPI, GFP and Cy3 respectively. This allowed high quality images (12 bit, 1024 pixels) to be reconstructed using the LSM 5 software, version 3.2.

2.7 Flow Cytometry Analysis

2.7.1 Analysis of integrin expression using flow cytometry

Cells to be labelled with different anti-integrin antibodies were trypsinised from tissue culture flasks, washed twice in chilled 0.1/0.1 DMEM (0.1% BSA / 0.1% sodium azide (w/v) in DMEM). Cells were then re-suspended to $4x10^6$/ml in 0.1/0.1 DMEM and 50µl transferred into Falcon 2054 centrifuge tubes to give a final cell number of $2x10^5$ cells per sample on ice. A final concentration of 10µg/ml of the antibody was added to the cells in suspension and was incubated for 45 minutes on ice. A class matched IgG was used as a negative control. After the incubation, the cells were pelleted by centrifugation (1200rpm for 3 minutes), washed in 0.1/0.1 DMEM three times and the appropriate alexafluor 488 secondary antibody added at a final concentration of 1:250 and incubated for 30 minutes at 4°C. The cells were washed in 0.1/0.1 DMEM by centrifugation three times and after the final wash, re-suspended in approximately 300µl of 0.1/0.1 DMEM.

Flow cytometry was performed on a FACS Calibur cytometer (BD Biosciences) using the Cell Quest Pro software version 4.0.2. Ten thousand events were collected within a gated population on the forward scatter (FSC) versus side scatter (SSC). A marker was set to include less than 1% of control labelled cells. The percentage of positive cells was quantified on a histogram of green fluorescence, detected by the FL-1 channel against the cell count. As the data obtained were not normally distributed, a geometric mean was plotted using the Cell Quest Pro software.

2.7.2 Cell cycle analysis

Cells were seeded at a density of $2x10^5$ cells per well of a 6 well plate and the following day treated with $\alpha v\beta 6$ blocking antibody or a control isotype antibody at a final concentration of 10µg/ml. After 96 hours post-treatment, samples were harvested by collecting both supernatant and attached cells by trypsinisation. Following neutralisation of trypsin and three washes in PBS, cells were pelleted by centrifugation and re-suspended in ice cold 70% ethanol whilst vortexing before fixing for a minimum of 24 hours at 4°C. The DNA content of the cells was analysed by washing the fixed cells with PBS (to remove the ethanol) and incubating with RNase A (Invitrogen) and 100µg of propidium iodide (PI) (Sigma Aldrich, UK), a DNA binding dye, in a total volume of 300µl of PBS for 30 minutes at 37°C in the dark.

Ten thousand events were acquired by flow cytometry on a FACS Calibur cytometer (BD Biosciences) with Cell Quest Pro software version 4.0.2. A primary gate on forward scatter (FSC) versus side scatter (SSC) was set to exclude debris and a second gate to exclude doublets on a dot plot of width (FL2-W) versus pulse area (FL2-A). PI fluorescence (FL3-H) was then plotted against cell counts on a linear scale to distinguish between the different phases of cell cycle. The G1 maximum peak was set by adjusting FL-3 H so that the first peak was at a value of 200 mean fluorescent intensity (MFI). Next, a G2/M marker was set at the second peak at the 4N DNA content. The S phase marker included all cells between these two peaks. A sub-G1 marker counted cells with <2N DNA and a fifth marker was also set to quantify cells with >4N DNA.

2.8 Western Blotting

2.8.1 Preparation of whole cell lysates

Cells nearing confluency in tissue culture flasks were washed with PBS and trypsinised to collect the cell pellet. Cell pellets were washed with PBS and lysed for 20 minutes on ice in RIPA buffer (50mM Tris HCl pH 8.0, 150mM NaCl, 1 mM EDTA, 1% Igepal CA-630 (NP-40), 0.1% SDS) containing a 1:100 dilution of protease inhibitor cocktail 1 stock (Calbiochem). After centrifugation at 13000rpm for 10 minutes, supernatant was transferred to clean 1.5ml centrifuge tubes and protein concentration determined using Bio-Rad DC Protein Assay (Bio-Rad Laboratories) according to manufacturer's instructions. Bovine serum albumin (BSA) (Sigma Aldrich, UK) standards (0-2000µg/ml) were prepared in distilled water. 5µl of either standard or sample added per well of a 96 well plate in duplicate. 25µl of activated solution A (1000µl of reagent A+ 20µl of reagent S (BioRad DC assay kit)) was added per well, followed by 200µl of Reagent B and incubated at room temperature for 15 minutes and absorbance was measured at 550nm using a spectrophotometer (SLT Lab instruments). A standard curve of absorbance *vs* concentration was constructed for the different concentrations of BSA and the protein concentration in each sample was calculated using this graph. The lysates were stored at -20°C till needed.

2.8.2 Sodium dodecyl sulphate polyacrylamide gel electrophoresis (SDS-PAGE).

Lysates were diluted, to either 10μg/μl or 20μg/μl, in RIPA buffer and an appropriate volume of 2x sample loading buffer (Sigma Aldrich, UK) (0.5M Tris, 0.2M NaH_2PO_4 [pH 7.8], 5% β-mercaptoethanol, 50% Glycerol, a few grains of bromophenol blue in distilled water) added to give a final concentration of 1X. Samples were heated at 100°C for 5 minutes. Samples were run on either a NuPAGE 4-12% Bis-Tris pre-cast gel (Invitrogen) or a 10% or 15% polyacrylamide gel. Resolving gels were made by mixing 3.8ml of 1.5M Tris-HCl (pH 8.8), 5ml of 30% polyacrylamide solution (National Diagnostics #EC890), 150μl of 10% SDS (National Diagnostics, #EC-874), 150μl of 10% ammonium persulphate (APS), 6μl TEMED (Sigma Aldrich UK, #T7024) in 5.9ml of distilled water and allowed to set. Stacking gel was prepared by mixing 670μl of 30% polyacrylamide solution, 500μl of 1M Tris-HCl (pH 6.8), 40μl of 10% SDS, 40μl of APS to 2.7ml of distilled water and added to the top of the resolving gel before inserting a comb and was allowed to set at room temperature. 10μg - 20μg of sample protein was loaded per well along with 5μl of PageRuler Pre-stained protein ladder (Fermentas UK, York, UK) for separation by electrophoresis at 120V for 90 minutes using Tris-Glycine SDS PAGE Running buffer (Invitrogen) for cast polyacrylamide gels, or 1X MOPS Buffer (Invitrogen) for precast gels.

2.8.3 Western blotting

Proteins were transferred onto Hybond nitrocellulose membranes (GE Healthcare, Buckinghamshire, UK) using a wet transfer Cell (Invitrogen). Briefly, nitrocellulose membrane along with the blotting paper and gel were soaked in transfer buffer (2.9g Tris, 14.5g Glycine, 200ml methanol in distilled water to a total volume of 1 litre) for a few seconds. A “sandwich” of blotting paper, gel, nitrocellulose membrane, blotting paper was placed in the holder inside the blotting cell. Electro-transfer of proteins was done at 30V for 90 minutes with nitrocellulose closest to the anode.

The membrane was blocked in 5% (w/v) non-fat milk and 1% Tween-20 in TBS (TBS-T) for a minimum of 20 minutes at room temperature. It was then rinsed with TBS-T before the addition of primary antibody in 5% milk overnight at 4°C with a gentle rocking motion. The next day, it was washed three times with TBS-T (1% Tween-20) for 10 minutes per wash. The appropriate HRP conjugated secondary antibody was added in TBS-T for 1 hour at room temperature followed by a further

three washes with TBS-T. Protein levels were detected using chemo-luminescent detection of HRP using ECL Western blotting detection reagents (GE Healthcare, Buckinghamshire, UK). Signal was visualised by exposure of the membrane to Hyperfilm ECL (GE Healthcare, Buckinghamshire, UK) and developed in a Curix 60 Developer (Agfa, Middlesex, UK).

2.9 Functional assays

2.9.1 Migration assay

Cell migration assays were performed using protein-coated polycarbonate filters (8 μm pore size (Transwell®, Beckton Dickinson) (Figure 27). 200μl of the protein solution, fibronectin (Sigma Aldrich, UK) at 10μg/ml final concentration, or LAP at 1μg/ml was added to the lower chamber of the Transwell® plate and incubated for 1 hour at 37°C. The protein solution was then replaced with 200μl of migration buffer (a-MEM containing 0.1% BSA) for 30 minutes at 37°C. Cells were plated in the upper chamber of the Transwell® at a density of $5x10^4$ in 200 μl of migration buffer for 16 hours. In blocking experiments, the cells were incubated with blocking antibodies at a final concentration of 10μg/ml (or chemical inhibitors) for 30 minutes at 4°C prior to plating. For RNAi (100nM final concentration) experiments, cells were used 24 hours post transfection.

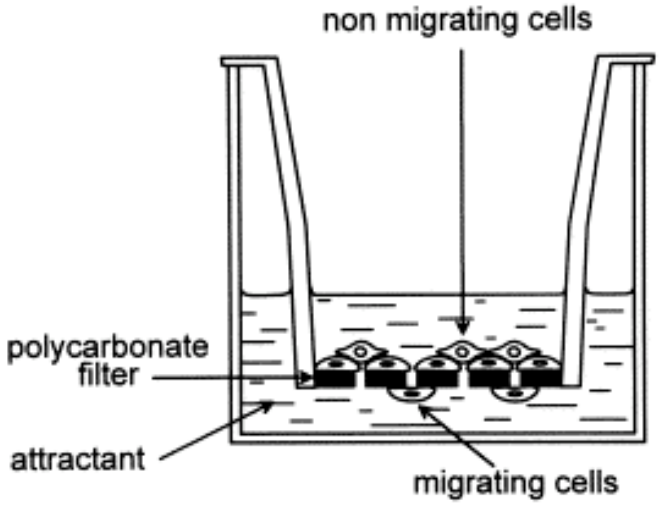

Figure 27: Schematic diagram of migration assay. Modified from Rochefort, H et. al, 1998.

After 16 hours, cells in the lower chamber (including those attached to the under surface of the membrane) were trypsinised and counted using a Casy cell counter (Sharfe System GmbH, Germany). Migration assays were set up in replicates of four and were repeated at least 3 times.

2.9.2 Transwell® invasion assay

Transwell® invasion assays were prepared using Matrigel™-coated polycarbonate filters, 8 μm pore size (Transwell®, Beckton Dickinson). 70μl of Matrigel™ (diluted 1:2 in serum free medium) was added to the upper chamber and allowed to gel for 1 hour at 37°C. Cancer cells were were then added to the Matrigel™ at a density of $5x10^4$ in 200 μl of serum free media per well. To act as a chemotactant, 500μl of serum containing medium was added to the lower chamber of the Transwell® plate (Figure 28). Samples were incubated for 72 hours at 37°C. In antibody blocking experiments, the cells were incubated with antibodies or chemical inhibitors at a final concentration of 10μg/ml for 30 minutes at 4°C prior to plating. For RNAi (100nM final concentration) experiments, cells were used 24 hours post transfection with siRNA. After 72 hours, the cells in the lower chamber (including those attached to the under surface of the membrane) were trypsinised and counted using a Casy cell counter (Sharfe System GmbH, Germany). Relative invasion was determined from a minimum of four replicate samples. Experiments were repeated at least 3 times.

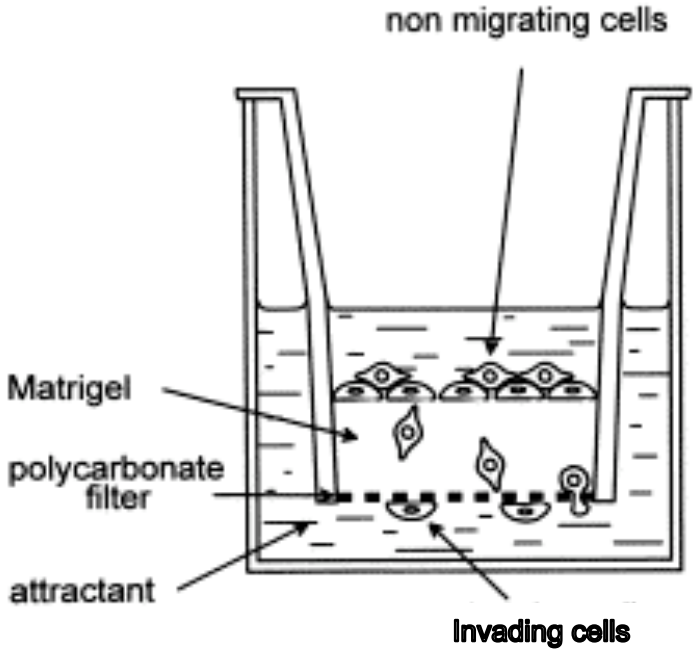

Figure 28: Schematic diagram of Transwell® invasion assay. Modified from Rochefort, H et. al, 1998.

2.9.3 Organotypic invasion assay

The organotypic invasion assay is a three-dimensional (3D) invasion assay that attempts to replicate the tumour-stroma interface. The assay requires 3 days to set up and can be left for 7-14 days as described.

2.9.3.1 Materials

The various materials required for setting up the organotypic co-culture gels are listed below.

• Rat tail collagen type 1 (BD Biosciences)
• Matrigel™ Basement Membrane Matrix (BD Biosciences, #354234)
• 25% glutaraldehyde (Sigma-Aldrich, #G5882)
• 10X DMEM (Media Production, Clare Hall, CR-UK)
• RPMI 10% Serum containing medium (PAA Laboratories)
• Fibroblasts
• Cancer cells (Different cell types of choice)
• Nylon Mesh (Tetko, Sefar LTD, #3-100/5)
• Steel Grids, 2cmx2cm with 5mm feet (Mechanical Workshop, BICMS London)
• Spatula, Forceps, Scalpel
• 6 well/24 well plates (NUNC, Beckton-Dickinson, UK)
• Shandon Cryomatrix (OCT), (Thermoelectron corporation, Ref: 676900)
• Cork Disks (Ref: E7.15/CD, Raymond A Lamb-Laboratory Supplies)
• Coverslips, (Menzel-Glaser, MNJ-380-020H)

Day 1

The gels are composed of collagen, Matrigel™, 10x DMEM, FCS and fibroblasts in the following ratio:

Collagen : Matrigel™ – 3.5 volume : 3.5 volume
10 X DMEM – 1 volume
FCS – 1 volume
Cell suspension (fibroblasts) – 1 volume
Total Volume – 10 volumes

The components were added together on ice. Fibroblasts were used at a final concentration of 5 x 10^5 cells/ml per gel and mixed thoroughly, to ensure even

distribution. The gel mix should appear pink in colour suggesting that it is in an optimal pH range (7.1-7.3). If the gel mix appeared as a pale yellow colour, 1M NaOH was added in about 100µl aliquots, till the mix attained a pink colour. 1ml of the gel mix was added per well of a 24 well plate placed at 37°C for an hour for the gels to solidify. After an hour 1ml of growth medium was added to each of the wells and plates returned to an incubator overnight.

Day 2

2cm squares of nylon supports were sterilised by autoclaving. Collagen gel mix was prepared according to the following recipe.

Collagen – 7 volumes

10X DMEM – 1 volume

FCS – 1 volume

E4 (10%FCS) – 1 volume

Total Volume – 10 volumes

The coating mix was prepared on ice and mixed thoroughly. 250µl of the above mix was added per nylon sheet and left at 37°C for 15-30 minutes. 1% glutaraldehyde solution was used to wash the nylon sheets and left at 4°C for an hour. The sheets were washed with PBS to remove any excess glutaraldehyde and stored in serum free growth medium until required. The PDAC cell lines were suspended in growth medium at $5x10^5$ cells per ml and 1ml plated onto the gels prepared on day 1and left at 37°C overnight.

Day 3

Using a metal spatula, gels were detached from the wells and raised onto a metal grid placed in a well of a 6 well plate. A collagen coated-nylon square was added to each grid. One gel was placed onto each nylon square and medium (approximately 5ml) added till it covered the nylon sheet (Figure 29). Medium was replaced every two days. After 11-14 days, the gels were removed and cut exactly in half with a scalpel. One half was fixed in formol saline and sent off to histopathology (BCI services) for paraffin embedding. The other half was frozen down in OCT and stored in the -80°C freezer.

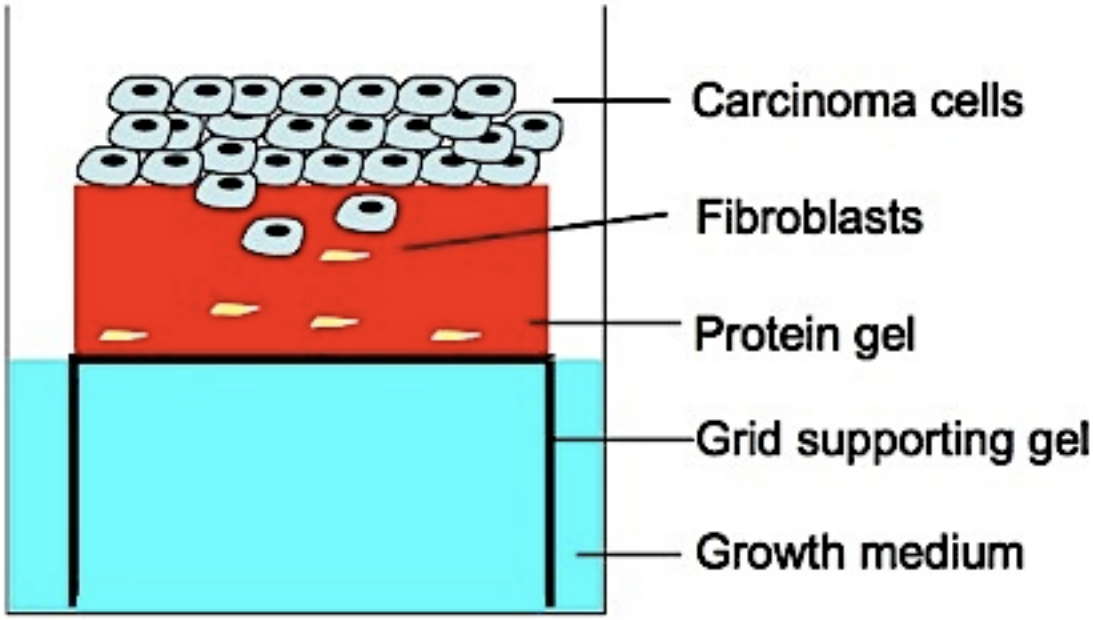

Figure 29: Schematic picture of organotypic co-culture system.

2.9.4 Cell Viability assay

Cell viability assays were performed in 96 well plates over a seven-day period. 3000-4000 cells, determined for each cell line in preliminary experiments (data not shown), were plated per well in 200μl of growth medium. The cells were left to adhere overnight and replaced with growth medium containing the antibody (53a.2 or 264RAD) at the required final concentration. At day 3, fresh antibody containing medium was added and plates re-incubated till day seven, unless otherwise stated. On day 7, (3-(4,5-Dimethylthiazol-2-yl)-2,5-diphenyltetrazolium bromide (MTT) (Sigma) was used to detect and quantify the number of cells that were viable after antibody treatment. MTT reacts with the mitochondrial dehydrogenase enzymes in living cells to be converted to water-insoluble formazan, which is purple in colour. The purple crystals are solubilised with dimethyl sulphoxide (DMSO) and the intensity is measured colourimetrically at 550 nm using a spectrophotometer (SLT Lab instruments). Absorbance values for wells with medium alone were subtracted from that of those containing cells (background value of MTT mixture in the absence of cells) and optical density (OD) values were plotted.

2.9.5 Cytotoxicity assay

A proprietary cytotoxic drug attached to the αvβ6-specific peptide A20FMDV2 [124] was generated by Spirogen, UK and this was tested *in vitro*. Initial studies using this drug on cytotoxic assays, even at very low concentrations, in αvβ6 positive pancreatic cancer cell lines showed very encouraging results.

3000 cells were plated in 200µl of growth medium in quadruplicate wells of 96-well plates. After 24 hours in culture, the medium was removed carefully and cells were treated with different doses of the cytotoxic drug (20, 10, 5, 1 and 0.2µM) plus an untreated control in a final volume of 200µl and then incubated for 72 hours. The medium was removed and 100 µl of 0.2mg/ml of MTT was added to each well for 60 minutes at 37°C. MTT binds to the living cells in the plate as described above and the intensity was measured colourimetrically at a wavelength of 550 nm using a spectrophotometer (SLT Lab instruments).

2.10 *In Vivo* models for pancreatic cancer

All *in vivo* experiments were carried out in the Biological Service Unit (BSU) at Queen Mary University of London. Animal care and treatment followed guidelines approved by the Home Office, United Kingdom.

Mice that were pathogen-free were either purchased from Charles River or Harlan and housed in the BSU, at Charterhouse Square, London. All experiments were performed using female CD1 nu/nu unless otherwise stated. All animals were housed in individually ventilated cages (IVC) in groups of five. Food and water were available *ad libitum*.

2.10.1 Subcutaneous models

2.10.1.1 Cancer cells alone

CFPac1 cells (Table 8) used for injection were harvested by trypsinisation, washed in growth medium and then washed three times in serum free media. Two million CFPac1 cells in 200µl of PBS were injected into the right flank of the mouse subcutaneously. Depending on the experiment, mice were maintained until the tumours reached a volume of 100mm^3 and further treatments were carried out as explained in the various treatment plans (2.10.3).

2.10.1.2 Cancer cells plus stellate cells

CFPac1 cells and PS1 (stellate cells) were harvested by trypsinisation, washed in growth medium and then and washed three times in serum free media. Half a million CFPac1 cells were mixed with one million PS1 cells (1:2 ratio) in 200µl of PBS and injected into the right flank of the mouse subcutaneously. Depending on the experiment, mice were maintained until the tumours reached a volume of 100mm^3 and further treatments were carried out as explained in treatment plan (2.10.3). Following the treatment regimen, tumours were excised and fixed in formol saline for 24 hours before transferring to 70% ethanol. Tissue was paraffin embedded and sections were cut (Pathology department, Barts Cancer Institute) for further immunochemical analysis.

2.10.2 Orthotopic pancreatic cancer model

All surgical procedures were carried out in a laminar airflow cabinet under sterile conditions. Mice were under anesthesia (inhalation of isoflurane with oxygen and nitrous oxide) during the procedure.

The flank wall of the mouse was wiped with a sterile cloth with 70% ethanol. A 2cm incision was made in the abdominal wall of the mouse alongside its right ribcage. The spleen together with the pancreas was carefully exteriorised and laid onto the skin. 40µl of cell suspension (two million CFPac1 alone or 1 million CFPac1 plus two million PS1 cells in a 1:2 ratio) was injected into the tail of the pancreas using an insulin syringe (29 gauge, ½ inch) (Southern Syringe Services, Leicester, UK). The injection site was dabbed with a sterile cotton swab to ensure no leakage had occurred and the organs placed back into the abdominal cavity. Skin and muscle were sutured using Vicryl 4.0 (Southern Syringe Services, Leicester. UK). Immediately after surgery, mice were transferred to a “recovery” cage, which contained food and water, and maintained at a warm temperature using a heater. A full recovery was observed within 30 minutes post operation and mice were monitored daily thereafter to ensure their sutures had healed adequately and that they were not showing any signs of ill health. The experiment was terminated six weeks post injection; mice were culled and tumours were harvested and processed.

2.10.3 Treatment plan

Tumour cells alone or tumour cells in combination with stellate cells were injected subcutaneously into the right flank. The tumours were measured twice weekly and tumour volume calculated using the formula –

$$Length \times (breadth)^2 / 2.$$

Once the tumours reached $100mm^3$ the mice were assigned randomly to one of the four treatment arms.

Treatment arm 1 – β6 blocking antibody – 10mg/Kg per mouse.

Treatment arm 2 – Gemcitabine treatment – 100mg/Kg per mouse.

Treatment arm 3 – β6 blocking antibody (10mg/Kg) plus gemcitabine (100mg/Kg) per mouse.

Treatment arm 4 – IgG control antibody in PBS – 10mg/Kg per mouse.

The treatments were given intraperitoneally twice a week (200µl) (400µl for treatment arm 3). The antibody treatment continued for a period of 6 weeks. Mice were culled when the tumours reached the maximum allowed tumour size as per Home Office guidance or if the animal showed any sign of distress.

RESULTS CHAPTER I

3. Expression of αvβ6 in PDAC

3.1 Preliminary clinical study

A small number of clinical samples of PDAC (n= 34) and normal (n= 12) pancreas were stained for αvβ6 expression. Figure 30A shows typical labelling of αvβ6 in normal pancreas and PDAC (Figure 30B) tissue, showing strong expression on the cancer and none on the normal tissue. Table 11 shows that 100% of PDAC samples expressed αvβ6 in varying levels, with 38% expressing it strongly. This positivity was limited to epithelial cells with no apparent staining of stromal cells. This was in agreement with previously published literature where 100% of PDAC samples tested were positive for αvβ6 [201]. In contrast, all but 1 sample of normal pancreas samples were negative for αvβ6 expression. Having established expression of αvβ6 in tissue samples, the expression and functional roles of αvβ6 on PDAC cell lines were examined *in vitro*.

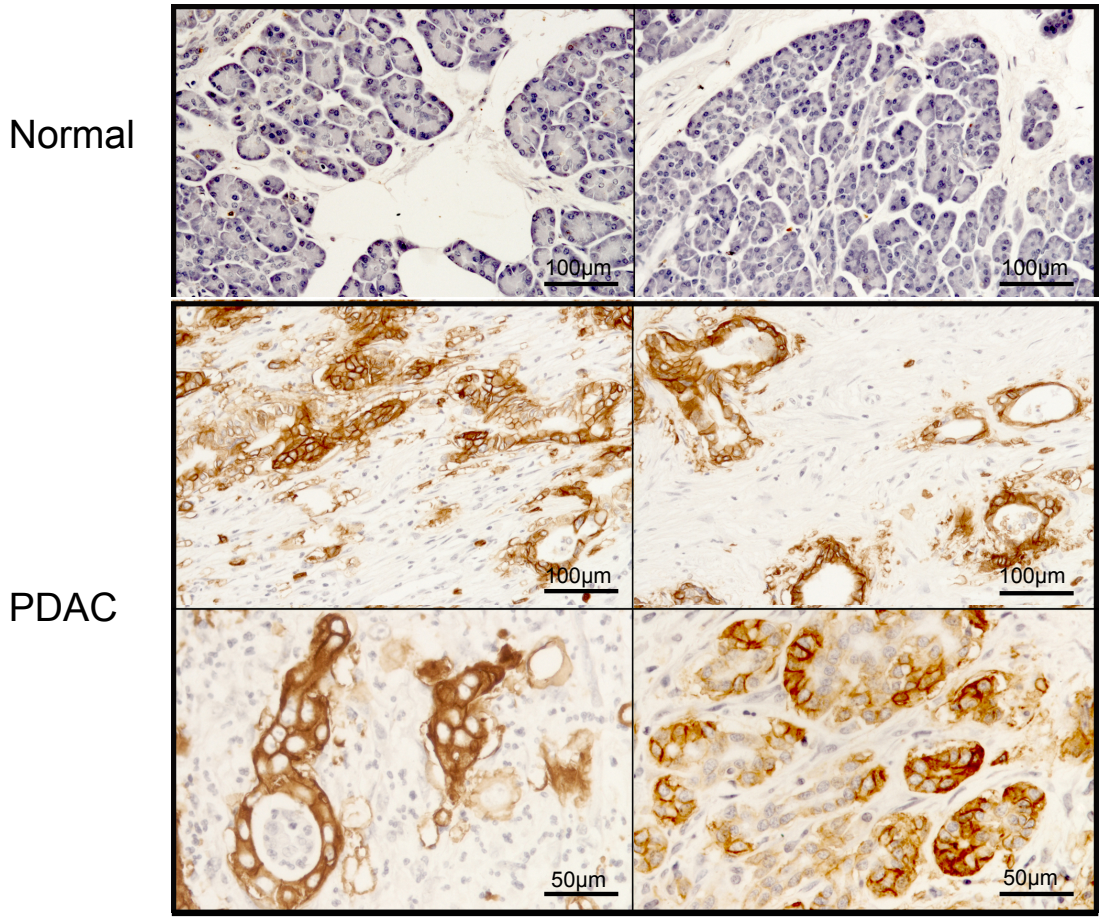

Figure 30: Expression of β6 on PDAC tissue samples. The normal pancreas was negative for β6 (A) whereas strong membranous expression was observed in PDAC tissue (B).

Cases	Negative	Low	Moderate	High
12 (normal)	11	1	0	0
34 (PDAC)	0	14	7	13

Table 11: Expression of αvβ6 in PDAC (n=34) and normal pancreas tissue (n=12) samples. Expression of αvβ6 varied in PDAC samples but 100% were positive with 38% expressing it strongly. Only 1 case of normal pancreas (n=12) showed low levels of staining for β6.

3.2 Flow cytometry screen of PDAC cell lines

Flow cytometry was used to screen a panel of 9 pancreatic cancer cell lines for a subset of RGD-dependent integrins using antibodies to αvβ3 (23C6), αvβ5 (P1F6), αvβ8 (14E5), α5 (P1F6) and αvβ6 (10D5); mouse IgG1 isotype (DAKO) was used as a negative control.

Cells in suspension were labelled with respective primary antibodies and the bound primary antibody detected using Alexa Fluor 488 conjugated secondary antibody (Figure 31). A Beckton Dickinson (BD) FACS Calibur flow cytometer machine was used to run the samples and results were analysed using Cell Quest Pro software to generate geometric mean fluorescence values (section 2.7). Flow cytometry experiments were performed regularly on cell lines routinely used for experiments to ensure that the expression profile of integrins did not vary between experiments.

A)

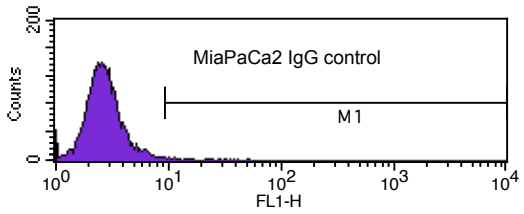

Marker	Left, Right	Events	% Gated	% Total	Geo Mean
All	1, 9910	10178	100.00	91.93	2.69
M1	9, 9910	62	0.61	0.56	14.69

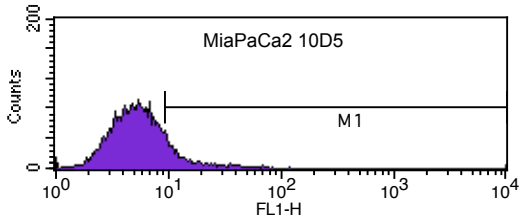

Marker	Left, Right	Events	% Gated	% Total	Geo Mean
All	1, 9910	10205	100.00	91.68	5.42
M1	9, 9910	1353	13.26	12.16	14.72

B)

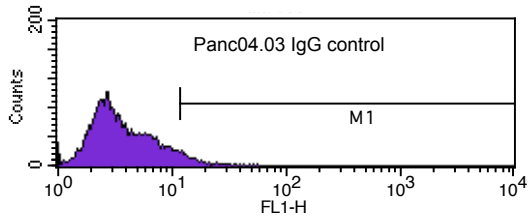

Marker	Left, Right	Events	% Gated	% Total	Geo Mean
All	1, 9910	9970	100.00	94.80	3.70
M1	12, 9910	440	4.41	4.18	15.14

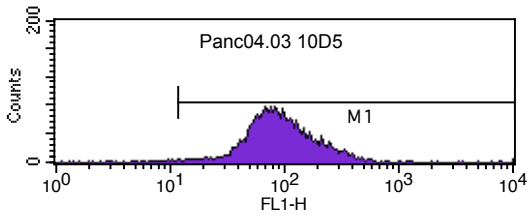

Marker	Left, Right	Events	% Gated	% Total	Geo Mean
All	1, 9910	9985	100.00	95.01	89.91
M1	12, 9910	9908	99.23	94.28	91.78

Figure 31: Representative flow cytometry histograms analysed using Cell Quest Pro software. A) an αvβ6 negative cell line, MiaPaCa2, stained with an IgG control and 10D5, an anti-αvβ6 antibody. B) an αvβ6 positive cell line Panc04.03 stained with an IgG control and 10D5, an anti-αvβ6 antibody (shift to the right of the purple curve denotes positivity). FL1-H is the excitation of alexa fluor 488.

Representative histograms showing αvβ6 expression in αvβ6 negative and αvβ6 positive cells lines are shown in Figure 31. Fluorescence intensity is plotted on a logarithmic scale on the x-axis, with shifts to the right denoting increased fluorescence. As data were rarely normally distributed, the geometric mean fluorescence intensity (MFI) was used.

Whilst MiaPaca2 cells were negative for αvβ6 expression, with a geometric mean of 5.42 (10D5) compared with 2.69 in cells stained for isotype control antibody, Panc04.03 cells demonstrated very strong expression of αvβ6. Geometric mean increased from 3.70 in the isotype control stained cells to 89.91 in the 10D5, anti-

αvβ6 antibody, treated cells. The data also show that approximately 99.23% of the gated population of Panc04.03 cells were positive for αvβ6 (Figure 31).

A panel of 9 pancreatic cancer cell lines (from ATCC), which originated from well differentiated or moderately/poorly differentiated PDAC tumours were screened for their integrin expression profile (Table 12). A subset of RGD-dependent integrins was screened together with αvβ6. α1 was expressed at low levels (geometric MFI between 11-20) in three out of the nine cell lines tested. The well differentiated cell lines tended to express more α1 compared to the poorly differentiated cell lines. In contrast, α2 was expressed in very high levels in all of the cell lines tested (geometric mean >100 in most cell lines) with the exception of MiaPaCa2 which was negative. α5 expression was relatively low (geometric mean between 11-20) but was expressed in five out of the nine cell lines tested, including MiaPaCa2. αvβ3 levels were also very low (geometric mean between 11-20) in the three cell lines that expressed it (CFPac1, BxPc3 and Panc1 stained positive). αvβ5 expression was low and expressed by five out of the nine cell lines tested regardless of their differentiation status (geometric mean between 11-20). αvβ8 expression was detected in three of the PDAC cell lines including CFPac1, AsPc1 and BxPc3. The levels of expression in these cells were very low (geometric mean between 11-20). αvβ6 was expressed in seven out of the nine cell lines tested in varying levels. The well differentiated cells expressed significantly higher levels (geometric mean between 21-100) compared with the moderately/poorly differentiated cell lines (geometric mean between 1-50).

	Well differentiated				Poorly/moderately differentiated			
Cell line	CFPac1	Capan1	Colo357	Panc0403	HPAF	AsPc1	BxPc3	Panc1	MiaPaCa2
α 1	++	++	++	+	-	-	+	-	-
α 2	+++	++++	+++	++++	+++	++++	++++	+++	-
α 5	+	-	-	+	-	-	+	+	+
αvβ3	+	-	-	-	-	-	+	+	-
αvβ5	+	+	-	++	-	+	-	++	-
αvβ6	++	++	++	+++	+++	+	++	-	-
αvβ8	+	-	-	-	-	+	+	-	-

Geometric Mean (MFI): 1-10 (-); 11-20 (+); 21-50 (++); 51-100 (+++); >100 (++++)

Table 12: Integrin screen of a panel of PDAC cell lines by flow cytometry. 8 out of 10 cell lines expressed αvβ6 at varying levels.

Data shown in Table 12 represent the mean of a minimum of two experiments, each performed in triplicate. Geometric mean fluorescence intensity was converted to a 'plus' score according to the key after subtracting the negative control (IgG score). It was shown that 7 out of 9 pancreatic cancer cell lines express αvβ6 endogenously in varying levels (Table 12). Expression levels of αvβ6 were highest in well-differentiated cell lines (Panc04.03, CFPac1, HPAF) compared to the poorly differentiated cell lines (AsPc1, Panc1, MiaPaCa2). BxPc3 was a moderately differentiated cell line expressing αvβ6 with a geometric mean of about 40 (Figure 32). In summary, the flow cytometry integrin analysis is consistent with the preliminary clinical study, since the majority of the cell lines expressed αvβ6 as did the PDAC tissues.

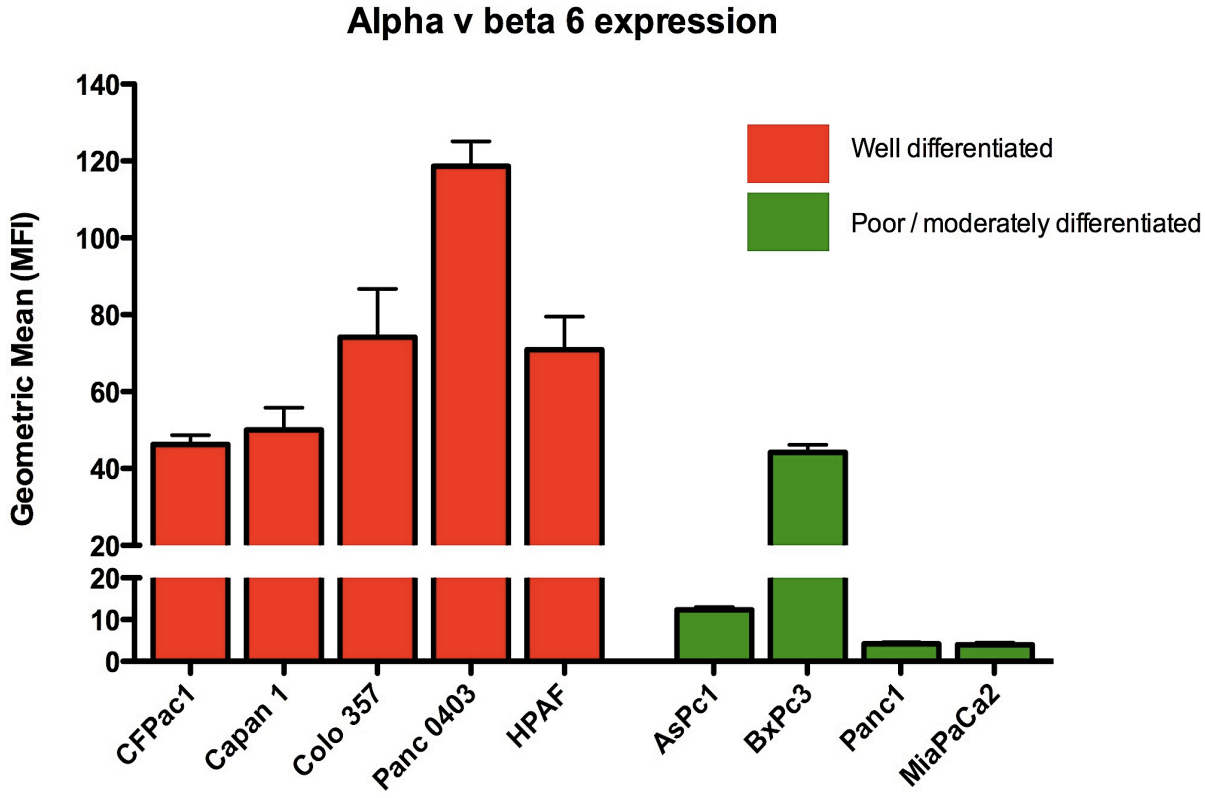

Figure 32: Expression of αvβ6 in PDAC cell lines grouped based on their differentiation status. Mean fluorescent intensity is represented by geometric mean values calculated using Cell Quest Pro software.

3.2.1 Integrin screen on pancreatic stellate cell line PS1

Pancreatic stellate cells isolated and immortalised in house in the laboratory, PS1 cells, were screened using flow cytometry for the same subset of RGD-dependent integrins as described previously and a few additional relevant integrins expressed by stromal cells (section 2.7).

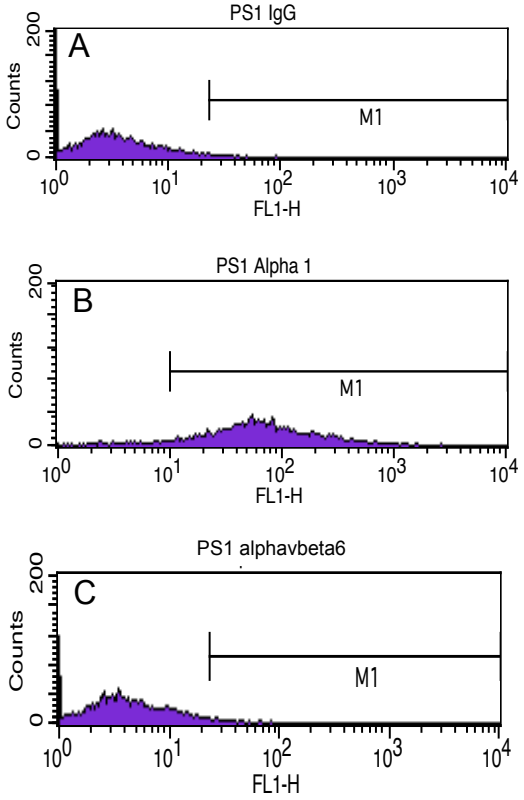

Marker	Left, Right	Events	% Gated	% Total	Geo Mean
All	1, 9910	5341	100.00	88.12	3.56
M1	23, 9910	53	0.99	0.87	35.58

Marker	Left, Right	Events	% Gated	% Total	Geo Mean
All	1, 9910	5345	100.00	89.79	60.08
M1	10, 9910	5155	96.45	86.59	65.98

Marker	Left, Right	Events	% Gated	% Total	Geo Mean
All	1, 9910	5313	100.00	88.56	4.27
M1	23, 9910	89	1.68	1.48	34.09

Figure 33: Representative histograms showing integrin expression in PS1 cells (pancreatic stellate cells) analysed using Cell Quest Pro software. IgG isotype staining is shown in (A). (B) shows integrin subunit α1 expression at high levels with a geometric mean of 60.09 (histogram shifts to the right). (C) shows that there is no αvβ6 expression in these cells (histogram shifts back to the left) with a geometric mean of 4.27, which is similar to the IgG control expression level.

Typical histograms are shown in Figure 33 and data from three separate experiments are summarised in Table 13. PS1 cells expressed high levels of α1 (geometric mean between 50-100) and α2, the latter at similar expression levels observed in the PDAC cell lines tested previously. PS1 cells expressed lower levels of α5 subunit (geometric mean between 21-50) but no α8 or α9 expression was detected. Both αvβ3 and αvβ5 were expressed at similar levels (geometric mean between 21-50).

However, PS1 cells did not express any αvβ6 or αvβ8 (geometric mean between 1-10).

Integrin Screened	Expression levels
α1	+++
α2	++++
α5	++
α8	-
α9	-
αvβ3	++
αvβ5	++
αvβ6	-
αvβ8	-

Geometric Mean (MFI): 1-10 (-); 11-20 (+); 21-50 (++); 51-100 (+++); >100 (++++)

Table 13: Integrin screen of PS1 (pancreatic stellate cells) cells. Data shown in the table represent the mean of three experiments performed in triplicate. Geometric mean fluorescence intensity was converted to a 'plus' score according to the key.

3.3 Western blotting to detect expression of β6

After establishing expression of αvβ6 at the cell surface of PDAC cell lines by flow cytometry, whole cell lysates were prepared to examine total cellular expression of β6 using Western blotting. The data in Figure 34 show endogenous expression of αvβ6, consistent with flow cytometry data. The double band observed is believed to be due to recognition of both the smaller immature (not fully glycosylated) and larger mature (fully glycosylated) form of β6 (determined in house in oral cancer cell lines, unpublished).

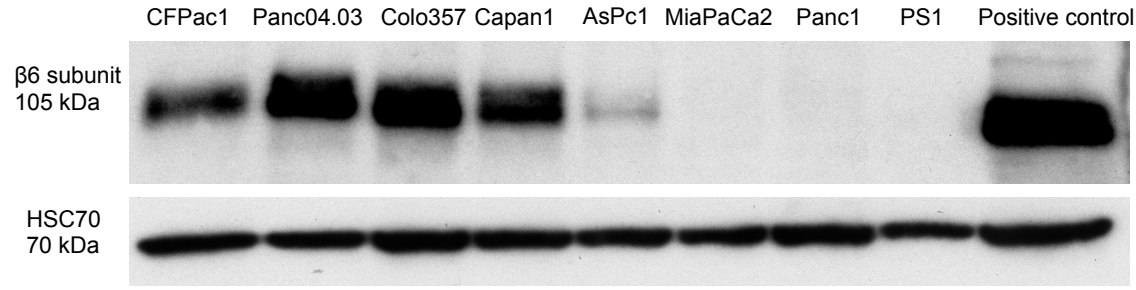

Figure 34: Western blotting of β6 from whole cell lysates from PDAC cell lines. β6 was detected using C19 polyclonal antibody (Santa Cruz Ltd) and HSC70 antibody used to confirm equal loading of samples. Image is representative of two independent experiments.

The genetically engineered melanoma cell lines, DX3β6, was used as a positive control. These cells express very high levels of αvβ6 compared with the endogenous levels of expression seen in PDAC cell lines. There were varying levels of expression of αvβ6 in the PDAC cell lines tested, and these generally were similar to the results observed using flow cytometry. PS1 cell line was negative for αvβ6 expression.

Thus, two separate methodologies were used to confirm β6 expression in a panel of PDAC cell lines. Based on the data obtained, Panc04.03, CFPac1 were the two positive cell lines selected and MiaPaca2 and Panc1 were the two negative cell lines picked for all further *in vitro* experiments.

3.4 Immunofluorescence labelling of αvβ6

CFPac1, Panc04.03 (αvβ6 positive cell lines) and Panc1 (αvβ6 negative cell line) were cultured as monolayers on coverslips and labelled for αvβ6 using 53A.2, a rat monoclonal anti-β6 antibody, and Alexa Fluor 488 was used to detect bound antibody. The cells were imaged using a confocal laser-scanning microscope (LSM 510, Ziess) (section 2.6.2).

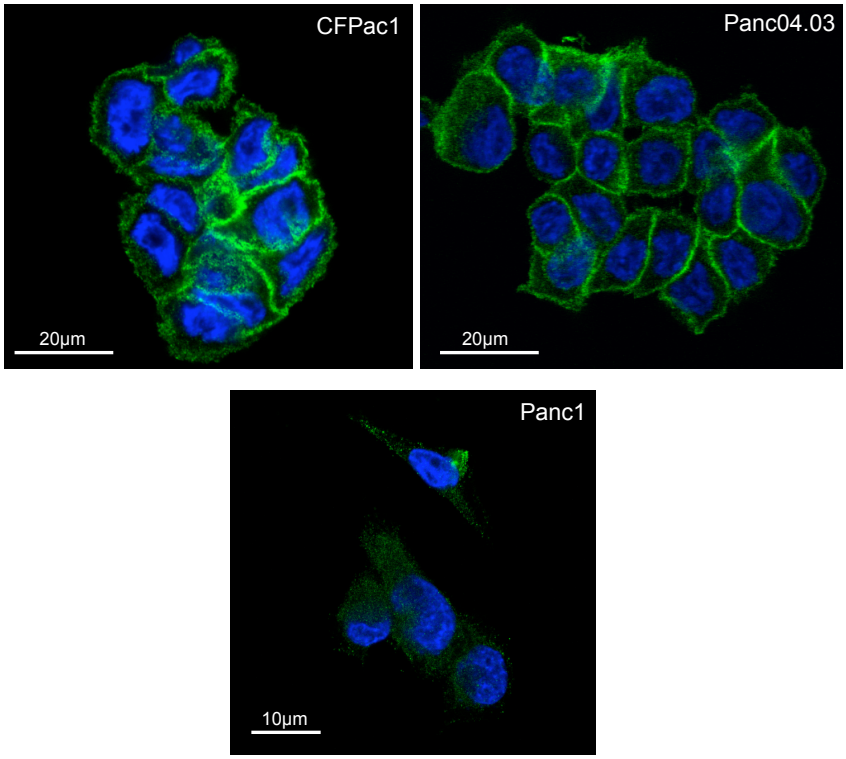

Figure 35: Expression of αvβ6 in PDAC cell lines using indirect immunofluorescence. Strong expression of αvβ6 in the cell membrane was observed in CFPac1 and Panc04.03 (green) while Panc1 cells showed weak cytoplasmic staining in the cytoplasm at background levels. Nuclei were labelled in blue (DAPI) and imaged using a confocal microscope.

αvβ6 was strongly expressed on the membrane of the two positive cell lines, particularly at the cell-cell junctions but was absent in the αvβ6 negative cell line (Figure 35), consistent with the flow cytometry and Western blotting data. Integrin αvβ6 was expected to be present on cells and the pattern of expression observed in cells was similar to human PDAC tissue samples stained for αvβ6 (Figure 30).

.

3.5 Functional role of αvβ6 in PDAC cell lines

3.5.1 Role of αvβ6 in PDAC cell proliferation

Uncontrolled cancer cell proliferation is considered to be the primary cause for tumour formation, thus cell proliferation has been the principal target in attempts to reduce tumour growth. So far there has been only one paper published where αvβ6 has been linked with PDAC cell proliferation. This study investigated whether blockade of αvβ6 function could affect growth of PDAC cell lines. Singh et al showed that knock down of β6 in the YAPC pancreatic cancer cell line resulted in a reduction of cell growth by 60%-80% [207].

3.5.1.1 Antibody blockade of proliferation in PDAC cell lines

Three different antibodies targeting αvβ6 were used for this study: 10D5 (mouse monoclonal antibody), 53A.2 (rat monoclonal antibody), 264RAD (human monoclonal antibody). All the antibodies have been established as αvβ6 function blocking antibodies [233] and both 53A.2 and 10D5 are available commercially.

CFPac1, Panc04.03 (αvβ6 positive) and Panc1, MiaPaCa2 (αvβ6 negative) cell lines were used for the proliferation assay, which was performed over 7 days. Once the appropriate cell numbers per well were optimised (3000 per well, established prior to assays, data not shown) cells were plated onto 96 well plates at day -1 (prior to antibody treatment). On day 0, αvβ6 function-blocking antibodies were added at multiple concentrations ranging from 0.2μg/ml to 10μg/ml. At day 4, the antibody was replaced (fresh media added) and the assay left till day 7. The control wells had an isotype negative control antibody at the respective concentrations and a no treatment well with only growth media was used as an additional control. Both the αvβ6 blocking antibodies and the control isotype antibody were prepared in 10% serum containing growth media. After 7 days an MTT assay was performed to quantify cell survival.

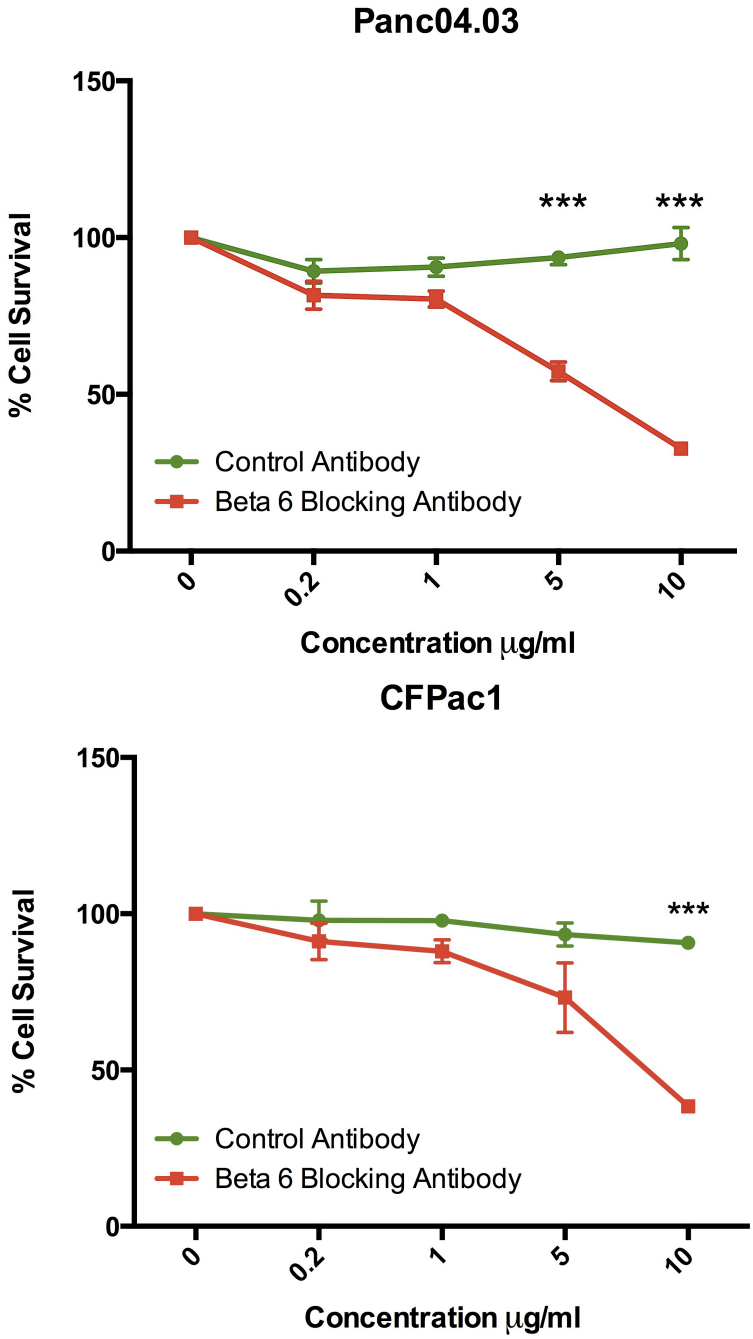

Figure 36: The effect of αvβ6 blocking antibody 53A.2 on *in vitro* growth of PDAC cell lines. Cell survival was quantified by MTT assay on day 7 and survival normalised to that of untreated cells. Results show that there is a significant reduction in proliferation (***) in the two αvβ6 positive cell lines Panc04.03 (top) and CFPac1 (bottom) when treated with a αvβ6 function blocking antibody 53A.2 at varying concentration compared to the control isotype IgG antibody. Student's t-test p= <0.0004 (Panc04.03) and p= <0.0008 (CFPac1). The graphs represent the mean and +/- standard error of mean of three experiments performed with replicates of four per dose in each experiment.

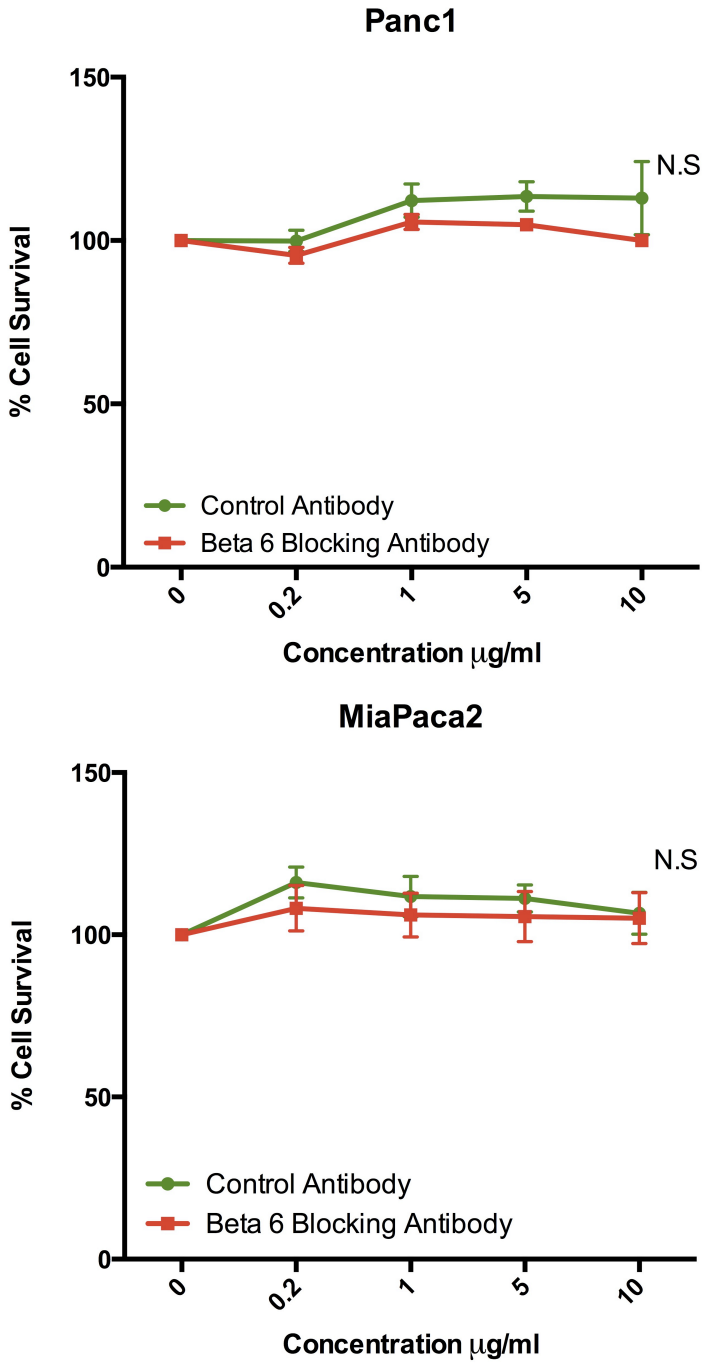

Figure 37: The effect of αvβ6 blocking antibody 53A.2 on *in vitro* growth of PDAC cell lines. Cell survival was quantified by MTT assay on day 7 and survival normalised to that of untreated cells. Results show that there is no reduction in proliferation in the two αvβ6 negative cell lines, Panc1 (top) and MiaPaCa2 (bottom) when treated with the αvβ6 function blocking antibody 53A.2 at varying concentrations compared to the control IgG isotype antibody. (Student's t-test non significant). The graphs represent the mean and +/- standard error of mean of three experiments performed with replicates of four per dose in each experiment.

The results shown in Figure 36 demonstrated that there was a significant reduction in the total percentage of αvβ6 positive cells that are alive after 7 days when treated with the αvβ6 function blocking antibody, 53A.2. Thus at 5μg/ml there is a 44% reduction in growth and this increased to 67% reduction at 10μg/ml in Panc04.03 cells. Similarly growth of CFPac1 in the presence of 10μg/ml 53A.2 was reduced by 62% after 7 days compared to the equivalent concentration of the isotype control antibody. It must be noted the MTT assay used measures mitochondrial metabolic activity as a surrogate measure of growth but does not measure cell number. The results in Figure 37 showed that the same antibody when used to treat two αvβ6 negative cell lines, Panc1 and MiaPaCa2, at the same concentrations over 7 days showed no significant difference in the percentage of cells that were alive. All four cell lines were set up for the cell survival assay at the same time under the same conditions. The 53A.2 used for performing the above experiments was purified from hybridoma supernatant by Dr. Veronika Jenei, University of Southampton, UK.

To confirm that the results in Figure 36 were due to blockade of αvβ6, and were not an irrelevant side effect of 53A.2, the proliferation assays were repeated with the function-blocking antibody 264RAD from Astra Zeneca-Medimmune. 264RAD antibody is a human antibody and has been shown to bind specifically to β6 and block human and mouse tumour growth *in vivo* [233].

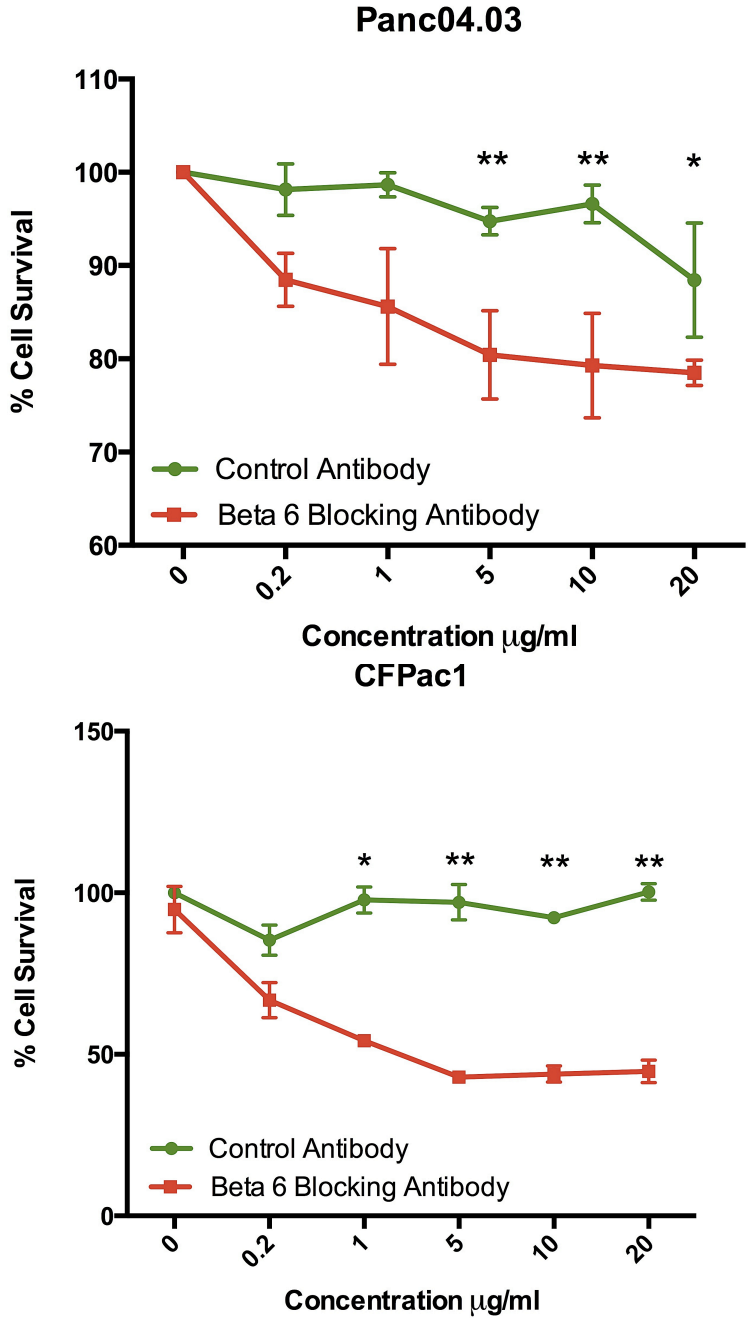

Figure 38: The effect of αvβ6 function blocking antibody 264RAD on *in vitro* growth of PDAC cell lines. Cell survival was quantified by MTT assay on day 7 and survival normalised to that of untreated cells. Results show that there is a significant reduction in proliferation (*/) in the two αvβ6 positive cell lines Panc04.03 (top) and CFPac1 (bottom) when treated with a αvβ6 function blocking antibody 264RAD at varying concentration compared to the control isotype IgG antibody. Student's t-test *p= <0.05, ** <0.005. The graphs represent the mean and +/- standard error of mean of three experiments performed with replicates of four per dose in each experiment.**

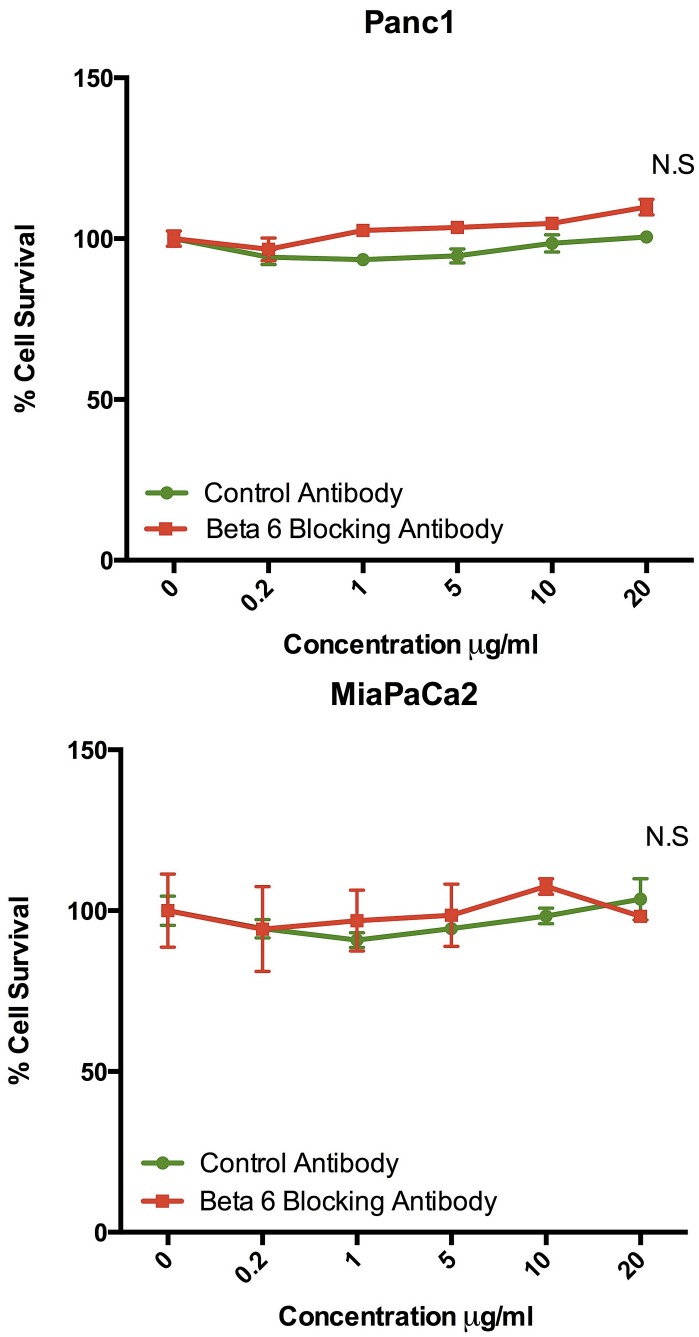

Figure 39: The effect of αvβ6 blocking antibody 264RAD on *in vitro* growth of PDAC cell lines. Cell survival was quantified by MTT assay on day 7 and survival normalised to that of untreated cells. Results show that there is no reduction in proliferation in the two αvβ6 negative cell lines, Panc1 (top) and MiaPaCa2 (bottom) when treated with the αvβ6 function blocking antibody 264RAD at varying concentrations compared to the control IgG isotype antibody. (Student's t-test non significant). The graphs represent the mean and +/- standard error of mean of three experiments performed with replicates of four per dose in each experiment.

264RAD was used at the same concentration range as that of 53A.2. Astra Zeneca also provided an isotype human IgG control antibody, which was used as the negative control. The graphs in Figure 38 again showed that there was a significant reduction in the total percentage of cells that are alive after 7 days when treated with the αvβ6 function blocking antibody, 264RAD at 5μg/ml, 10μg/ml and 20 μg/ml concentration for Panc04.03 and CFPac1 compared to the equivalent concentration of the isotype control antibody. There was a reduction in cell numbers up to about 30%-40% in the treated group at varying concentrations for Panc04.03 and a reduction of 50%-55% in the treated group at varying concentrations for CFPac1. In contrast, the data in Figure 39 showed that the same antibody when used to treat two αvβ6 negative cells, Panc1 and MiaPaCa2, at the same concentrations over 7 days evoked no significant difference in growth.

3.5.2 A20FMDV2 Ad5 knob protein mediated blockade of αvβ6

Previous studies from our laboratory have generated a recombinant adenovirus type 5 (Ad5) fibre knob protein incorporating a peptide (A20FMDV2) that specifically binds to and inhibits αvβ6 [234]. This A20FMDV2 knob protein was tested for its effects on the growth of PDAC cell lines.

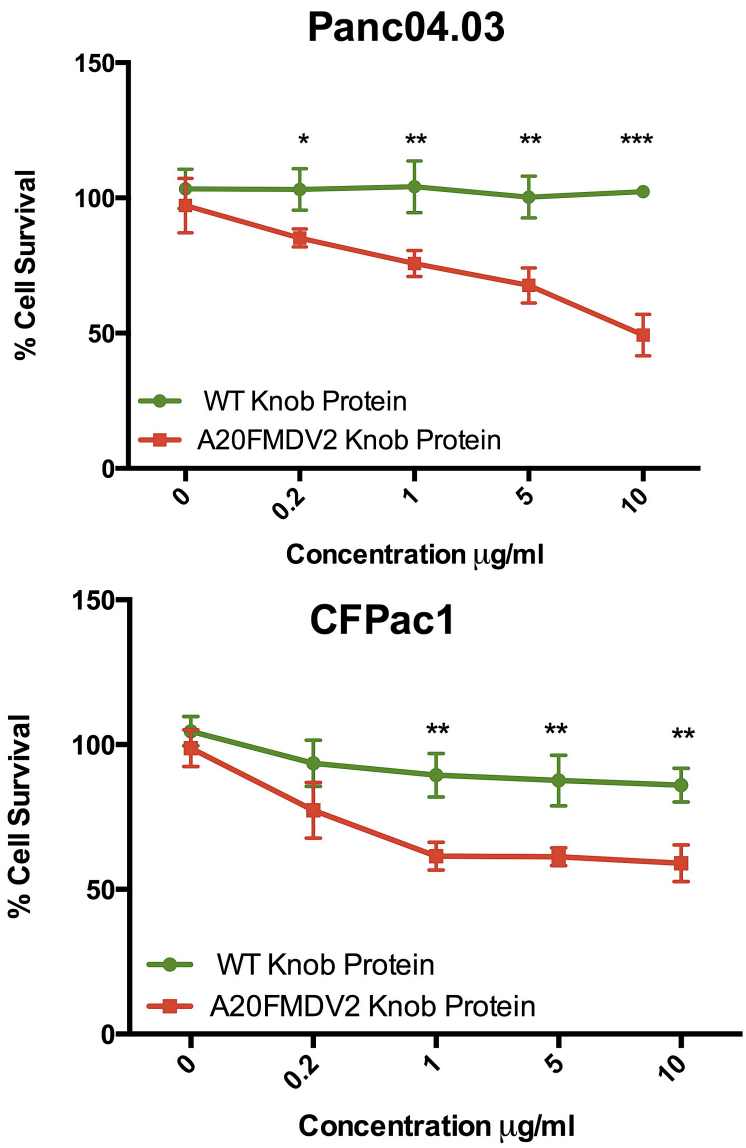

Figure 40: The effect of αvβ6 blocking protein A20FMDV2 knob protein on *in vitro* growth of PDAC cell lines. Cell survival was quantified by MTT assay on day 7 and survival normalised to that of untreated cells. Results show that there is a significant reduction in proliferation in the two αvβ6 positive cell lines Panc04.03 (top) and CFPac1 (bottom) when treated with a αvβ6 function blocking A20FMDV2 knob protein at varying concentration compared to the control wild-type knob protein. Student's t-test * p= <0.05, ** p= <0.001 and *** p=<0.0001. The graphs represent the mean and +/- standard error of mean of three experiments performed with replicates of four per dose in each experiment.

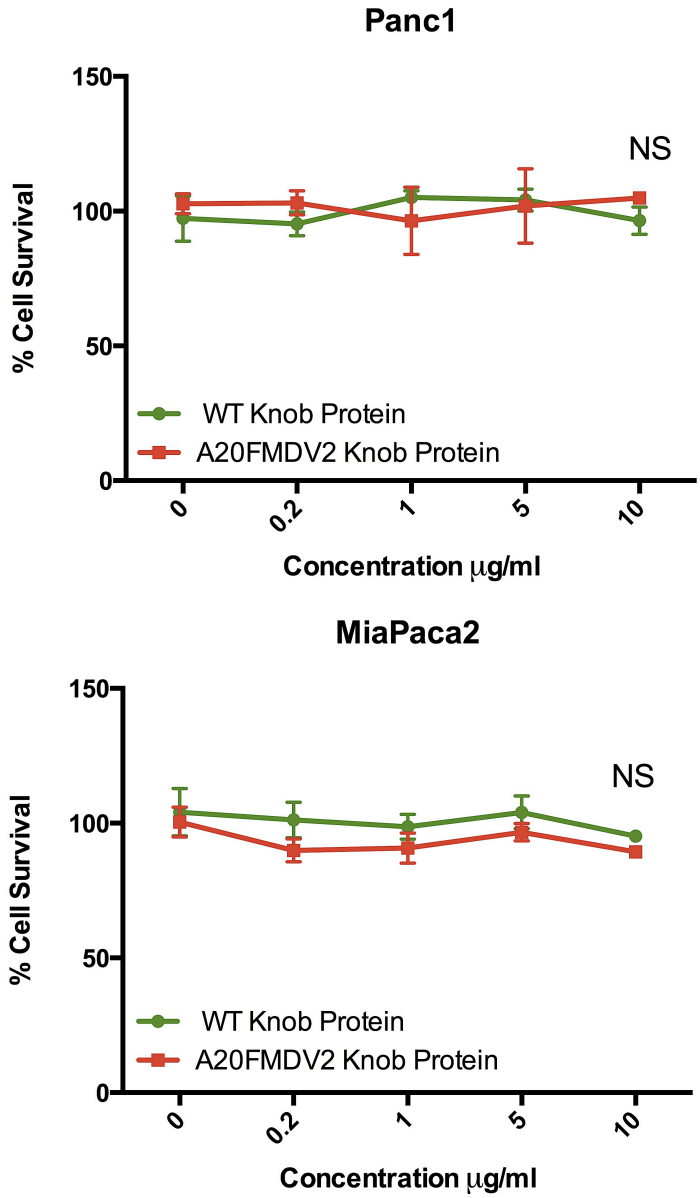

Figure 41: The effect of αvβ6 function blocking A20FMDV2 knob protein on *in vitro* growth of PDAC cell lines. Cell survival was quantified by MTT assay on day 7 and survival normalised to that of untreated cells. Results show that there is no reduction in proliferation in the two αvβ6 negative cell lines, Panc1 (top) and MiaPaCa2 (bottom) when treated with the αvβ6 function blocking A20FMDV2 knob protein at varying concentrations compared to the control wild type knob protein. (Student's t-test non significant). The graphs represent the mean and +/- standard error of mean of three experiments performed with replicates of four per dose in each experiment.

With the assistance of Dr. Lynda Coughlan, an Ad5 knob protein and a control wild type knob protein (without A20FMDV2) were generated as described previously [234]. The data in Figure 40 showed that there was a significant reduction in the total percentage of PDAC cells that were alive after 7 days when treated with the αvβ6 function blocking A20FMDV2 Ad5 knob protein at 0.2μg/ml, 1μg/ml, 5μg/ml and 10μg/ml concentration for Panc04.03 and for CFPac1 at 1μg/ml, 5μg/ml and 10μg/ml compared with the equivalent concentration of the wild type knob protein. Thus, at 10 μg/ml there was a 51% reduction in growth of Panc04.03 and a 43% reduction in growth of CFPac1 and these changes were significant ($p=<0.0001$ and $p=<0.001$ respectively). Again, in contrast, the data in Figure 41 showed that the same A20FMDV2 Ad5 knob protein when used to treat two β6 negative cell lines, Panc1 and MiaPaCa2, at the same concentrations over 7 days induced no significant difference in the percentage of cells that were alive after 7 days, relative to the same concentrations of wild-type knob protein.

3.5.3 Attempts to knock down of β6 using siRNA to inhibit proliferation

Since two blocking antibodies and a blocking adenoviral protein produced a similar reduction in proliferation in the αvβ6 positive cell lines, a genetic knock down of β6 using siRNA was performed to observe if the effect on proliferation could be reproduced. Multiple attempts to achieve a significant knock down of β6 in Panc04.03 and CFPac1 cells proved unsuccessful. Despite various optimisation steps to the lipid mediated siRNA protocol a significant reduction in levels of β6 expression was never achieved (data not shown). In order to confirm if the siRNA sequences were targeting the correct gene, the Capan1 cell line (another αvβ6 positive cell line) was used together with a positive control for αvβ6 expression (A375β6 puro – a melanoma cell line).

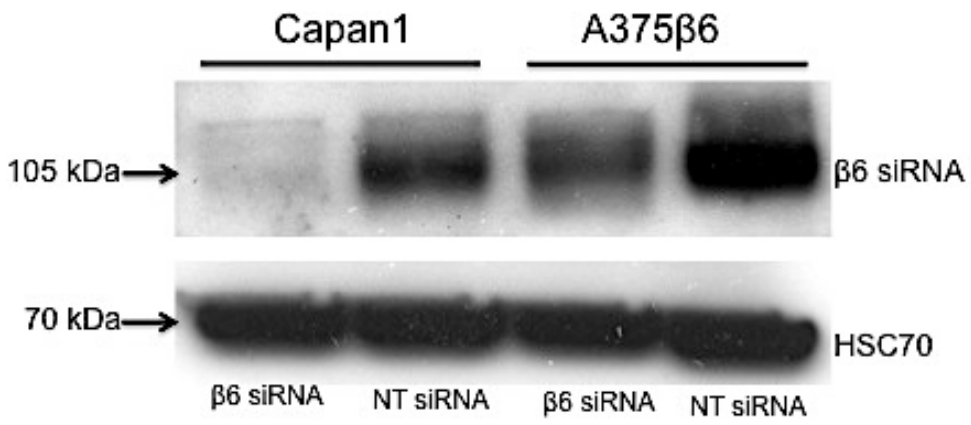

Figure 42: Western blot to confirm knock down of β6 in Capan1 and A375β6P cell lines using Oligofectamine™ 5 days post transfection. HSC70 was used as a loading control. (NT- non-targeting).

siRNA was purchased from Dharmacon Ltd (gene pool with four individual sequences) to target β6 specifically. A non-targeting siRNA sequence was purchased from the same company. 5 days post transfection; the cells were lysed and quantified using pico green (DNA binding dye) and read at 450nm in a spectrophotometer. Figure 42 confirmed that the β6 siRNA knock down technique was working and suggested that the two positive cell lines used in previous experiments happened to be difficult to transfect using the lipid mediated transfection techniques. Fellow colleagues in the laboratory who have used the two cell lines (Panc04.03 and CFPac1) for siRNA-mediated knock down of other proteins using lipid mediated transfection reagents have encountered similar problems, indicating this was not a consequence of my technique.

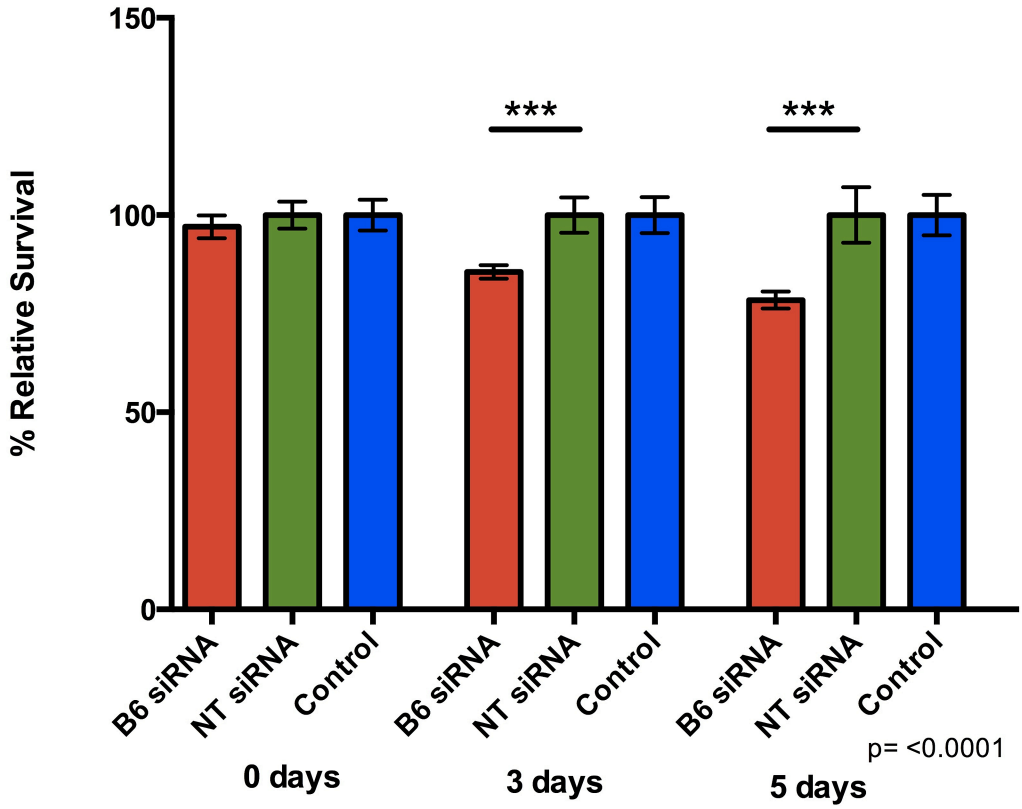

Figure 43: Histogram above shows a significant reduction (***) in proliferation of Capan1 cells over 5 days when β6 is knocked down specifically (red bars). The non-targeting (NT) siRNA had no effect on the cells (green bars). Control cells are grown without any treatment in the growth media. Student's t-test p= <0.0001 (***). The histogram above represents the mean and +/- standard error of mean of two experiments performed with replicates of six per treatment in each experiment.

The data in Figure 43 showed that inhibiting β6 at the mRNA level reduced cell proliferation in Capan1 cells similar to the effect of αvβ6 function-blocking antibodies, albeit observed in different cell lines. There was a significant reduction in proliferation from day 3 post transfection (20% decrease) compared to the NT siRNA treated cells. By day 5 post transfection there was a further dip in the rate of proliferation (30%) compared with the NT siRNA treated cells. The control cells served as an additional negative control to ensure the transfection protocol alone did not affect cell growth. It is worth noting that the reduction in proliferation when β6 is knocked down is less than that observed when using the αvβ6 function-blocking antibodies (30% inhibition compared with >50% using 53A.2). Whilst it would have been ideal to directly compare the effects of blocking antibodies and β6 knock down in the same

cell lines, the fact that neither Panc04.03 nor CFPac1 cell lines could be transfected with β6 siRNA meant that an alternative cell line (Capan1) had to be utilised.

3.5.4 Effect of αvβ6 blocking antibody on the growth of PS1 cells

The majority of the PDAC stroma is comprised of the pancreatic stellate cells and pancreatic fibroblasts along with other stromal cells. Our laboratory had isolated and characterised pancreatic stellate cells, termed PS1. As these will be used later (section 2.9.4) for *in vivo* xenograft models, it was essential to test the effect of the β6 function blocking antibody 264RAD on the growth of PS1 cells. 3000 cells per well were plated onto 96 well plates at day -1 (prior to antibody treatment). On day 0, αvβ6 function blocking antibody was added at multiple concentrations ranging from 0.2µg/ml to 10µg/ml. At day 4, the antibody was replenished (fresh media with antibody added) and left until day 7. The control wells had an isotype negative control antibody at the respective concentrations and a no treatment well with only growth media was used as an additional control. Both the β6 blocking antibody and the control isotype antibody were prepared in 10% serum containing growth medium. The data in Figure 44 showed that there was no significant difference in proliferation of the pancreatic stellate cell line PS1 when treated with αvβ6 blocking antibody 264RAD compared with the control isotype IgG antibody used at the same concentration.

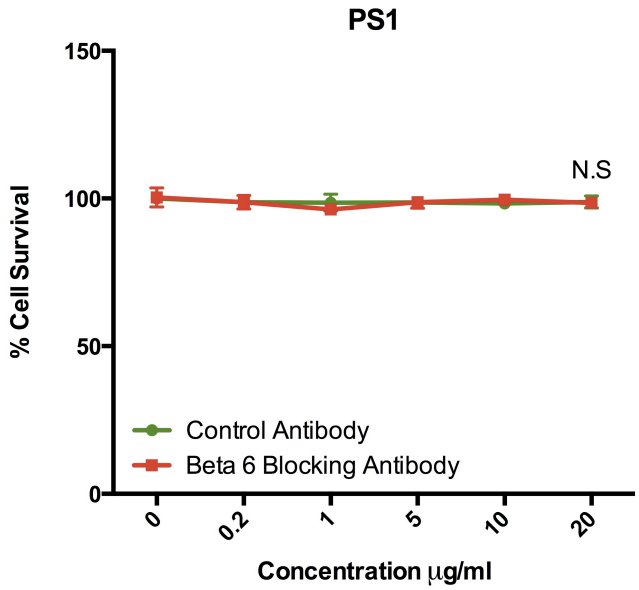

Figure 44: The effect of 264RAD function blocking antibody on *in vitro* growth of PS1 cell line. Cell survival was quantified by MTT assay on day 7 and survival normalised to that of untreated cells. Results show that there is no reduction in proliferation. (Student's t-test non significant). The graphs represent the mean and +/- standard error of mean of two experiments performed with triplicates per dose in each experiment.

3.6 Effect of αvβ6 blockade on cell cycle progression

Blockade of αvβ6 using a function blocking antibody or αvβ6 specific protein led to a significant reduction in proliferation in the two αvβ6 positive cell lines tested (Panc04.03 and CFPac1) and had no effect on the αvβ6 negative cell lines (Panc1 and MiaPaCa2). The antibodies had maximum effect on proliferation when used at a final concentration of 10μg/ml final concentration. Since the difference in proliferation was dramatic compared to the isotype control antibody in these cell lines a cell cycle analysis was performed to understand how the reduction in proliferation was achieved.

Panc04.03, CFPac1 (αvβ6 positive cell lines) and Panc1 (αvβ6 negative cell line) were treated with the αvβ6 blocking (53A.2) or the control antibody at 10μg/ml for a period of four and seven days. Residual adherent cells were harvested and added to floating cells in the supernatant and treated with propidium iodide (PI), a DNA binding dye. PI binds to the DNA in the cells and thus the cell cycle profile was analysed by flow cytometry.

The two αvβ6 positive cell lines, Panc04.03 and CFPac1, showed a significant difference in their cell cycle profile when treated with the αvβ6 blocking antibody 53A.2 at 10µg/ml over seven days compared with the control IgG antibody treated cells, while there was no effect on the αvβ6 negative cell line, Panc1 (Figure 45). In Panc04.03 cells, there was a significant increase in cells in G2/M phase (Figure 46), whilst in CFPac1 cells a significant increase was observed in the sub-G1 phase (Figure 46). In all the three cell lines tested, there were a high percentage of cells in the Gap1 (G1) phase of the cell cycle (Figure 45 white bar). This is typical to cells when left in culture for a week, although this high percentage (e.g. >80% of Panc04.03) could potentially have masked any subtle differences in other stages of the cell cycle. There was no change in the percentages of cells in the synthesis (S) phase, (DNA replication) or in the >4N phase (polyploid cells) in all the cell lines tested.

In contrast, there was a significant increase in the percentage of cells arrested in the Gap 2/Mitosis (G2/M) phase in Panc04.03 when treated with the αvβ6 blocking antibody (Figure 46) compared with the untreated cells or the IgG control antibody, from 6.5% to 16%. CFPac1 cells treated with the αvβ6 blocking antibody showed a significant increase in the sub-G1 population, from 8.5% to 46%, compared with the untreated or IgG antibody treated cells (Figure 46). Sub-G1 population usually is an indicator of cell death and an increase in percentage of the sub-G1 population suggested that there were dying or dead cells. This could be due to the fact that the treated cells went through apoptosis as a result of blocking αvβ6 function.

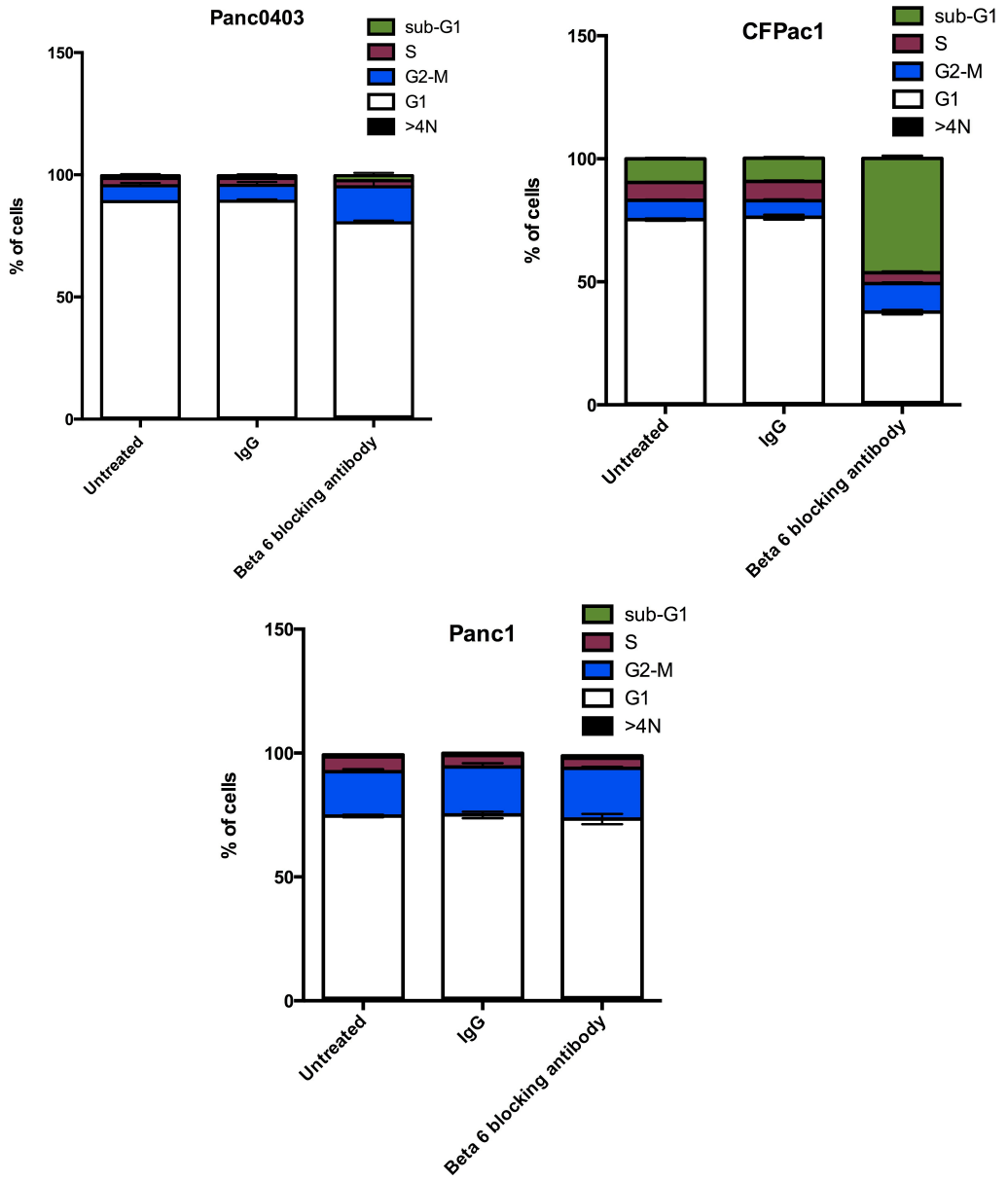

Figure 45: Cell cycle analysis of Panc04.03, CFPac1 and Panc1 cells when treated with the αvβ6 blocking antibody 53A.2 at 10 µg/ml over 7 days. There was an increase in the percentage of cells in G2/M phase (blue) in the antibody treated Panc04.03 cells and an increase in the percentage of cells in the sub-G1 (green) in the antibody treated CFPac1 cells. No differences in cell cycle profile were observed in the Panc1 (αvβ6 negative) cells when treated with the antibody. The data represents the mean and +/- standard error of mean of two experiments performed with triplicates per experiment.

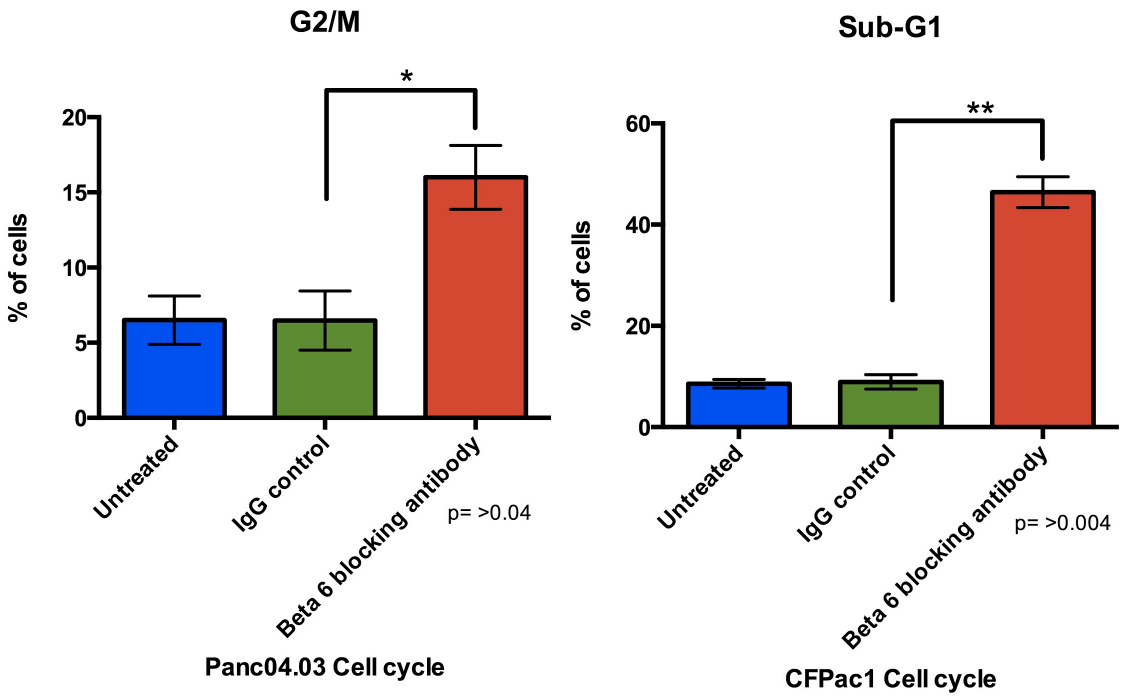

Figure 46: Histograms showed a significant increase in the percentage of cells in different phases of the cell cycle in the αvβ6 antibody (53A.2) treated cells. The G2/M phase (*) in Panc04.03 and Sub-G1 (**) (red bars) in CFPac1 cells were significantly higher when compared to the control isotype antibody (green bars). Student's t-test p= >0.04 (*) p= >0.004 (**). The data represent the mean and +/- standard error of mean of two experiments performed with triplicates per experiment.

3.7 Effect of αvβ6 blockade on downstream signalling pathways in PDAC cell lines

In order to further investigate the apparent cell cycle arrest (G2/M) and apoptosis observed in cells treated with the αvβ6 blocking antibody 53A.2, downstream signalling pathways were investigated. There are very few studies detailing the signalling pathways associated with ligation of the αvβ6 integrin. Investigations on interaction of αvβ6 with other proteins have begun to shed more light on its effects on cellular functions. ERK-2 and Fyn are the only two 'classical' signalling molecules, which have been reported to bind directly to αvβ6 and, as a consequence, evoke a functional response down stream [181, 190].

Panc04.03 and CFPac1 cells were treated with the αvβ6 blocking antibody 264RAD or a control isotype IgG at 10μg/ml over a time period of 24 to 96 hours. Every 24 hours, the cells and the supernatant were harvested and whole cell lysates were prepared. These lysates were probed for the two molecules that have been shown to interact with β6, ERK and Fyn, by Western blotting. Due to the significant increase of sub-G1 phase in the cell cycle analysis, expression levels of caspase 3 were also investigated.

3.7.1 Expression levels of ERK in αvβ6 blocked PDAC cell lines

Whole cell lysates were prepared and subjected to SDS PAGE and the membranes were probed for phospho ERK, stripped and probed for total ERK. HSC 70 was a loading control and was probed in the same blot (molecular weight 70kDa). There was no striking difference in the expression levels of phospho ERK or total ERK in the CFPac1 cells (molecular weight 41-42kDa) that were treated with the αvβ6 function-blocking antibody compared to the control antibody over 24 to 96 hours time period (Figure 47). There was a slight, but reproducible, reduction in expression of phospho ERK in αvβ6 blocking antibody treated cells compared with the control antibody treated cells at 24 and 48 hours, with expression reduced by 18% and 24% respectively. No difference in phospho ERK expression was observed at 72 and 96 hours. This result suggested that the effect on proliferation observed when treated with the αvβ6 blocking antibody may be dependent on ERK and its interaction with αvβ6 in the CFPac1 cell line.

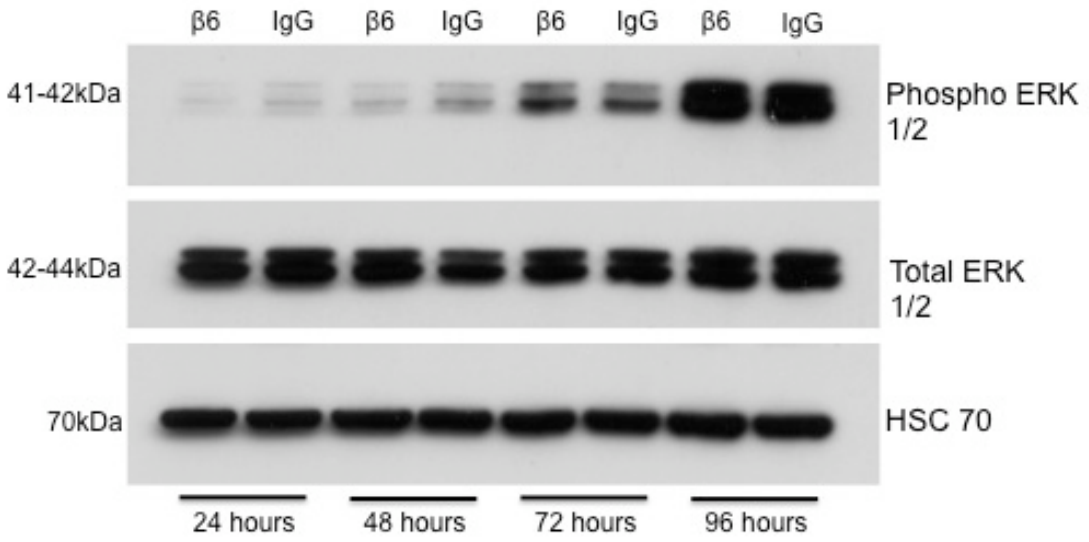

Figure 47: Western blot probing for phospho and total ERK 1/2 in CFPac1 cells treated with 264RAD αvβ6 blocking antibody or control IgG isotype antibody at 10µg/ml for 24, 48, 72 and 96 hours. HSC70 served as a loading control. The above image is representative of two experiments carried out under the same conditions.

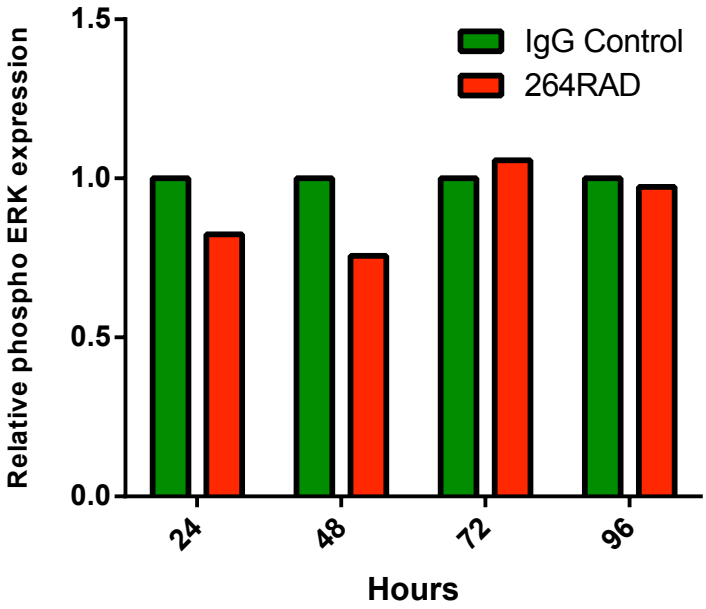

Figure 48: Quantification of phospho ERK following treatment with 264RAD in the CFPac1 cell line. Protein expression was quantified using image J software. Expression of phospho ERK in each lysate was normalised to expression of HSC70, which served as a loading control. Phospho ERK expression in 264RAD treated cells was then expressed relative to that in IgG control antibody treated cells.

3.7.2 Expression levels of Fyn in αvβ6 blocked PDAC cell lines

Fyn is a member of the Src family of proteins and is located on the cytoplasmic side of the plasma membrane. Tyrosine phosphorylation of target proteins by Fyn regulates intercellular signalling pathways. Fyn has been shown to interact directly with β6 [185].

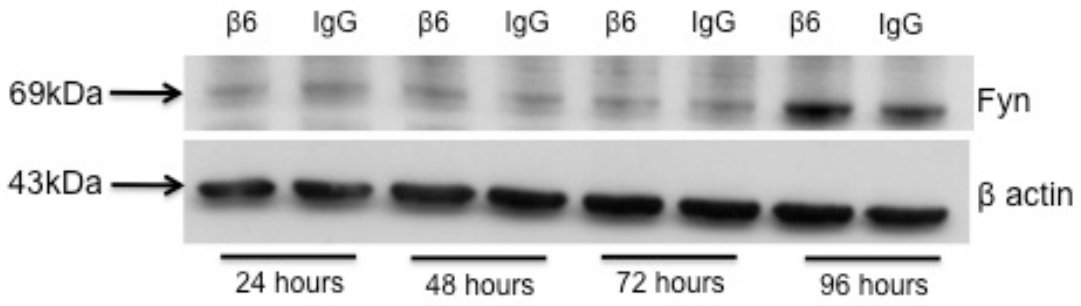

Figure 49: Western blot probing for expression levels of Fyn in CFPac1 cells treated with αvβ6 blocking antibody, 264RAD or an isotype control antibody at 10µg/ml for 24, 48, 72 and 96 hours. Beta actin served as a loading control. The above image is representative of two experiments carried out under the same conditions.

The expression level of Fyn was not affected by the antibody treatment in the CFPac1 cell line over a 24 – 96 hour time period. Expression of Fyn was observed to be higher in the αvβ6 blocking antibody treated cell lysate and control antibody treated cell lysate at the 96 hour time point compared to the other time points (Figure 49). Beta actin served as a loading control in this experiment with a molecular weight of 43kDa. The above result suggested that the effect of proliferation observed when treated with the αvβ6 blocking antibody was not dependent on changes in levels of expression of Fyn in CFPac1 cell line.

3.7.3 Expression levels of caspase 3 in β6 blocked PDAC cell lines

As blocking β6 using 53A.2 antibody resulted in a significant increase in sub-G1 DNA (Figure 46), which may be indicative of apoptosis, levels of caspase 3 were investigated in CFPac1 cells. Caspase 3 is a key executioner of apoptosis and is either partially or totally responsible for proteolytic cleavage of many proteins such as poly ADP ribose polymerase (PARP). It also interacts with other members of the caspase family like caspase 8 and caspase 9. Cleavage of caspase 3 is generally used as an indicator of apoptosis in cells and is usually detected as p17 and p12 fragments. It should be noted that there are caspase-independent mechanisms of cell death; so cleaved caspase 3 is not an absolute marker for apoptosis.

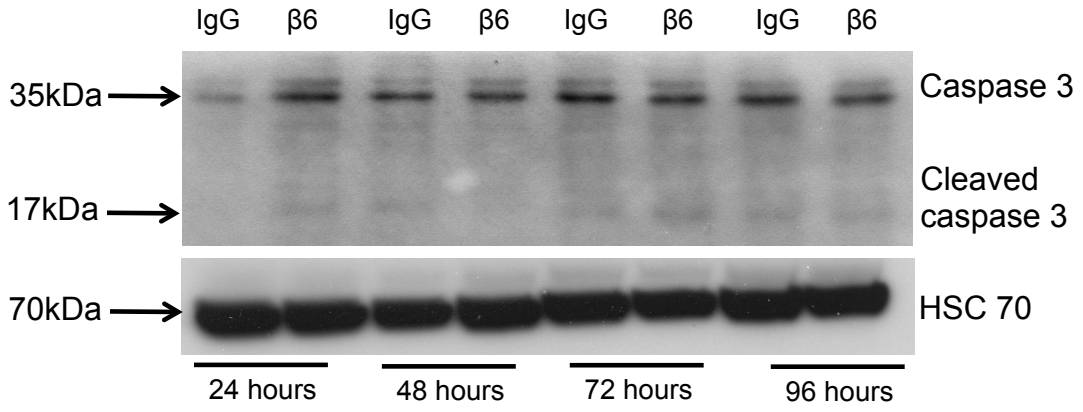

Figure 50: Western blot probing for expression levels of Caspase 3 in CFPac1 cells treated with β6 blocking antibody 264RAD or an isotype control antibody at 10µg/ml for 24, 48, 72 and 96 hours. HSC70 served as a loading control. Blots are representative of two experiments carried out under the same conditions.

CFPac1 cells were treated with αvβ6 blocking antibody 264RAD for 24, 48, 72 and 96 hours. Cells were lysed and Western blotting performed to detect both pro and cleaved caspase 3. Despite a significant increase in sub-G1 DNA at day 7 post-treatment with αvβ6 blocking antibody (Figure 46), from 8.5% to 46%, the expression level of caspase 3 was not affected by the antibody treatment in CFPac1 cell lines. Expression of cleaved caspase 3 was observed to be higher in the β6 blocking antibody treated cell lysate compared to the control antibody treated cell lysate at the 24 hour time point, although expression of total caspase 3 was also higher suggesting that protein loading may have been higher in this lane. There was no

difference in caspase 3 expression levels at any other time points. This result suggested that the significant increase in sub-G1 phase that was observed during cell cycle analysis on CFPac1 cells treated with the αvβ6 function-blocking antibody *in vitro* (Figure 46) may not be caspase mediated. However, tumours *in vivo* treated with the αvβ6 function-blocking antibody 264RAD showed significant difference in levels of caspase 3 expression suggesting that there occurs a difference in activation of caspase 3 between cells grown in tissue culture and *in vivo* as discussed later (section 5.4.1.4).

3.7.4 Expression levels of cyclin B1 in αvβ6 blocked PDAC cell lines

Cyclin B1 is a mitosis regulatory protein expressed predominantly during the G2/M phase of cell cycle. Its activation is involved in early events of mitosis such as chromosome condensation and nuclear envelope breakdown. Cells generally express increased inactive cyclin B1 prior to mitosis and therefore a cell cycle block at the G2/M phase should result in even higher levels of cyclin B1. As an increase in G2/M from 6.5% to 16% was observed in Panc04.03 cells following treatment with 53A.2 antibody (Figure 46), levels of cyclin B1 were investigated in whole cell lysates of cells also treated with an αvβ6 function blocking antibody.

Expression of cyclin B1 was higher in the αvβ6 blocking antibody-treated cell lysate compared with the control antibody treated cell lysates at 24 and 48 hours with an increase of 16% and 21% respectively (Figure 52), suggesting a possible early induction of G2/M arrest. However, there was no difference observed between the αvβ6 blocked lysates and the control antibody-treated cells at either 72hrs or 96hrs post-treatment with antibody (Figure 52), indicating that a single dose of αvβ6 blocking antibody does not lead to a sustained anti-proliferative effect, despite some early changes in cyclin B1 levels. Interestingly, levels of cyclin B1 also increased in control IgG treated cells (Figure 51) from 48hrs to 72hrs post-treatment which may have masked the modest increase in cyclin B levels induced by the αvβ6 blocking antibody.

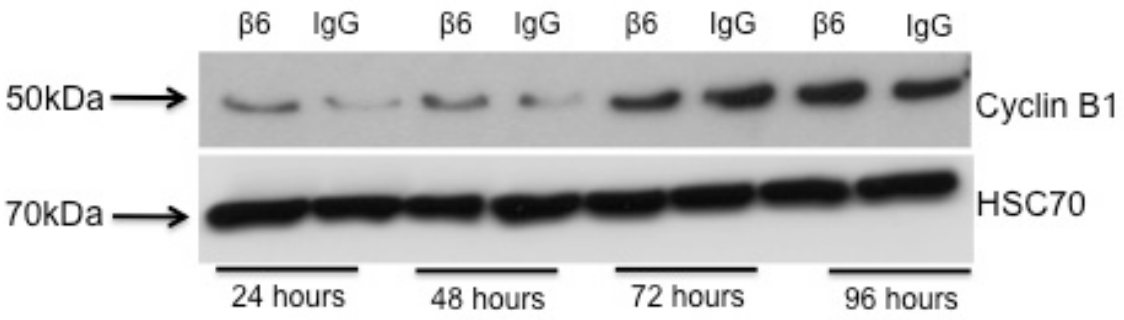

Figure 51: Western blot probing for expression levels of cyclin B1 in Panc04.03 cells treated with αvβ6 blocking antibody, 264RAD, or an isotype control antibody at 10µg/ml for 24, 48, 72 and 96 hours. HSC70 served as a loading control. The above blot is a representative image of three experiments carried out under the same conditions.

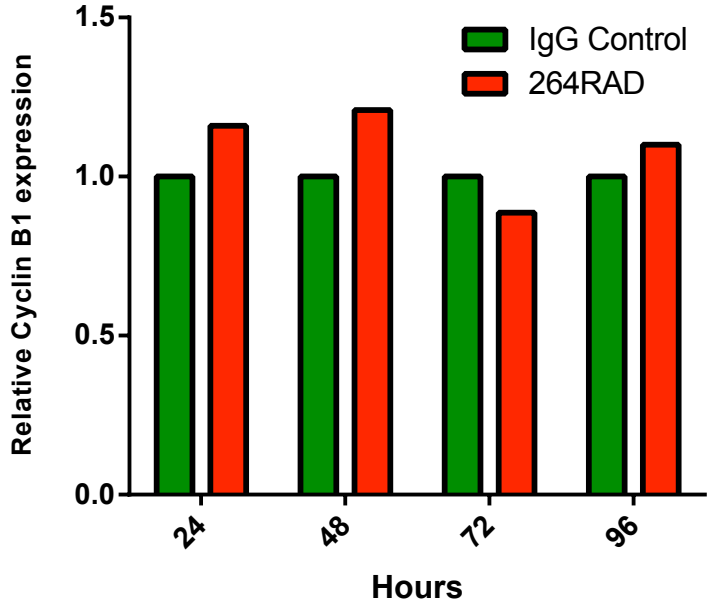

Figure 52: Quantification of cyclin B1 in Panc04.03 following treatment with 264RAD αvβ6 function blocking antibody. Protein expression was quantified using image J software. Expression of cyclin B1 in each lysate was normalised to expression of HSC70, which served as a loading control. Cyclin B1 expression in 264RAD treated cells was then expressed relative to that in IgG control antibody treated cells.

It is worth noting that significant increases in cells in G2/M arrest or containing sub-G1 DNA in Panc04.03 or CFPac1 cells respectively were observed at Day 7 following two doses of β6 blocking antibody on day 1 and day 4 (Figure 46), whereas levels of both cyclin B1 and caspase 3 were investigated after a single dose of αvβ6 blocking antibody over a 96hr time period. It was hypothesised that any changes in proteins associated with proliferation, and particularly induction of apoptosis, would be apparent prior to changes observed in cell cycle analysis. However, it may be that one dose of αvβ6 blocking antibody is not sufficient to lead to a sustained anti-proliferative state and a second dose is necessary. This could be one explanation as to why the changes in cell cycle data were not reflected as dramatically in downstream signalling proteins such as Erk, Fyn, cyclin B1 and caspase 3. The other reason being that none of the above molecules may be affected as a result of αvβ6 blockade.

3.8 Role of αvβ6 in PDAC cell migration

αvβ6 expressing oral cancer cells have been shown to have an increased migratory capacity and this contributes towards a more malignant phenotype [209]. In order to investigate the role of αvβ6 in PDAC cell migration, migration of PDAC cells towards the αvβ6 ligands, fibronectin and LAP of TGFβ1 were conducted. αvβ6 has a strong binding affinity for fibronectin, which is an important ECM protein upregulated in the pancreatic tumour stroma. The same subset of cell lines used for proliferation assays, Panc04.03, CFPac1 (αvβ6 positive cell lines) and Panc1, MiaPaCa2 (αvβ6 negative cell lines) were used to study antibody-mediated blockade of β6 and its role in modulating cell migration.

3.8.1 Migration of PDAC cells towards fibronectin

50,000 cells were plated onto Transwell® membranes where the underside of the membrane, had previously been coated with fibronectin at 10µg/ml (section 2.9.1). Cells were incubated for 16 hours in serum free media, harvested and counted. Cells were incubated at 4°C with αvβ6 blocking antibody 53A.2 or a control isotype antibody at 10µg/ml final concentration for 60 minutes prior to plating them onto Transwell® membranes.

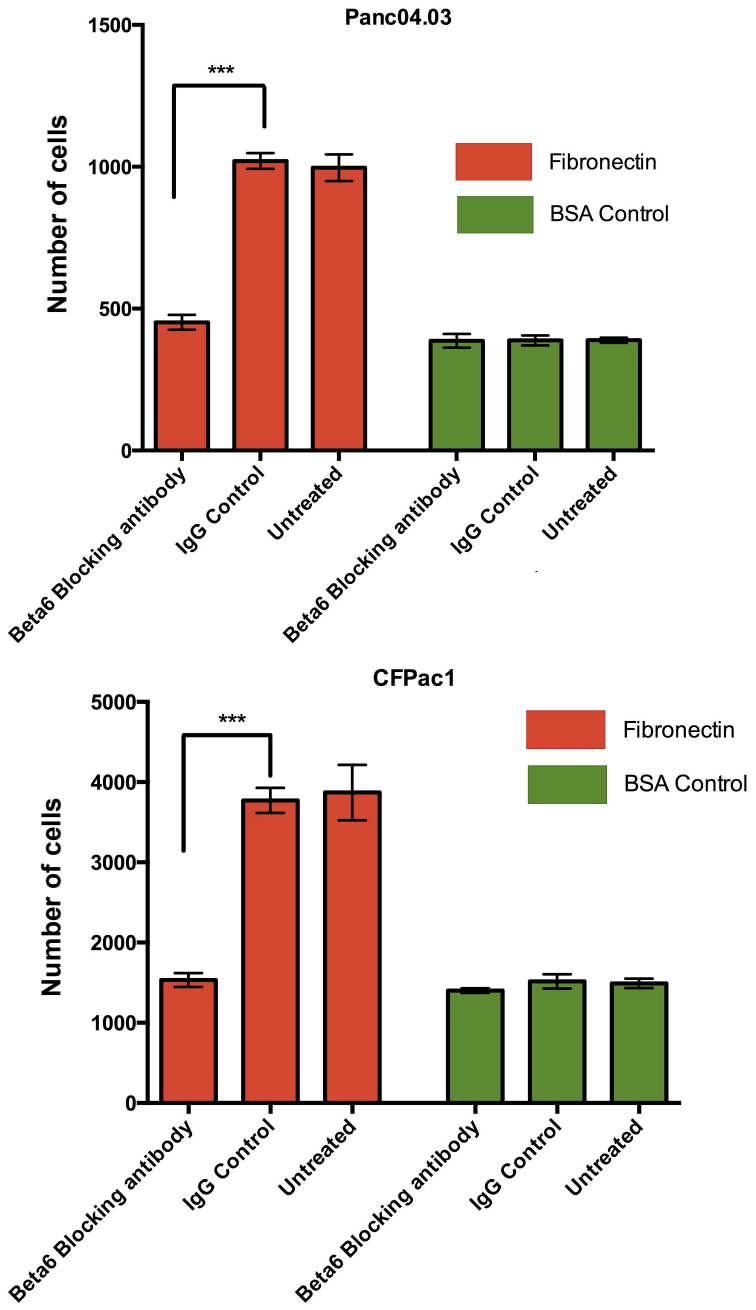

Figure 53: Effect of antibody-mediated blockade of αvβ6 on migration towards fibronectin by the two αvβ6 positive cell lines Panc04.03 and CFPac1. Cells were treated with 53A.2 at 10µg/ml for 1 hour before migration towards fibronectin over a 16 hour period was quantified. There was a significant reduction in migration towards fibronectin compared to the isotype IgG control Student's t-test p= <0.0001 (***). The antibody did not have any effect in migration of cells towards BSA, which was a negative control (Student's t-test p= non significant). Histograms represent mean ± SEM of two experiments, each performed with four replicates for each treatment condition.

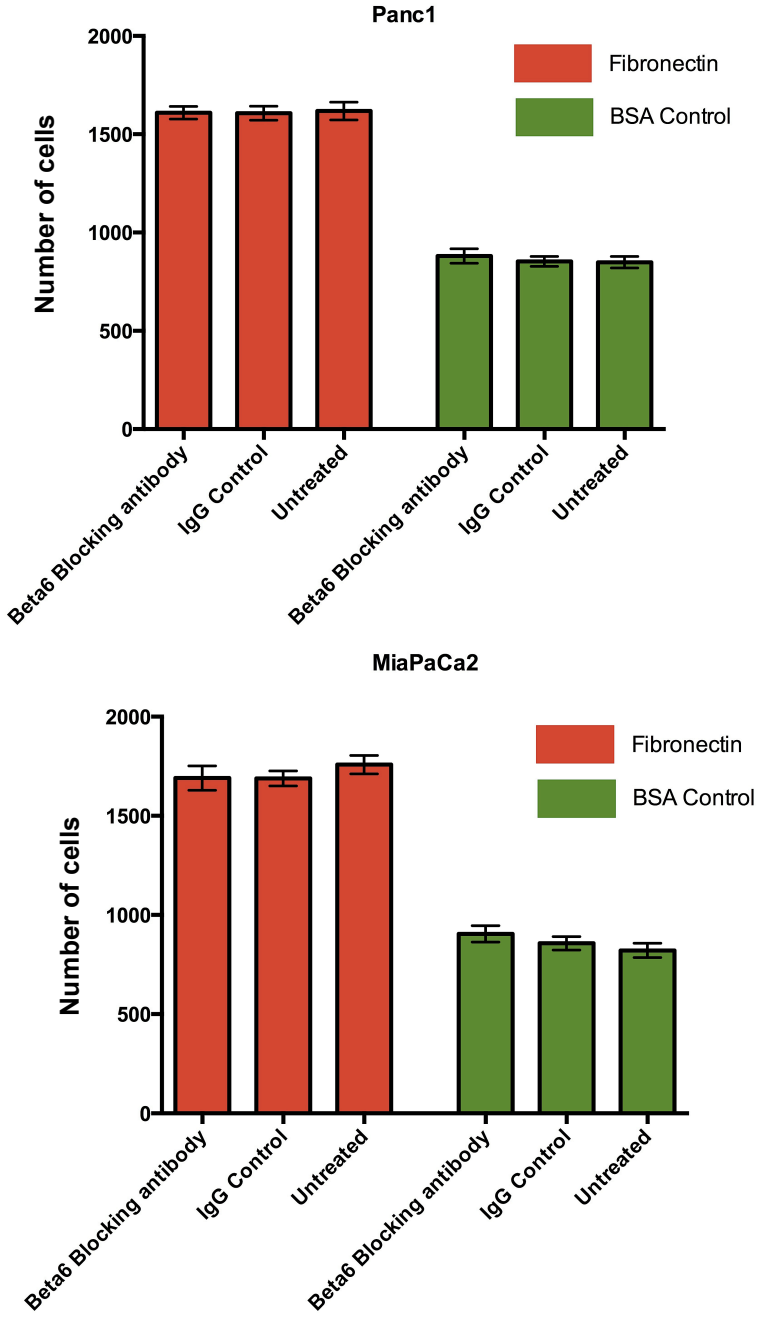

Figure 54: Effect of antibody-mediated blockade of αvβ6 on migration towards fibronectin by the two αvβ6 negative cell lines Panc1 and MiaPaCa2. Cells were treated with 53A.2 at 10µg/ml for 1 hour before migration towards fibronectin over a 16 hour period was quantified. There was no significant reduction in migration towards fibronectin compared to the isotype IgG control (Student's t-test: non significant). The antibody did not have any effect in migration of cells towards BSA, which was a negative control. Histograms represent mean ± SEM of two experiments, each performed with four replicates for each treatment condition.

The data in Figure 53 showed that there was a significant reduction in migration by 59% in Panc04.03 and by 44% in CFPac1 towards fibronectin over 16 hours when αvβ6 was blocked using a function blocking antibody, 53A.2 (p= <0.0001). The untreated samples did not have any antibody and served as a control for basal levels of migration. Levels of migration were not increased by the addition of the IgG control antibody demonstrating that it did not have any non-specific effects on the cells. The migration towards BSA served as an additional control to highlight the fact that cells tend to exhibit an enhanced migratory phenotype in the presence of fibronectin and any reduction in this migration observed was as a direct result of inhibition of binding of αvβ6 to fibronectin.

Furthermore, the data in Figure 54 showed that there was no difference in migration in Panc1 and MiaPaCa2 over 16 hours when treated with a αvβ6 function blocking antibody 53A.2. This demonstrates that the antibody was specific and does not have any off target effects in αvβ6 negative cell lines.

3.8.2 Migration of PDAC towards LAP

Similarly, 50,000 cells were plated onto Transwell® membranes where the underside of the membrane had previously been coated with LAP at 1µg/ml. Cells were incubated for 16 hours in serum free media, harvested and counted. Cells were incubated at 4°C with αvβ6 blocking antibody 53A.2 or a control isotype antibody at 10µg/ml final concentration for 60 minutes prior to plating them onto Transwell® membranes.

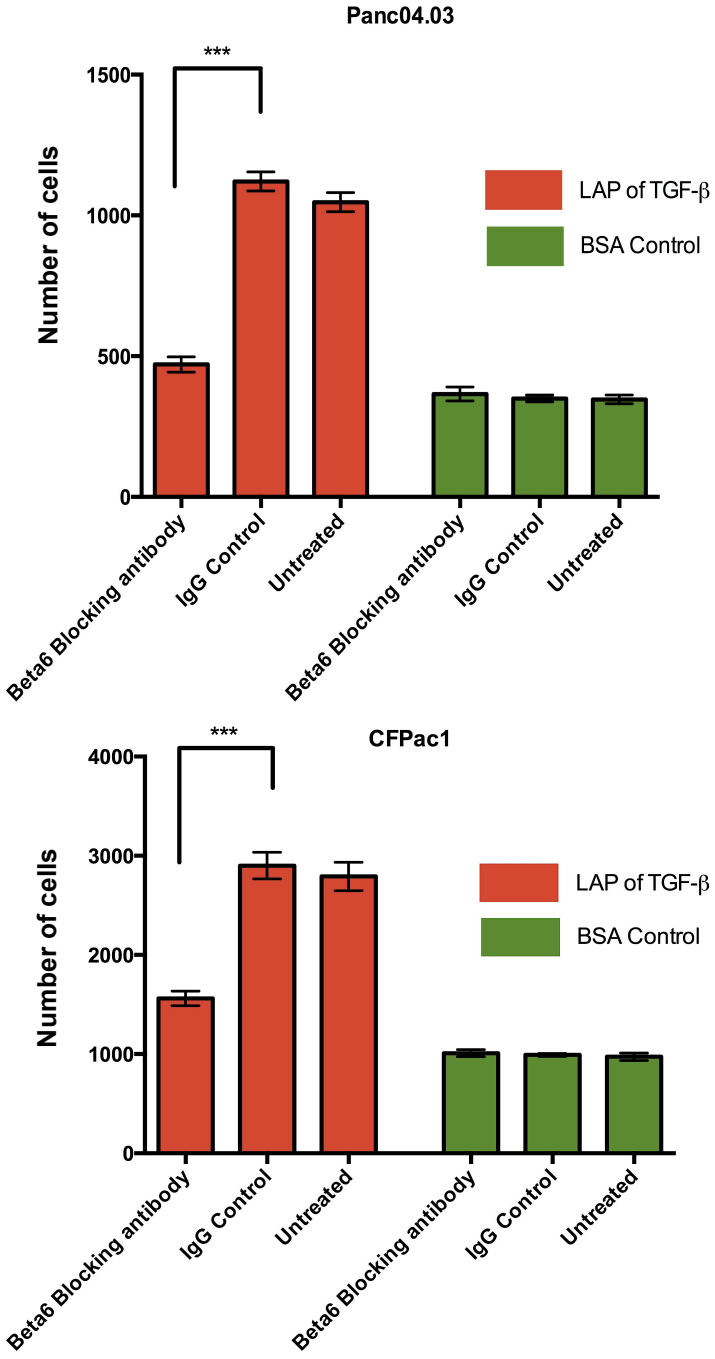

Figure 55: Effect of antibody-mediated blockade of αvβ6 on migration towards LAP in the two αvβ6 positive cell lines Panc04.03 and CFPac1. Cells were treated with 53A.2 at 10µg/ml for 1 hour before migration towards LAP over a 16 hour period was quantified. There was a significant reduction in migration towards LAP compared to the isotype IgG control (Student's t-test p= <0.0001). The antibody did not have any effect in migration of cells towards BSA, which was a negative control (Student's t-test: non significant). Histograms represent mean ± SEM of two experiments, each performed with four replicates for each treatment.

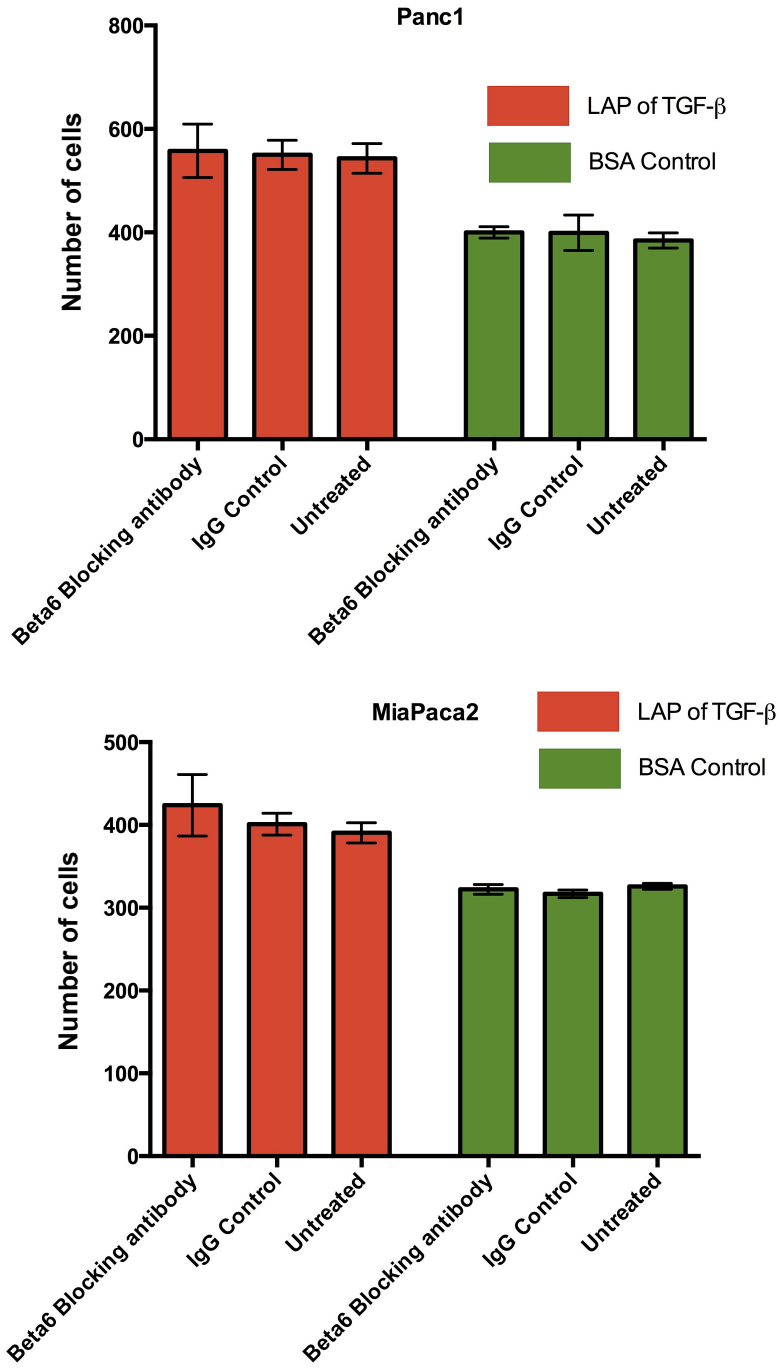

Figure 56: Effect of antibody-mediated blockade of αvβ6 on migration towards LAP in the two αvβ6 negative cell lines Panc1 and MiaPaCa2. Cells were treated with 53A.2 at 10µg/ml for 1 hour before migration towards LAP over a 16 hour period was quantified. There was no significant reduction in migration towards fibronectin compared to the isotype IgG control. The antibody did not have any effect in migration of cells towards BSA, which was a negative control (Student's t-test: non significant). Histograms represent mean ± SEM of two experiments, each performed with four replicates for each treatment.

LAP is one of the major ligands of αvβ6 since binding to LAPs on latent TGFβ activates TGFβ. The data in Figure 55 showed that there was a significant reduction in migration towards LAP of 58% in Panc04.03 and 46% in CFPac1 over 16 hours when αvβ6 is blocked using a function blocking antibody 53A.2 (p= <0.0001). Untreated samples served as a control for basal levels of migration and also showed that the IgG control antibody did not have any non-specific effects on the cells. The migration towards BSA was unaffected by treatment with either 53A.2 or IgG control. In contrast, the results in Figure 56 showed that there was no difference in migration towards LAP of TGFβ in Panc1 and MiaPaCa2 over 16 hours when treated with a αvβ6 function blocking antibody 53A.2. As these cells do not express αvβ6, this result was not surprising and demonstrates the specificity of 53A.2 in evoking this effect upon migration.

3.9 Role of αvβ6 in PDAC invasion

As migration was inhibited in PDAC cell lines by blockade of αvβ6, its role in invasion was next investigated. Epithelial cell invasion occurs when carcinoma cells breach the basement membrane, migrate into and come in contact with the stromal ECM. This is an extremely complicated process where the cells are required to secrete various factors including proteases such as MMPs, which in turn will favour invasion. αvβ6 expression in OSCCs has been shown to correlate with an increase in expression of MMP9 and MMP2 and αvβ6 has been shown to be responsible for increased oral cancer invasion in an MMP9-dependent manner [125].

3.9.1 Invasion assay using a β6 blocking antibody

Transwell® inserts coated with Matrigel™ were prepared to test the ability of a panel of six αvβ6 positive pancreatic carcinoma cell lines to invade through this barrier. The cells were first incubated with the αvβ6 function blocking antibody 10D5 (Table 9) or an isotype control antibody at a final concentration of 10μg/ml at 4°C for up to 60 minutes before plating onto Matrigel™ coated membranes (section 2.9.2). The Transwell® plates were harvested 72 hours later and the invaded cells in the lower chamber collected and counted using an automated cell counter.

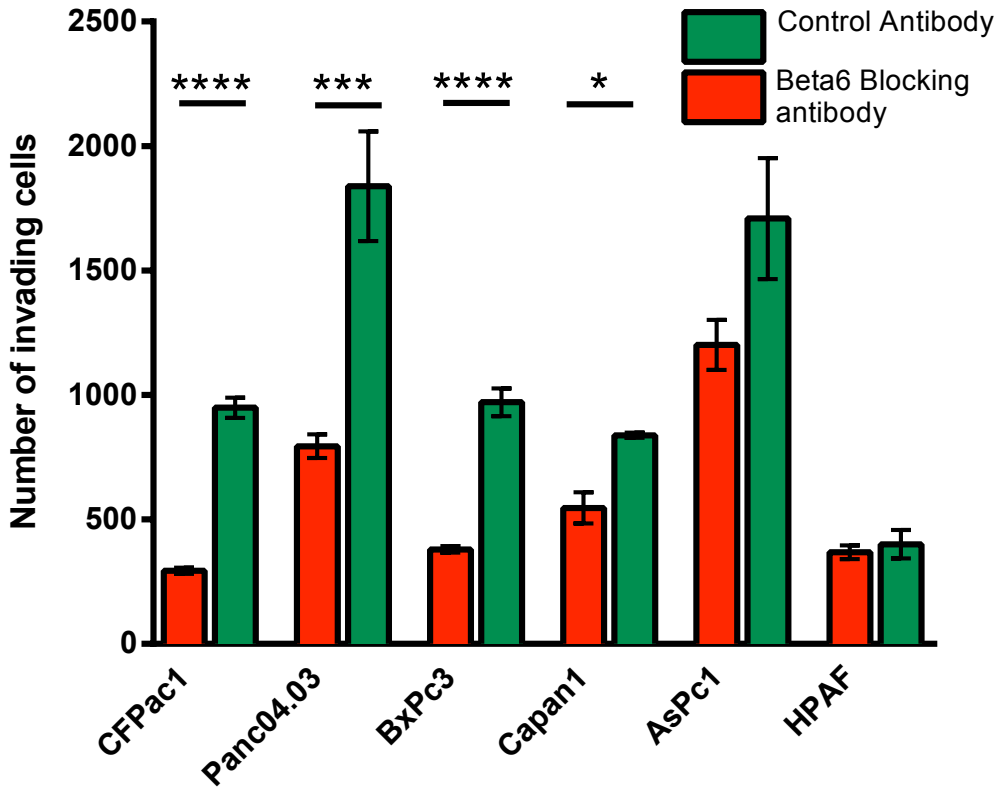

Figure 57: Effect of blocking αvβ6 on invasion of PDAC cells. Cells were treated with 10µg/ml of 10D5 αvβ6 function blocking antibody or an isotype control antibody for 1 hour. Cells were then plated onto matrix-coated membranes and invading cells were counted 72 hours later. Data show the mean ± SEM from a minimum of two experiments each performed with triplicates for each condition. Student's t-test p= <0.0001 (****), p= <0.001 (***). p= <0.02 (*).

The data in Figure 57 showed that 5 out of the 6 PDAC cell lines had invasive propensity and there was a significant reduction in invasion in four out of the five PDAC cell lines tested when blocked with an αvβ6 function-blocking antibody 10D5 at 10µg/ml. There was a reduction in invasion by 69% in CFPac1, 56% in Panc04.03, 61% in BxPC3 and 34% in Capan1 compared with the control antibody. Whilst a 21% reduction in invasion was also observed in the AsPc1 cell line this difference was not statistically significant.

Although all six cell lines tested in Figure 57 expressed αvβ6, their invasive potential varied greatly with Panc04.03 and AsPc1 cells showing higher levels of invasion compared with the other cell lines. The level of αvβ6 expression did not correlate with increased inhibition of invasion when αvβ6 was blocked. HPAF had high levels of αvβ6 comparable to that in Panc04.03 but were non-invasive. Thus, it is possible that

in certain PDAC cell lines, the mere expression of αvβ6 is not in itself sufficient to promote invasion.

In separate assays, the αvβ6 blocking antibody, 264RAD, was used on a smaller subset of PDAC cell lines, Panc04.03 and CFPac1 (αvβ6 positive cell lines) and Panc1 (αvβ6 negative cell line) to confirm that the observed reduction in invasion was due to specific blocking of αvβ6 in the cells and not due to any off target effect. IgG antibody was used as a control and results are shown in Figure 58.

.

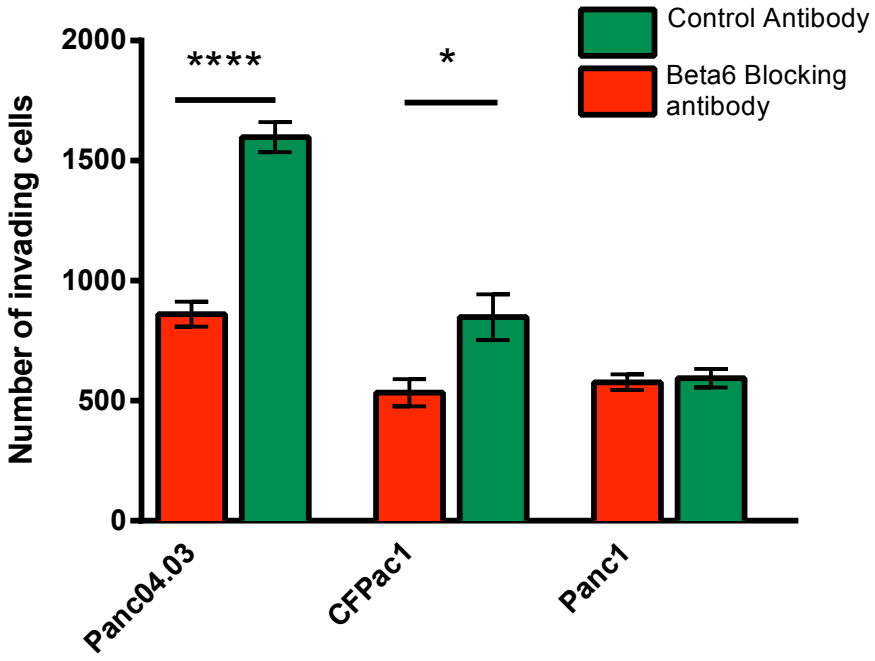

Figure 58: Effect of blocking αvβ6 on invasion of PDAC cells. Cells were treated with 10µg/ml of 264RAD αvβ6 function blocking antibody or an isotype control antibody for 1 hour. Cells were then plated onto matrix-coated membranes and invading cells were counted 72 hours later. Data show the mean ± SEM from a minimum of three experiments each performed with triplicates for each cohort. Student's t-test p= <0.0001 (****), p= <0.02 (*).

The results in Figure 58 showed that there was a significant reduction in invasion in the two αvβ6 positive cell lines, Panc04.03 and CFPac1 when blocked with the αvβ6 function blocking antibody 264RAD at 10µg/ml whereas there was no effect on the β6 negative cell line Panc1. There was a reduction in invasion by about 46% in Panc04.03 and 43% in CFPac1 compared to the control antibody. Proliferation assays were carried out in parallel with the invasion assay to ensure that the

reduction in invasion observed was not an indirect result of reduced proliferation in the αvβ6 positive cell lines over the assay time frame.

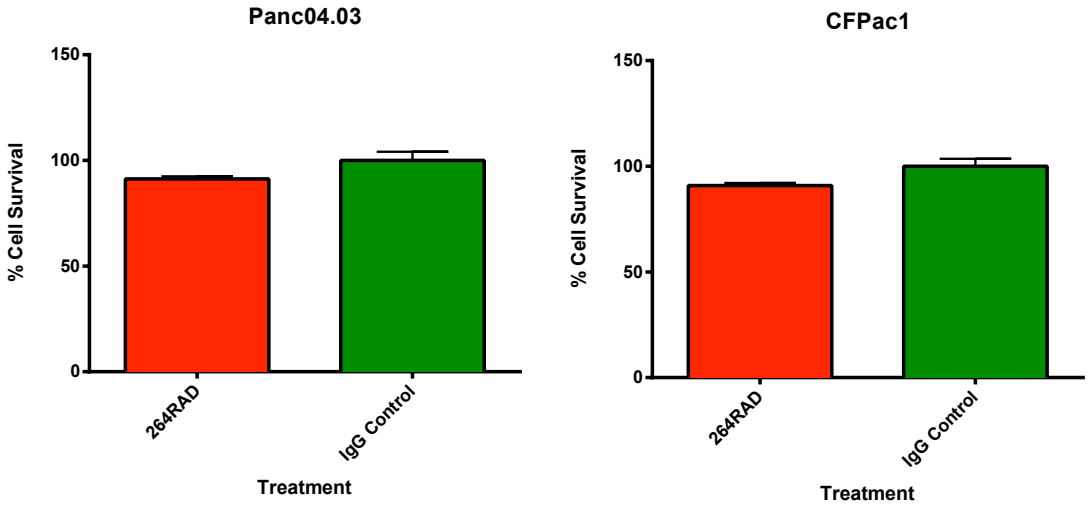

Figure 59: Treatment of Panc04.03 and CFPac1 cell lines with the αvβ6 blocking antibody 264RAD over 72 hours does not inhibit proliferation. Cells were treated with 10µg/ml 264RAD and cell survival quantified by MTT assay 72 hours later. Data show the mean ± SEM of three experiments performed with replicates of four per treatment in each experiment. Student's t-test (p= non significant).

Data in Figure 59 showed that there was no significant difference in proliferation of Panc04.03 and CFPac1 cell lines when treated with the αvβ6 blocking antibody 264RAD at 10µg/ml over 72 hours compared with the control isotype IgG antibody. The proliferation assays were performed in parallel with each invasion assay experiment for all the cell lines tested with no significant difference in proliferation over 72 hours.

3.9.2 Developing a 3D organotypic co-culture

Monolayer cultures do not provide even an approximate simulation of *in vivo* tissue because monoculture in 2 dimensions (2D) lacks cell-cell, cell-ECM and cell-stromal interactions, which are key players in control of gene expression and behaviour of cells. An *in vitro* tissue model, which allowed us to better replicate these cell-stromal interactions and their effects on tumour cell growth and invasion, was essential. Therefore organotypic 3D co-cultures of PDAC cells and fibroblasts were developed to model epithelial-stromal interactions. The growth, differentiation and invasive behaviour of cells was observed in this assay, which was modelled on organotypic co-cultures as described previously [90].

Briefly, collagen; Matrigel™ gels embedded with human fibroblasts were overlaid with PDAC cells. The structures were raised to an air-liquid interface and cultures maintained for 14 days, feeding every other day. The co-culture model was optimised so that it can be used to culture PDAC cells in a more physiologically relevant manner. Representative images of pancreatic cancer cell lines that have been tested are shown in the following two figures and these images illustrate that the different cell lines show distinct patterns of growth and invasion.

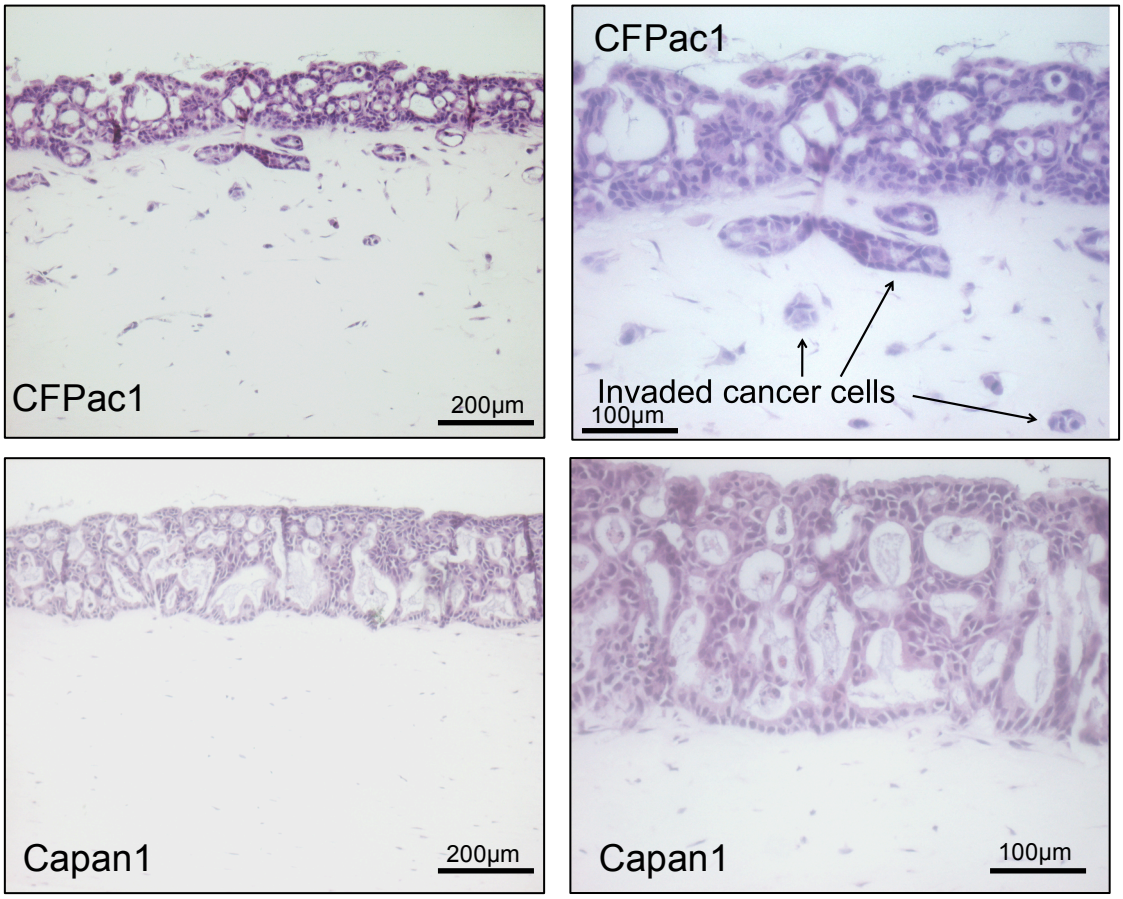

Figure 60: Representative H&E images of 3D organotypic co-cultures with PDAC cell lines CFPac1 and Capan1 co-cultured with MRC5-hTert fibroblasts over two weeks.

Figure 60 shows H&E images of CFPac1 and Capan1 cell lines growing on organotypic gels. Both cell lines formed deep epithelial structures filled with luminal spaces, typical of adenocarcinoma. There was clear evidence that CFPac1 but not Capan1 or Panc04.03 (Figure 61) invaded the fibroblast rich matrix. This was in contrast to the 2D Transwell® invasion assay, where all three cell lines exhibited invasive propensity. This was a clear example demonstrating the different behaviour of cancer cell lines in a 3D matrix when co-cultured with stromal cells. Since these gels can be treated similarly to human tissue, they were stained for $\alpha v\beta 6$ expression using the protocol described (section 2.6.1).

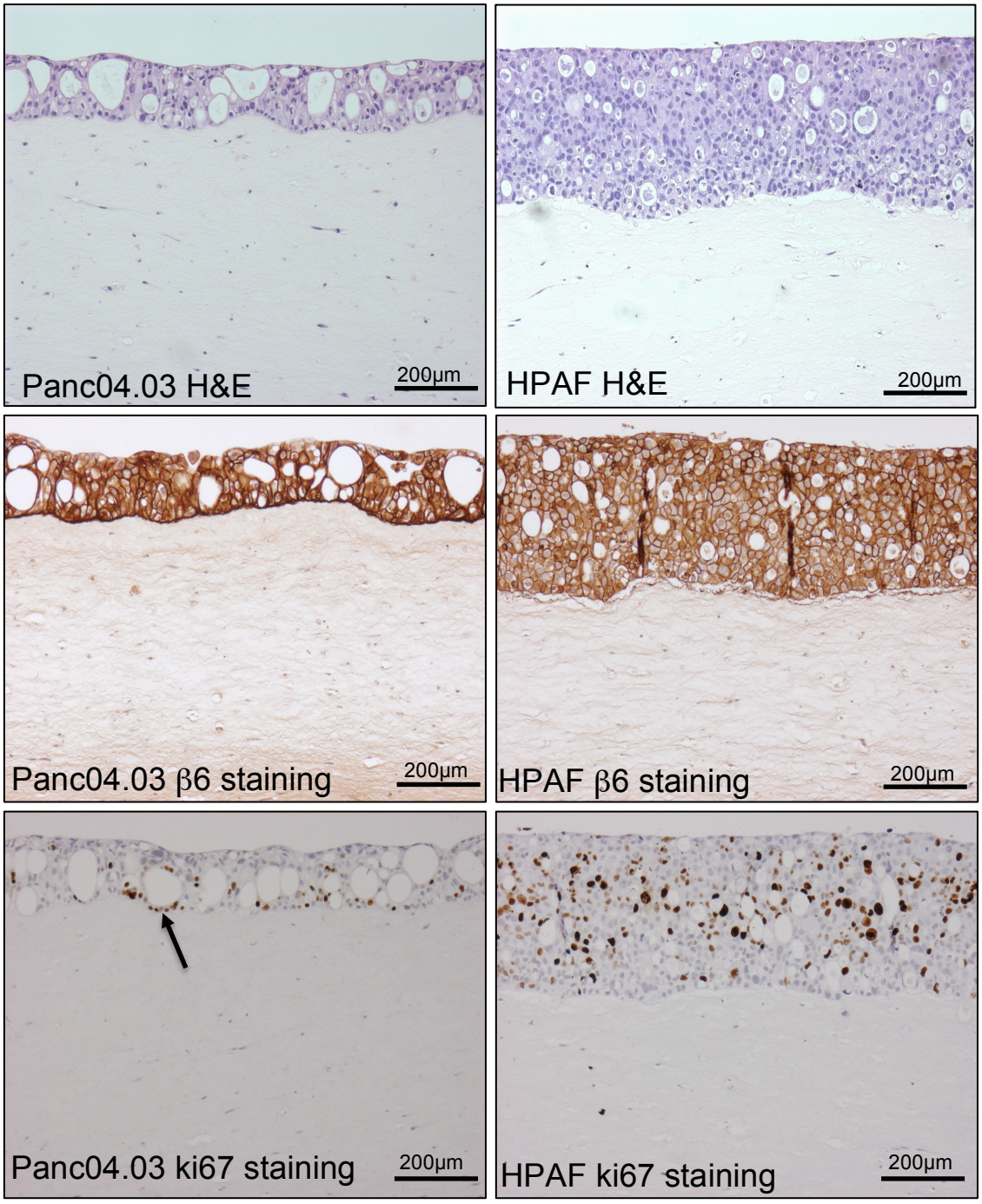

Figure 61: Organotypic co-cultures stained for αvβ6 and ki67. Panc04.03 and HPAF cells were co-cultured with MRC5-h-Tert for 14 days and then processed for IHC. Sections were stained for αvβ6, ki67 and with H&E.

The results showed that both Panc04.03 and HPAF PDAC cell lines retained strong expression of αvβ6, as observed by the brown colour in the epithelial cells (Figure 61). Ki67 staining showed that a significant fraction of the cells retained their ability to divide (brown dots in the nuclei of the cell) in Panc04.03 and HPAF PDAC cell lines (Figure 61). It should be noted that αvβ6 typically was expressed strongly on the membrane at the cell-cell junctions. These data may also suggest that Panc04.03

may undergo changes in cell polarity since most ki67 positive nuclei are near, or at, the baso-lateral surface (shown by an arrow in Panc04.3 ki67 staining x10, (Figure 61).

Even though both PDAC cell lines formed a thick layer of epithelium on the gel with ductal structures, typical of PDAC tumours, and continued to grow and multiply in the 3D cultures, only CFPac1 showed invasion in this assay out of a panel of PDAC cell lines that was tested. Different fibroblasts and pancreatic stellate cells were also used to co-culture with PDAC cell lines, with no or very little invasion (data not shown). This could be due to the poor invasive potential of the PDAC cell lines tested in this assay. Each experiment (cell line) was prepared in triplicate and was repeated a minimum of three times. Since blocking $\alpha v\beta 6$ significantly reduced proliferation and invasion in PDAC cell lines in 2D cultures, the organotypic co-cultures were a good model to test the role of $\alpha v\beta 6$ in PDAC cell line proliferation and invasion in a more physiologically relevant 3D setting. Since these cultures were grown for fourteen days, siRNA mediated knock down of $\beta 6$ on cell lines was not possible. Antibody mediated block of $\alpha v\beta 6$ was not considered to be an option either because of the technical difficulties involved in treating the cells in 3D culture. A stable knock down of $\alpha v\beta 6$ in PDAC cell lines was deemed essential to test its effect on proliferation and invasion over this long-term assay.

3.10 Stable knock down of β6 in PDAC cell lines

Three lentiviral shRNA sequences in pGIPZ vectors (section 2.4.1) were purchased from Open Biosystems to knock down β6 in pancreatic cancer cell lines. The pGIPZ vector also had a turbo-GFP as a read out to measure the levels of expression. The vector contains both puromycin and zeocin antibiotic selection. After confirming, by sequencing, that the plasmids did indeed target the published sequences HEK 293 FT cells were used to make the lentivirus particles, using a three vector transfection method as detailed in methods (section). The PDAC cell lines CFPac1 and Panc04.03 were incubated with the supernatant containing the viral particles together with polybrene (hexadimethrine bromide) for 4 hours at 37°C. Following incubation, fresh 10% FCS containing growth medium was added and cells left to grow. Since the viruses also expressed GFP driven by an IRES promoter, up stream to the target shRNA sequence, infected cells would express this fluorochrome in proportion to the expression of the shRNA in the cell. Disappointingly two of the three plasmids failed to reduce αvβ6 expression (data not shown). However, the plasmid (V3LHS_374274, Open Biosystems), when used to infect Panc0403 and CFPac1 cells did seem to suppress αvβ6 expression based on flow cytometry. Post infection, the increase in GFP expression in Panc04.03 correlated to a decrease in αvβ6 expression (figure below).

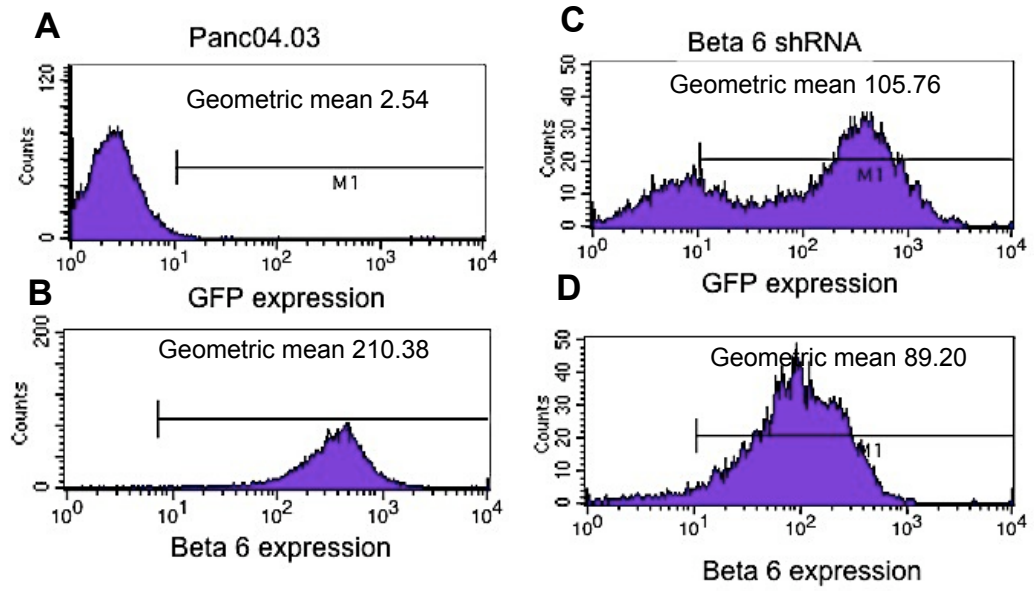

Figure 62: Lentiviral shRNA knockdown of αvβ6 in Panc04.03 cells. GFP and αvβ6 expression was determined prior to (A), (B) and post (C), (D) transfection. GFP was analysed as a measure of transfection and αvβ6 expression was determined using 10D5 antibody.

Panc04.03 were analysed by flow cytometry before and after infection with the lentiviral construct V3LHS_374274. Data show that after infection GFP levels increased (geometric MFI 105.76 from 2.54) and αvβ6 detected by antibody 53A.2 decreased (geometric MFI 210.38 to 89.2).

Expression of αvβ6 in the infected cell population was reduced dramatically following lentiviral infection after three to five days in culture (geometric mean of 89.20) compared with the uninfected parent population of cells (geometric mean 210.38). Note that expression was reduced by >50% three weeks after infection when compared to the uninfected parental control (Figure 62). There was a dramatic increase in GFP positive cells following infection, which was an indicator for successful infection of the lentivirus into the cells (top) (geometric mean 105.26).

The co-expressed fluorescent marker GFP was then used to select the most GFP-positive cells (>90%) by FACS. Following sorting, the growth rate of cells was very slow until 6-8 weeks, after which their growth rate returned to normal permitting further analysis by flow cytometry.

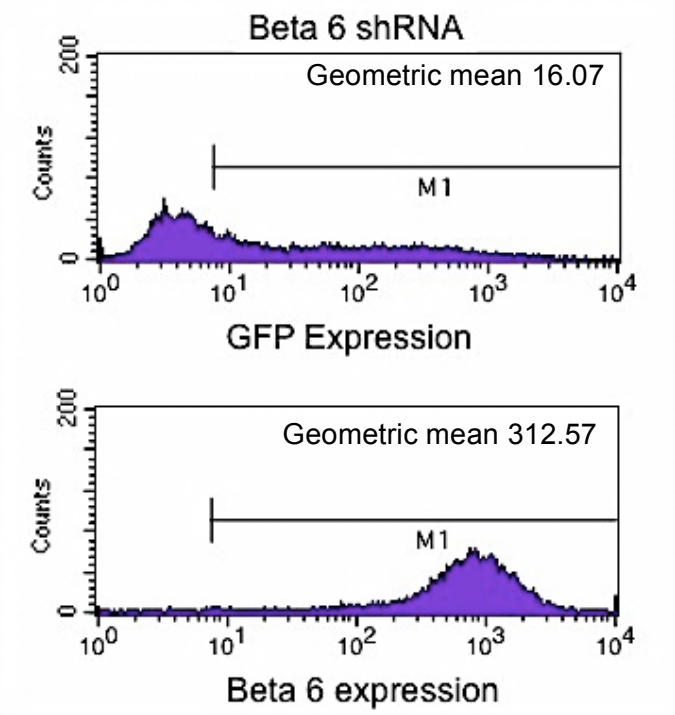

Figure 63: Lentiviral infected Panc04.03 cells do not stably express GFP. Six weeks after selection of αvβ6 high expressing cells, cells were analysed for both GFP and αvβ6 expression by flow cytometry.

Six weeks after sorting for high GFP expressers, cells were reanalysed by flow cytometry. Data showed that the cells lost expression of GFP with a geometric mean of 16.07 at six weeks compared with >105.76 (Figure 62) just after transfection. Similarly, αvβ6 expression returned to high levels, geometric mean 312.57 (Figure 63) compared with geometric mean of 89.2 at the time of sorting (Figure 62).

This loss of GFP and loss of αvβ6 suppression could be due to multiple reasons. The fact that the plasmid was in the cells and could be detected by flow cytometry 3-4 days post infection showed that the infection worked, but following a positive GFP sort, the rate of cell growth dramatically slowed down for about 6-8 weeks; then the growth rate returned to the normal rate of growth. Once the growth rate returned to normal, enough cells could be collected to perform a flow cytometry analysis, which revealed that the cells had lost expression of GFP indicative of either loss of plasmid from cells or silencing of the lentiviral plasmid.

This loss of GFP correlated with a return to high levels of αvβ6 indicating that the shRNA was not working. These data suggested that β6 might be crucial for the growth and survival of the PDAC cell lines tested, Panc04.03 and CFPac1 (data not shown), and any attempt to knock down αvβ6 stably is not possible as it is not compatible with cell growth and survival. All three shRNA sequences showed very similar results and it was not possible to generate a stable knock down for β6 in the two cell lines tested. A doxycycline (dox) inducible shRNA plasmid to knock down β6 is currently available to purchase and it might be worth attempting to generate a stable dox-inducible knock down of β6 to overcome the dependence of these cells on αvβ6 for survival.

3.11 Discussion

Integrins are major contributors to the development of cancer because of their dual capacity to generate pro-oncogenic signals (e.g. increased secretion of proteases, generation of survival signals) as well as their ability to physically mediate tumour cell motility and invasion. The role of αvβ6 in PDAC is relatively unknown and only few studies have linked αvβ6 expression with pancreatic cancer [201, 207]. Sipos and colleagues reported αvβ6 to be overexpressed in pancreatic cancer from tissue samples obtained from a cohort of 34 patients. 100% of the PDAC tissue samples screened were positive for αvβ6. In *in vitro* studies, Singh et al, reported that αvβ6 was part of a "gene signature" that was essential for mutant *KRAS* dependent pancreatic cancer cell survival [207]. The study used a panel of seven pancreatic cell lines; although shRNA mediated transient knock down of β6 was performed in three of these, a significant decrease in cell survival (60% to 80%) compared to control knock down was only observed in the YAPC cell line, using *in vitro* cell proliferation assays [207]. If this result with a single cell line were extrapolatable to the clinical situation then αvβ6 could be an ideal therapeutic target since it appears to be entirely absent from normal tissue. Moreover, for the same reasons, it could prove to be an ideal imaging target. In fact, a subcutaneous inoculum of the αvβ6 positive BxPC3 cell line was used to image αvβ6 positive tumours specifically using a radiolabelled peptide [(^{18}F)] FBA-A20FMDV2 (A20FMDV2 is a peptide that binds specifically to αvβ6) using positron emission tomography (PET) [235]. Current non-invasive imaging using radio-tracers to detect metastatic PDAC pre-operatively has limited success due to non-specific uptake in tissues. A radiolabelled αvβ6 specific peptide improves tumour uptake due to expression of αvβ6 solely in the tumour tissue and this could have important implications in clinical outcome.

3.11.1 Characterising αvβ6 in PDAC cell lines

This study aimed to determine the functions that αvβ6 expression would impart to PDAC cells and whether these would potentially enhance PDAC growth and invasion. A pilot IHC study of tissue obtained from 34 PDAC patients and 12 normal cases, was conducted and the tissues were analysed for αvβ6 expression. All PDAC cases were positive for αvβ6 with 38% expressing very high levels. In contrast, only 1 of the 12 normal cases expressed αvβ6 at a very low level. This preliminary study

served to confirm findings from Sipos et al, and suggested that αvβ6 could be a potential therapeutic target in PDAC.

A panel of 9 pancreatic human cell lines (Table 12) was screened to check for αvβ6 surface expression levels using flow cytometry. αvβ6 recognises its target ligands using the RGD tri-peptide sequence and binds to a variety of ECM proteins including fibronectin, LAP, tenascin-c and vitronectin. Seven out of the nine PDAC cell lines tested were positive for αvβ6 expression, consistent with the high expression seen in PDAC tissue. Varying levels of positivity were observed, with some cell lines expressing αvβ6 at very high levels (CFPac1, Panc04.03), some at moderate levels (AsPc1, BxPC3) and some with no expression (Panc1, MiaPaCa2). Published literature has always associated β6 with well-differentiated tumours [201], so when the cell lines were grouped based on their differentiation status (at the time of origin) it was not surprising to observe higher levels of αvβ6 expression in the well differentiated cell lines (Figure 32). These early events were encouraging because they meant that there was now a panel of PDAC cell lines available, some expressing varying levels of endogenous αvβ6 and some αvβ6 negative cell lines to study the functional role of endogenous αvβ6 in PDAC.

Having looked at the surface expression levels of αvβ6 in PDAC cell lines, whole cell lysates from a subset of cell lines tested were prepared to measure total levels of αvβ6 expression and to determine if these results matched the flow cytometry data (Figure 34). The levels showed a similar pattern of expression to that observed with flow cytometry. Thus, two separate methodologies were used to confirm αvβ6 expression in the same panel of PDAC cell lines. Based on these data, Panc04.03 and CFPac1 were the two high αvβ6 expressing cell lines selected and MiaPaca2 and Panc1 were the two negative cell lines selected for further investigation.

3.11.2 Functional role of αvβ6 in PDAC cell lines

Studies conducted to date have not looked into the functional role of αvβ6 in pancreatic cancer cells. In other tumour systems αvβ6 has been shown to promote activities that could increase tumour progression by increasing migration, invasion, survival and MMP secretion [209]. Very recently, an αvβ6 blocking antibody 264RAD was assessed as a possible new targeted therapy to treat αvβ6 positive oral and breast cancer tumours in xenograft models where they showed that the αvβ6

function-blocking antibody significantly reduced tumour size compared to the control antibody treated tumours in recipient mice [233]. The authors of this study also showed a dose dependent decrease in expression of Ki67 in the 264RAD antibody treated tumours indicative of a reduction in proliferation.

3.11.2.1 Role of αvβ6 in regulating cell proliferation

Targeting integrins using specific antibodies has long been used as a possible therapeutic approach to treat various cancers. An αvβ3 function blocking antibody, etaracizumab, targets ovarian cancer cell lines that express αvβ3 and significantly reduces proliferation and invasion in a phospho AKT and phospho mTOR dependent manner [236]. Another study has shown that the αv blocking antibody 17E6 inhibited the growth of melanoma cells in nude mice, although no obvious mechanisms were reported [4].

Blockade of αvβ6 in PDAC cell lines showed there was a significant and dose dependent decrease in cell survival in two αvβ6 positive cell lines (Panc04.03, CFPac1) when treated with either of the αvβ6 function-blocking antibodies 53A.2 or 264RAD (Figure 36, Figure 38). The 264RAD αvβ6 function-blocking antibody has also been shown to bind with low affinity to αvβ8 [233]. However there are several reasons to believe that the effect of 264RAD in this model is predominantly due to interaction with αvβ6. Panc04.03 do not express αvβ8 and CFPac1 cells express αvβ8 at very low levels. Furthermore, two αvβ6 negative cell lines (Panc1, MiaPaCa2) did not show any difference in cell survival when treated with the same αvβ6 function-blocking antibody at similar concentrations (Figure 37, Figure 39). These results suggested that the anti-αvβ6 function-blocking antibody blocked αvβ6 specifically and this led to a decrease in proliferation. It also confirmed that the antibody did not have any non-specific off target effects because the αvβ6 negative cell lines were not affected by the treatment and continued to look healthy without the rounding and increased nuclear size observed in the αvβ6 positive cell lines.

The potential power of blocking αvβ6 function as a method for therapy was further confirmed using a fragment of adenovirus modified to incorporate the peptide A20FMDV2. A20FMDV2 is a peptide derived from the foot-and-mouth disease virus, with a high affinity and specificity for αvβ6 [124]. A recombinant adenovirus type 5 (Ad5) fibre knob protein incorporating A20FMDV2 in the H1 loop was generated to

target αvβ6 positive tumours specifically [234]. This Ad5 knob protein was generated as part of an independent study on viral gene therapy performed by a colleague in the laboratory at the time. It was decided to test this recombinant protein on αvβ6 dependent PDAC cell proliferation. The modified Ad5 A20FMDV2 had a similar dose-dependent effect on Panc04.03 and CFPac1 cells, inhibiting their proliferation significantly (Figure 40). In contrast, the two negative cell lines were not affected by the treatment (Figure 41). Thus, three independent targeting agents that block αvβ6 significantly reduced PDAC cell proliferation in αvβ6 positive, but not in αvβ6 negative tumour cell lines. These data suggest that in PDAC cell lines, αvβ6 signalling is an essential survival factor. In support of these conclusions, when Singh et al, used shRNA to knock down αvβ6 in PDAC cell lines, there was no effect on proliferation in the Panc1 cell line but a significant decrease in proliferation in the αvβ6 positive YAPC cell line [207]. They also observed similar effects on cell survival in the two αvβ6 positive *KRAS* dependent lung cancer cell lines tested (H358 and A549).

The next step in this study was to try and knock down β6 using siRNA on the two αvβ6 positive cell lines to observe if there was a similar effect on cell proliferation seen by the blocking antibodies, an approach similar to that used by Singh et al [207]. Unfortunately, this proved to be not possible; a consequence perhaps of Panc04.03 and CFPac1 proving to be extremely difficult to transfect. Different lipid mediated transfection agents were used (lipofectamine, oligofectamine, interferin, gene juice) with no success. Electroporation was performed and although it yielded a 70% knock down of αvβ6 expression (data not shown), many dead or dying cells were seen after treatment with the non-targeting siRNA as a consequence of the electroporation. These many attempts, over a protracted time period, were disappointing and frustrating and occupied a considerable amount of time. For whatever reason, αvβ6 expression could not be reduced in Panc04.03 or CFPac1 cells. Accordingly Capan1, another αvβ6 positive cell line, was used instead to knock down β6 using oligofectamine mediated siRNA transfection. There was a significant difference in proliferation in the β6 siRNA treated cells compared with the non-targeted siRNA control treated cells over 5 days (Figure 43). Note that the antibody-mediated function blocking (2 doses) of αvβ6 over 7 days yielded better inhibition of proliferation compared with the siRNA-mediated inhibition of proliferation over 5 days. This may be due to the lack of a 100% knock down of β6 in the cells over a 5 day

period. It could also be that the cells where β6 was still expressed (no knock down) started to out grow the slow growing low β6 expressers thereby masking any differences in proliferation between the β6 siRNA and NT siRNA treated cells.

Importantly, it was necessary to confirm that neither of the αvβ6 blocking antibodies had any effect on pancreatic stellate cells. Using the pancreatic stellate cell line PS1, it was confirmed that neither 53A.2 nor 264RAD (data not shown) had any effect on PS1 proliferation (Figure 44). Thus in later *in vivo* studies, any effect of the antibody on xenograft growth is unlikely to be via a direct effect on the proliferation of stellate cells.

3.11.2.2 Effect of αvβ6 on cell cycle progression in PDAC

Although blockade of αvβ6 has been shown to reduce PDAC cell survival significantly, the exact mechanism by which it exerts this regulation is unknown. Routine microscopic observation of cells revealed phenotypic changes with cells appearing to be more rounded with bigger nuclei in the αvβ6 blocking antibody treated cells (Panc04.03, CFPac1) compared with the control cells. Other studies have shown that blocking integrins can have an effect on cell cycle progression. Knockdown of the α6 subunit and overexpression of the α5 subunit in the murine breast cancer cell line 4T1 showed inhibition of tumour growth *in vivo*. In these cells, there appeared to be a S phase block in the cell cycle and an increase in p27 with a corresponding decrease in the CyclinE/CDK2 [237]. In order to better understand the reduction in proliferation observed as a result of αvβ6 blockade, cell cycle analysis was performed on Panc04.03 and CFPac1 cells. The antibody treated Panc04.03 cells showed a small, but significant, increase in the G2/M phase compared to the IgG treated cells, which meant there was a block in cell cycle progression as the cells prepared to enter the mitotic phase (Figure 46). The CFPac1 cells treated with the αvβ6 blocking antibody showed a significant increase in the sub-G1 phase compared to the control IgG antibody treated cells (Figure 46). An increase in G2/M phase was also observed at day 7 in the CFPac1 cells but was not statistically significant. It is also possible that the cells blocked in the G2/M phase could have died, thus showing an increase in the sub-G1 phase. It might be worth considering earlier time points in the cell cycle assay to identify if there occurs any change in the G2/M phase in CFPac1 cells.

Increase in the sub-G1 population in cell cycle analysis is often mistaken for apoptosis and further analysis needs to be done in order to confirm if indeed it was apoptosis that contributed to the increased sub-G1 population in CFPac1 cells. In a pilot study, detection of surface annexin V was performed on CFPac1 cells treated with the αvβ6 blocking antibody 53A.2 (data not shown). The results obtained were inconclusive, however the assay needs to be optimised further before any conclusions can be made. Whilst Panc04.03 and CFPac1 cells showed similar levels of inhibition of proliferation upon treatment with αvβ6 function blocking antibodies, the mechanisms behind this may be different in each of the cell lines. Understanding the mechanism of action of the αvβ6 function blocking antibodies are vital and perhaps markers for cell cycle progression such as cyclin A, cdk2, cdk6, p16, p21, p27 need to be tested, which might provide an answer. Preliminary experiments conducted to test some of the above mentioned markers did not reveal any significant changes (data not shown).

3.11.2.3 Effect of αvβ6 on downstream signalling pathways

It was hypothesised that blocking αvβ6 was having an effect on the downstream signalling pathways involved in apoptosis and proliferation. αvβ6 has been previously shown to bind and activate Fyn, which activates the Raf-ERK/MAPK pathway and promote OSCC invasion [185]. αvβ6 has also been shown to interact with the ERK signalling pathway directly and deletion of the ERK2 binding site from the β6 cytoplasmic tail led to a decrease in tumour growth in colon carcinoma cell lines [181]. Phosphorylation of ERK leads to activation of down stream signalling, which induces cell proliferation and survival. When levels of phospho ERK (proliferation), Fyn (integrin mediated signalling), caspase 3 (cell death by caspase dependent apoptosis) and phospho SMAD2/3 (activation of TGFβ) were examined in the cells treated with the αvβ6 blocking antibody or the control IgG antibody for 5, 15, 30, 45, 60 minutes and 24 hours, disappointingly, no differences were observed between the two treatment groups at any of the time points (data not shown). It was then decided to examine later time points as the differences in proliferation observed in the cell cycle was at day 7. It was hypothesised that any changes in the signalling would happen prior to this time point. Lysates from the αvβ6 antibody treated and control IgG treated cells were prepared 24, 48, 72 and 96 hours post treatment and tested. However, no significant differences were observed at these time points when probed

for phospho and total ERK, Fyn, caspase 3 and cyclin B1 (Figure 47, Figure 49, Figure 50, Figure 51).

A slight decrease in the expression levels of phospho ERK in CFPac1 cells at 24 hours and 48 hours in the αvβ6 blocking antibody treated cells compared with the IgG treated cells was seen (decrease of 18% and 24% respectively). However, I cannot be certain if the differences observed in cell proliferation in CFPac1 cells as a consequence of αvβ6 blockade can be attributed to this decrease in phospho ERK observed. Nevertheless, it is worth bearing in mind that ERK2 has been shown to interact directly with the β6 subunit cytoplasmic tail and perhaps like Ahmed and colleagues have shown in colon cancer cell lines [181], mutating the ERK binding site in the β6 subunit in CFPac1 cells and studying its downstream signalling might be worth pursuing in the future.

Cyclin B1 is an important regulatory subunit of Cdk1, essential for mitotic exit and completion of cell cycle and if cells are blocked at the G2/M phase, a corresponding increase in levels of cyclin B1 is usually expected. An increase in cyclin B1 was observed in Panc04.03 cells at 24hours and 48 hours (increase of 16% and 21% respectively). The levels of change observed were in line with the proportion of cells blocked at the G2/M phase upon αvβ6 blockade. Although encouraging, this change was not observed at the later time points tested, which made it difficult to make any conclusive inferences. Perhaps a more quantitative and sensitive technique (flow cytometry, qPCR) might reveal any subtle differences, if any, at the later time points.

Generally, caspase 3 cleavage is considered to be a marker for apoptosis and is a convergent point for both intrinsic and extrinsic apoptotic pathway. Since there was a dramatic increase in the sub-G1 population in the αvβ6 function blocking antibody treated CFPac1 cells, lysates prepared at 24, 48, 72 and 96 hours were tested for caspase 3 activation. Disappointingly, no difference was observed in caspase 3 activation at any of the time points. However as previously mentioned, the presence of sub-G1 DNA in itself is not definitive of apoptosis and furthermore caspase independent pathways of apoptosis have been described [238]. Apoptosis inducing factor (AIF) is released from the mitochondria during apoptosis and contribute to DNA fragmentation in the nucleus [239]. Importantly, release of AIF can be triggered independently of the caspase cascade by cathepsin D [240] and can also proceed in cells derived from a caspase 3 null mice [241].

It was disappointing that none of the potential markers showed any significant changes in response to αvβ6 treatment *in vitro* but it has to be borne in mind that signalling pathways are affected by multiple factors including the environment in which it is grown (plastic as opposed to a 3D matrix) and the surrounding microenvironment. These pathways are better reflected *in vivo* and some of these markers were significantly different between the αvβ6 blocking antibody treated tumours and control IgG antibody treated tumours, which will be further discussed later.

3.11.2.4 Effect of αvβ6 on migration and invasion of PDAC cell lines

Integrin signalling has been shown to be involved in both migration and invasion [242]. αvβ6 overexpression in OSCC cell lines promoted greater migration and invasion compared with control αvβ6 negative cell lines [209]. It has also been shown that up regulation of αvβ6 leads to an increase in MMP9 secretion which, in turn, promotes cancer cell migration and invasion [210]. Thus, there has been a strong link between αvβ6 and its role in cancer cell invasion and migration [208]. Invasion of pancreatic cancer cells into the surrounding nerves (perineural invasion) and blood vessels (vascular invasion) have been linked with local recurrence of PDAC in patients [243].

This study has shown that αvβ6 function-blocking antibodies can significantly reduce migration of αvβ6 positive PDAC cell lines towards fibronectin and LAP, the two most common ligands associated with αvβ6 (Figure 53, Figure 55). No change in migration was observed in the αvβ6 negative cell lines (Figure 54, Figure 56). Fibronectin has been shown to be one of the primary ECM components in the stroma surrounding pancreatic cancer [82]. Binding of αvβ6 to LAP exposes the TGFβ allowing activation of the TGFβ signalling pathway, which in turn can promote cancer cell migration and invasion [51]. TGFβ can also activate stellate cells to become myofibroblast-like. Thus, it is perhaps not surprising that enhanced expression of TGFβ has been linked to poor prognosis in PDAC patients [244].

A significant reduction of invasion was observed in four out of the five αvβ6 positive invasive cell lines treated with an αvβ6 function-blocking antibody, 10D5 (Figure 57, Figure 58) over 72 hours compared with control antibody. Proliferation assays were

set up in parallel to ensure that there were no differences in cell numbers over 72 hours (the time period employed for the invasion assay) between the αvβ6 function blocking antibody treated and control IgG treated groups. Interestingly, the HPAF cell line did not show any invasion even though it had high levels of αvβ6 expression. One possible explanation for this could be that the αvβ6 expressed by HPAF is in a different conformational state, and thereby does not promote invasion or it may simply be that this cell line was not invading in an αvβ6 dependent manner.

There is a strong expression of Cyclooxygenase 2 (cox 2) in pancreatic stellate cells present in the tumour stroma surrounding PDAC [245]. Cox 2 has also been shown to be expressed by tumour cells and upregulate MMP9 expression, in turn promoting invasion of BxPC3 cells [246]. In a separate study, Cox 2 inhibition has been shown to suppress αvβ6 dependent invasion in oral carcinoma cell lines in 3D invasion assays [247] and MMP9 has been shown to promote invasion in an αvβ6 dependent manner in OSCCs [125]. Given more time, it would be interesting to check for levels of cox2 and MMP9 expression by PDAC cell lines tested in this study. It could very well be that invasion of PDAC cells lines tested in this study could be driven by MMP9 expression in response to Cox 2 expression in an αvβ6 dependent manner.

3.11.3 Development of 3D co-culture model

Pancreatic cancer is associated with a very strong desmoplastic response. Cancer cells behave differently when co-cultured with stromal cells in a 3D matrix because of varied gene expression as a result of the tumour-stroma interactions. Pancreatic stellate cells form the major cell component of this stromal response with the fibroblasts, nerve cells, blood vessels and immune cells providing the remaining cells [81].

An air-liquid interface organotypic co-culture was previously established for studying OSCC invasion in vitro [90] and this model was later modified for generating a 3D organotypic model for studying PDAC [59]. This model allowed better replication of the tumour-stroma interaction, more relevant to the dense stromal response observed in human PDACs. Data obtained so far show that the organotypic gels revealed some of the cellular complexity of pancreatic carcinoma growth, differentiation and their impact on invasive potential. Four αvβ6 positive cell lines were co-cultured with MRC5 h-TERT immortalised fibroblasts (neo-natal lung

fibroblasts). MRC5 cells were used as these are reported to express high levels of HGF, a chemotactic and invasive factor for carcinomas [248]. It would have been more relevant to use the Pancreatic stellate cells (PS1), available in-house, in this co-culture model but their rate of growth was incredibly slow and attaining enough number of cells to set up the co-culture experiment was incredibly time consuming. However, considerable time and effort was spent to grow these cells in bulk in the later stages of this study, as they were crucial for *in vivo* experiments, which will be discussed in detail later.

In the co-culture system, CFPac1 cell line was found to be the only invasive cell line compared with Panc04.03, Capan1 and HPAF, where no invasion was observed (Figure 60, Figure 61). In contrast, all four cell lines tested in a 3D organotypic co-culture system exhibited invasive capability at varying levels in the 2D invasion assay. An independent study which I performed comparing OSCC invasion in response to a panel of fibroblasts in this co-culture model revealed that the cancer cell lines' invasive propensity varied in response to fibroblasts of different origin. For example, VB6 (OSCC) cells showed high level of invasion when co-cultured with MRC5 fibroblasts but a complete absence of invasion in the presence of FSF44 (foreskin fibroblast 44) (data not published). Therefore, it is worth investigating if the same holds true for the PDAC cell lines tested above and perhaps PS1 cells might induce a more invasive response from these cells. A further consideration for the lack of invasion observed (with the exception of CFPac1 cell line) would be the proximity of tumour cells to stromal cells in the co-culture system. In a model for squamous cell carcinoma, Sahai and colleagues demonstrated that in order for cancer cells to invade collectively, close proximity to fibroblasts is required, as these fibroblasts create tracks via RhoA and ROCK dependent actin-myosin activity with MMP-mediated proteolysis [249]. As there was no direct cancer cell-to-stromal cell contact in the co-culture system tested in this study, it is possible that the proteolytic activity by the fibroblasts is absent and thus invasion does not occur.

Both Panc04.03 and HPAF retained $\alpha v\beta 6$ expression in the 3D co-culture system and the cells were proliferating as confirmed by the Ki67 staining, a marker for proliferation. Higher magnification images revealed luminal structures that were formed in the epithelial layer, which were very similar to *in vivo* PDAC tumours. In fact, images from the 3D organotypic co-culture model and orthotopic xenograft tumours (shown in results chapter III) reveal very similar features further confirming that this co-culture model provides a morphologically similar pattern of cellular

distribution. Close examination of the Panc04.03 co-culture shows that αvβ6 expression is more pronounced along the tumour-stroma interface, which is consistent with the published literature where αvβ6 expression has been shown to be higher in the invasive front of the tumour [250]. Strong αvβ6 expression at the interface with stromal cells has also been observed in other cancers such as head and neck cancer [203]. Other studies in our laboratory have shown that in OSCCs, expression of αvβ6 mRNA, detected by *in situ* hybridisation, was greatest at the tumour-stroma interface (unpublished). Perhaps a similar effect might be occurring in the Panc04.03 cell line tested in this model, where β6 mRNA might be overexpressed at the invasive front.

These co-culture models were generated to study αvβ6 dependent PDAC cell invasion with the aim of using shRNA mediated β6 stable knock down or non-targeted knock down cell lines (discussed later). Using an antibody to block the function of αvβ6 in these co-culture models was challenging due to a variety of factors. It was impossible to assess whether the antibody would target all the cancer cells, including ones in the matrix, while a large amount of antibody was required for this assay and there was only a limited amount of the antibody (received from Astra Zeneca) available for the purposes of this study. Since no invasion was observed in the cell lines tested, with the exception of CFPac1, in this co-culture system it was decided not to use the *in vitro* co-culture model and proceed directly to *in vivo* experiments. As the challenges of antibody delivery hold true *in vivo* as well in the 3D co-culture model tested above, it was thus necessary to generate a β6 shRNA stable knock down cell line for use directly in the murine models.

3.11.4 Development of stable knock down cell lines

It is worth noting that attempts to knock down β6 with shRNA began before the studies on the role of αvβ6 in proliferation and actually fuelled their development. Having screened and characterised many PDAC cell lines for expression of αvβ6, it was decided to generate β6 stable knock down cell lines using lentivirus-mediated transfection of β6 shRNA into Panc04.03 and CFPac1. As discussed previously, siRNA mediated knock down of Panc04.03 and CFPac1 proved extremely difficult using a lipid-mediated method of transfection. It was hypothesised that lentiviral-mediated transfection of shRNA would help generate matched pairs of the same cell line with the only difference in αvβ6 expression levels. This would have proven to be

an extremely useful tool to study the functional role of αvβ6 in 3D co-culture models in vitro and also in vivo in xenograft animal models. Despite trying three different commercially available and verified β6 shRNA-targeted sequences, it was not possible to successfully generate a stable cell line for both CFPac1 and Panc04.03. It was possible to monitor the transfection efficiency by following the GFP expression, which was driven by an IRES promoter. The cells when treated with the lentivirus carrying the shRNA plasmid showed lower levels of αvβ6 and higher levels of GFP compared with the non targeted (NT) control shRNA treated cells, meaning the transfection had worked and αvβ6 levels were low compared to the parent control (Figure 62). The infected cells were then positively sorted by FACS for the top 10% GFP expressers (indicative of high shRNA transfection levels) and re-plated. Once sorted, these cells (high GFP, low αvβ6) were extremely slow growing compared to the NT shRNA control treated cells (high GFP, high αvβ6). It took on average between six to eight weeks before these cells started to grow faster allowing for enough cells to be collected to check for expression levels of αvβ6 and GFP using flow cytometry (Figure 63). The sorted cells, which were GFP positive and low expressers of αvβ6 at the time of plating, had lost their GFP expression, indicating loss of plasmid from the cell and expressed high levels of αvβ6 comparable to the parent control cells. The above data suggested that αvβ6 might be crucial for the survival of the PDAC cell lines tested (Panc04.03 and CFPac1) and any attempt to knock down αvβ6 stably was not possible because the plasmid was ejected from the host genome.

This dramatic reduction in cell growth when transfected with shRNA targeting β6 has been observed in another study using YAPC PDAC and A549 lung cancer cell lines [207], which are both *KRAS* dependent (activating mutation in *KRAS*) cell lines. Both Panc04.03 and CFPac1 have activating *KRAS* mutations at codon 12 and thus these results correlate with my results presented in this study. Providing more time were available, it might be worth repeating the knock down of β6 in a PDAC cell line without an activating *KRAS* mutation using the shRNA sequences to study the effect on proliferation. More recently, a dox -nducible shRNA plasmid to knock down β6 has become available (Open Biosystems Ltd). It would be worth trying the inducible plasmid on the same cells to try and generate an inducible knock out model, which will help overcome the dependence of these cells on αvβ6 for survival.

So in summary, blockade of αvβ6 function in the αvβ6 positive PDAC cell lines significantly reduces growth, migration towards fibronectin and LAP and invasion, suggesting that αvβ6 might be an interesting molecule to study in human PDAC with the potential of being a therapeutic target.

RESULTS CHAPTER II

4 Human PDAC and αvβ6

4.1 Bioinformatics analysis of αvβ6-associated gene changes in pancreatic cancer

The Pancreatic expression database (PED) was developed at the Barts Cancer Institute, Queen Mary University of London, comprising data published by multiple research groups who focus on pancreatic cancer [251, 252]. It contains of 56,015 expression measurements and 6363 DNA copy number alterations obtained from 59 different published studies. The collected data were profiled using multiple transcriptomics (e.g. Affymetrix GeneChip® Human Genome arrays), proteomics (e.g. Matrix Assisted Laser Desorption/Ionization Time-of-Flight (MALDI-TOF) Mass spectrometry), miRNAs (e.g. human miRNA Agilent array) and genomics (e.g. Affymetrix GeneChip® Human Mapping 100K SNP Set) platforms [252]. The PED interface also incorporates functional data from Ensembl Mart 56, allowing users to link PDAC genes to the pathways they control.

4.1.1 *ITGB6* expression at the mRNA level

In collaboration with Dr. Claude Chelala, the pancreatic expression database (PED) was used to examine expression of integrin *ITGB6* gene expression in pancreatic cancer versus normal pancreas at the mRNA transcript level. The Affymetrix GeneChip® Human Genome array U133 Plus 2.0 platform was used to determine the expression level in the dataset. The dataset had a total of 96 human PDAC cases and 4 normal donor pancreas (normal pancreas tissue is extremely rare to obtain, hence the small sample size). Interrogation of the pancreatic expression database revealed that the expression of the β6 gene (*ITGB6*) was significantly up regulated in PDAC tumour tissue compared to the normal tissue (Figure 64). Three different probes for the *ITGB6* gene (Figure 65) showed similar results confirming that *ITGB6* is up regulated in PDAC patients at the mRNA level.

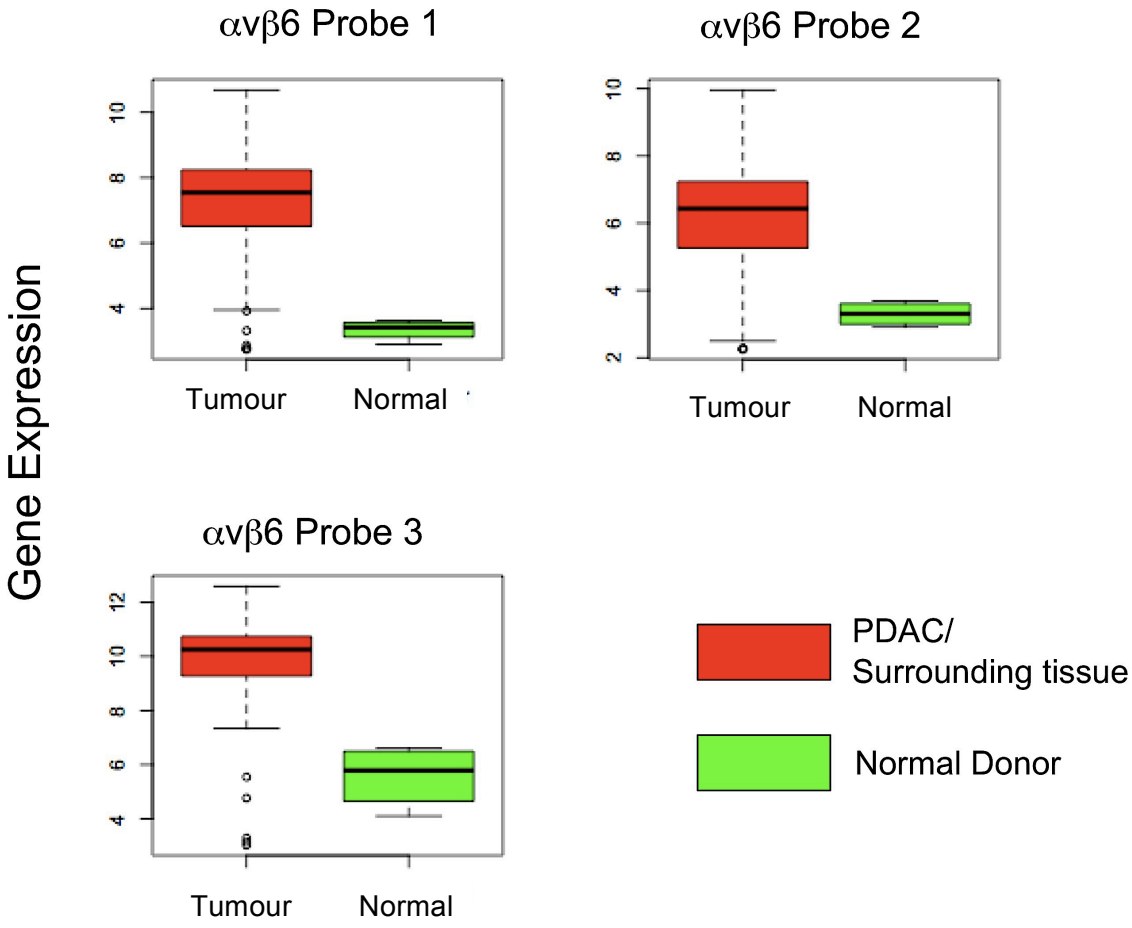

Figure 64: Expression of *ITGB6* gene in PDAC (whole tissue) versus normal pancreas (whole tissue).

There is an overexpression of *ITGB6* at the mRNA level (red) in the PDAC tumour tissue compared to the normal pancreas (green). Data shown above are box and whisker plots showing the median expression (black line) of *ITGB6* with a confidence interval between 5% and 95%. Three different Affymetrix probes 208083_S_AT (probe 1), 208084_AT (probe 2) and 226535_AT (probe 3) are present in the Affymetrix U133 Plus 2.0 chip that recognise *ITGB6*. The probes and their target sequences in *ITGB6* are shown in the table below. Integrin *ITGB6* has 2397 base pairs with 15 exons. Each probe has at least 11 different recognition sites within the exons and these are shown in the figure presented below.

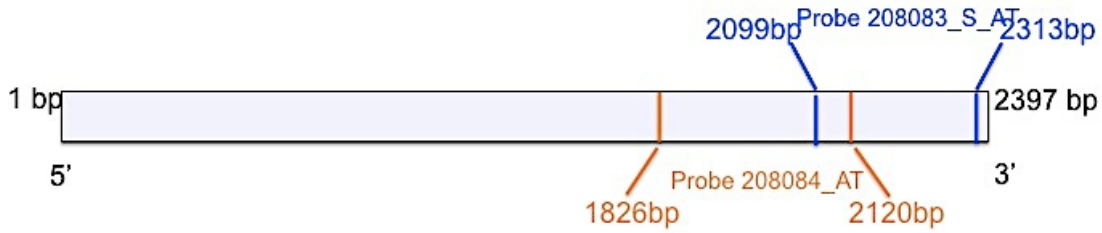

Probe Sequence(5'-3') 20803_S_AT	Probe X	Probe Y	Probe Interrogation Position
AAAACCATCATTCACAGCATCAATG	651	221	2099
GGTTGTCCTACTGTGCATCTGGAAG	1025	833	2197
CCTACTGTGCATCTGGAAGCTACTG	1006	447	2203
ATCTGGAAGCTACTGGTGTCATTTC	479	47	2213
AAGCTACTGGTGTCATTTCATGATC	1010	247	2219
ACTGGTGTCATTTCATGATCGTAAA	518	165	2224
GCAGAACGATCAAAAGCCAAGTGGC	295	531	2267
GGCAAACGGGAACCAATCCACTCTA	516	871	2289
CAAACGGGAACCAATCCACTCTACA	438	305	2291
CAATCCACTCTACAGAGGATCCACA	669	293	2302
ACAGAGGATCCACAAGTACTTTTAA	254	187	2313
Probe Sequence(5'-3') 208084_AT	**Probe X**	**Probe Y**	**Probe Interrogation Position**
GGCAAGTGTGTTTGCACAAACCCTG	234	871	1826
GACCAACCTGTGAACGATGTCCTAC	38	625	1860
TGAACGATGTCCTACCTGTGGTGAC	821	951	1870
ACCCCTGTAACTCTAAACGGAGCTG	651	147	1893
AACGGAGCTGCATTGAGTGCCACCT	474	239	1908
GCTGCATTGAGTGCCACCTGTCAGC	1015	501	1914
GCCAAGCCCGAGAAGAATGTGTGGA	521	469	1944
GTGCAAACTAGCTGGTGCGACCATC	778	767	1972
CTAGCTGGTGCGACCATCAGTGAAG	893	371	1979
CAAAGGATGGTTCTGTTTCCTGCTC	589	305	2016
AATGAAAAAGATTGTCCGAAGCCTC	459	275	2120

Figure 65: Recognition sites of Probe 1 and Probe 2 in the *ITGB6* gene.

A list of 10,000 genes was up or down regulated in PDAC with a cut off log fold change of 2, including *ITGB6* with a log fold change of 4.261 (p=4.59E-06). Potentially, expression of some of these genes may be as a result of *ITGB6* overexpression in PDAC. In an attempt to identify those genes that are likely to have changed due to changes in *ITGB6*, further analyses were conducted on the list of 10,000 genes using a high threshold of 8 in order to obtain a set of genes that had maximum correlation with *ITGB6* expression. 40 genes were up regulated and one gene (FAM107A) was down regulated. The genes and their log fold change in expression along with p values obtained are shown in Table 1.

Gene of interest	Gene name	Log Fold change	p value
Integrin alpha 2	ITGA2	4.5273	1.8E-10
Capping protein (actin filament), gelsolin-like	CAPG	2.4702	1.09E-05
Matrix metalloproteinase 7	MMP7	2.0468	0.00618
Matrix metalloproteinase 11	MMP11	5.2970	5.46E-06
Laminin gamma 2	LAMC2	4.6285	2.28E-05
Laminin alpha 3	LAMA3	4.3512	9.66E-05
Tumour necrosis factor receptor superfamily, member 21	TNFRSF21	2.4503	5.76E-05
S100 calcium binding protein A6	S100A6	3.5582	0.00082
Cathepsin E	CTSE	6.0343	4.66E-06
Collagen, Type X, alpha 1	COL10A1	7.1897	5.69E-14
Chemokine like factor	CKLF	2.4139	2.90E-09
Keratin 19	KRT19	4.3910	9.13E-05
Claudin 18	CLDN18	5.5356	0.00315
Bcl-2 interacting killer (apoptosis inducing)	BIK	2.4062	0.00172
EPS8-like 1	EPS8L1	2.5512	0.00940
Family with sequence similarity 107, member A	FAM107A	-2.5839	0.00381

Gene of interest	Gene name	Log Fold change	p value
Hematological and neurological expressed 1	HN1	2.4300	4.48E-04
ADAM metallopeptidase domain 10	ADAM10	2.2388	2.06E-07
Laminin, beta 3	LAMB3	3.7281	0.0004
Pleckstrin homology-like domain, family A, member 2	PHLDA2	3.8929	2.53E-05
Fermitin family homolog 1 (Drosophila)	FERMT1	2.5231	0.00204
Transmembrane channel-like 5	TMC5	3.8931	0.00209
UEV and lactate/malate dehydrogenase domains	UEVLD	2.2070	7.52E-08
GAP junction protein, beta 2, 26kDA	GJB2	5.9666	4.46E-08
Solute carrier family 44, member 4	SLC44A4	2.43909	0.0324
CD58 molecule	CD58	2.8020	5.87E-11
Anoctamin 1, calcium activated chloride channel	ANO1	4.5766	1.19E-07
Chromosome 15 open reading frame 49	C15orf48	4.0073	7.03E-06
Sperm associated antigen 1	SPAG1	3.3445	3.32E-07
Epithelial cell transforming sequence 2 oncogene	ECT2	4.7843	5.32E-09
Rhophilin, Rho GTPase binding protein 2	RHPN2	2.0807	0.00775
Kruppel-like factor 5 (intestinal)	KLF5	4.7366	1.02E-08
Epiplakin 1	EPPK1	3.4071	0.0001
Chromosome 19 open reading frame 33	C19orf33	4.2576	0.0005
Heparan sulphate (glucosamine) 3-O-sulphotransferase 1	HS3St1	4.8245	2.24E-06
Calpain 8	CAPN8	4.2043	0.00130
Spermatogenesis associated, serine-rich 2-like	SPATS2L	3.2409	9.25E-08
Adhesion molecule with Ig-like domain 2	AMIGO2	3.2254	6.94E-08
FXYD domain containing ion transport regulator 3	FXYD3	3.19357	0.00186
Transmembrane protease, serine 4	TMPRSS4	4.7028	0.00032
ADP-ribosylation factor-like 14	ARL14	3.3263	0.010851

Table 14: Top 41 genes whose expression changed at the same time as *ITGB6*.

4.1.2 q-PCR analysis

To determine whether the observed changes were αvβ6-dependent, Capan1 cells were treated with siRNA to knock down *ITGB6* or a control non-targeting siRNA. mRNA was isolated from the treated cells and a quantitative PCR (qPCR) assay was set up to determine whether the expression levels of three genes that were relevant to cancer, integrin alpha 2 (ITGA2), capping protein (actin filament) gelsolin-like (CAPG) and matrix metalloproteinase 11 (MMP11) changed in response to β6 knock down. Ct values were normalised to the endogenous expression of the house-keeping gene 18s and relative % fold change was plotted as below.

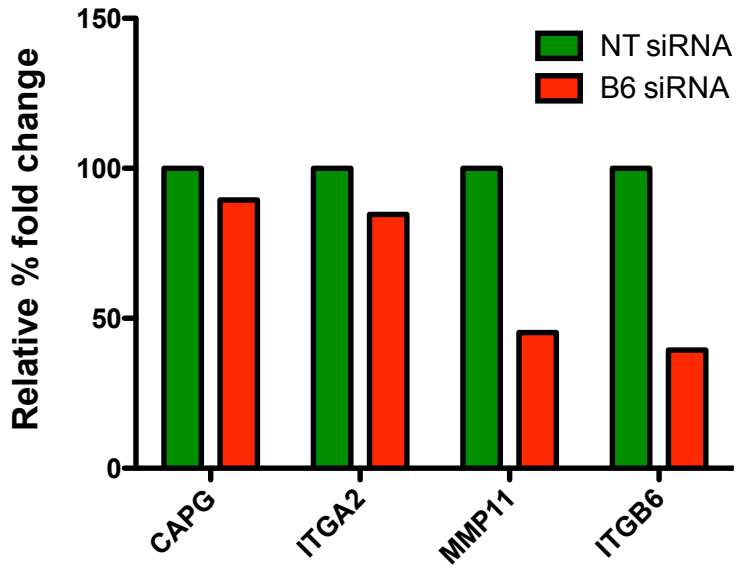

Figure 66: qPCR analysis of genes selected from the gene-list that were up or down regulated in PDAC along with ITGB6 in Capan1 cells. RNA from siRNA mediated knock down of β6 in Capan1 cells (red) were analysed for changes in gene expression and compared with non-targeted siRNA control (green). *Note that n=1 for this experiment.*

CAPG is an actin-filament capping protein and is shown to be involved in actin-cytoskeleton regulation. Previous studies have noted its up regulation in pancreatic cancer [253]. Its expression was marginally reduced when β6 was knocked down in Capan1 cells (Figure 66). There was a marginal reduction in the expression levels of ITGA2 when β6 was knocked down. ITGA2 when associated with integrin subunit β1, forms the major collagen receptor integrin, α2β1, a most relevant molecule in a desmoplastic tissue [254]. MMP11 encodes for matrix metalloproteinase 11 (Stromelysin 3); previously this protease has been linked strongly with breast cancer

[255]. There was a 50% reduction in the expression levels of MMP11 in the β6 knock down cells compared to the NTsiRNA. It should be noted that the Pancreatic Expression Database data also includes stromal cells and it is entirely possible that any or all of the genes in our top 40 could be stromal in origin. However preliminary data obtained suggest that there is a drop in MMP11 gene expression as a consequence of knockdown of *ITGB6* and there also may be a moderate reduction in both CAPG and ITGA2. The results shown are for n=1 and it is necessary to repeat the qPCR assay before any inference can be drawn from these results.

4.1.3 IHC analysis

A pilot experiment performed on five human PDAC tissue samples and one normal control tissue sample by immunohistochemical staining showed expression of two genes that were shown to be upregulated in the bioinformatics study. FERMT1, more commonly known as Kindlin1 is a focal adhesion protein, belonging to the fermintin family homolog-1 and loss of function mutations of this gene have been associated with Kindler syndrome, an autosomal recessive disorder characterised by skin atrophy and blistering [256] and it has also been identified as part of a gene signature in predicting lung and breast cancer metastasis [257].

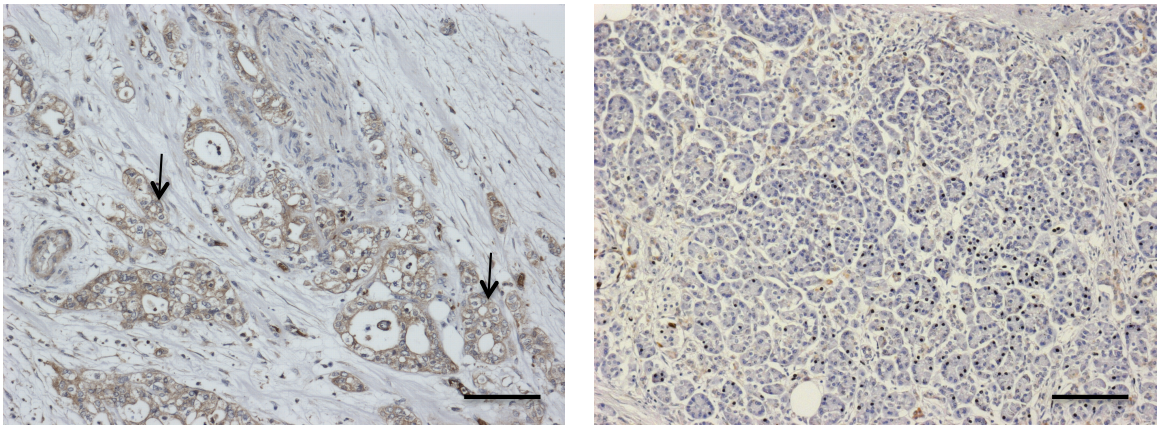

FERMT1 PDAC **FERMT1 normal pancreas**

Figure 67: Representative image of FERMT1 (brown membranous stain, arrows) on PDAC tissue and its absence in normal pancreas tissue. (Scale bar represents 100μm).

LAMC2 or laminin gamma 2 has shown to be up regulated in oesophageal squamous cell carcinomas and patients with high expression are linked with poor prognosis [258].

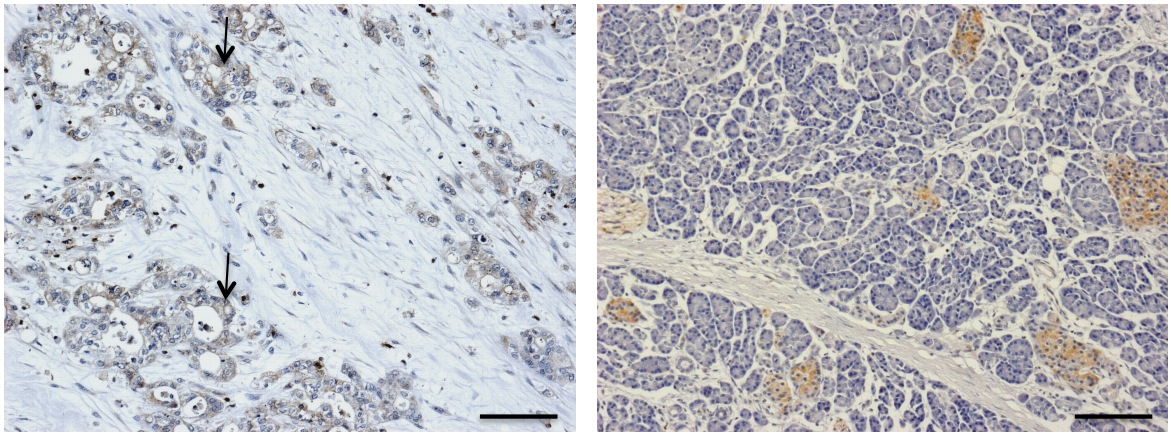

LAMC2 PDAC **LAMC2 normal pancreas**

Figure 68: Representative image of LAMC2 (brown cytoplasmic/membrane stain, arrows) on PDAC tissue and absent in normal pancreas tissue. Note: background staining observed in the Islet cells. (Scale bar represents 100µm).

Immunohistochemical analyses revealed overexpression of FERMT1 and LAMC2 in the cell membrane/cytoplasm of PDAC cells in all the cases tested (Figure 67, Figure 68). The normal pancreas tissue was negative for both the proteins.

4.2 ITGB6 expression at mRNA level and survival in PDAC patients

There are no studies looking at expression of $\alpha v\beta 6$ and its influence on survival in patients with pancreatic ductal adenocarcinoma. Using bioinformatics, the expression of *ITGB6* at the mRNA level was examined for the first time to determine if *ITGB6* overexpression in pancreatic cancer had any correlation with survival in patients. Kaplan-Meier (KM) survival curves of *ITGB6* mRNA abundance across five publically available data sets [259-263] and one in-house cohort of PDAC patients (BCI) were plotted. A total of 292 patients were dichotomised into low expressers and high expressers based on expression levels of *ITGB6*, top 25% quartile versus the bottom 75%.

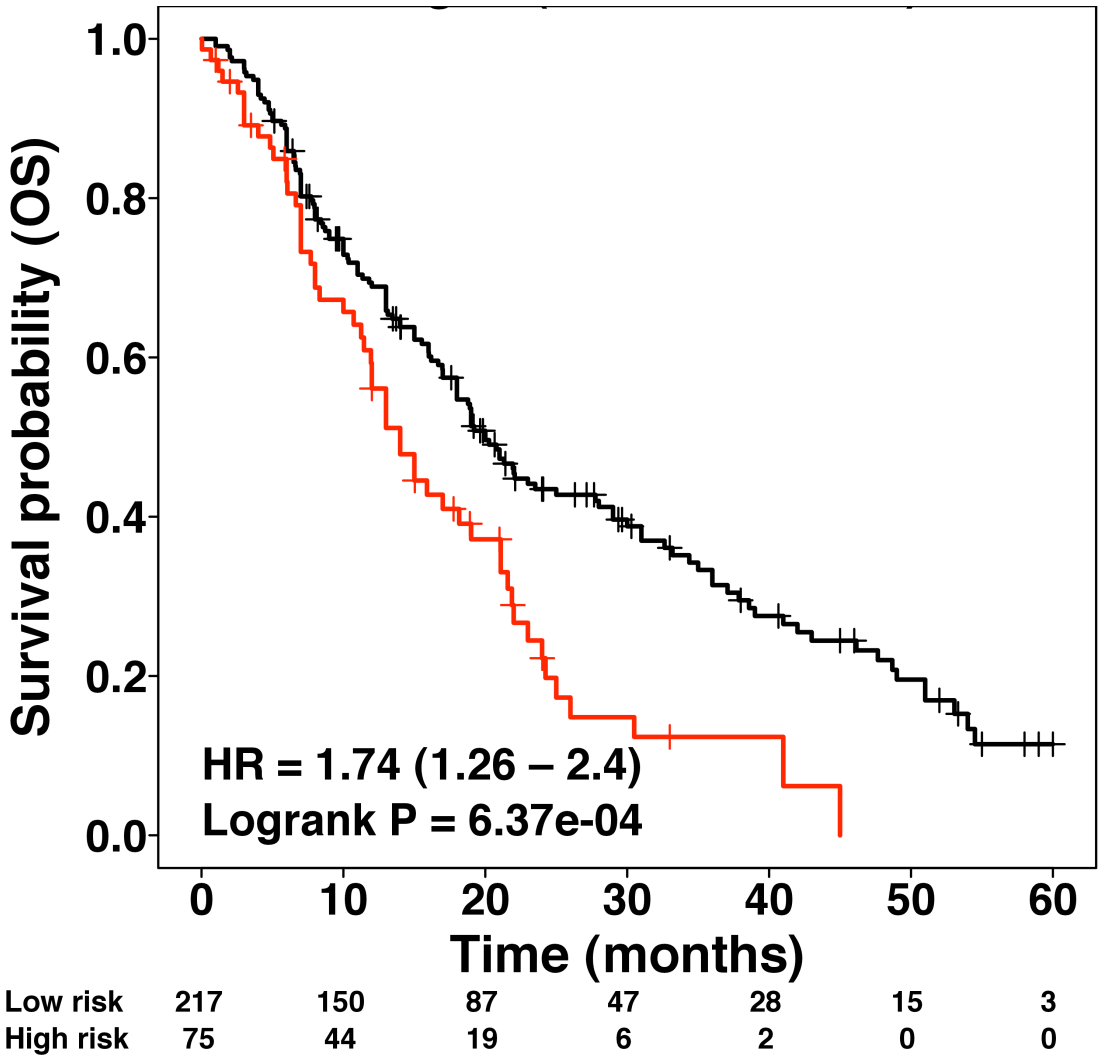

Figure 69: Kaplan-Meier survival curve of PDAC patients based on ITGB6 expression. (n=292). Logrank test p= 6.37×10^{-4}. Red line is *ITGB6* positive (top 25%), Black line is *ITGB6* weakly positive or negative (bottom 75%). Hazard Ratio (HR)= 1.74.

Kaplan-Meier curves are used for estimating survival as a function of various markers in patients and usually are represented in a series of horizontal steps of declining magnitude. When a large enough number of samples are analysed, it provides a true survival function for that group. It is a method that takes into consideration certain types of right censoring. E.g. it takes into account if a patient withdraws from a study (i.e. data is lost before the final outcome). On the curve, tiny vertical marks indicate any survival time that has been censored.

Red and black curves represent high (top quartile 25%) and low (bottom quartile 75%) expression groups. There were 217 patients in the low *ITGB6* expressing group and 75 in the high *ITGB6* expressing group at time zero. Based on predictive survival only 6 patients in the high *ITGB6* expressing group were alive at 30 months compared to 47 patients in the low *ITGB6* expressing group. There is a significant difference in overall survival between the two groups, with those expressing high levels of *ITGB6* tending to have lower overall survival compared to the weak expressers of *ITGB6* (Figure 69). There is a median survival difference of 6 months between the two groups. At 24 months, there were only 11 patients alive in the high *ITGB6* expressing group (3.76%) compared to the 64 patients alive in the low *ITGB6* expressing group (21.91%). At three years, there were only 4 patients alive in the high *ITGB6* expressers (1.36%) compared with the 35 patients alive in the low *ITGB6* expressers (11.98%). Survival analysis was conducted for overall survival (OS) truncated at 60 months. Survival at 60 months was low for both groups, with just 3 and no patients alive in the *ITGB6* low and high expressers respectively reflecting poor prognosis of pancreatic cancer patients as a whole. Difference between the dichotomised groups was assessed using the Cox proportional hazards model and significance of difference was evaluated using the Log-rank test.

4.3 Expression of αvβ6 in human PDAC tissue samples

Having looked at expression of αvβ6 at the mRNA level and establishing a correlation between αvβ6 expression and overall survival in PDAC patients, we wished to investigate this on PDAC tissue samples and determine if there were similar observations at a protein level.

Sipos et al, (2004) first showed the expression of αvβ6 in human PDAC. They had a small sample set of 34 PDAC cases and stained them for expression of β6 using a novel monoclonal antibody [201]. They found αvβ6 to be expressed in varying levels in all 34 PDAC tissue samples (section 2.6.1). They did not perform any further analysis or correlation studies presumably due to the limited number of PDAC samples. A large number of patient samples with follow up data were required for conducting a clinical analysis to identify the role of αvβ6 in PDAC progression. In collaboration with the Beatson Institute, Glasgow, UK and the University of Verona, Verona, Italy, a large number of tissue microarrays (TMA) of human pancreatic ductal adenocarcinoma and ampullary cancer patients were obtained. Both sets of

TMAs had clinical follow up data, which made it possible to carry out correlation studies with regards to expression of αvβ6.

4.3.1 αvβ6 staining in PDAC tissues

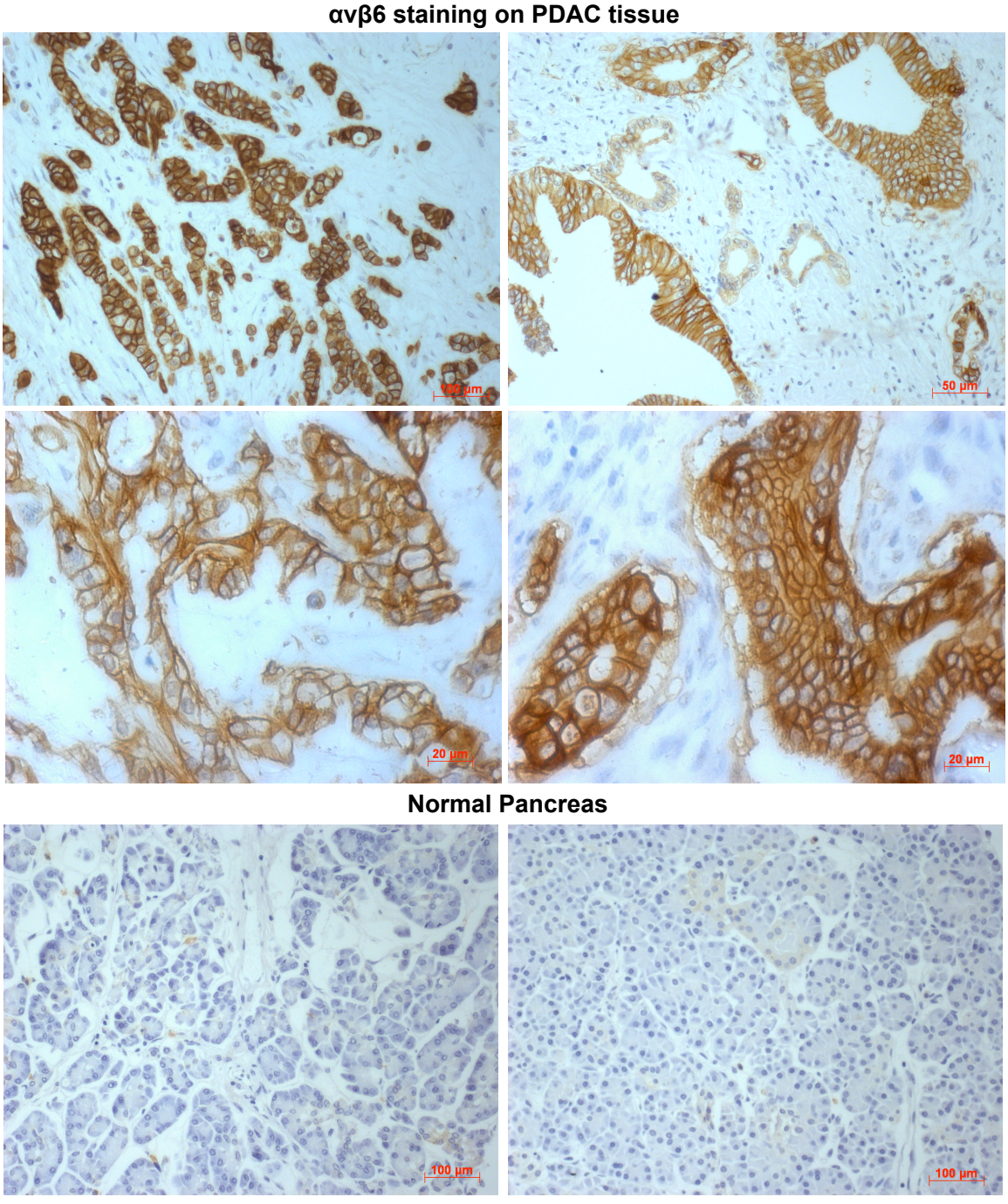

Figure 70: Expression of αvβ6 in human PDAC tissue sample. The tumour cells are strongly positive (brown stain) for αvβ6 expression while the normal pancreas is entirely negative for αvβ6. Strong and distinct membrane staining can be observed on the epithelial cells with the surrounding stromal cells entirely negative for αvβ6.

The above picture is a typical representation of a TMA stained for αvβ6 using 62G2 antibody. The x10 magnification image shows a TMA core with normal pancreas and PDAC. The antibody 62G2 picks up αvβ6, which is expressed only by the cancer cells and the normal cells are all negative. The higher magnification of the image shows the membranous localisation of αvβ6 particularly at the cell-cell junctions. It should be noted that the staining is restricted to the epithelial cells and the surrounding stromal cells are all negative. This was the case for all the TMAs stained and they were scored and quantified for further analysis.

4.3.2 Clinical analysis of PDAC TMAs from the Beatson Institute

A total of 118 PDAC patients in the data set and six cores per slide represented each patient. Scores of all six cores were averaged to get a single score per patient. As it was not possible to release the clinical data associated with TMAs, the scores of individual cores were sent to the Beatson Institute for further clinical analysis.

Kaplan-Meier (KM) survival curves were plotted based on β6 expression scores for a total of 118 PDAC cases (Figure 71). Based on the scores, any patient with a score greater than or equal to the median score of 3 was considered as positive and the remaining patients with a median score of less than 3 were considered negative. A logrank test was performed to check for significance. The Logrank test is used widely to compare survival distribution of two sets of data. It is a non-parametric test and was appropriate to be used in this particular data set because the data was not normally distributed. The logrank test often is referred to as the Mantel-Cox test.

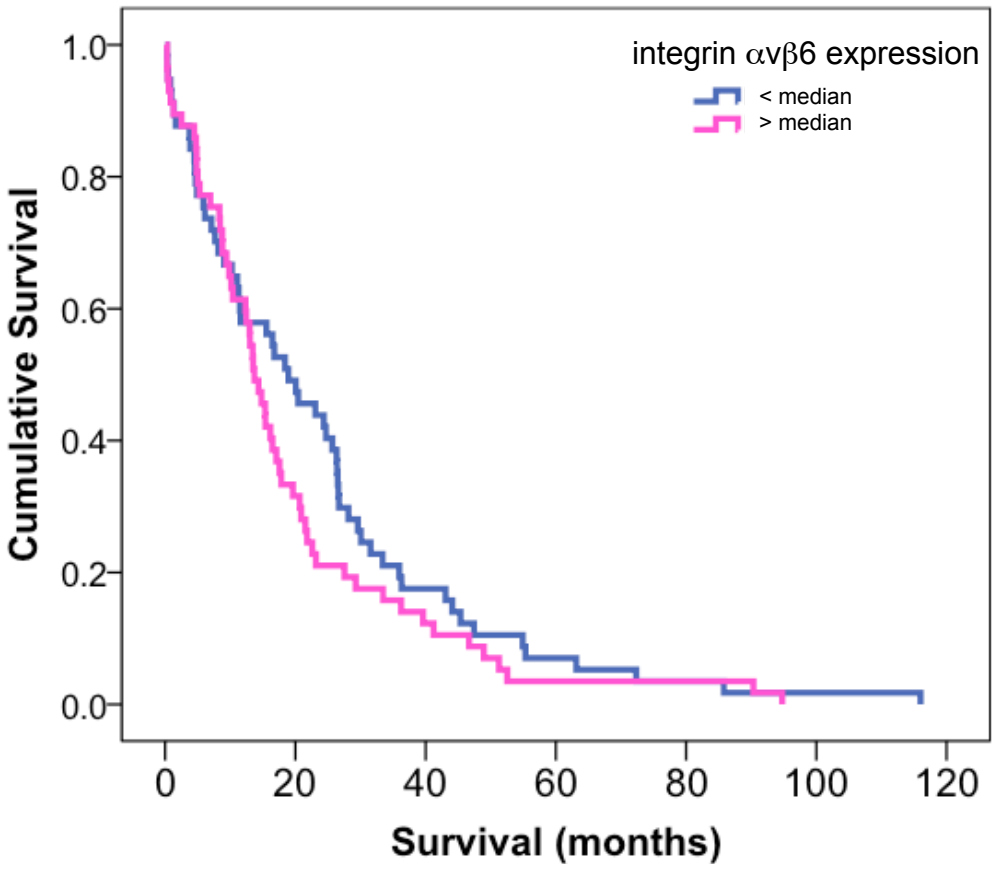

Figure 71: Kaplan-Meier survival curve of PDAC patients (n= 118) based on αvβ6 expression (median score of 3). Logrank test p= 0.241.

The pink line in the graph represents a group of 98 patients with a median score greater than or equal to three and the blue line represent 20 patients with a median score less than three (Figure 71). Despite a moderate shift in the curve to the left, indicative of poor prognosis in the high expressers of αvβ6, a logrank test revealed no significant difference between the two groups of patients (p=0.241) followed over a time period of 120 months from the time of surgery (Figure 71).

The Beatson Institute TMA data set had a variety of clinical data in addition to the survival data shown in Figure 71. The grade of tumours, the stage of tumour and the differentiation status of the tumour at the time of surgery were some of the other parameters which were examined in relationship to αvβ6 expression based on the same scores used for survival analysis. All further analyses were done as part of a collaboration with Dr. Jeniffer Morton, at the Beatson institute.

4.3.2.1 Correlation of tumour grade with αvβ6 expression

Patients with follow up data for the grade of pancreatic cancer at the time of diagnosis/surgery were divided into two groups, low and high grade PDAC, and these groups were correlated with expression of αvβ6 based on the TMA scores. A Mann-Whitney test was used to test for significance. Mann-Whitney test is a non-parametrical test used to check if one of the two data sets of independent observations have a higher value than the other. It is commonly referred to as the Wilcoxon rank-sum test.

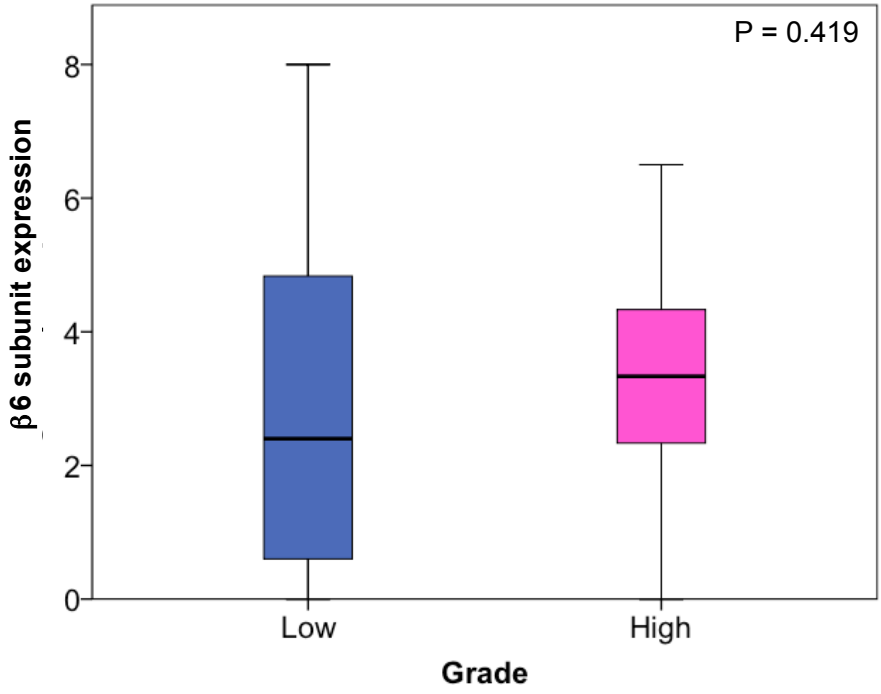

Figure 72: Correlation of αvβ6 expression with patients having low (n=84) or high grade (n=34) PDAC. Mann-Whitney test p= 0.419.

The results in Figure 72 show that there was no significant correlation between αvβ6 expression and the grade of pancreatic cancer in the samples analysed from this particular data set with a p value of 0.419 using the Mann-Whitney test. The median represented by the black line in the box and whisker plot suggested that the level of expression of αvβ6 in the low grade tumours (blue) and high grade tumours (pink) was statistically not significantly different, although the median for the high grade tumours was slightly higher in comparison to the low grade tumours.

4.3.2.2 Correlation of tumour stage with αvβ6 expression

The classical method to analyse the stage of the tumour is the TNM method of classification. T stands for primary tumour, N stands for regional lymph nodes, M stands for distant metastasis. The Beatson Institute data set had clinical follow up data associated with the T stage 2 and 3 for all patients. The T stage of classification can be divided into various sub-stages, Tx, T0, T1, T2, T3 and T4. Each stage denotes the size of the primary tumour.

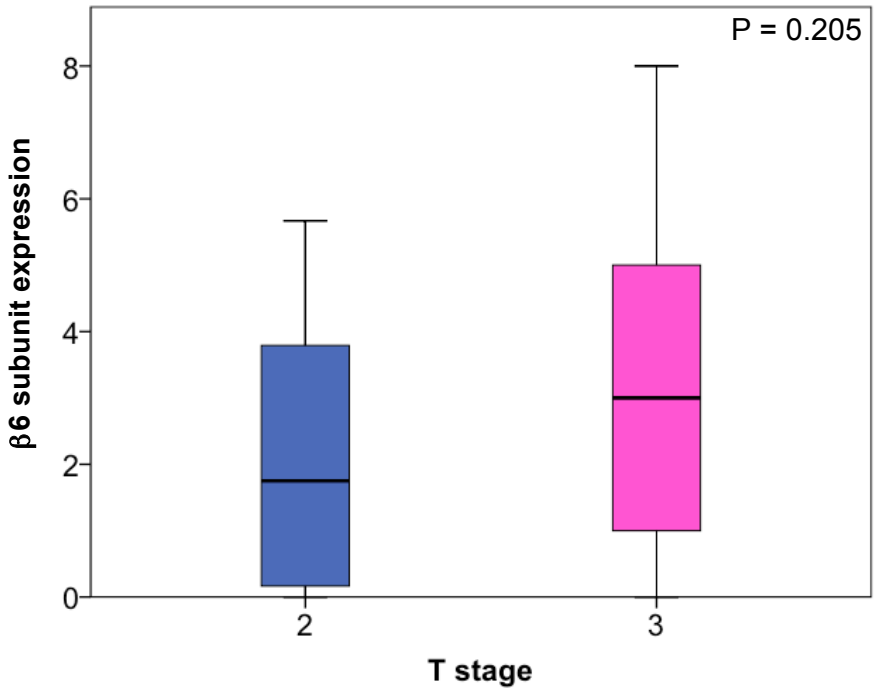

Figure 73: Correlation of αvβ6 expression and T stage classification of PDAC tumours in patient samples. Mann-Whitney test p= 0.205.

The data in Figure 73 showed that there was no significant correlation between αvβ6 expression and the T stage 2 (n= 13) (blue) where tumours are limited to the pancreas, (2 centimetres or less in the greatest dimension) versus T stage 3 (n= 105) (pink), where tumours extend beyond the pancreas but without involvement of the coeliac axis or superior mesentery using Mann-Whitney test p= 0.205. The median score suggested that the level of expression of αvβ6 was not significantly different between the different stages but a slight increase in median β6 expression was observed in the T3 stage compared to the T2 stage of PDAC in this data set.

4.3.2.3 Correlation of differentiation status with αvβ6 expression

It is characteristic for pancreatic ductal adenocarcinomas to have glandular structures embedded in an extremely desmoplastic stroma. The extent of changes in PDAC morphology from the typical glandular duct-like structures to a more squamoid or spindle cell like cellular architecture are indicators of PDAC differentiation. There are variations in the levels of differentiation in PDACs and they behave differently depending on the stage of differentiation. The well differentiated PDACs consist of large duct-like structures in tubular or cribriform patterns embedded in a desmoplastic stroma. They retain more epithelial cell-like features. Moderately differentiated PDACs comprise a combination of medium sized incomplete duct-like structures and tubular structures in a desmoplastic stroma. Poorly differentiated PDACs are less common and consist of tiny irregular glands with almost no duct-like structures. They also tend to lose their epithelial cell-like phenotype (WHO classification of tumours, 2000).

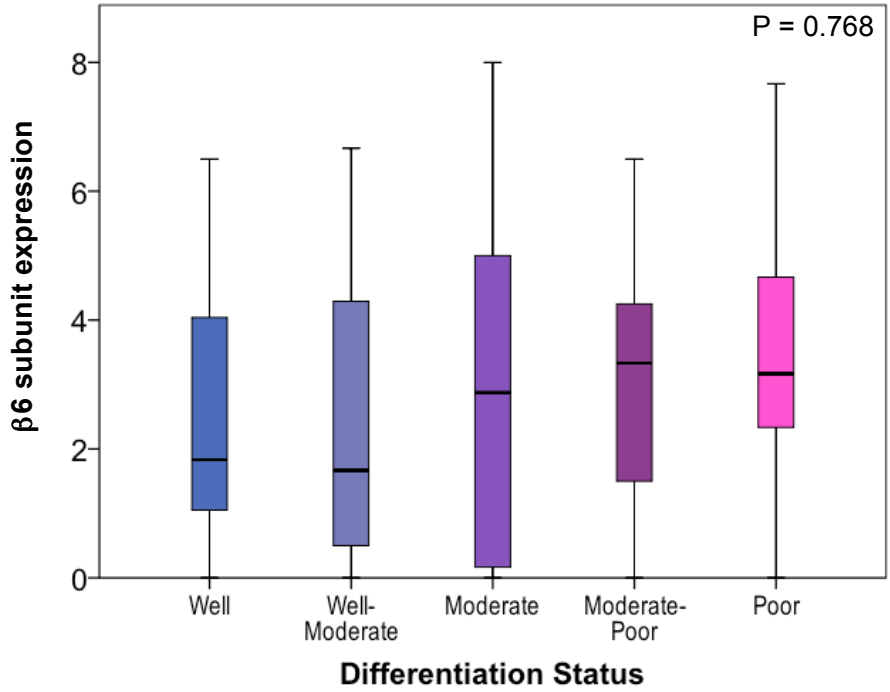

Figure 74: Correlation of αvβ6 expression and cellular differentiation of PDAC in patient samples. Kruskal-Wallis test p= 0.768.

The data in Figure 74 showed that there was no significant correlation between αvβ6 expression and differentiation status of human pancreatic cancer in the samples tested using the Kruskal-Wallis test (p= 0.768). This test can be used as an alternative to the one-way independent-samples ANOVA to compare between groups. The p value represents differentiation status compared across all the groups. The median expression of αvβ6 was found to be lower in both the well differentiated (n=7), well to moderate differentiated (n=12) compared to the moderately differentiated tumours (n=65). This is contrary to what was expected considering well differentiated tumours retain more epithelial cell-like features and αvβ6 is an epithelial specific integrin. The moderate to poorly differentiated tumours (n=13) and the poorly differentiated tumours (n=21) expressed more β6 than the well differentiated tumours in this particular data set.

4.3.2.4 Correlation of αvβ6 expression with lymph node positivity

One of the major routes of dissemination in pancreatic cancer is lymph node metastasis. The lymph node ratio (number of lymph nodes containing tumour cells compared to the number of lymph nodes examined in total) is considered to be a strong prognostic marker in pancreatic cancer [264]. A high lymph node ratio means significantly reduced survival in PDAC patients who have undergone surgical resection of the pancreas.

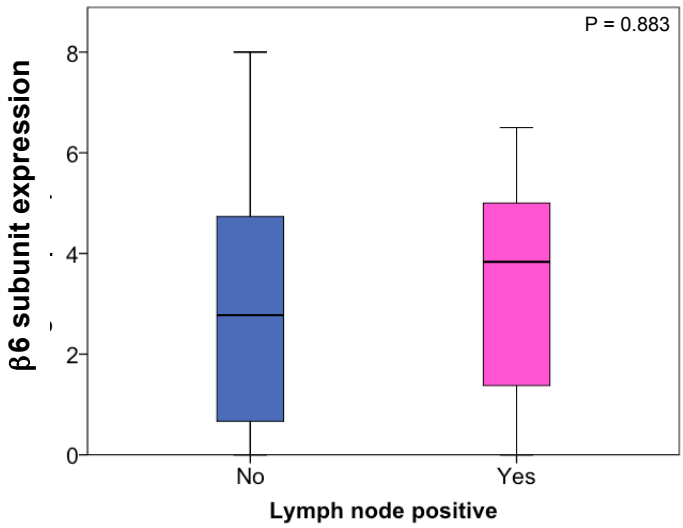

Figure 75: Correlation of αvβ6 expression and lymph node positivity in PDAC patient samples. Mann-Whitney test p= 0.883.

The data in Figure 75 showed that there was no significant correlation between αvβ6 expression and lymph node positivity in PDAC patients using the Mann-Whitney test (p= 0.883). The box and whisker plot with lymph node positivity (n=94) (pink) tended to show a marginally higher median score of αvβ6 expression compared to the plot with no lymph node positivity (n=24) (blue).

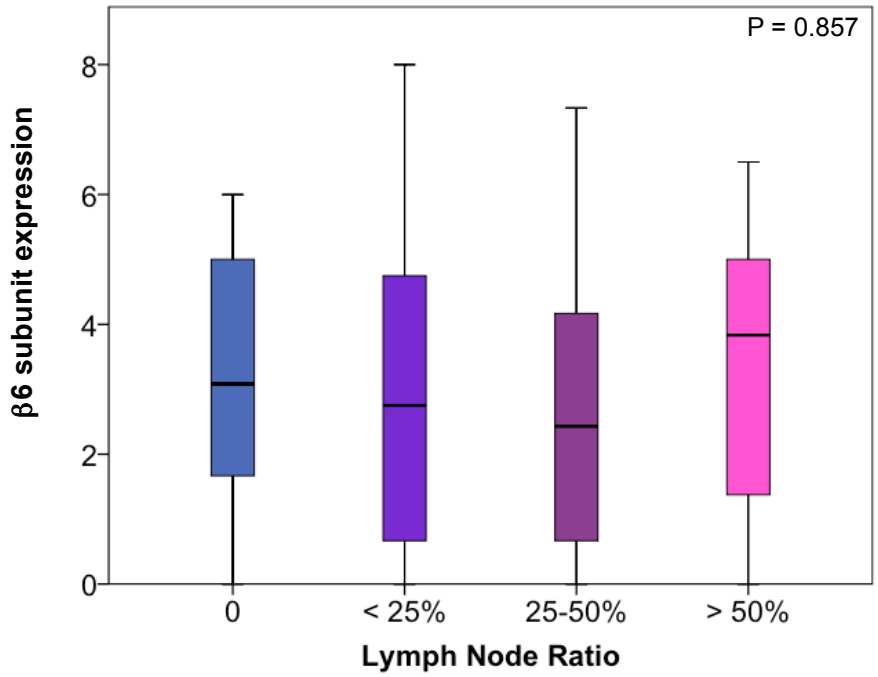

Figure 76: Correlation of αvβ6 expression and lymph node ratio in PDAC patient samples. Mann-Whitney test p= 0.857. n=24 for 0 lymph node ratio, n=60 for <25%, n=24 for 25-50% and n=10 for >10% lymph node ratio.

The data in Figure 76 show that there was no significant correlation between αvβ6 expression and lymph node ratio in the PDAC patients in this data set using the Mann-Whitney test (p= 0.857). High lymph node ratio is a poor prognostic marker in pancreatic cancer and although there was no significant difference in αvβ6 expression between patients with lymph node positivity, the median score for αvβ6 expression was highest for patients with a lymph node ratio of >50% (n=10) (pink) suggesting that β6 could contribute to poor prognosis in PDAC.

4.3.2.5 Correlation of αvβ6 expression with perineural invasion

Perineural invasion is a characteristic feature of pancreatic cancer. The cancer cells invade the surrounding nerves and metastasise. It is believed that more aggressive tumours tend to spread to the nerves causing significant back pain to patients. The infiltration accounts for local recurrence following surgical resection, usually involving a negative margin only a few millimetres wide [243].

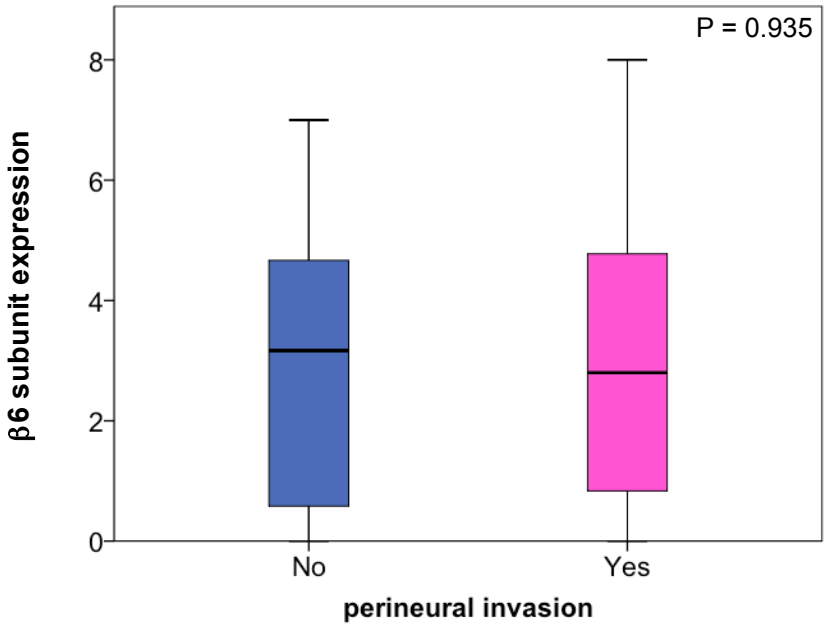

Figure 77: Correlation of αvβ6 expression and perineural invasion in PDAC patient samples. Mann-Whitney test p= 0.935.

The data in Figure 77 show that there is no significant correlation between αvβ6 expression levels and perineural invasion in the PDAC patients analysed using the Mann-Whitney test (p= 0.935). n=112 for patients with no perineural invasion and n=6 for patients with perineural invasion.

4.3.2.6 Correlation of αvβ6 expression with vascular invasion

Detection of vascular invasion in pancreatic cancer is a very difficult challenge and in the absence of evident metastatic disease, the presence of vascular invasion plays an important role in determining how resectable the tumour is and what the likely success of such resection will be. Recent improvements in imaging techniques allow better detection of vascular invasion [265].

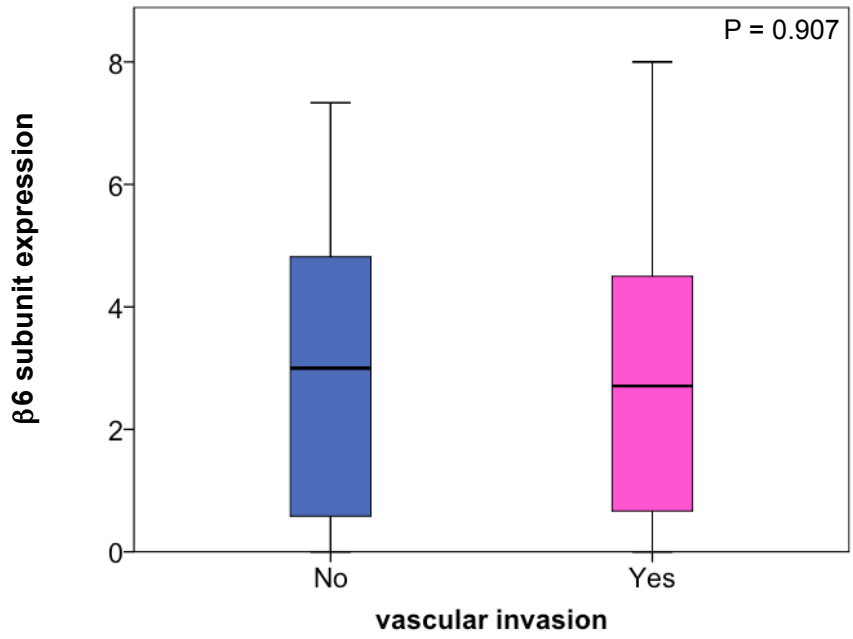

Figure 78: Correlation of αvβ6 expression and vascular invasion in PDAC patient samples. Mann-Whitney test p= 0.907.

The data in Figure 78 show that there is no significant correlation between αvβ6 expression and vascular invasion in PDAC patients in the data set analysed using the Mann-Whitney test (p= 0.907).

4.3.3 Clinical analysis of PDAC TMAs from the University of Verona

Tissue Microarray Cores (TMA) of PDAC patients were stained for αvβ6 expression using the monoclonal antibody 62G2 (Biogen) by IHC (section 2.6). There was a total of 147 PDAC patients in the data set. Four cores per slide represented each patient and the scores of all four cores were averaged to obtain a single score per patient. The scores of individual cores were matched to the follow up data and all further clinical analyses were performed at Barts Cancer Institute, Queen Mary University of London, with help from Mr. Hemant Kocher and Dr. Colan Ho-Yen.

The X-tile software has been developed by Yale University, USA and is a robust and increasingly used statistical platform to determine the best "cut point", while dividing patients into subsets based on expression of a potential biomarker It has been validated on a number of well established prognostic markers (tumour size, p53 expression) in breast cancer [266]. Despite the existence of various statistical tests for determining the optimal cut point, X-tile provides a more rigorous evaluation by dividing a single cohort into "training" and "validation" subsets for estimating the p value. It also performs additional Monte Carlo simulations to generate corrected p values to assess statistical significance of the data assessed by multiple cut points. Monte Carlo simulations try to define a possible input from a probability distribution, thus the cut off value generated by the X-tile software is more robust than testing multiple cut points and accepting the value and gives the best p value.

The median scores for all patients on the data set based on αvβ6 expression were uploaded on to the X-tile software along with the survival data, and a "cut off" median score of five was determined by the software. All PDAC patients with a median score greater than or equal to five were referred to as high expressers and all patients with a median score of less than five were referred to as the low expressers of β6 for the purposes of further analyses.

		Number	Percentage
Cases available in analysis	Event[a]	114	76.5
	Censored	33	22.1
	Total	147	98.7
Cases dropped	Cases with missing values	2	1.3
	Cases with negative time	0	0
	Censored cases before the earliest event in a stratum	0	0
	Total	2	1.3
Total		149	100

a- dependent variable: survival

Table 15: Total number of PDAC samples that were available for further clinical analysis in the data set from the University of Verona.

There were a total of 149 PDAC cases available for analysis out of which two patients had to be removed because of lack of clinical data follow up (Table 15). Kaplan-Meier (KM) survival curves were plotted based on integrin β6 subunit expression scores for a total of 147 PDAC cases (Figure 79). A logrank test was performed to test for significance between high expressers (≥5) or low expressers (≤5).

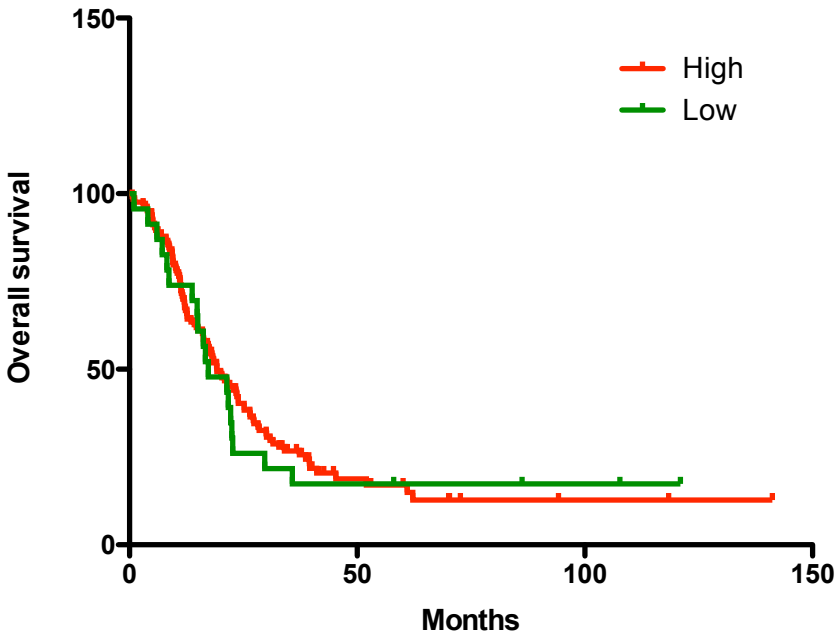

Figure 79: Kaplan-Meier survival curve of Verona PDAC patients (n=147) based on expression levels of αvβ6 (median cut off score used was 5). Logrank test p= 0.776.

The red line in the graph represents a group of 124 patients with a median score greater than or equal to five and the green line represents 23 patients with a median score less than five (Figure 79). A logrank test showed no significant statistical difference between the high expressers (red line) of αvβ6 and the low expressers (green line) of αvβ6 with a p value of 0.776.

The University of Verona TMA data set had a variety of clinical data in addition to the survival data shown in Figure 79. The grade of tumours, the stage of tumour, sex and the age of the patient at the time of surgery, perineural and vascular invasion, were some of the other parameters, which were correlated to αvβ6 expression. A Spearman's rho test compares how well the relationship between two variables can be described using a function, in this case αvβ6 expression levels (median scores) and the various parameters in the clinical follow up data. It also indicates the direction of correlation between the X and the Y variable. If Y tends to increase with an increase in X, then it is a positive correlation and if Y tends to decrease with an increase in X, then it is considered to be a negative correlation. If X and Y are perfectly related, then the Spearman correlation coefficient becomes 1. A Spearman's rho test was used to test for significance and work out the relationship

between αvβ6 expression levels and various other parameters available for testing as part of the follow up clinical analyses.

4.3.3.1 Correlation of tumour stage with αvβ6 expression

The PDAC patients in the data set were divided into two groups depending on the stage of the tumour based on the American Joint Committee on Cancer (AJCC) classification. Any patient with a stage greater than or equal to IIB was classified as high stage and any patient below the IIB stage was classified as low stage. This was done because there is no nodal involvement or metastasis of cancer until stage IIB in pancreatic cancer (Table 16, AJCC pancreatic cancer staging, edition 7).

Anatomic stage / Prognostic groups			
Stage 0	Tis	N0	M0
Stage IA	T1	N0	M0
Stage IB	T2	N0	M0
Stage IIA	T3	N0	M0
Stage IIB	T1	N1	M0
	T2	N1	M0
	T3	N1	M0
Stage III	T4	Any N	M0
Stage IV	Any T	Any N	M1

Table 16: Table showing the TNM scoring and characterisation of stage in PDAC patients according to AJCC. *(Table modified from AJCC 7th edition).*

Table 16 shows the staging of PDAC patients according to the AJCC system of classification. T represents the tumour size, N represents nodal involvement of the disease and M represents metastatic spread. A PDAC patient is classified as stage IIB regardless of T stage 1, 2 or 3 and if regional lymph node metastatic spread can be detected as denoted by N1. N0 means there is no lymph node metastatic spread. M0 means there is no distant metastasis, while M1 indicates that there is metastatic spread to a distant organ.

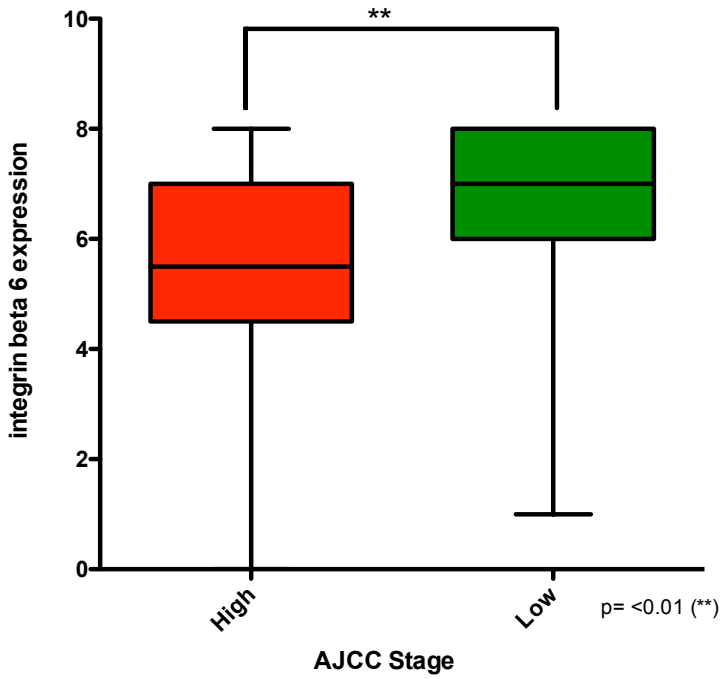

Figure 80: Correlation between AJCC stage of Verona PDAC patients in the data set with αvβ6 expression. Spearman's rho test p= <0.01 (**).

The data in Figure 80 showed that there was a significant difference in the expression levels of αvβ6 and the stage in PDAC patients in this data set with a p value of <0.01 using the Spearman's rho test. The patients categorised as high stage (red) (n=100) had a lower median score for expression of αvβ6 expression compared to the patients in the low stage (green) (n=47). A Spearman's correlation coefficient calculated using the SPSS platform revealed that there was a negative correlation of -0.299 between αvβ6 expression levels and the stage of PDAC in patients in this data set. This means that αvβ6 expression levels were higher in patients with low stage PDAC compared to people with high stage disease, where expression levels of αvβ6 was found to be significantly lower.

4.3.3.2 Correlation of tumour grade with αvβ6 expression

Patients with a follow up data for the grade of pancreatic cancer at the time of diagnosis/surgery were divided in to three groups: grade 1 (low grade), grade 2 (medium grade) and grade 3 (high grade). This was correlated with expression of β6 based on the TMA scores. A Spearman's rho test was used to test for any statistical significance between tumour grade and β6 expression levels in PDAC patients in this data set.

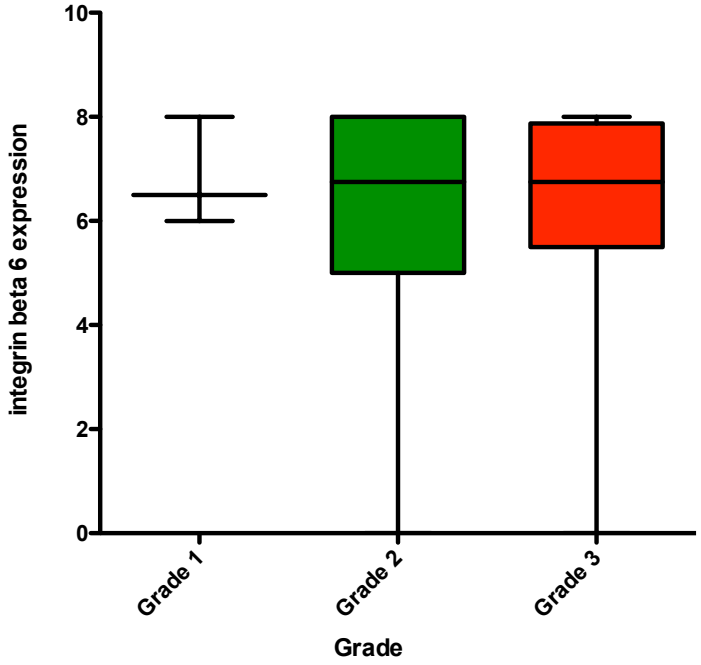

Figure 81: Correlation between tumour grade and αvβ6 expression levels in Verona PDAC patients. Spearman's rho test p= 0.994.

The data in Figure 81 showed no significant correlation between αvβ6 expression levels (median scores) and grade of pancreatic ductal adenocarcinoma tumours in patients in this data set tested using the Spearman's rho test (p= 0.994). It should be noted that there were only three cases with a grade 1 disease and majority of the cases were classified as grade 2 (n= 88) and grade 3 (n= 56).

4.3.3.3 Correlation of αvβ6 expression with sex of PDAC patients

The clinical follow up data included the sex of patients and PDAC is a type of cancer where the incidence rates between men and women are similar. αvβ6 expression levels were never correlated to gender in any previous published reports in cancer patients.

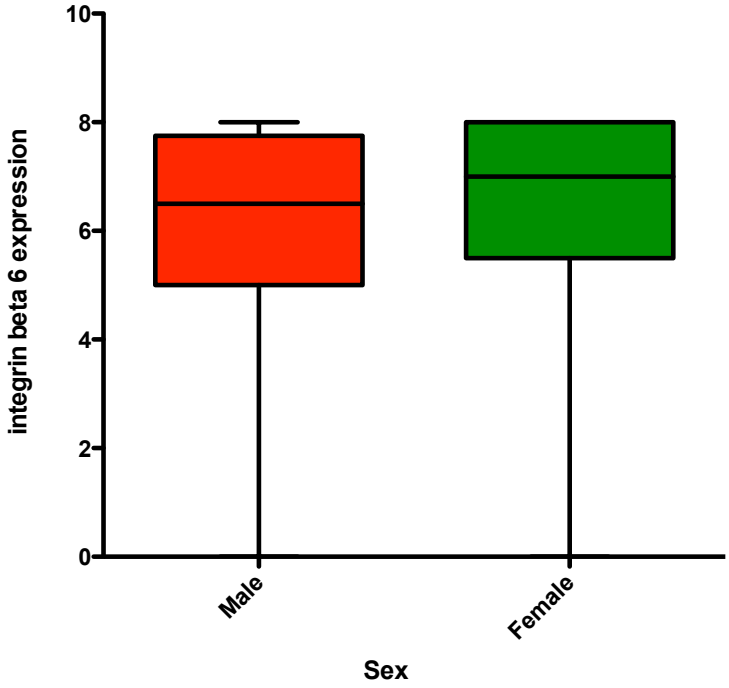

Figure 82: Correlation between αvβ6 expression levels and gender in Verona PDAC patients. Spearman's rho test p= 0.406.

The graph in Figure 82 showed that there was no significant correlation between expression levels of αvβ6 and gender of PDAC patients tested using the Spearman's rho test (p= 0.406). There is a very slight increase in the median score in females (green) compared to the men (red) with a negative correlation coefficient of 0.069.

4.3.3.4 Correlation of αvβ6 expression with T stage in PDAC

The classical method to analyse the stage of the tumour is the TNM method of classification, where T stands for the size of the primary tumour. The University of Verona data set had clinical follow up data associated with the T stage 2, 3 and 4 for all patients. The T stage of classification can be divided into various sub-stages, Tx, T0, T1, T2, T3 and T4. Each stage denotes the size of the primary tumour.

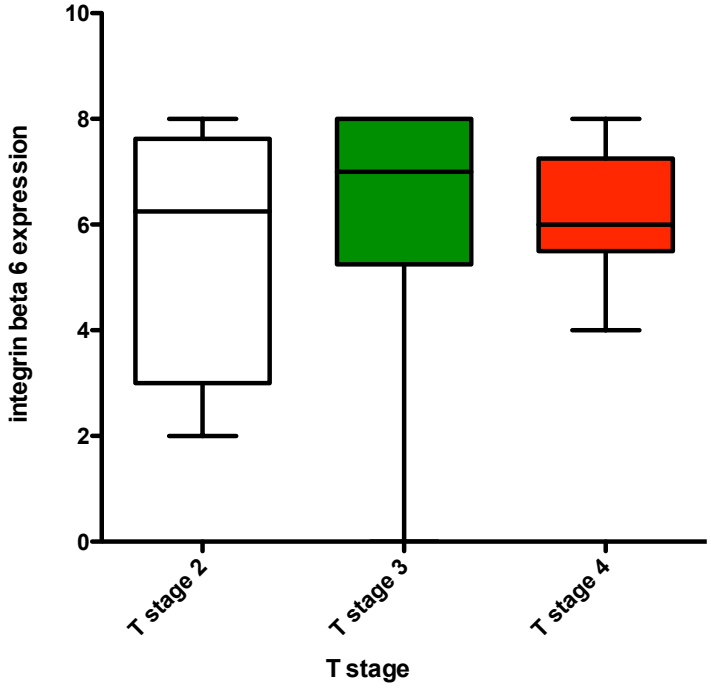

Figure 83: Correlation between αvβ6 expression levels and T stage classification in Verona PDAC patients. Spearman's rho test p= 0.856.

The graph in Figure 83 showed no significant correlation between αvβ6 expression levels and T stage of tumours in PDAC patients tested using the Spearman's rho test (p= 0.856). T stage 2 (no colour) had a small number of patients (n= 5), stage 3 (red) had the most number of cases (n= 129) and stage 4 (green) had slightly more patients compared to stage 2 (n= 13). The median score for αvβ6 expression tended to be slightly higher in the T stage 3 when compared to stage 3 and stage 4.

4.3.3.5 Correlation of αvβ6 expression with vascular invasion

Vascular invasion in pancreatic cancer is extremely difficult to detect though recent improvements in imaging technologies have made it feasible to detect it more easily. In the absence of metastatic disease, vascular invasion plays an important role in determining how resectable the tumour is.

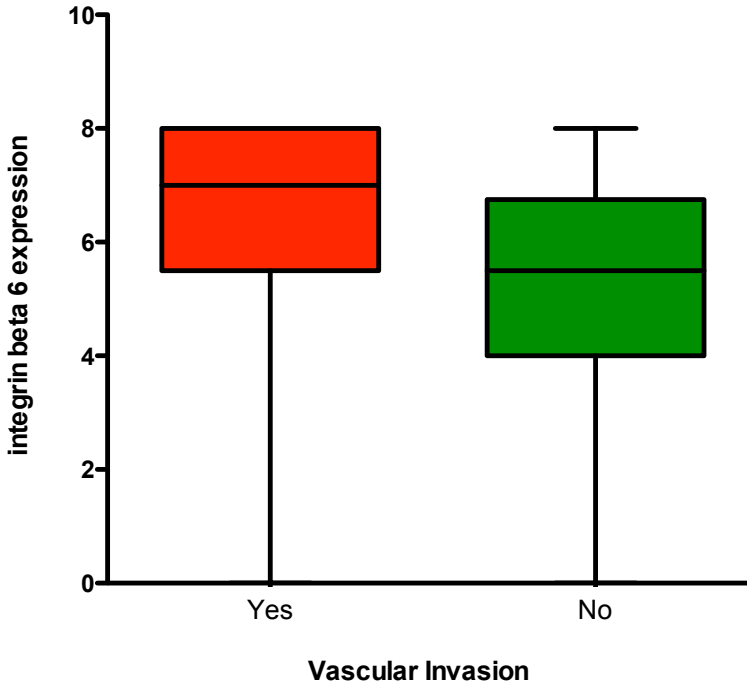

Figure 84: Correlation of αvβ6 expression levels with vascular invasion in Verona PDAC patients. Spearman's rho test p= 0.075.

The data in Figure 84 show that there was no significant correlation between the level of αvβ6 expression and vascular invasion in PDAC patients in this data set using the Spearman's rho test (p= 0.075). The median score of αvβ6 expression in patients with vascular invasion (red) tended to be higher than the patients with no vascular invasion (green). The Spearman's test p value of 0.075 was just out of significance and perhaps more data points would have shown a significant difference in correlation between the two variables.

4.3.3.6 Correlation of αvβ6 expression with perineural invasion

Perineural invasion is a process in which the pancreatic cancer cells invade the surrounding nerves and metastasise. The more aggressive tumours tend to metastasise to the nerves causing significant back pain to patients.

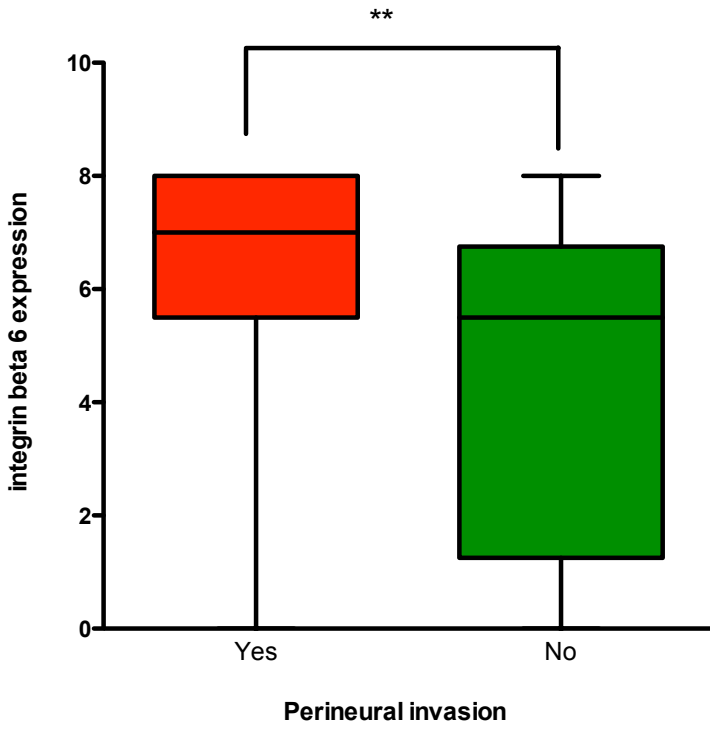

Figure 85: Correlation of αvβ6 expression levels with perineural invasion in Verona PDAC patients. Spearman's rho test p= <0.01.

The data in Figure 85 showed that there was a significant difference in correlation between the expression level of αvβ6 and perineural invasion in PDAC patients in this data set tested using the Spearman's rho test (p= <0.01). The patients with perineural invasion (red) tended to show a higher expression of αvβ6 (higher median) compared to the patients with no perineural invasion (green). A Spearman's correlation coefficient calculated using the SPSS platform revealed that there was a positive correlation of 0.221 between β6 expression levels and perineural invasion in PDAC patients within this data set.

4.4 Discussion

αvβ6 has been linked with poor prognosis in many cancers. Bates et al showed that there was a significant difference in median overall survival between the αvβ6 low expressers (16.5 years) and αvβ6 high expressers (5 years) in colon cancer patients [173]. A significant difference in overall survival was observed in cervical cancer patients with only 54% of patients with strong αvβ6 expression surviving for 5 years compared to 91% who were negative for αvβ6 expression [267]. In lung cancer (NSCLC) patients, αvβ6 was shown to be a potential prognostic marker, with >75% of αvβ6 weak expressers surviving over 5 years compared with only <50% in the strong αvβ6 expressers [204]. It is worth mentioning that the high 5 year survival rate in the NSCLC patients in the above study was due to patients being treated at a very early stage of the disease. αvβ6 has also been shown to be a prognostic marker in breast cancer patients with a significant difference in overall survival between the αvβ6 low (10 years) and high (5 years) expressers (in-house data, not published). Thus, four different cancers with high αvβ6 expression have been associated with poor survival. To date, no study has compared the levels of αvβ6 expression and overall survival in PDAC patients.

Through collaboration with the Beatson Institute, Glasgow and the University of Verona, Verona, two independent cohorts of PDAC patients were available for the purposes of this study. Barts Cancer Institute also has a public domain, pancreatic expression database, which provided data on β6 mRNA expression levels. This meant I could examine expression of αvβ6 both at the mRNA and protein level in independent cohorts of patients.

Bioinformatics studies are often used as a tool to check for expression of genes at the mRNA level. It can also be used to identify differential gene expression based on expression levels of a gene of interest. Results obtained here have shown that *ITGB6* is overexpressed in PDAC tumour tissue when compared with normal pancreas (Figure 64). Further correlation and analysis using stringent cut offs (high threshold ≥8) generated a list of forty genes, which were up regulated and one gene which was down regulated as the same time as *ITGB6* was overexpressed in PDACs (Table 14). Thus, it is a possibility that one or more of these genes was regulated directly by ITGB6 or regulated as a result of ITGB6 overexpression.

In order to ascertain if any of the genes identified were under the influence of *ITGB6* expression, qPCR analysis was performed on a small subset of genes picked out from the list due to their link with pancreatic cancer [253, 254]. As these studies occurred late in my project, the data must be considered preliminary. However, these results suggested that MMP11 expression is decreased when αvβ6 expression is knocked down in Capan1 cells using siRNA (Figure 66). Since very little is known about αvβ6 downstream signalling in cancer, the aim was to identify key genes relevant to pancreatic cancer using the pancreatic expression database. This list of genes generated in this study can potentially provide possible target genes, which could be under the influence of αvβ6 or influence αvβ6 activity in PDAC tumour tissue. More validation assays have to be performed, which may provide further clues to determine the role of αvβ6 in PDAC.

To date no studies have attempted to correlate *ITGB6* expression and survival in cancer. In this study, using bioinformatics, high mRNA expression levels of *ITGB6* were linked to poor prognosis with a significant difference in mean overall survival in PDAC patients (n=292, p= 6.7×10^{-4}). The difference in overall survival was 6 months for high expressers compared to 12 months for low expressers. Admittedly, the difference in survival is very modest compared with correlation of αvβ6 expression, at the protein level, and survival in colon cancer [173]. However, as only about 24% of PDAC patients have a one-year relative survival rate (American Cancer Society, facts and figures, 2010) after diagnosis and as this falls to about 5%- 6% of patients over a period of five years (WHO report, Pancreatic cancer, 2010), a doubling of overall survival in this challenging disease is encouraging. Having observed a significant difference in survival at the mRNA level, it was critical to check if the same could be observed at the protein level.

Since patients with PDAC present at a late stage, it usually is inoperable. Tissue samples are often limited to biopsies, thus conducting tissue studies in PDAC is challenging. It is usually difficult to obtain statistically significant and robust follow up data because of the limited number of patient samples combined with the exceptionally poor prognosis of the disease. Tissue microarrays from the Beatson institute dataset had a total of 118 PDAC cases and 20 normal cases and the University of Verona has a total of 147 PDAC cases and 12 normal cases in their data set. The two centres also had valuable follow up clinical data that was collected and matched to every patient included in the data set. Analyses for the Beatson

Institute data set including statistical analyses was performed at the Beatson Institute, as the follow up clinical data were not available to the author in order to maintain data security. The follow-up data for the cohort of patient tissue from the University of Verona was available and I performed all further analyses. Due to restrictions in sharing follow up clinical data between institutes, all further analyses for both cohorts had to be presented separately.

As discussed previously, three independent assessors scored the TMAs separately and the median of the scores was used to carry out all further clinical analyses. Of the 118 PDAC cases stained for αvβ6 in the Beatson data set, 98 cases were positive with a median score ≥1 (83%) and out of the 147 in the Verona data set, 144 were positive for αvβ6 with a median score ≥1 (98%). The control normal pancreas samples in both data sets were completely negative for αvβ6. This strong up regulation of αvβ6 is typical for many solid epithelial cancers [203] but the very high percentage positivity is typical to the PDAC cases (91% if scores from both data sets were combined) is higher than any other cancer reported to date but in agreement with the original study that reported 100% αvβ6 expression in human PDAC [201]. In comparison, only 58% out of 85 cervical cancer patients tested were positive for αvβ6 expression [267] and 54% out of the 311 NSCLC cases tested were positive for αvβ6 [204]. It came as a surprise that 20 PDAC cases were scored negative for αvβ6 in the Beatson data set (83%) considering only three cases of PDAC tumours from the Verona data set were negative for αvβ6 (98% positive). This could be due to a variety of factors including poor tissue preservation and differentiation status of the tumours tested. It should be noted that aside from the studies carried out by Sipos et al [201], using 34 PDAC cases, this data here are probably the biggest collection of PDAC samples that were tested for αvβ6 expression to date. Thus, there exists a possibility that more αvβ6 negative PDAC tumours might be identified with an increase in the number of PDAC tumours being tested for αvβ6 expression. It should be noted that, overall the samples in the Beatson data set did show a weaker αvβ6 staining compared with the Verona data set suggesting that tissue preservation might be a more plausible explanation for the differences in positivity observed.

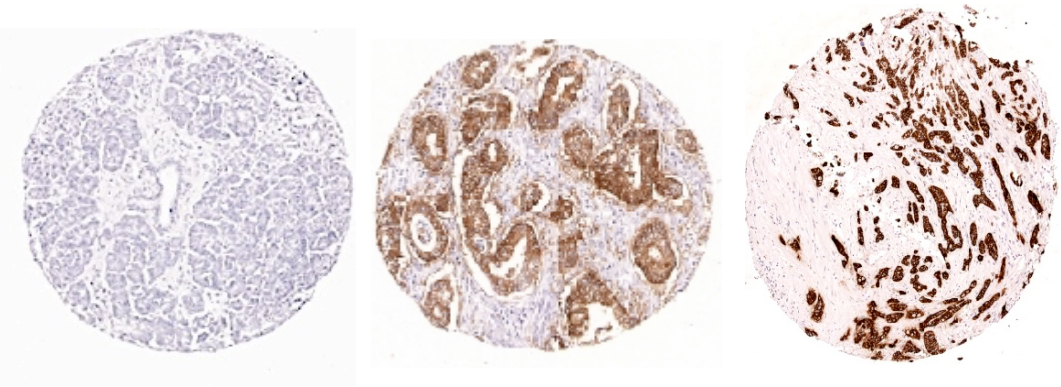

Figure 86: Low magnification pictures of examples showing a normal pancreas core stained for αvβ6 (left), a core stained for αvβ6 (median score 8) from the Beatson data set (centre) and a core stained for αvβ6 (median score 8) from the Verona data set (right).

Thus, Figure 86 clearly illustrates the difference in the intensity of the staining between the two data sets (centre and right), even though staining was performed at the same time using the same set of reagents. Care was taken to score both data sets independently and this difference in intensity of staining was taken into account while scoring the cores.

Having established αvβ6 expression in the TMAs tested, the next logical step was to check if there was any relation between αvβ6 expression and overall survival in the two independent data sets. Kaplan-Meier survival curves were plotted to relate αvβ6 expression levels and survival in patients. Surprisingly, neither the Beatson data set (Figure 71) nor the Verona data set (Figure 79), plotted separately, showed any significant relationship between αvβ6 expression and survival tested using the logrank test. This was unexpected considering all the available literature that was reported showed αvβ6 as a poor prognostic marker for cancer. In the Beatson data set, there was a slight shift of the curve observed in the high expressers of αvβ6, indicative of poorer prognosis, but the difference was not significant (p= 0.241). However, in the Verona dataset the low expressers of αvβ6 tended have a marginally poorer survival rate but this was not significantly different from the high expressers of αvβ6 (p= 0.776). Even though αvβ6 has been shown to be a poor prognostic marker in other cancers, the obvious conclusion here is that the expression of αvβ6, at the protein level, cannot be used as a prognostic marker in PDAC.

This lack of correlation between αvβ6 expression and survival in PDAC patients could be attributed to a variety of factors. Incidence rates of PDAC are relatively low compared with many other solid cancers like breast or lung cancer. Even though this study had 2 separate data sets with 118 and 147 cases, which is a significantly large number of cases compared to other PDAC studies published so far, it may still not be enough to carry out the rigorous statistical analyses that are required to study patient survival based on high and low αvβ6 expression at the protein level. The p values obtained suggested that even if the two data sets were to be combined, it would not have changed the overall conclusions. Another reason could be the very high percentage positivity of αvβ6 in PDAC (91%), combined with the high mortality rate, making it difficult to follow patients for a sufficiently long period of time before any differences in survival are observed. The majority of patients who have PDAC tend to die of the disease within a few weeks or months after diagnosis, making survival analysis studies extremely difficult. If compared with other solid cancers such as breast cancer, where the incidence rates are higher, only about 30-35% of the tumours are positive for αvβ6 and five-year survival rates (85.1%, 2005-2009) (Cancer Research UK, 2012) are remarkably better than PDAC (3.8%, 2005-2009) (Cancer Research UK, 2012), there is a more even distribution of patients between the two cohorts (high and low) divided based on the levels of αvβ6 expression with greater follow up time, making it feasible to conduct statistically robust long-term survival analysis.

So far, the clinical data generated appear to conflict when comparing αvβ6 expression levels at the mRNA and the protein level. High expression of mRNA encoding the β6 integrin subunit correlates with significant reduction in overall survival (p= 6.7x10-4) (Figure 69) but there was no significant difference in overall survival observed in analysis of two independent sets of clinical samples for αvβ6 at the protein level (Figure 71, Figure 79). Since the mRNA data seem so compelling it is possible the data indicate the β6 protein and mRNA are differentially regulated in PDAC tissue. Preliminary data from our laboratory suggest that such a regulation occurs in oral SCCs. *In situ* hybridisation for β6 mRNA on OSCCs show non-uniform density of expression, with much higher levels at the tumour stroma interface (unpublished data). This will be an important issue to examine in future studies. Thus, while it remains a speculation that such a mechanism occurs in PDAC, the presence of αvβ6 on 91% of PDAC tissue but not in the normal tissue still makes it potentially a valuable target for therapy.

4.5 Clinical follow up data

Both the Beatson and the Verona data set had clinical follow up data for all the patients: grade, stage, age, differentiation status, perineural invasion, vascular invasion, lymph node metastasis were some of the parameters correlated with αvβ6 expression from both data sets.

4.5.1 Beatson data set

118 patients with follow up data were available for further clinical analyses in the Beatson data set. None of the parameters analysed showed a significant correlation with αvβ6 expression. Follow up data analysed was tested using the Mann-Whitney test and even though there was no significant difference observed there was a general trend observed in the pattern of αvβ6 expression. Thus, patients with higher grade or higher stage of PDAC had a higher median score of αvβ6 expression (Figure 72, Figure 73). Patients with greater lymph node metastasis, usually a sign of poor prognosis, tended to express higher levels of αvβ6 (Figure 75, Figure 76). These results showed that there was a tendency for patients with more severe disease to express higher levels of αvβ6 albeit at levels that were not significant in this cohort. The analysis shows that moderate and poorly differentiated cancers expressed slightly higher levels of αvβ6 when compared to the well differentiated cancers, which had a lower median score than expected. This was a surprise as our previous observations in the laboratory suggested that αvβ6 is stronger in the more epithelial-like tumours. It could be that the total numbers of patients in the well and well-moderately differentiated group (n=19) was too small and happened to score lower compared to the total numbers in the moderate and poorly differentiated tumours (n=99); as such no correlation was observed. There was no trend observed between αvβ6 expression levels and perineural or vascular invasion, which are markers for poor prognosis in PDAC patients. Even though αvβ6 has been shown to be involved in promoting tumour growth and metastasis in other cancers [268], no correlation was observed between αvβ6 expression levels and the parameters tested in this data set. The presence of a trend in αvβ6 expression in patients with severe disease suggests that, perhaps with more samples in this particular data set, some of the clinical parameters might become significantly associated with αvβ6 expression.

4.5.2 Verona data set

147 patients with clinical follow up data were available for further clinical analyses in the Verona data set (Table 15). Follow up data were analysed using the Spearman's rho test. There was a significant negative correlation between αvβ6 expression levels and the stage of the PDAC in patients (Figure 80). The low stage tumours (up to stage IIA) had higher levels of αvβ6 compared with the high stage tumours (stage IIB to stage IV). This was contrary to what was expected and what has been published in literature so far about the expression of αvβ6, where it has been associated with higher stage colon cancer [173]. The exact reason as to why this inverse correlation between αvβ6 expression and stage is observed in PDAC remains unclear but perhaps in this data set, the patients in the high stage cohort had poorly differentiated tumours leading to the decreased expression of αvβ6. This could not be verified because differentiation status for this data set was not available as part of the follow up clinical data.

Some of the other parameters listed below as part of the clinical follow up data analyses did not show any significant correlation with αvβ6 expression when tested using the Spearman's rho test. The patients were grouped on the basis of grade of the tumour (Figure 81), gender of the patients (Figure 82), T-stage (Figure 83) and a vascular invasion (Figure 84). It is a possibility that there might be no relationship between αvβ6 protein expression and the above mentioned clinical parameters but it should be noted that there is also a possibility that with more patients included in the study, some of the parameters tested might have shown a significant correlation with αvβ6 expression. This was highlighted when patients in the data set were divided into two cohorts based on vascular invasion. There was a very clear trend observed, where the patients with vascular invasion had high levels of αvβ6 expression compared with the low αvβ6 expression in patients with no vascular invasion. The data were very nearly significant (p value= 0.07) and may well have been significant if there were more patients in the data set (Figure 84). Interestingly, in the current breast cancer studies in my laboratory, strong expression of αvβ6 correlated with vascular but not lymphoid metastasis (data not published). αvβ6 has been shown to promote invasion of tumour cells and just like in other cancers, αvβ6 expression is higher in PDAC tumours that invade the surrounding vasculature.

There was a significant positive correlation between αvβ6 expression levels and perineural invasion in patients (Figure 85). Individuals with perineural invasion had higher levels of αvβ6 compared to the patients with no perineural invasion with low levels of αvβ6 expression (p value= <0.01). It was no surprise that αvβ6 has been shown to correlate with perineural invasion in PDAC patients. It has been shown that the more aggressive PDAC tumours tend to invade into the surrounding nerves and is usually associated with local recurrence of the disease in patients. It also causes severe pain and discomfort to the patient [243]. Even though a significant difference in perineural invasion was observed, it has be noted that the perineural invasion data from the Beatson data set did not show significant difference. This clearly highlights the importance of screening a large cohort of patient material before making any conclusions with regard to selecting a potential marker can be made. It will be interesting to study the data from the two cohorts of patients in greater detail to try and answer some of the questions.

Although a total of 118 patients and 147 patients were included in the analyses carried out for the purposes of this study, it is still necessary to expand these numbers. A larger number of samples in the study are vital for carrying out robust statistical analyses on the follow up data before it is possible to draw definite conclusions.

In contrast, high β6 mRNA levels in PDAC tumours is a poor prognostic marker at the mRNA level with significant difference in overall survival. The high percentage (91%) of PDAC tumours that express αvβ6 and the absence of αvβ6 on normal pancreas suggests that αvβ6 can still be used a potential therapeutic target to treat PDAC, and this is discussed in the following chapter.

RESULTS CHAPTER III

5. Development of *in vivo* models for screening anti-αvβ6 therapy

This study has so far examined protein expression of αvβ6 in 118 and 147 PDAC patients from two independent cohorts, of which 91% were scored positive for αvβ6. Survival analysis on two independent cohorts of patients revealed that there was no significant correlation between αvβ6 expression and patient survival. In contrast, there was a very strong correlation with *ITGB6* gene expression and survival. Thus it seems likely that the role of αvβ6 is perhaps more complex than I first considered. Regardless of this, since αvβ6 is absent from normal pancreas but expressed by most PDAC, it constitutes a possible therapeutic target to treat pancreatic cancer patients.

To develop anti-αvβ6 cancer therapy, a xenograft model that most closely replicated the human pancreatic cancer had to be generated. In this study novel orthotopic xenograft models with CFPac1 and Panc04.03 and a subcutaneous xenograft model (CFPac1) with and without co-injected pancreatic stellate cells (PS1) were developed. The latter model, with PS1 cells introduced, recapitulated key aspects of PDAC and was used for therapeutic antibody studies.

5.1. Generation of novel αvβ6 positive orthotopic xenograft mouse models

Having established that Panc04.03 and CFPac1 cell lines exhibit human PDAC-like features and express αvβ6 in 3D organotypic co-culture models, both cell lines were tested in orthotopic xenograft models. Intra-peritoneal laparotomy was performed (section 2.10.2) on mice, the pancreas was exposed and injected with two million cells per animal. After 6-8 weeks, mice were killed and tumours and neighbouring organs were harvested for analysis.

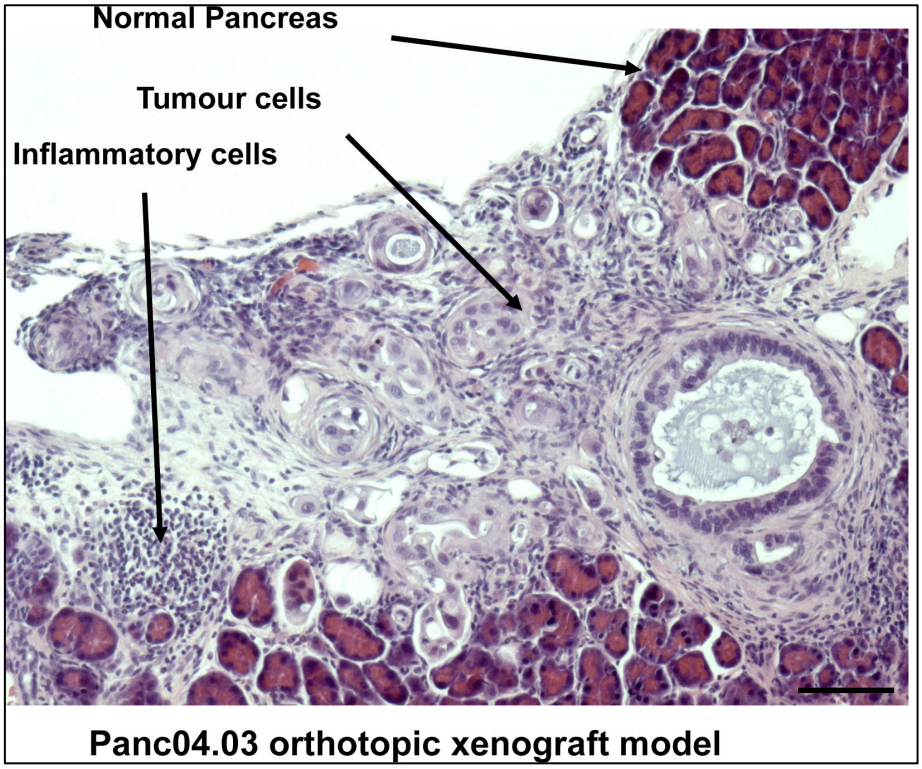

Figure 87: Orthotopic xenograft of Panc04.03. Cells were grown as an orthotopic xenograft in the mouse (CD1nu/nu) pancreas. After 6 weeks growth, tumours were harvested and processed to paraffin. Image shows an H&E stained section showing tumour cells infiltrating the normal pancreas. (Scale bar represents 100μm).

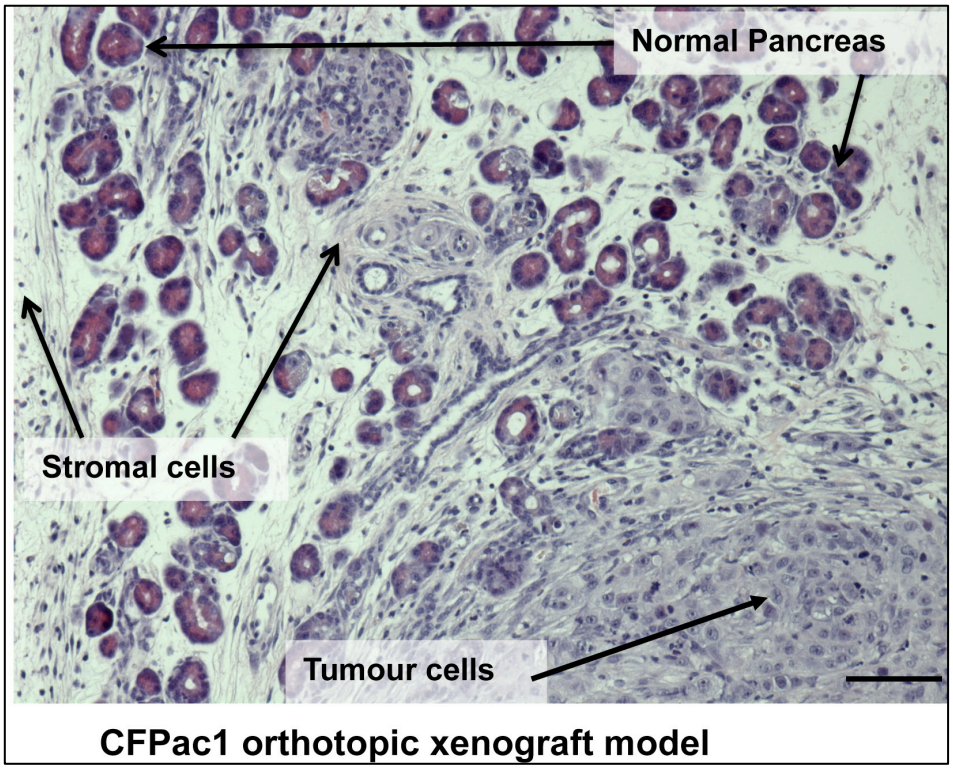

Figure 88: Orthotopic xenograft of CFPac1. Cells were grown as an orthotopic xenograft in the mouse (CD1nu/nu) pancreas. After 6 weeks growth, tumours were harvested and processed to paraffin. Image shows an H&E stained section (10X) showing tumour cells infiltrating the normal pancreas. (Scale bar represents 100µm).

Images show typical histology of Panc04.03 (Figure 87) and CFPac1 (Figure 88) tumours infiltrating the host pancreas with immune infiltrate and stromal response clearly visible. The CFPac1 cell line was particularly good as an orthotopic xenograft model with local metastasis observed in the spleen and distant metastasis to the liver (Figure 89).

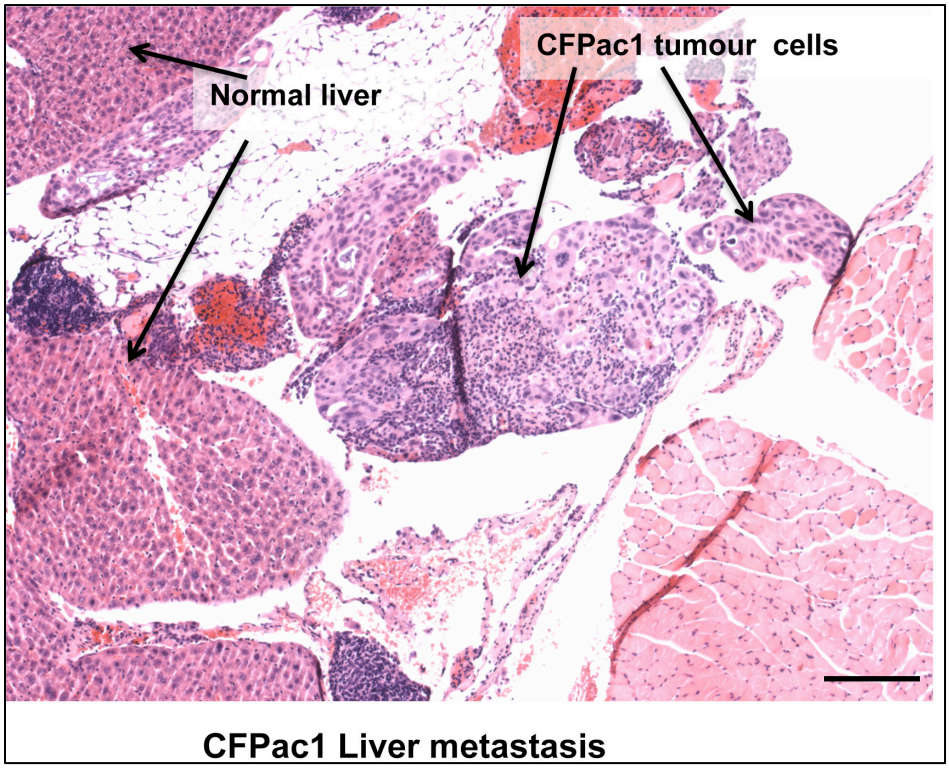

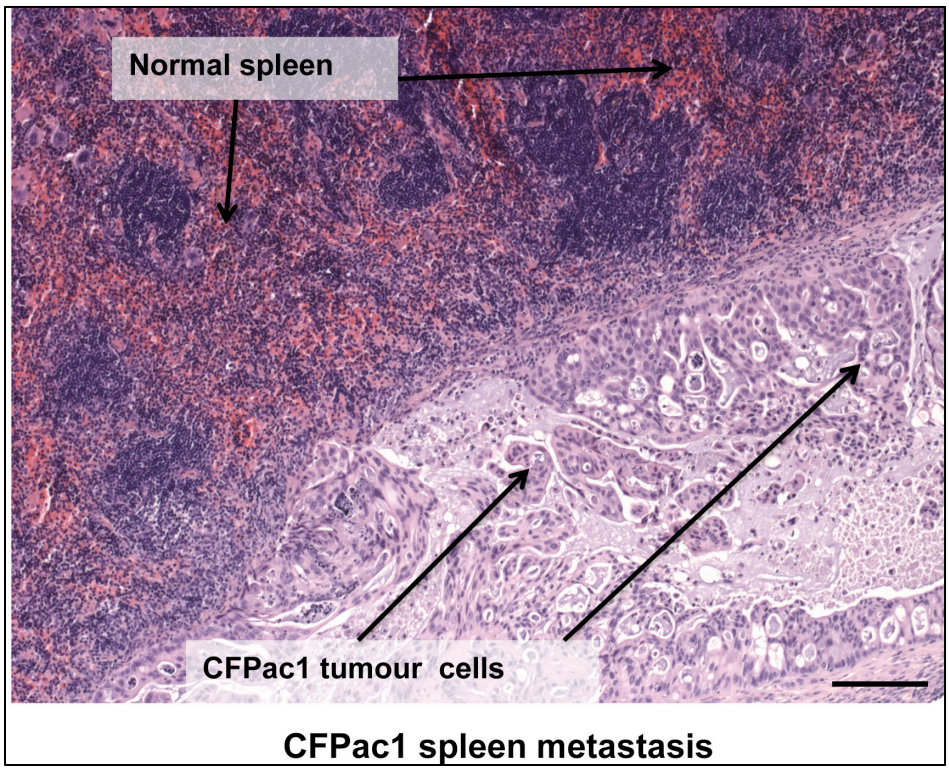

Figure 89: Metastasis of CFPac1 to the liver and spleen in an orthotopic xenograft model. 10X H&E stained images of distant metastases of the liver and local metastases of the spleen observed in CFPac1 orthotopic xenograft mouse model harvested six weeks post injection. CFPac1 tumour cells can clearly be seen infiltrating both normal liver and spleen. (Scale bar represents 100µm).

A total of 10 animals per group were used for generating and validating each of the orthotopic models using CFPac1 and Panc04.03 cell lines. All 10 animals in the CFPac1 group developed tumours. Two animals had metastasis to the liver (Figure 89) and four animals had local metastasis to the spleen (Figure 89) although metastases to the lung were not observed in either of the orthotopic models. Seven out of the 10 animals in the Panc04.03 group developed tumours. Images depicted are representative images and all tumours were harvested at the same time (6 weeks post injection). Tumour sizes were roughly the same in all animals at approximately 7mm length (Figure 90).

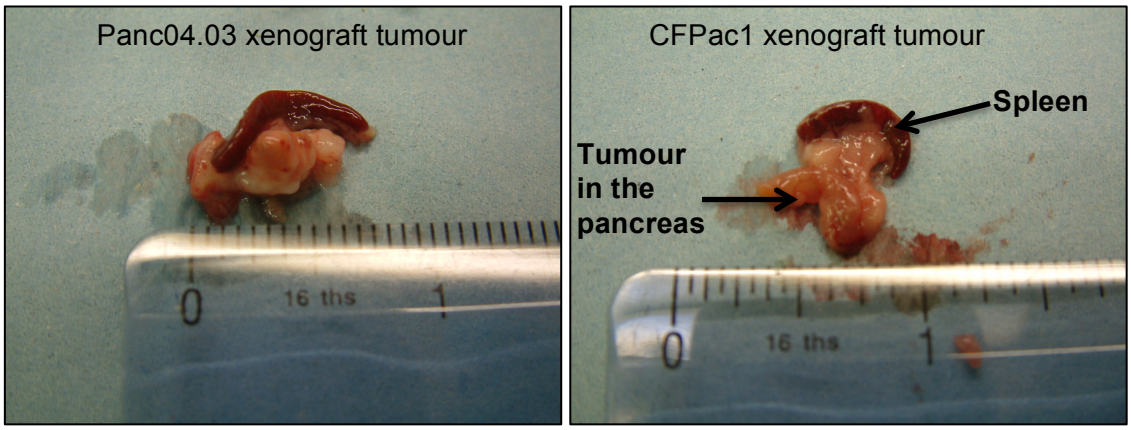

Figure 90: Panc04.03 and CFPac1 orthotopic xenograft tumours. Tumours were excised 6 weeks post injection of two million tumour cells directly into the pancreas of CD1nu/nu mice. Images are representative of tumour bearing mice from 10 per group.

5.1.1. Expression of αvβ6 in Panc04.03 and CFPac1 orthotopic models

Both orthotopic models generated using Panc04.03 and CFPac1 cell lines were tested for their retention of αvβ6 expression. The pancreata from all the animals were harvested six weeks post injection together with the spleen, liver and lungs. Post fixation and processing, the pancreas tissues were stained for αvβ6 using the same antibody used for staining the human TMA samples but using a mouse-on mouse (M.O.M) immunohistochemistry kit from Vector laboratories, UK. This kit was used in order to reduce non-specific binding of the mouse primary antibody to mouse tissue and thus background.

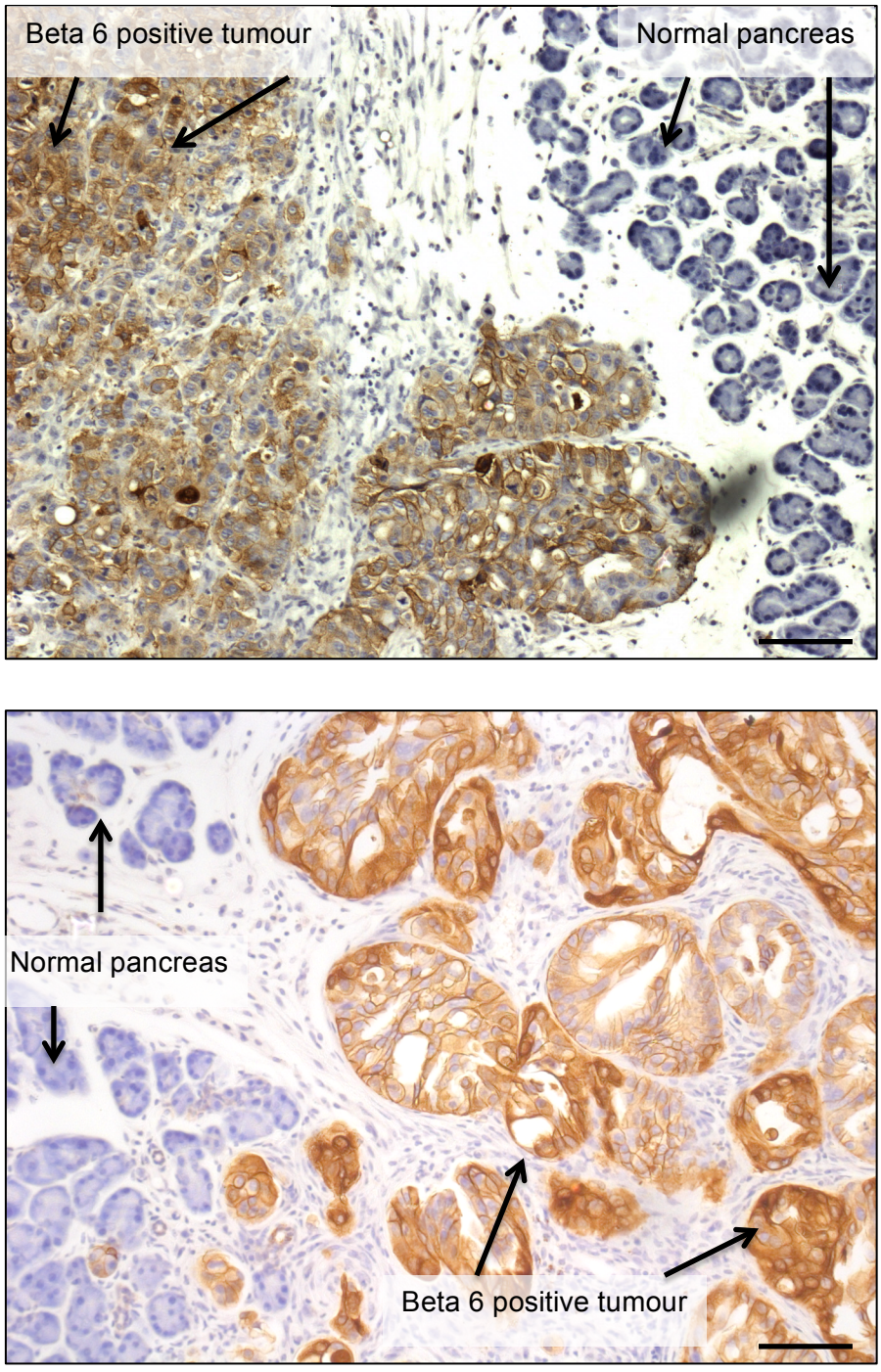

Figure 91: Expression of αvβ6 in CFPac1 (top) and Panc04.03 (bottom) orthotopic xenograft models. Pancreases were harvested six weeks post injection of 2 million CFPac1 or Panc04.03 cells into the pancreas of CD1nu/nu mice. Sections were stained with 62G2 (Biogen) antibody used at 1µg/ml. Strong brown membranous staining of αvβ6 was observed in CFPac1 and Panc04.03 tumour cells and the normal pancreas, in blue, was negative for αvβ6. (Scale bar represents 100µm).

There was a strong expression of β6 specific to the epithelial cell membrane in all the tumours harvested from the orthotopic xenograft models. Both CFPac1 (Figure 91) and Panc04.03 (Figure 91) showed high levels of αvβ6 expression as observed by the brown coloured staining. The pattern of staining was very similar to that observed in the human TMA samples. Also, as in human tissues, the normal mouse pancreas together with the surrounding stroma was negative for αvβ6. There was a very slight increase in background staining of the xenograft tumours compared to human tissue because of using a mouse antibody on mouse tissue but this was overcome by using an M.O.M kit to carry out IHC on the samples.

Thus, two new orthotopic models were successfully generated and both models maintained expression of αvβ6. Even though this was perhaps an ideal model to use from a physiological point of view, it was not possible to carry out testing of new therapeutic agent targeting αvβ6 using these models due to lack of an accurate method to monitor tumour growth in the pancreas on a daily basis. An ultrasound scanner to measure tumour growth or luciferase tagged tumour cell lines to image using an IVIS scanner were the two options available to overcome this issue. The latter was more feasible and Panc04.03 and CFPac1 luciferase tagged cell lines were generated but too late for use in this study (data not shown). Based on data obtained from colleagues who performed PDAC orthotopic experiments using a different pancreatic cancer cell line, it was evident that the luciferase tagged cells imaged using an IVIS scanner did not provide an accurate read out proportional to the tumour size in the pancreas. This was a major set back in terms of using the orthotopic models generated for further experiments to test the efficacy of anti-αvβ6 therapy using function blocking antibodies. A subcutaneous model seemed like the most viable option to carry the study forward but this model had to be modified to try and overcome its major drawback, which is the lack of a relevant tumour-stroma interaction.

5.2. Generation of an αvβ6 positive subcutaneous xenograft mouse model

Two million CFPac1 cells were injected subcutaneously in 200µl PBS into five CD1nu/nu mice. Tumour growth was monitored twice a week and tumours were harvested six weeks post injection. Following tissue processing, these tumours were stained with 62G2, an anti-αvβ6 antibody to determine expression levels of αvβ6.

CFPac1 cells injected subcutaneously into CD1nu/nu mice grew in approximately six weeks to give rise to tumours. Tumour cells frequently showed mitotic morphology and the developing masses contained small luminal structures as shown by H&E staining. The tumour cells (CFPac1) maintained strong membranous αvβ6 expression as detected by the brown staining. Higher levels of background staining were observed in all subcutaneous xenograft sections that were stained for αvβ6. This was probably due to the non-specific binding of the mouse primary antibody onto host tissue even though a M.O.M kit was used to reduce background staining.

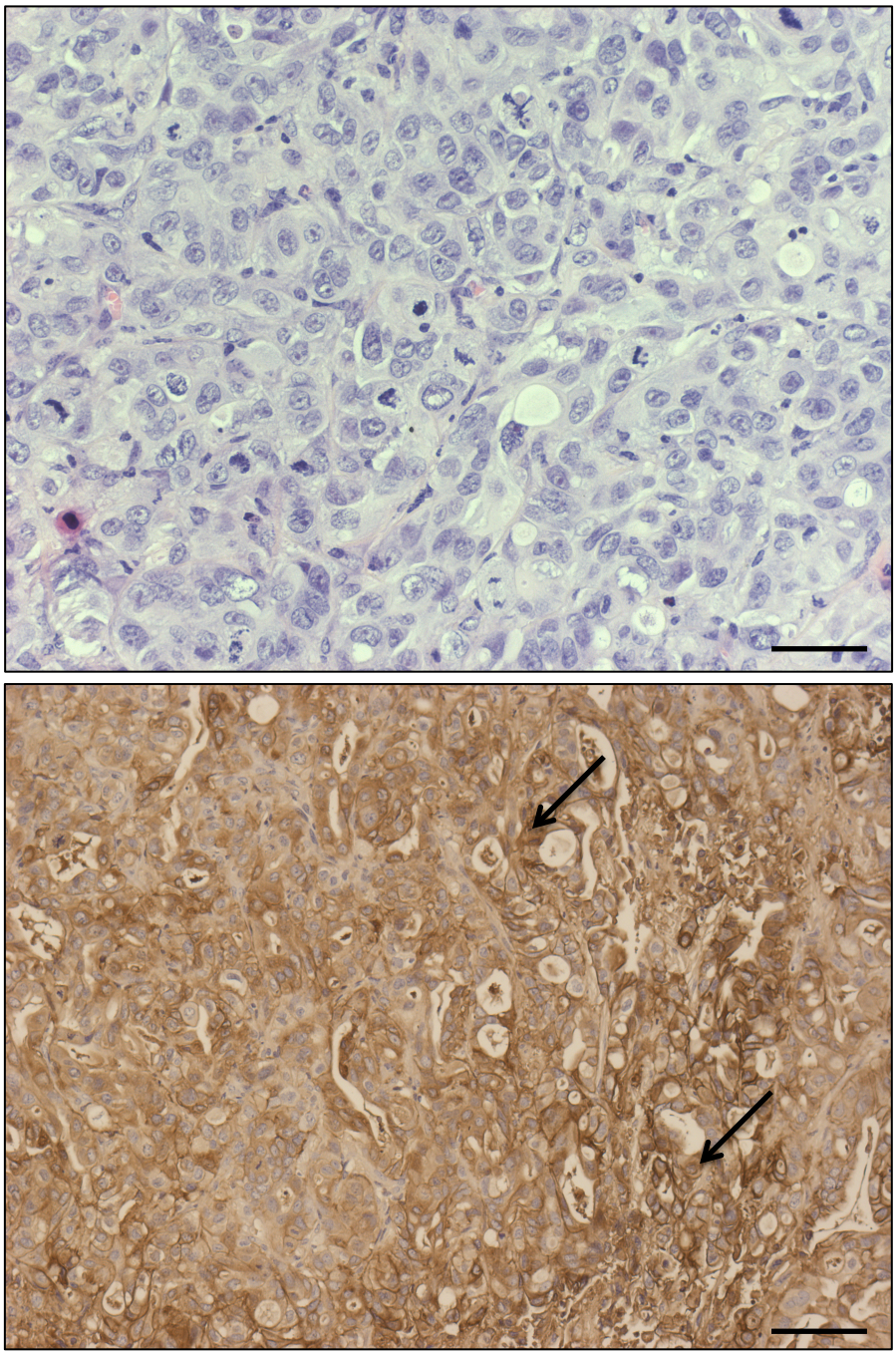

Figure 92: αvβ6 expression in a CFPac1 subcutaneous tumour. CD1nu/nu mice were injected with 2 million tumour cells subcutaneously and the tumour harvested six weeks later. Strong expression of β6 (brown staining) was observed in the epithelial cell membrane (arrow). H&E staining showed the presence of luminal structures. The above pictures are representative of images obtained from tumours in five animals. (Scale bar represents 50μm).

An αvβ6 positive subcutaneous xenograft model was successfully generated but this model lacked a key feature, tumour-stroma interactions, which is a very important feature of PDAC tumour growth and progression. A xenograft model that more closely replicated human pancreatic cancer therefore had to be generated for pre-clinical validation of anti-αvβ6 therapy. Human PDACs have a very strong desmoplastic reaction and usually up to 70% of the tumour is composed of stroma. This desmoplastic reaction had to be mimicked in the xenograft model in order to make it more physiologically relevant. Pancreatic stellate cells (PS1) isolated and immortalised from human pancreatic cancer patients were available in-house. This cell line was characterised by colleagues, who have shown that the ratio of the number of stellate cells to cancer cells plays an important role in determining the growth and invasion of PDAC cell lines grown in 3D organotypic co-culture models (data not published, manuscript submitted). Their data suggested that a ratio of 1:2, cancer cells to stellate cells, provided the maximum growth and invasion in the *in vitro* 3D co-culture analysis performed. Thus, before attempting therapeutic approaches, I set out to determine whether the incorporation of pancreatic stellate cells in the subcutaneous injection resulted in a tumour appearance which more closely approached the morphology seen in human pancreatic cancer.

5.3. Development of novel xenograft models incorporating pancreatic stellate cells

PS1 cells were co-injected with CFPac1 tumour cells in a 2:1 ratio both into the pancreas and subcutaneously in to CD1nu/nu mice. The subcutaneous tumours were measured every two days and tumours harvested fifteen days after injection. As expected the introduction of the stellate cells increased the rate of growth compared to the growth of CFPac1 in the absence of stellate cells (Figure 94). All mice that were injected with CFPac1 together with PS1 cells in a 1:2 ratio, had measurable tumour volumes from day 3. In contrast, only three of the five mice injected with CFPac1 tumour cells alone developed tumours and this was only apparent from day 11. At day 15, the mean tumour volume of CFPac1/PS1 tumours was 349mm^3 compared to just 5.4mm^3 in the tumours with CFPac1 cells alone.

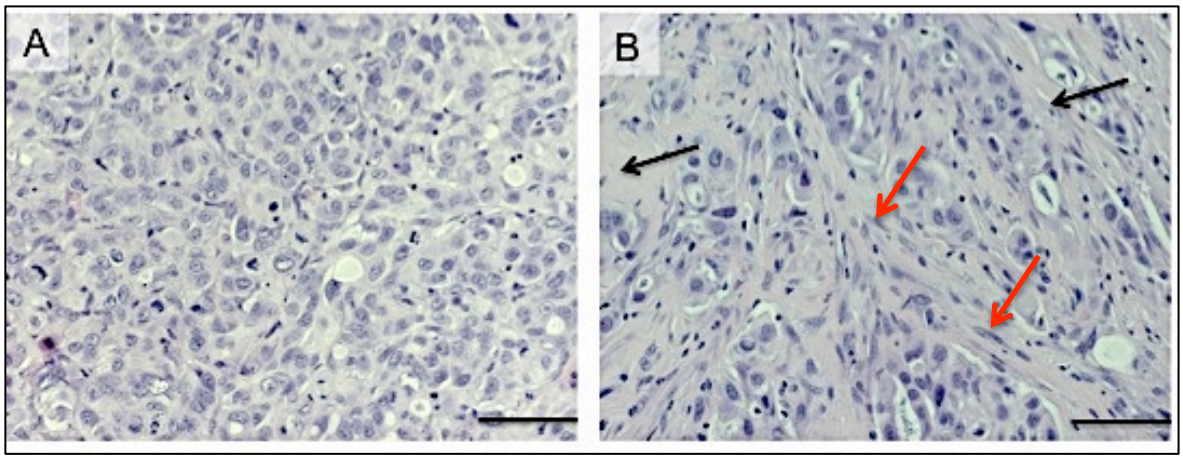

Figure 93: Introduction of PS1 cells into a CFPac1 subcutaneous model increases desmoplastic reaction. 1 million CFPac1 tumour cells alone (A) or 1 million CFPac1 with two million PS1 stellate cells (B) were injected subcutaneously into CD1nu/nu mice (n=5 per group). Tumours were harvested from mice fifteen days post injection. The black arrows in (B) point to increased desmoplastic response observed in the cancer cell and stellate cell co-injected subcutaneous xenograft model. The red arrows in (B) point towards the fibroblast-like stellate cells (PS1) interspersed in the tumour stroma. The above pictures are representative images (Scale bar represents 100µm).

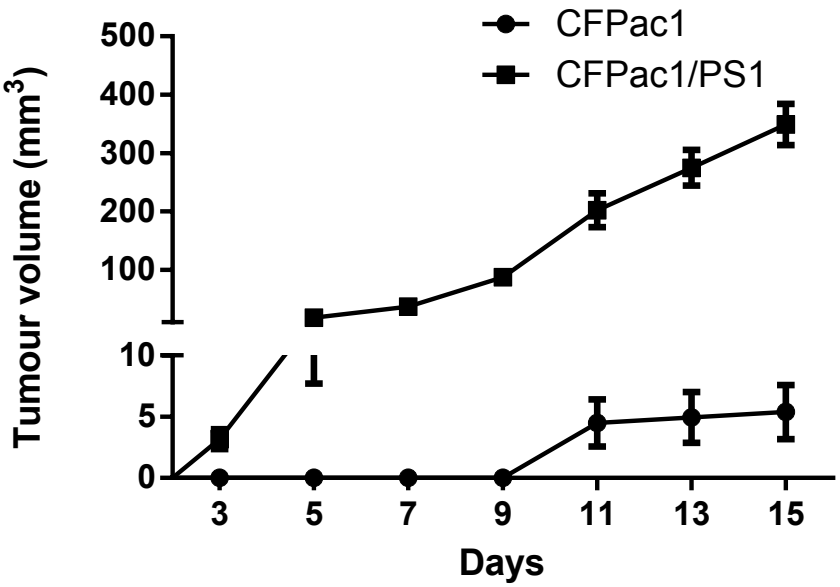

Figure 94: Accelerated growth of CFPac1/PS1 (1:2 ratio) subcutaneous tumours compared to CFPac1 cells alone. 1 million CFPac1 and 2 million PS1 cells were co-injected subcutaneously into the CD1nu/nu mice and tumour growth compared to that of CFPac1 cells alone (n=5 per group). Data show the mean tumour volume ± SEM.

It was observed that the introduction of the stellate cells with the cancer cells stimulated a desmoplastic response similar to that which has been observed in human PDAC (Figure 93). The stellate cells could be seen in the surrounding tumour stroma (shown by red arrows). This increased desmoplastic response was not observed in the CFPac1 cells alone subcutaneous model generated previously (Figure 92- top). The addition of the stellate cells into the subcutaneous model also significantly increased the rate of tumour growth (Figure 94). This was a significant step towards achieving a more physiologically relevant subcutaneous model. A similar response was also observed in the orthotopic model (Figure 95) but this model is, of course, more technically demanding and places greater stress on the experimental animals.

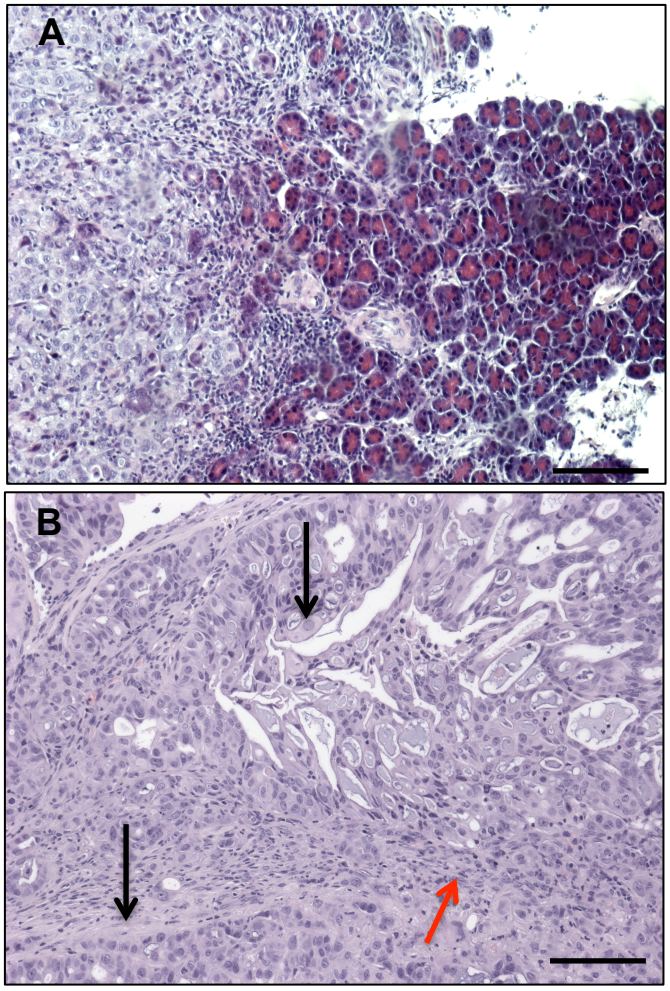

Figure 95: Introduction of PS1 cells into a CFPac1 orthotopic model increases desmoplastic reaction. 1 million CFPac1 tumour cells alone (A) or 1 million CFPac1 with two million PS1 stellate cells (B) were injected orthotopically into the pancreas of CD1nu/nu mice (n=5 per group). Tumours were harvested from mice six weeks post injection. The black arrows in (B) point to increased desmoplastic response observed in the cancer cell and stellate cell co-injected orthotopic xenograft model. The red arrows in (B) point towards the fibroblast-like stellate cells (PS1) interspersed in the tumour stroma. The above pictures are representative images and scale bar represents 100µm.

In order to determine that αvβ6 expression was retained in the modified subcutaneous model (CFPac1/PS1) tumour sections were stained for αvβ6. Figure 96 shows CFPac1 cells expressed αvβ6 strongly on the cell membrane. A strong desmoplastic response also was observed, which is typical of the human disease. Multiple tumour sections from all animals in the CFPac1/PS1 cohort were observed by two independent pathologists (Dr. Colan Ho-Yen and Prof. Louise Jones), who confirmed the similarity of these tumours to human pancreatic cancer.

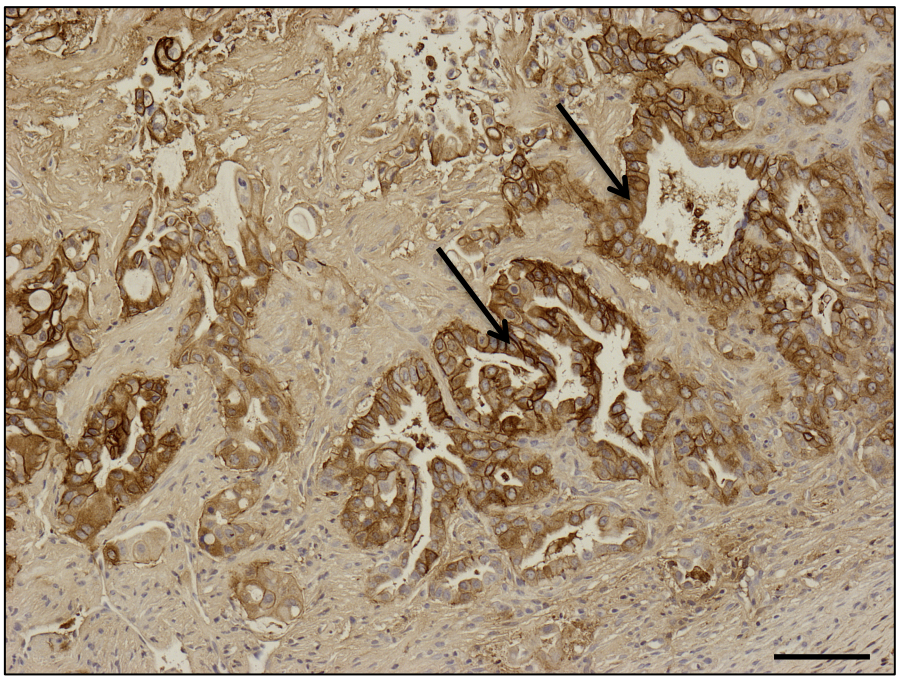

Figure 96: Expression of αvβ6 in a CFPac1/PS1 subcutaneous tumour. Tumours were harvested fifteen days post injection and stained for αvβ6. Arrows point towards β6 staining (brown) on the cell membrane of CFPac1 cells. Note also the marked stromal response in between islands of tumour cells. The above picture is representative of tumour sections from five animals per group. (Scale bar - 100μm).

5.3.1. Direct comparison of CFPac1/PS1 subcutaneous model with CFPac1/PS1 orthotopic model

In the absence of a genetically modified spontaneous mouse model for pancreatic cancer, it was important to validate the modified subcutaneous xenograft model against the orthotopic model, the latter seeming most likely to represent the more physiologically relevant and comparable model to the human disease. H&E stained sections showed that the CFPac1/PS1 subcutaneous model had an increased desmoplastic response compared to the injection of CFPac1 cells on their own (Figure 93) and certainly these tumours looked morphologically similar to the CFPac1/PS1 orthotopic xenograft model (Figure 93 compared with Figure 95). This was considered to be promising and more experiments were carried out to validate the new modified subcutaneous model further.

5.3.1.1. Desmoplastic response in CFPac1/PS1 xenografts.

PDAC disease is typified by the presence of an intense desmoplastic stroma. This stromal response has been attributed largely to the presence of the activated pancreatic stellate cells in the stroma surrounding the tumour [86]. It has also been shown that orthotopic models for pancreatic cancer where tumour cells and stellate cells have been co-injected tend to replicate the desmoplastic reaction seen in humans making them suitable models to study PDAC growth and progression [77]. The modified subcutaneous xenograft model tumours were stained for collagen using Sirius red dye, which binds specifically to the helical structure on fibrillar collagen (type 1-4). Therefore it was used as a measure to compare total collagen deposition between the orthotopic and subcutaneous xenograft models.

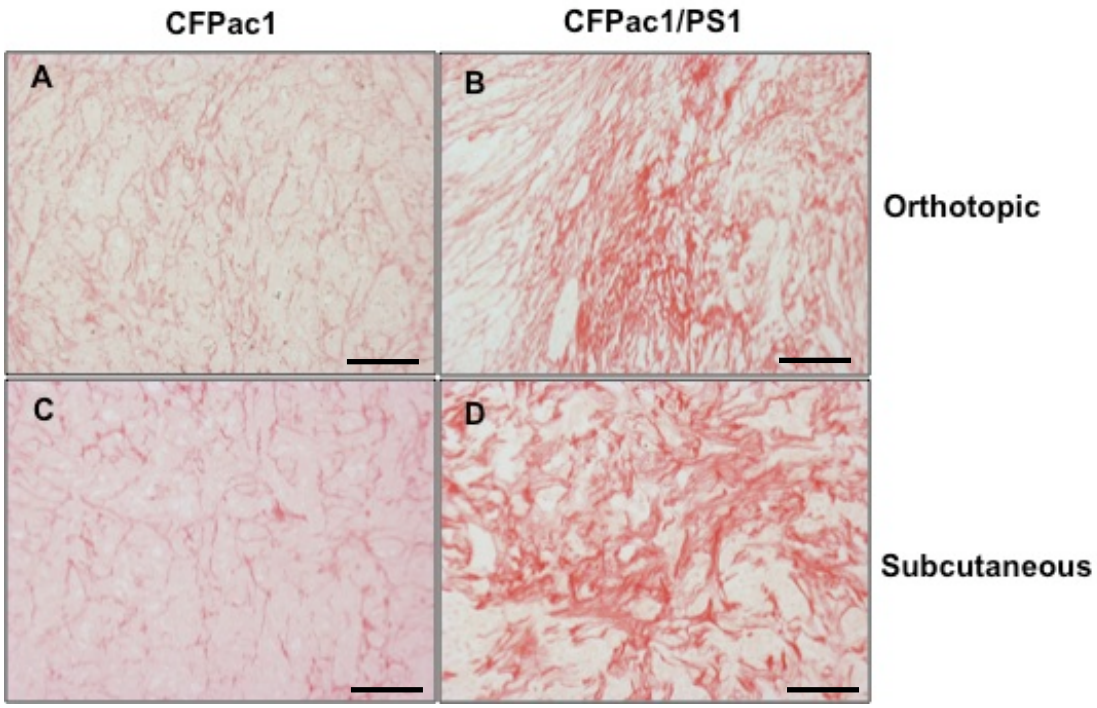

Figure 97: Increased collagen deposition in CFPac1/PS1 orthotopic and subcutaneous xenograft models. Representative images show total levels of collagen deposition using Sirius red staining on tumour sections from CFPac1 cells alone or tumours produced by CFPac1 cells in combination with PS1 cells in an orthotopic model (A and B) and subcutaneous model (C and D) (Scale bar - 100µm).

There was no difference observed in terms of total collagen deposition between the CFPac1/PS1 orthotopic and CFPac1/PS1 subcutaneous xenograft models when stained with Sirius red (Figure 97). The red colour of the dye was observed where there was collagen deposition and the addition of the stellate cells into the subcutaneous model significantly increased the desmoplastic response observed as seen in Figure 97D compared to the CFPac1 alone when injected subcutaneously Figure 97C. This increase in collagen deposition was also observed in the orthotopic model upon addition of PS1 cells (Figure 97B compared with Figure 97A). The CFPac1 alone subcutaneous model still had some collagen deposition; presumably as a result of the host stromal response but the level of collagen deposition was dramatically lower than that when PS1 cells were incorporated. All sections from the different models were stained at the same time using the same procedure. This suggested that the modified subcutaneous model with CFPac1/PS1 was as good as the CFPac1/PS1 orthotopic model in terms of laying down a desmoplastic stroma thereby mimicking human disease.

5.3.1.2. Tumour vascularity in the xenograft models

Poor vascularity is a common feature in human PDAC and one of the major reasons why chemotherapeutic agents do not reach the tumour. This poor vascularity is also observed in the genetically modified mouse model (KPC), widely used in pancreatic cancer research and considered the gold standard to recapitulate human disease. In contrast, transplanted tumours, either orthotopic or subcutaneous have been shown to be highly vascularised thereby not replicating the physiological scenario observed in human PDAC [269]. Tumour vascularity therefore was investigated in both the tumour models generated previously to determine if these novel xenograft models were more morphologically relevant to the human disease (Figure 98).

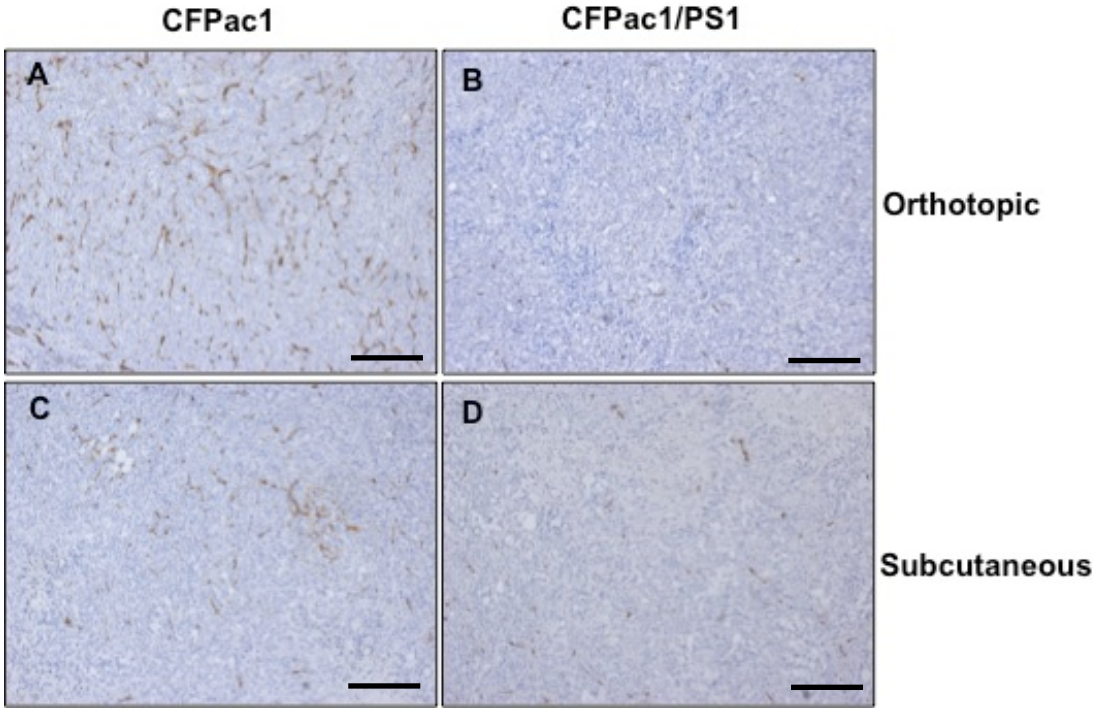

Figure 98: Decreased tumour vascularity in CFPac1/PS1 orthotopic and subcutaneous xenograft models. Representative images show blood vessels, identified by being stained for endomucin, on tumour sections from CFPac1 alone or in combination with PS1 cells in an orthotopic model (A and B) and subcutaneous model (C and D) (Scale bar - 100μm).

The tumours harvested from CFPac1 and CFPac1/PS1 orthotopic xenograft models were stained for blood vessels using a rat anti-endomucin antibody; endomucin is a blood vessel marker specifically expressed on the endothelial cells. It was clearly apparent from visual inspection that the addition of the PS1 stellate cells with the CFPac1 cells significantly reduced the number of blood vessels in both the subcutaneous and orthotopic tumour models (Figure 99). The numbers of blood vessels were quantified by counting the number of endomucin positive blood vessels in four high power fields per tumour sample. There was a significant reduction in the number of blood vessels in the CFPac1/PS1 orthotopic model compared to the CFPac1 orthotopic model ($p = <0.01$). The tumours in both cohorts were harvested at the same time and the counting was done blind to avoid any element of bias in the analysis (Figure 99A). Similarly, there was a significant reduction in the number of endomucin positive blood vessels in the CFPac1/PS1 subcutaneous tumours compared with the CFPac1 tumour cells alone ($p = <0.03$). The number of blood vessels was quantified using the Ariol microscope, which uses automated software to analyse the number of blood vessels and express it relative to the area of the tumour (Figure 99B). The blood vessels around the edge of the tumour were not included for the analysis.

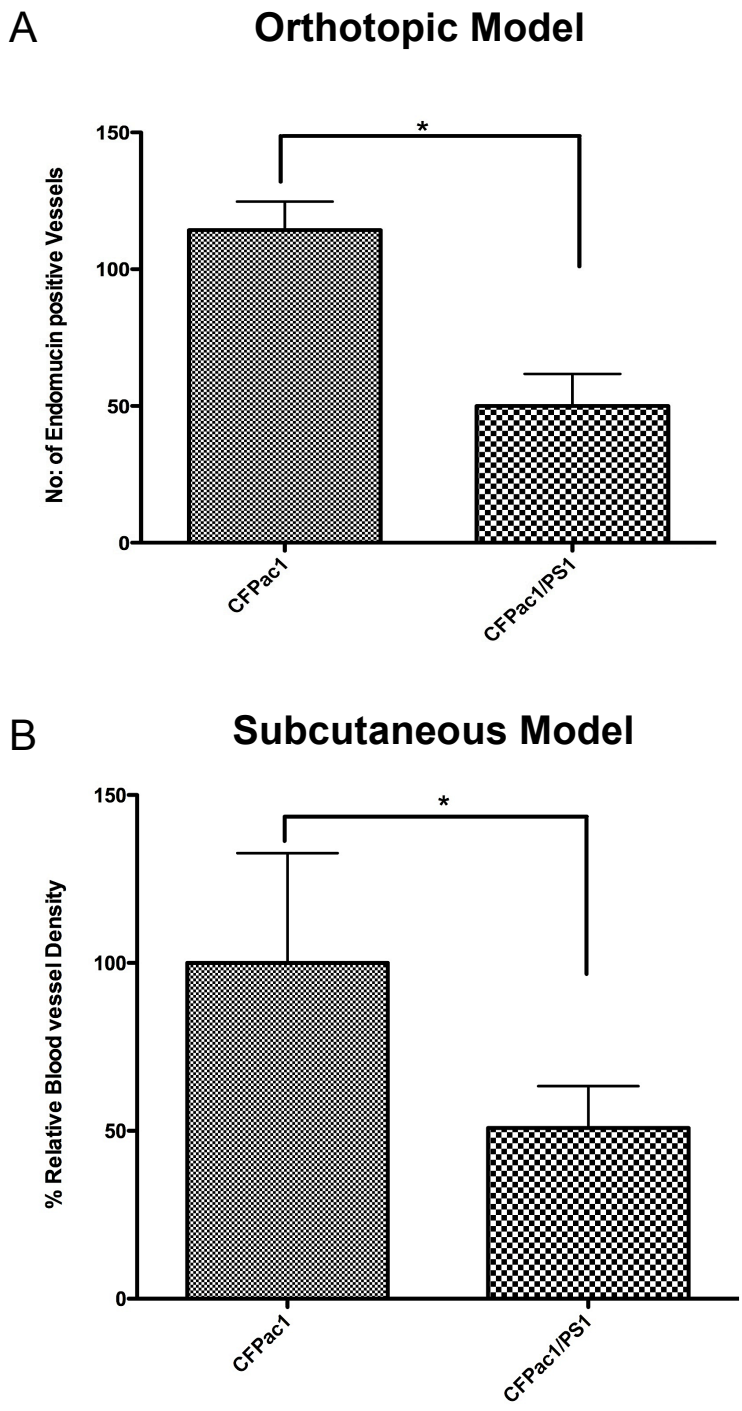

Figure 99: Quantification of blood vessels in CFPac1 and CFPac1/PS1 orthotopic and xenograft tumour models. Blood vessels were stained for endomucin. A) Four high power fields per tumour sample (n=3 per group) were used to quantify the number of endomucin positive blood vessels in the orthotopic models. B) Ariol scanning microscope was used for quantifying the number of endomucin positive blood vessels and expressed relative to area of the tumour sample (n=3 per group). Student's t-test p= <0.01 (orthotopic models) and p= <0.03 (subcutaneous models).

These results suggested that another important aspect of PDAC tumours, hypovascularisation, was retained in both the CFPac1/PS1 subcutaneous and orthotopic xenograft models. There was a strong and near identical desmoplastic response observed in both the subcutaneous and orthotopic models, which could be the reason for the significant reduction in vascular density in the tumours. The modified subcutaneous model was comparable to the modified orthotopic model in terms of the desmoplastic response observed (collagen deposition) and reduced vascularity (endomucin quantification) in the tumours. These parameters were physiologically relevant and comparable to the published data using the genetically modified KPC mouse model [93, 269]. Although the modified subcutaneous model may still not be considered the perfect model, in terms of representing human disease, this study addressed some of the key issues that arise from using a subcutaneous mouse model.

5.4. Anti-αvβ6 targeted therapy in a subcutaneous xenograft mouse model of pancreatic cancer

Having established a suitable subcutaneous xenograft model that retained major features of human PDAC, a novel human anti-αvβ6 antibody was next tested as a potential therapeutic. In a pilot experiment (n=3 mice per arm) 1 million CFPac1 cells were co-injected with 2 million PS1 cells subcutaneously into female CD1nu/nu mice. Mice were given antibody 264RAD at 10mg/Kg or isotype control at 10mg/Kg once tumours reached a size of 100mm^3. The animals were treated twice a week and the antibodies were administered intra-peritoneally (IP). Tumour volume was assessed twice a week by bilateral Vernier-caliper measurement.

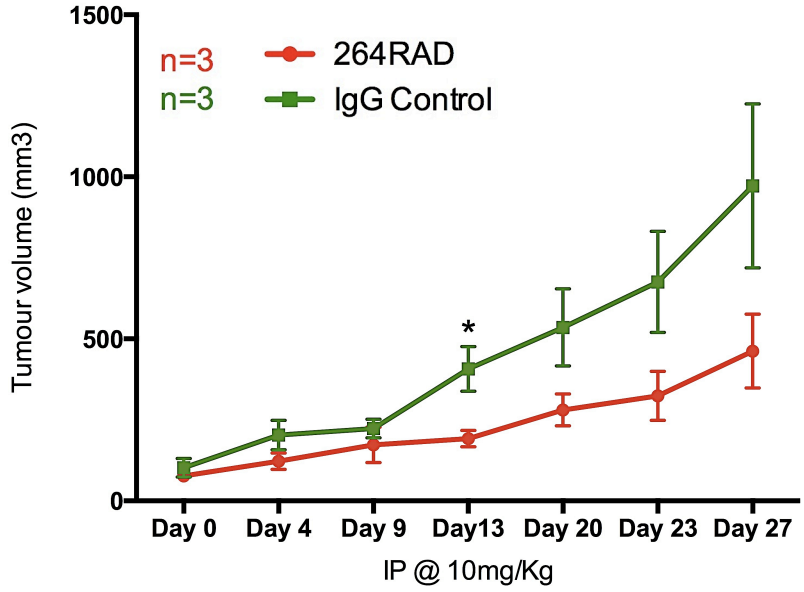

Figure 100: Pilot experiment testing the therapeutic efficacy of 264RAD antibody against CFPac1/PS1 subcutaneous tumours. CD1nu/nu mice bearing subcutaneous CFPac1/PS1 tumours were treated with 264RAD at 10mg/Kg or IgG control antibody at 10mg/Kg twice a week. Data represent the mean tumour volume and standard deviation of 3 animals per group. Student's t-test p= <0.04.

The preliminary experiment, with only n=3 per group, showed that the anti-β6 therapy delayed tumour progression compared to the IgG control antibody treated group. There was a significant difference between the two groups at day 13 (p= <0.04) but the differences in size did not attain significance in the later stages as the treatment progressed (Figure 100). This is likely due to the very small numbers of animals used per group and also because the animals in the control group reached the upper limit of tumour size under the Home Office regulations and had to be killed before a significant difference between the two groups could be observed. The tumours from these animals were harvested and processed for further IHC analyses.

5.4.1. IHC analysis on tumour tissue

Effective antibody therapy in humans requires biomarkers to prove that the therapeutic is causing real biological change. Expression of αvβ6, Ki67, phospho ERK and caspase3 levels were thus analysed in 264RAD and IgG treated tumours.

5.4.1.1. Expression levels of αvβ6 on tumours

It has been shown that when tumours are treated with 264RAD, they lose expression of αvβ6 [233]. Since the tumours were treated with the anti-αvβ6 blocking antibody for 27 days, it was decided to check expression levels of αvβ6 in the tumour samples.

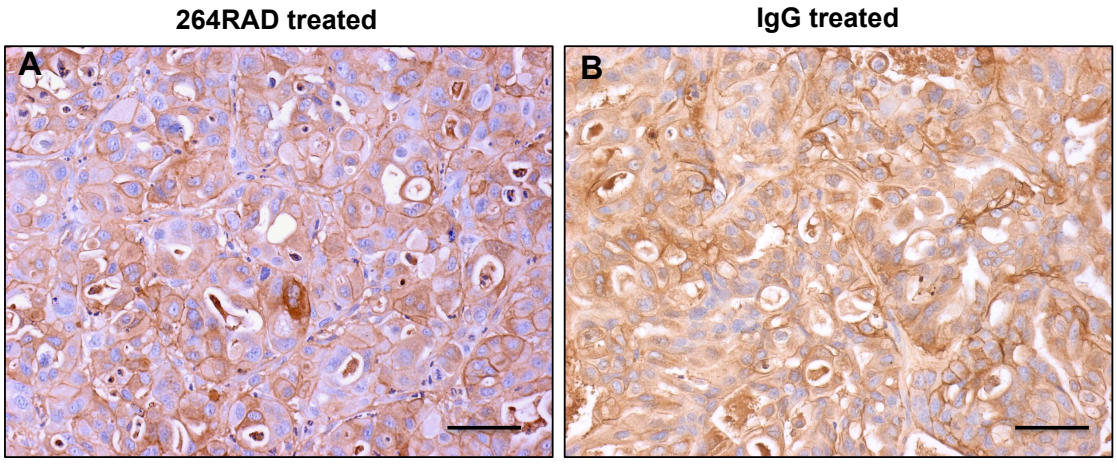

Figure 101: αvβ6 expression in 264RAD and IgG treated CFPac1/PS1 subcutaneous tumours. Representative images of αvβ6 expression in tumours treated with A) 264RAD and B) IgG antibody. Tumours were harvested after 27 days of treatment (n-3 per group). Brown membranous staining was observed on both 264RAD and IgG treated tumours. (Scale bar represents 50µm).

There was no clear observable reduction in the levels of expression of αvβ6 between the 264RAD treated and the control IgG treated tumour samples (Figure 101). This was not in agreement with the published literature but it could be that the tumours were not treated long enough in order to significantly affect levels of expression of αvβ6. The high background staining, which made comparison difficult, was because of using a mouse primary antibody on mouse tissue despite using the M.O.M kit, which aims to reduce background staining.

5.4.1.2. Expression of phospho ERK in 264RAD/IgG treated tumours

ERK phosphorylation plays an important role in cellular proliferation, differentiation and survival and αvβ6 has been shown to interact directly with the ERK pathway and generate survival signals [181]. Since a significant decrease in proliferation was anticipated in the tumour sections that were treated with 264RAD compared with the IgG control treated antibody, because of the slower growth rate of the tumours, it was decided to examine expression levels of phospho ERK at the tissue level between the two treatment groups.

Four high power fields per tumour sample were taken at random and the number of positive nuclei was counted (Figure 102). There was a significant reduction in the expression levels of phospho ERK in the 264RAD treated tumours in comparison with the IgG control antibody treated tumour sections ($p = <0.0001$). These data showed the down stream effects of blocking αvβ6 using an αvβ6 function blocking antibody in the tumours treated with 264RAD compared with the IgG control antibody treated tumours.

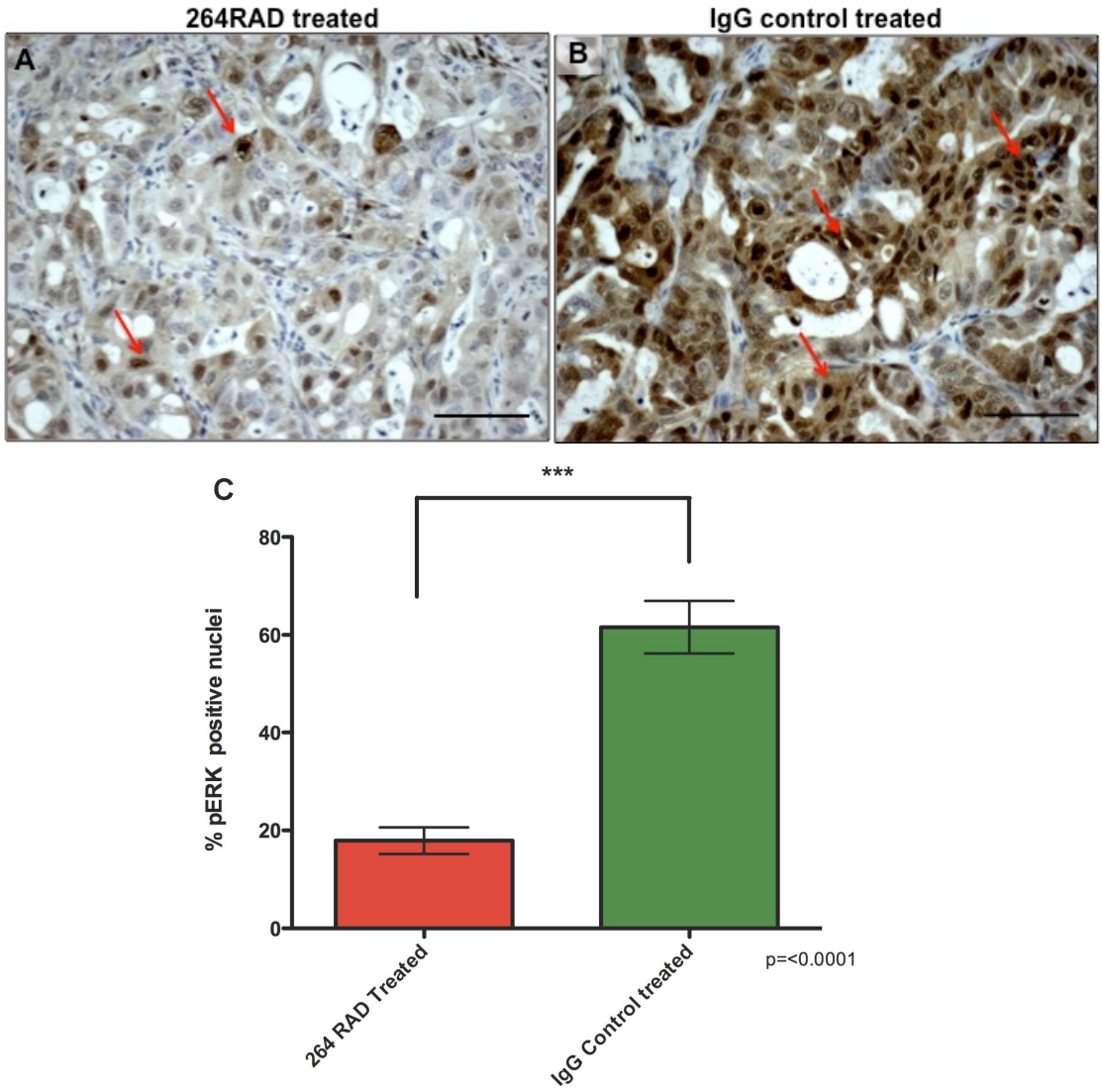

Figure 102: Phospho ERK expression in 264RAD and IgG treated CFPac1/PS1 subcutaneous tumours. 10X magnification representative images of phospho ERK expression in tumours treated with A) 264RAD and B) IgG antibody. Tumours were harvested after 27 days of treatment. C) Data show % mean ± SEM of phospho ERK positive cells (n-3 per group). Student's t-test p= <0.0001. (Scale bar represents 50µm).

5.4.1.3. Expression of Ki67 in 264RAD/IgG treated tumours

Ki67 is a nuclear protein and marker for cellular proliferation. Ki67 is present during all phases of the cell cycle but is absent in the resting (G0) phase. Since there was a marked decrease in tumour volume in the 264RAD treated tumours compared to the control IgG antibody treated animals, the tumour sections were stained for Ki67 to check if there was any difference in cell proliferation between the two groups.

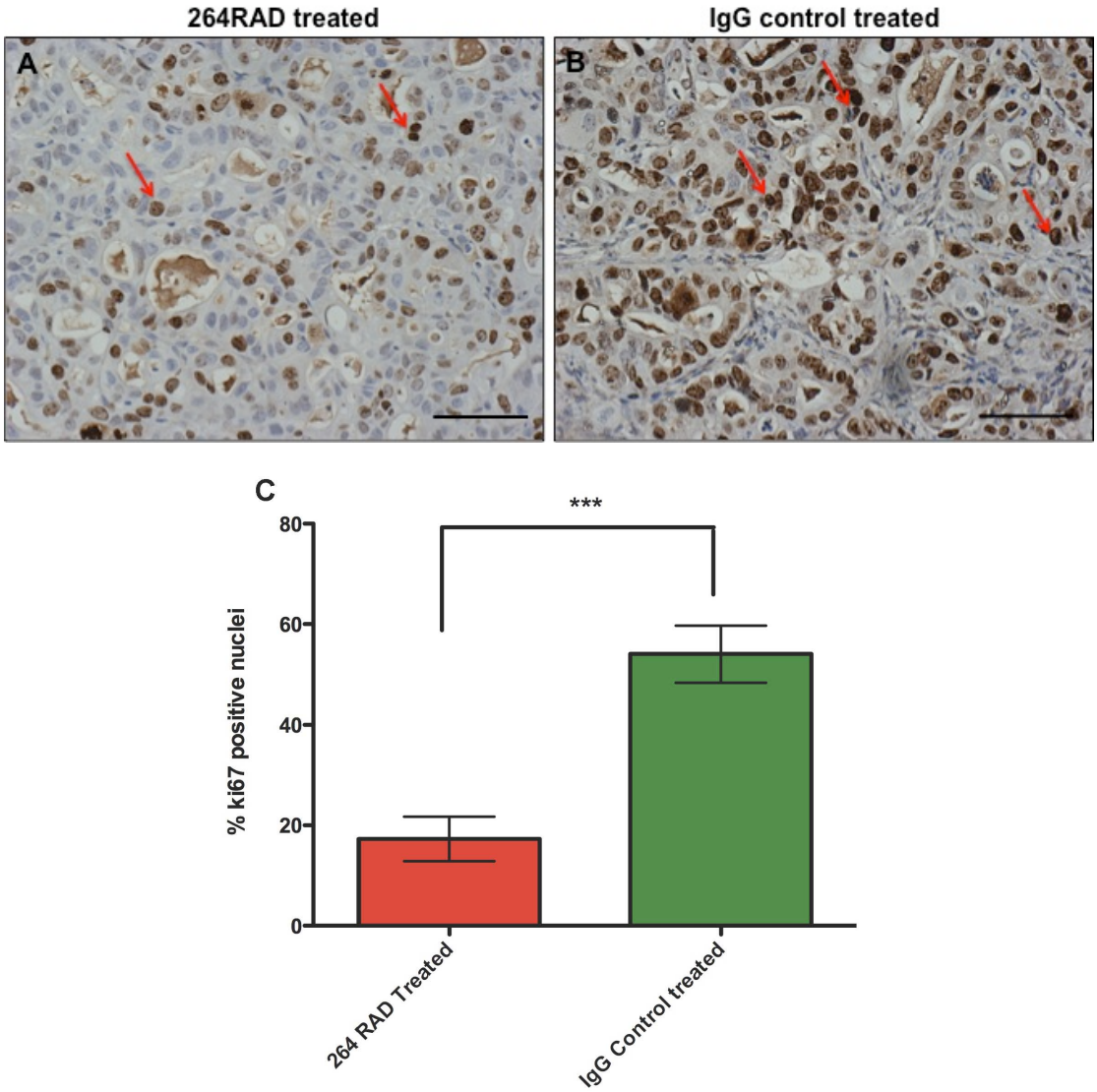

Figure 103: Ki67 expression in 264RAD and IgG treated CFPac1/PS1 subcutaneous tumours. 10X magnification representative images of Ki67 expression in tumours treated with A) 264RAD and B) IgG antibody. Tumours were harvested after 27 days of treatment. C) Data show % mean ± SEM of Ki67 positive nuclei (n-3 per group). Student's t-test p= <0.0001. (Scale bar represents 50µm).

Four high power fields per tumour sample were taken at random and the number of positive nuclei was counted (Figure 103). There was a significant reduction in the expression levels of Ki67 on the 264RAD treated samples in comparison to the IgG control antibody treated tumour sections (p= <0.0001). These data confirmed that the tumour cells treated with 264RAD αvβ6 blocking antibody were proliferating less compared to the IgG control antibody treated tumour cells thus perhaps accounting in part for the difference in tumour volumes observed between the two treatment groups.

5.4.1.4. Expression of activated caspase 3 in 264RAD/IgG treated tumours

Activated or cleaved caspase 3 is considered a marker for apoptosis. In general, cells positive for activated caspase 3 have undergone or are undergoing apoptosis through a caspase dependent pathway. Since there was a substantial difference in tumour volume between the 264RAD treated and IgG control antibody treated tumours, sections were stained for activated caspase 3 to determine if there was any difference in apoptotic cell death between the two groups.

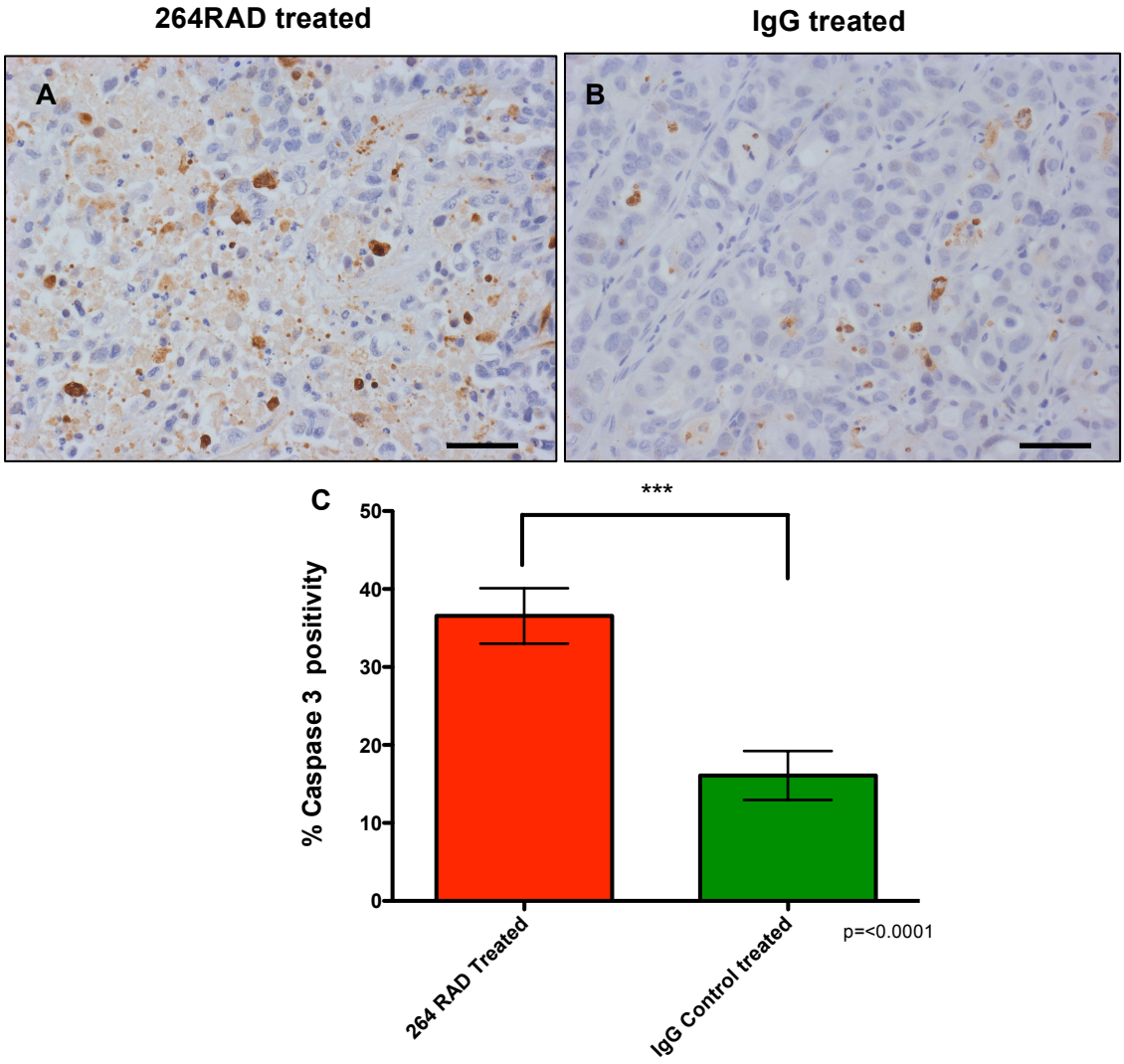

Figure 104: Activated caspase3 expression in 264RAD and IgG treated CFPac1/PS1 subcutaneous tumours. Representative images of activated caspase 3 expression in tumours treated with A) 264RAD and B) IgG antibody. Tumours were harvested after 27 days of treatment. C) Data show % mean ± SEM of activated caspase 3 positive cells (n-3 per group). Student's t-test p= <0.0001. (Scale bar represents 50µm).

Four high power fields per tumour sample were taken at random and 200 nuclei per field of the number of caspase 3 positive or negative cells (nuclear/cytoplasmic brown stain) were counted. There was a significant increase in the expression levels of caspase 3 on the 264RAD treated samples in comparison with the IgG control antibody treated tumour sections (p= <0.0001). This data confirmed that the tumours treated with 264RAD β6 blocking antibody were apoptotic and dying compared with the IgG control antibody treated tumours (Figure 104) possibly accounting in part for the difference in tumour volumes observed between the two treatment groups.

5.4.2. Targeting αvβ6 in a CFPac1/PS1 xenograft model using 264RAD and gemcitabine

Having observed a significant difference between the two treatment arms in the pilot experiment, it was decided to conduct a larger experiment with more animals per group and also include a gemcitabine single agent therapy and 264RAD + gemcitabine combination therapy treatment arm. The number of cells injected per animal was also halved, as PS1 cells are slow growing.

0.5 million CFPac1 were co-injected with 1 million pancreatic stellate cell line, PS1 (1:2 ratio) subcutaneously into female CD1nu/nu mice. Tumour growth was measured twice weekly and treatment started on an individual basis when tumour size reached approximately 100mm3. Mice were randomised to one of four treatment groups (Figure 105).

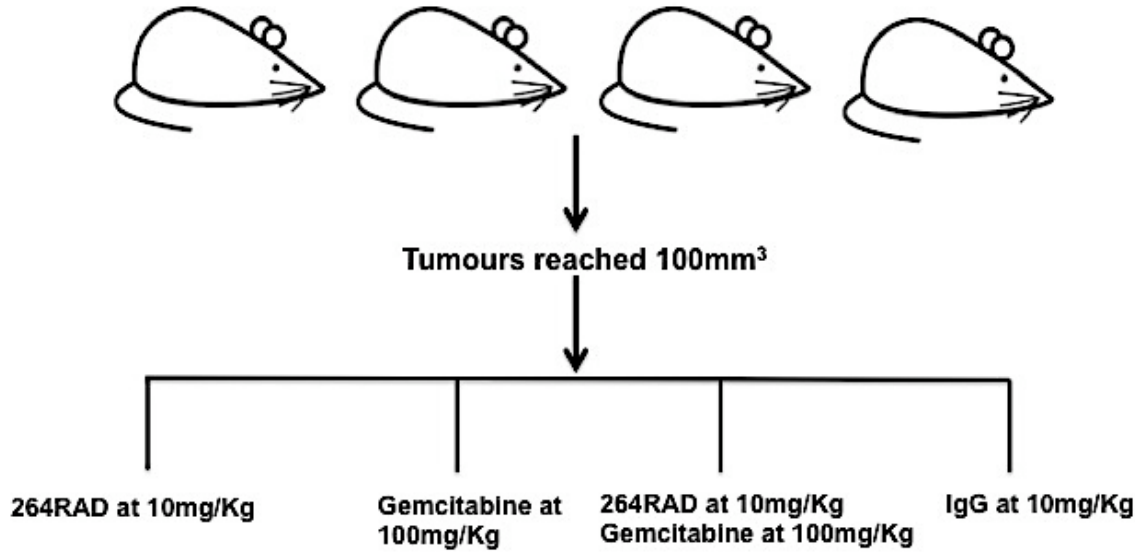

Figure 105: Treatment plan for the 264RAD/gemcitabine therapy of CFPac1/PS1 xenografts. Animals were randomised and entered into one of the four groups when tumours reached 100mm^3.

The four treatment arms included the αvβ6 function blocking antibody 264RAD as a single agent therapy used at 10mg/Kg final concentration, gemcitabine as a single agent (current therapy available for PDAC patients) at 100mg/Kg, a combination arm, 264RAD used at 10mg/Kg and gemcitabine at 100mg/Kg and a control arm with IgG isotype antibody used at 10mg/Kg (Figure 105). The animals were treated twice a week and the drugs were administered intra-peritoneally (IP). Each animal in the single agent group received 200µl of the drug per injection and the combination group received 400µl (200 each of the two drugs) per injection. Therapy was continued until 6 weeks (day 42) from the first dose (day 1). There were 9 animals per group and tumour volumes were assessed twice a week by bilateral Vernier-caliper measurement and calculated (taking length to be the longest diameter across the tumour and width to be the corresponding perpendicular diameter) using the formula- [length x (breadth)^2]/2.

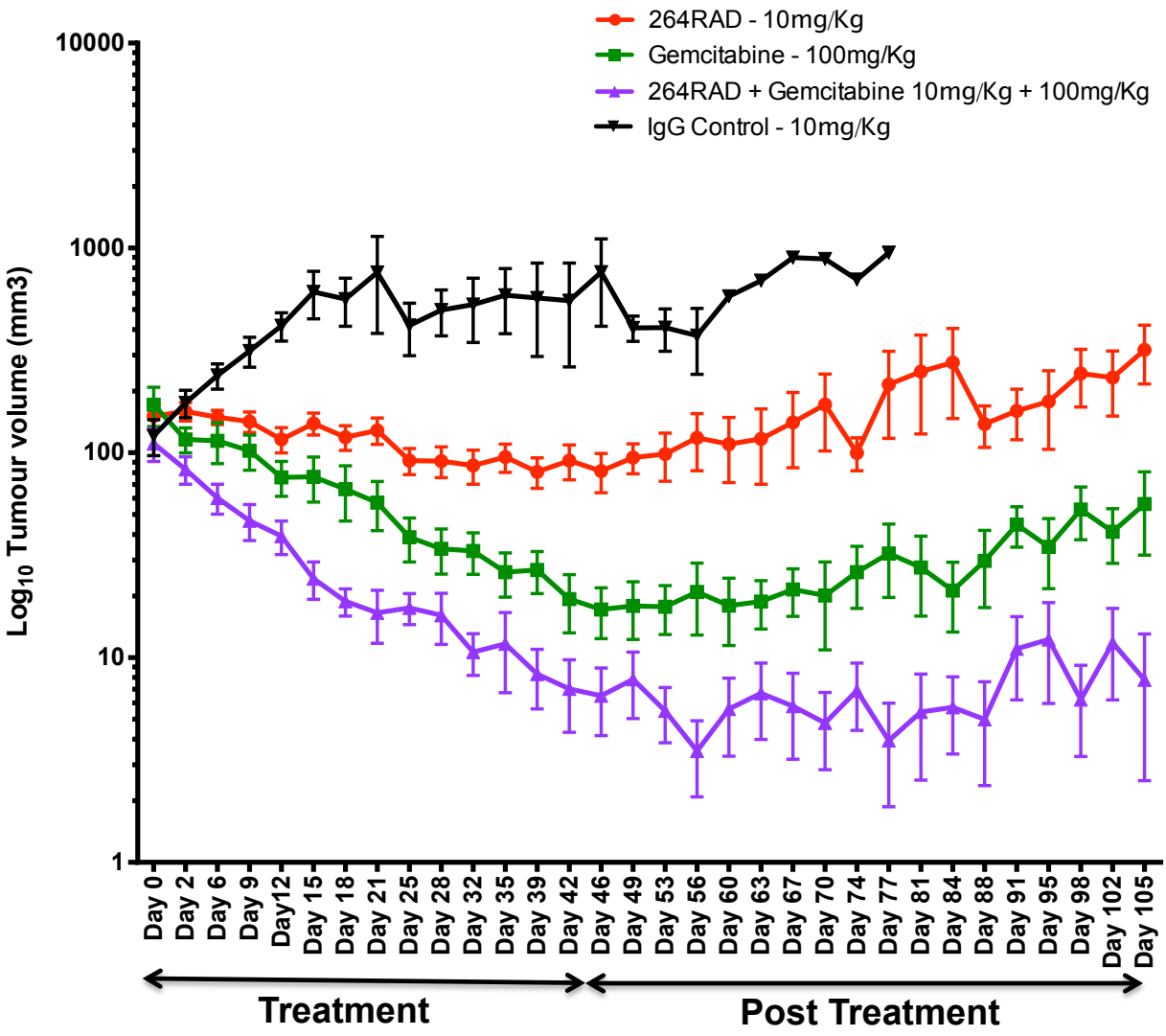

Figure 106: Treatment of CFPac1/PS1 subcutaneous tumours with 264RAD/gemcitabine. Mice bearing subcutaneous CFPac1/PS1 tumours were treated with 264RAD at 10mg/Kg, gemcitabine at 100mg/Kg, 264RAD (10mg/Kg) + gemcitabine (100mg/Kg) or IgG control antibody at 10mg/Kg twice a week up to day 42. Data were log transformed and represent the mean and standard error of mean of 9 animals per treatment arm.

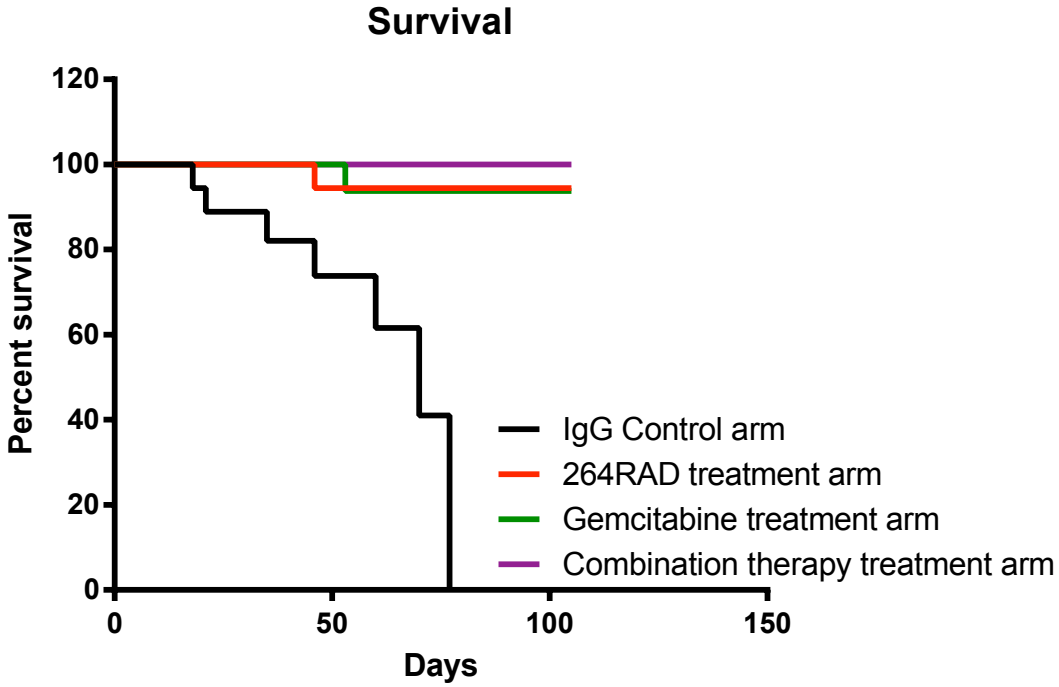

Figure 107: Kaplan-Meier survival curves showing response to the therapy administered. Animals in the IgG group were all dead by day 77 after treatment started. 8 out of 9 animals survived in both the single agent treatment arms whereas all animals were alive at day 105 in the combination group.

There was a significant decrease in tumour growth in all the treatment arms when compared to the IgG control antibody treated animals over the six-week treatment period (Figure 106). Growth inhibition was calculated from start of treatment based on the change in tumour volume. Since the variance in mean tumour volume data increases proportionally with volume (and is therefore disproportionate between the groups), data were log-transformed to remove any size-dependency. There was considerable variation observed in the IgG control antibody treatment arm (Figure 106) and this was because animals had to be culled as the experiment was in progress either due to poor health or the tumour had reached the maximum permitted size as per Home Office regulations (Figure 107). Note that by day 56 only 2 animals in the IgG group survived and they were culled by day 77 (Figure 107). There was one animal each from both the single agent therapy arm, which had to be culled due to poor health even though their tumour burdens were well within the size limit (Figure 107).

The 264RAD single agent therapy arm inhibited tumour growth as soon as treatment was administered with >50% reduction in tumour growth observed just 9 days after treatment commenced when compared to the IgG control antibody treated animals (Figure 106). Once treatment stopped at day 32, it was observed that the tumours in the 264RAD treated mice started to grow but at a much slower rate than the IgG group. In contrast, all animals in the IgG control antibody treated treatment arm were dead by day 74 (Figure 106). The gemcitabine single therapy treatment arm significantly reduced tumour size over the treatment period when compared to the IgG control antibody treated animals. Once therapy had stopped, tumour size seem to remain static but the tumour masses started to grow again by day 63. The rate at which the tumours were growing was slower than the IgG control arm (Figure 106). The combination therapy arm with both 264RAD and gemcitabine reduced tumour burden the most effectively of all treatment arms when compared with the IgG control antibody treated animals. Once combination therapy stopped, tumour size remained static for an additional 49 days since mean tumour size did not increase until day 91. Although it appears that tumour re-growth occurs following the end of treatment in all treatment arms, the combination therapy arm had the lowest tumour volume at day 105.

5.4.1. Statistical analyses comparing the four treatment arms from day 0 to day 42

Tumour measurements from day 0 to day 42 (end of treatment) were analysed using the generalised linear mixed model, which focuses more on the inverse link function rather than the link function to model the relationship between the linear predictor (time) and the conditional mean (tumour volume). The adjusted p values were calculated (Table 17). There was a significant difference in the rate of growth of the tumours in the 264RAD single therapy arm from day 6 to day 32 as denoted by the p values (***) when compared with the IgG treated animals. There was a significant difference in the rate of tumour growth in the gemcitabine single therapy treatment arm from day 6 to day 42 when compared with the IgG control antibody treated animals as denoted by the p values (***). There was a significant difference in the rate of tumour growth in the combination therapy treatment arm from day 2 to day 42 when compared to the IgG control antibody treated animals as denoted by the p values (***). When comparisons were made between the combination therapy treatment arm and the gemcitabine single agent therapy arm, there was a significant difference in the rate of tumour growth between the two groups from day 9 to day 21

and from day 32 to day 42 as denoted by the p values (*). More interestingly, there appeared to be a significant difference between the rate at which the tumour was growing back when comparing the gemcitabine single agent therapy arm and the combination therapy treatment arm. This experiment is still on going and further statistical analyses will be carried out when the experiment is terminated.

Days	IgG - 264RAD	IgG - Gemcitabine	IgG - 264RAD +gemcitabine	Gemcitabine +264RAD - 264RAD	Gemcitabine +264RAD - gemcitabine
0	*0.406*	*0.497*	*0.5983*	*0.1470*	*0.2407*
2	*0.818*	*0.072*	0.0043 **	0.003 **	*0.1454*
6	0.010 *	0.008 **	1.35E-05 ***	0.0004 ***	*0.1144*
9	0.004 **	0.0003 ***	2.42E-05 ***	0.0009 ***	0.0136 *
12	0.0001 ***	2.98E-05 ***	4.46E-06 ***	0.001 **	*0.0577*
15	0.003 **	9.51E-05 ***	2.30E-07***	9.86E-06 ***	0.0049 **
18	0.001 **	0.0001 ***	1.85E-06 ***	0.0001 ***	0.011 *
21	0.015 *	0.0002 ***	2.25E-05 ***	0.0002 ***	0.0108 *
25	0.003 **	4.70E-05 ***	8.65E-06 ***	0.0007 ***	*0.0811*
28	0.025 *	0.0007 ***	0.0001 ***	0.001 **	*0.0768*
32	0.007 **	0.0001 ***	5.97E-06 ***	9.94E-05 ***	0.0102 *
35	*0.090*	0.0001 ***	0.0003 ***	0.0003 ***	0.0375 *
39	*0.109*	0.010 *	0.0002 ***	0.0002 ***	0.0128 *
42	*0.444*	0.049 *	0.0001 ***	0.0001 ***	0.0121 *

Generalized linear mixed model- adjusted p values (***) denotes significance

Table 17: Statistical analyses comparing the four treatment arms. Values with *//*** denote significant statistical difference between two groups at a particular time point. Italicised p values are non-significant.**

5.5. Discussion

Treatment options available to PDAC patients have not improved over the past few decades with gemcitabine or a combination of chemotherapeutic drugs with gemcitabine and radiotherapy being the only treatment available for patients with locally advanced unresectable disease. Only about 20% of patients who present with the disease can undergo surgical resection and a further 50%-60% have metastatic disease at a stage where palliative care usually is the only option. Currently there are 18 active clinical trials for pancreatic cancer patients (source: clinical trials.gov, 2012). Of these, two active trials are investigating potential biomarkers in PDAC patients (source: clinical trials.gov, 2012) and one utilises PET imaging to study hypoxia in PDAC tumours (source: clinical trials.gov, 2012). There are two active trials providing vaccines to PDAC patients to modify the immune system (source: clinical trials.gov, 2012) but there are no active trials currently for antibody-mediated therapy to treat pancreatic cancer. This could be due in part to the history of poor performance by novel antibodies in treating pancreatic cancer or that there are no new agents, which are clinically efficient and good enough to enter clinical trials to target pancreatic tumour specifically.

As discussed in the previous chapter, even though $\alpha v\beta 6$ failed to be a reliable novel prognostic marker at the protein level for PDAC, at the mRNA level in a separate cohort of 292 patients, individuals expressing high $\alpha v\beta 6$ showed significantly poorer prognosis compared with the low expressers. The most important piece of information from the two data sets that were tested for $\alpha v\beta 6$ at the protein level was that 91% (median score ≥1) of PDAC patients were tested positive and this is dramatically more than what is observed in other cancers studied to date [201, 203, 204, 267]. Since PDAC patients have very limited treatment options available to them and thus developing new treatment options are essential to improve clinical outcome, targeting $\alpha v\beta 6$ may provide an additional strategy. Integrin $\alpha v\beta 6$ is expressed only on cancer cells and is absent in normal adult tissues, making it a potential therapeutic target for treating PDAC patients. Currently there are no $\alpha v\beta 6$ targeting antibodies in any active clinical trials to target cancer, although a function-blocking antibody against $\alpha v\beta 6$ (STX-100), is being used in the clinic to treat patients with pulmonary fibrosis (source: clinical trials.gov, 2012). Thus, there remains a clinical opportunity for antibody mediated targeting of $\alpha v\beta 6$. However, such studies require pre-clinical validation.

5.5.1. Generation of mouse models

Pre-clinical validation of novel therapeutic agents is essential before setting up clinical trials. Such experiments also enhance understanding of the kinetics and efficacy of the agent. Selection of the correct pre-clinical animal model is extremely important because results obtained from these pre-clinical experiments form the basis for any further clinical trials conducted in patients. A recent study using the KPC model for PDAC used a hedgehog inhibitor (IPI-926) to block hedgehog signalling in the surrounding stromal cells. This was targeted to inhibit the anti-angiogenic functions of the stellate cells to temporarily increase blood supply to the pancreatic tumours, before administering gemcitabine to target the cancer more efficiently [269]. This combination of inhibitor and gemcitabine showed extremely promising results in the KPC mouse model but phase II clinical trails conducted on PDAC patients with metastatic cancer showed no significant difference in clinical outcome in patients treated with the hedgehog inhibitor/gemcitabine (<6 months overall survival) or placebo/gemcitabine (>6 months overall survival) (Infinity Pharmaceuticals report, 2012). Thus, choosing the correct animal model and finding the optimal treatment strategy, such that it is physiologically relevant to humans, is crucial to get novel therapeutics into the clinic. As demonstrated with IPI-926, there is still the possibility that humans will not respond in a fashion that mirrors the animal model.

I investigated the use of a human anti-$\alpha v\beta 6$ function-blocking antibody 264RAD as a therapeutic agent, to treat pancreatic cancer in xenograft mouse models, used both as a single agent and in combination with gemcitabine, the existing chemotherapeutic drug of choice to treat PDAC in humans. 264RAD has been validated by *in vitro* tests performed both in this study and in an independent study, which reaffirm that 264RAD can block $\alpha v\beta 6$ function in cancer cells specifically [233]. Indeed, the independent study also used the 264RAD antibody as a single agent to target the xenografts of murine breast and human OSCC cell lines 4T1 and Detroit 562 respectively, grown in mice [233]. The study showed a significant inhibition of tumour growth when the animals were treated with 20mg/Kg of the 264RAD antibody compared to a control isotype IgG antibody. The authors of this study also observed a decrease in the number of lung metastases from 4T1 tumours in the animals treated with the 264RAD antibody compared to the controls. Studies performed by a colleague in our laboratory have used 264RAD in combination with Herceptin to treat subcutaneous breast cancer xenograft models, with the combination therapy arm

performing significantly better than the single agent therapy (data not published). These results reaffirmed that αvβ6 is a promising therapeutic target to treat cancer.

Based on the results from the above-mentioned studies, it was decided to test the αvβ6 function-blocking antibody on a xenograft mouse model for PDAC. This study has used 264RAD at 10mg/Kg (half the concentration used in the published literature) or a combination of 264RAD and gemcitabine at 10mg/Kg and 100mg/Kg respectively administered to mice twice a week, intraperitoneally (Figure 105). A gemcitabine single agent therapy arm was also included in the study to compare how effective the αvβ6 function-blocking antibody, as a single agent would be, and also to test if there was any synergistic or additive effect when used in combination with gemcitabine. Since Astra Zeneca – Medimmune provided the 264RAD and control IgG antibody for the purpose of this study; dosage of antibody administered was based on their previous data. However, previously published literature has used gemcitabine at 100mg/Kg to treat mice twice a week, with a significant difference in tumour growth in the treated animals compared to the control [269]. This was used as a reference and the same concentration was given to experimental animals in this study.

5.5.2. Orthotopic mouse model

Two orthotopic models (Figure 87, Figure 88) were generated as part of this study using Panc04.03 and CFPac1 PDAC cell lines. Both cell lines grew successfully *in vivo*, with the CFPac1 model developing both local and distant metastasis (Figure 89). Both the tumour cell lines grown in mice retained expression of β6 *in vivo* as confirmed by IHC (Figure 91). The surrounding stroma and the normal pancreas was negative for αvβ6. In the absence of a genetically engineered mouse model for PDAC for this study, the orthotopic xenograft model was the next most physiologically relevant model to investigate. Although models were generated and tested for expression of αvβ6, it was soon apparent that using them for antibody mediated therapy experiments would not be possible. This was partly due to the limitations in the technology available to measure tumour growth kinetics daily and also due to time and cost restrictions, since orthotopic models took longer to grow and required more mice. Therefore, initially we chose to luciferase tag the tumour cells to allow tumour growth in the mice to be imaged using the IVIS scanner. Unfortunately, further discussion regarding the imaging of orthotopic pancreatic

tumours highlighted problems with this technique; colleagues in the laboratory found that bioluminescence detected by the IVIS was not proportional to tumour growth and thus subtle changes in the tumour size could not accurately be assessed. This was a set back in terms of using these models for further therapy experiments and subsequently a subcutaneous model was generated for therapeutic experiments. While it is accepted that a subcutaneous model for PDAC is not ideal, it does obviate the need for laparotomy and thus, presumably, places less stress and discomfort on the experimental animals.

5.5.3. Subcutaneous mouse model

Although subcutaneous xenograft models are widely used, they often are not considered to be physiologically relevant primarily due to the lack of an appropriate tumour-stroma interaction. A $\alpha v\beta 6$ positive subcutaneous model was generated using the CFPac1 PDAC cell line, (Figure 92). This model was modified by co-injecting human pancreatic stellate cells, PS1, together with the CFPac1 cells in a 2:1 ratio respectively. The hypothesis was that by introducing the stellate cells into the model it would create a relevant tumour-stroma interaction, thereby making the subcutaneous model a closer physiomimetic of pancreatic cancer tissue. Activated pancreatic stellate cells form the major component in the tumour stroma and are known to be important for PDAC progression in humans [84]. The stromal response in PDAC tumours is extremely high, in some cases up to 70%-80% of the tumour is composed of stromal cells. Unpublished data obtained from our laboratory determined that mixing stellate:cancer cells in a 2:1 ratio generated the optimum levels for maximum tumour growth and invasion. Previous studies have co-injected stellate cells with cancer cells orthotopically in a 5:1 ratio and shown that the rate of tumour growth is accelerated by the presence of the stellate cells [84]. Stellate cells have also been shown to induce fibrosis and also stimulate secretion of MMPs including MMP9 [270]. This could be one of the mechanisms used by PDAC tumour cells to promote tumour invasion. As mentioned previously, $\alpha v\beta 6$ has been shown to promote OSCC invasion in an MMP9 dependent manner [125]. I have not looked in my studies whether a similar mechanism might be operative. However, preliminary studies conducted using the pancreatic expression database suggest that MMP11 (stromelysin 3) may be regulated by $\alpha v\beta 6$ in PDAC. This relationship between $\alpha v\beta 6$ and MMP regulation is likely to be a fruitful area to pursue in the future.

5.5.4. Comparison and validation of the two modified models

No previous studies have co-injected pancreatic stellate cells (PS1) with CFPac1 cell line and compared the subcutaneous and orthotopic models. In fact, I found no reports studying CFPac1 cell line *in vivo*. Co-injecting stellate cells with CFPac1 in the modified subcutaneous model invoked a strong desmoplastic response compared with the model with the tumour cells alone as confirmed by H&E staining (Figure 93). The new xenograft model also retained expression of $\alpha v\beta 6$ in the tumour cells and the surrounding stromal cells were completely negative (Figure 96).

Two pathologists confirmed, independently, that the modified subcutaneous tumours were similar to the human disease, but the model still had to be validated against the orthotopic model before being used to carry out any therapy experiments. A modified orthotopic model was generated simultaneously with the subcutaneous model using the same ratio of PS1 and CFPac1 cells and tumours from both models were harvested and stained for collagen deposition. Collagen type I has been shown to be one of the major ECM proteins deposited in the highly desmoplastic PDAC tumours as a result of the presence of the activated pancreatic stellate cells [86]. The presence of PS1 cells dramatically increased expression of collagen compared with tumours lacking PS1 cells. Thus, the addition of PS1 cells replicated the fibrotic phenotype observed in human PDAC. It was also noted that the fibrosis developed was similar in both the orthotopic and subcutaneous models, suggesting that the subcutaneous model faithfully reproduced the orthotopic phenotype (Figure 97).

Poor vasculature is another key feature of PDAC in humans. Unlike most tumours, the blood supply to the PDAC tumours is significantly lower and this could be due to the strong desmoplastic response observed [269]. Recent studies have shown that one of the major reasons for the poor response of PDAC patients to chemotherapeutic agents is the lack of adequate blood supply to the tumour [269]. The same was true in the case of the KPC mouse model where poor vasculature in the tumour meant gemcitabine could not reach the tumours. Hedgehog inhibitor (IPI-926) could temporarily increase blood supply to the tumours by depleting the tumour-associated stromal cells (reducing the desmoplastic reaction) thus enhancing drug delivery to the tumour [269]. Since there was a strong desmoplastic response observed in both the modified orthotopic and subcutaneous models generated, the sections were stained for a mouse blood vessel marker, endomucin. There was a significant decrease in the number of blood vessels in the PS1-containing orthotopic

and subcutaneous models when compared with the cancer cell alone model (Figure 98). Thus, the addition of stellate cells with the cancer cells affected the tumour vasculature similarly in both orthotopic and subcutaneous models. This hypo-angiogenic response could be due to the increased desmoplasia observed as a result of the addition of the stellate cells. Importantly, both subcutaneous and orthotopic models behaved similarly and were comparable to the KPC mouse model and human pancreatic cancer. In conclusion, the co-injection of pancreatic stellate cells generated PDAC xenografts that appeared morphologically similar to human PDAC tumours, regardless of the site of injection. This highlights the importance of pancreatic stellate cells in determining the appearance and growth of PDAC tumours. This model also provides an excellent new system for studying the molecular basis of how pancreatic stellate cells influence matrix deposition and blood vessel density.

Having established a valid new model I was still concerned that the consequence could be a poor response to antibody therapy due to the high desmoplasia and poor blood supply. It was decided to go ahead and provide antibody therapy to the experimental models bearing subcutaneous CFPac1/PS1 tumours. If response was poor then it was planned to consider an approach similar to that adopted by the Tuveson group in Cambridge, UK, to perhaps try and modulate the blood supply to the tumour to enhance drug delivery.

5.6. Antibody mediated αvβ6 therapy of PDAC

Many novel chemotherapeutic agents used to target PDAC, whether on their own or in combination with existing chemo/radiotherapy, have brought about no or at best only a modest, improvement in the overall survival of patients. A list of some of the antibodies or small molecule inhibitors used in clinical trials so far to treat PDAC is shown in Table 18.

Therapeutic agent	Target	Used in combination with gemcitabine	Comments	Reference
Cetuximab (Erbitux®) (monoclonal antibody)	EGFR	No	Phase III trial. No significant difference in survival compared to gemcitabine	Philip, P.A., et al., 2010 (221)
Bevacizumab (Avastin®) (Mono clonal antibody)	VEGF	Yes	Phase III trial. No significant difference in overall survival	Kindler, H.L., et al., 2010 (222)
Tipifarnib (Zarnestra®) (Small molecule inhibitor)	RAS	Yes	Phase III trial. No significant difference in overall survival	Van Cutsem, E, et al., 2004 (292)
Erlotinib (Tarceva®) (Small molecule inhibitor)	EGFR	Yes	Pase III trial. Modest but significant improvement in survival.	Moore, M.J., et al., 2007 (219)

Table 18: Monoclonal antibodies or small molecule inhibitors used in clinical trials to treat PDAC patients as a single agent or in combination with gemcitabine.

A monoclonal antibody targeting αvβ6 (264RAD) used as a single agent or in combination with existing chemotherapy was hypothesised to be a novel therapeutic option for PDAC patients. Validating this in the pre-clinical model was crucial and the modified subcutaneous CFPac1/PS1 xenograft mouse model was used to test this.

The 264RAD single agent therapy arm started to show a significant difference in tumour volume when compared to the IgG control therapy arm from day 10 (Table 17).

It should be noted that the rates of tumour growth in the 264RAD treated tumours were slower and the single agent therapy arm showed a significant reduction in tumour volume during the whole course of the treatment up to day 42 when compared with the control IgG treatment arm (Figure 106). Following the end of treatment, tumour recurrence was observed in all animals treated with 264RAD but at a much slower rate in comparison with the control IgG treatment arm as shown in Figure 106. In fact, by day 56 there were only two animals left in the control IgG treatment arm (Figure 107) either because the tumour volume reached the maximum

allowed Home Office limit or the tumours were starting to ulcerate. This shows that the treatment with 264RAD alone was sufficient to reduce the rate of growth of the tumours thus preventing it from progressing. This effect on reduction in rate of tumour growth was similar to the that observed in previously published data where 264RAD has been used as a single agent at 20mg/Kg to target αvβ6 to prevent the growth and metastasis of 4T1 tumours in an orthotopic xenograft mouse model [233]. This data confirmed that the antibody was reaching the target αvβ6 positive tumour cells and blocking the functional role of αvβ6 in the modified subcutaneous PDAC xenograft model.

The gemcitabine single agent therapy arm also showed a significant effect on tumour volume when compared with the IgG control from day 6 (Table 17). The growth of the tumour was significantly inhibited by gemcitabine; in fact it was better than the 264RAD single agent treatment arm. Tumour volumes continued to fall until the treatment was stopped and tumour recurrence was slower when compared with the 264RAD single agent treatment arm post treatment (Figure 106). This was not entirely surprising because gemcitabine is the best drug available to treat pancreatic cancer and PDAC tumour cells. It should also be noted that when the two single agents are compared, the molar concentration of gemcitabine used was 10 times more than the antibody concentration although its serum half-life is likely to be much shorter.

Combination therapies have been used to treat cancer for many years. ABVD therapy to treat Hodgkin's disease is a combination of four chemotherapeutic drugs given to patients (doxorubicin, bleomycin, vinblastine and darcarbicine) and work best in combination with almost 100% cure rates [271]. Some combination therapies have drugs, which work through different mechanisms sometimes in order to target and kill the cancer cells or sometimes to alleviate symptoms with some regimens showing increased toxicity compared to gemcitabine treatment alone. Gemcitabine is used in combination with fluorouracil as therapy given to PDAC patients has modestly improved the clinical outcome of patients [216]. Very recently, a combination drug regimen consisting of oxaliplatin, irinotecan, fluorouracil and leucovorin (FOLFIRINOX) used in combination with gemcitabine have given a significant improvement in overall survival (11.1 months) compared with gemcitabine treatment alone (6.8 months) in PDAC patients with metastasis [218].

The combination of 264RAD and gemcitabine caused a significant reduction in tumour volume when compared to the IgG control from day 2 (Table 17). It was evident that the combination therapy was working better than either 264RAD or gemcitabine mono therapy showing a significant decrease in tumour volume till day 42. Tumour volumes continued to fall following post treatment and tumour recurrence appeared to be significantly slower than both the single agent treatment arms (Figure 106, Table 17). Even at day 105 (2 months post treatment) the combination therapy arm tumour volumes were still very small and the rate of tumour progression was very slow. The addition of 264RAD antibody with the gemcitabine seems to have made an improvement in the outcome by lowering tumour volumes and greater overall survival, which might be indicative of an additive effect. The tumour volumes in the combination therapy arm were significantly smaller than the single agent therapy arms, 264RAD alone (from day 2) and gemcitabine alone, (from day 15) (Table 17). This was similar to the results observed in the breast cancer study, where the combination therapy arm of 264RAD and Herceptin performed better than either of the single agent therapy arms in a subcutaneous xenograft mouse model (data not published).

Even though the above results are in complete agreement with a number of other previously published data linking $\alpha v\beta 6$ with poor prognosis and cancer progression, it was entirely contradictory to a recent study showing that antibody-mediated blockade of TGFβ (1D11) or $\alpha v\beta 6$ (3G9) promoted pancreatic tumour growth, both in the early and late stages of the disease in a genetically modified mouse model [212]. The researchers behind this report went on to show that blocking $\alpha v\beta 6$ or TGFβ attenuated the tumour suppressor role of TGFβ signalling in the tumours resulting in an increased rate of tumour growth. These experiments studying the role of $\alpha v\beta 6$ blocking antibody (3G9) and TGFβ blocking antibody (1D11) in early stages of cancer, were performed in mice at 5 weeks of age, a point at which the pancreas was relatively normal or at the earliest stage of PanIN formation, where $\alpha v\beta 6$ expression levels were very weak (data not published). Moreover, TGFβ has been shown to be a tumour suppressor in the early stages of cancer before turning into a tumour promoter in the late stages of cancer [272]. Biomarkers that delineate the exact switch from a tumour suppressor to tumour promoter are not available. Yet another strange observation made was the complete lack of effect on the stromal cells when TGFβ function was blocked. TGFβ has been shown to activate fibroblasts into myofibroblasts, which in turn promote cancer [273-275]. The authors specifically

reported that there were no changes in the surrounding stromal cells, immune cells and vasculature as a result of blocking TGFβ function compared with control antibody treatment [212]. *KRAS/p53*$^{lox+}$ mice with *Smad4* deletion where tumours arise from cystic neoplasms rather than from PanINs were used at 9 weeks to repeat the same study in order to show that blocking αvβ6 or TGFβ in "late stages" of PDAC promote pancreatic cancer. The authors also mention that at that age, the animals only develop focal PDAC with large parts of the pancreas still normal. I do not think this is the right model and from a physiological point of view with relevance to the human disease. The experimental design would be similar to starting therapy as soon as the patient develops the earliest form of pancreatic cancer or, from a xenograft model perspective, it would be similar to starting treatment even before the tumours get a chance to develop. It should also be pointed out that none of the mice in either the control or the antibody treated groups developed any metastases. Nevertheless, it is worth taking on board some of the comments made by the authors in terms of the role of αvβ6 in the TGFβ pathway and perhaps performing IHC analyses to check for SMAD4 expression in the 264RAD treated tumours and compare it to the control antibody treated tumours. It might also be worth screening the minority of patients diagnosed at a very early stage of PDAC for *SMAD4* mutations before giving anti-αvβ6 therapy, considering the 50% of patients with *SMAD4* mutations tend to have a poorer prognosis compared to the wild type SMAD4 expressing patients [52].

5.7. IHC analysis of treated tumour samples

The tumours harvested from a pilot experiment, where mice bearing subcutaneous tumours (CFPac1/PS1) were treated with 264RAD αvβ6 function-blocking antibody or control IgG antibody for 27 days, were stained to check for expression levels of αvβ6 (Figure 101). Both 264RAD treated and IgG blocking antibody treated tumours expressed αvβ6 and there was no obvious difference in the levels of expression between these two groups. This was contrary to what was reported in a recent study in an oral SCC model, where bi-weekly treatment with 264RAD seemed to reduce expression levels of αvβ6 in the tumours [233]. This might be due to the fact that the antibody treatment was carried out for a significantly longer time period (>8 weeks) and at double the concentration (20mg/Kg). So there arises the possibility that cells that were expressing αvβ6 failed to proliferate in the 264RAD treated tumours at the

same rate as the IgG control antibody treated tumours, leading to the significant difference in αvβ6 expression levels.

Having observed significant difference in the tumour volumes between the 264RAD treated animals and the control IgG treated animals, it was interesting to determine how this difference in tumour growth was attained. Caspase 3 is at the convergent point of both the intrinsic and extrinsic pathway of apoptosis. Activation of pro-caspase 3 is indicative of apoptosis and IHC staining on the 264RAD treated and control IgG tumour sections revealed a significant increase in levels of activated caspase 3 (Figure 104). This suggests that the tumour cells treated with the αvβ6 blocking antibody 264RAD were dying through apoptosis as compared with the control IgG treated antibody. Although Western blotting on cell lysates from CFPac1 monolayers treated with 264RAD did not show any changes in levels of expression of activated caspase 3, these results were in concordance with the cell cycle analysis carried out, where 264RAD treatment on CFPac1 cells over 7 days led to a significant increase in the sub-G1 population. Increased cell death (apoptosis) also explains the differences in tumour volumes observed in the current experiment compared to the IgG control treated animals (Figure 106).

IHC staining on treated tumour sections showed that there was a significant decrease in proliferation in the αvβ6 function-blocking antibody treated tumours compared to the IgG treated tumours as indicated by Ki67 staining (Figure 103). This meant that the αvβ6 blocking antibody treated tumours were proliferating less and dying more (apoptosis), thereby preventing tumour progression. A similar effect was seen in the recently published literature where tumours treated with 264RAD at 20mg/Kg showed a significant decrease in the levels of Ki67 staining compared to the control IgG treated antibody [233]. Anti-integrin targeted therapies to block cancer cell proliferation have been published previously. Blocking αvβ3 using a specific function-blocking antibody LM609 has been shown to reduce proliferation in breast cancer xenograft mouse models, although human trials using this antibody did not show any significant difference in overall survival [276].

Reducing proliferation and enhancing apoptosis in the αvβ6 positive tumour cells specifically makes αvβ6 an attractive therapeutic target for treatment of PDAC. Results obtained so far clearly indicate that 264RAD could be used as a potential new therapeutic agent to treat PDAC when used in combination with gemcitabine.

Given the strong response observed in the rate of tumour growth as a result of treatment with the 264RAD antibody, it was hypothesised that some of the key signalling pathways could likely be affected as a result of blockade of αvβ6. ERK/MAPK signalling plays an important role in regulating a variety of cellular functions including cell proliferation and survival. ERK can control transcriptional activity of the cell directly or indirectly through multiple pathways. The cytoplasmic tail of the β6 subunit has been shown to bind directly to and activate ERK2 signalling pathway in colon cancer [181]. Phosphorylated ERK is an indicator of activation of the ERK pathway and IHC staining showed a significant difference in the expression levels of phospho ERK between the two treatment groups. 264RAD treated tumours had significantly lower levels of phospho ERK compared to the control IgG antibody treated tumours (Figure 103). Even though there were no significant differences observed in the levels of phospho and total ERK *in vitro*, a distinct and significant difference was observed *in vivo*. This could be due to multiple factors including tumour-stroma interactions or growing cells in a 3D as opposed to plastic environment; an environmental change, which can de-regulate signalling pathways. A similar effect on levels of phospho ERK expression was also reported in a recently published study where breast cancer xenograft models were treated with 264RAD or control IgG antibody [233]. The data obtained could mean that some of the downstream signalling pathways, which are activated as a result of αvβ6 activity in PDAC tumours, were no longer functional, possibly as a result of the blockade of αvβ6 by 264RAD antibody. Thus blocking the function of αvβ6 using an αvβ6 function-blocking antibody, 264RAD, can significantly slow down tumour progression by decreasing proliferation of tumour cells, possibly in an ERK/MAPK pathway dependent manner, and increase caspase dependent apoptosis in the CFPac1/PS1 subcutaneous xenograft mouse model for pancreatic cancer. The results from the pre-clinical model used in this study suggests that αvβ6 is a potential therapeutic target and by using a specific monoclonal antibody, 264RAD, as a potential new therapeutic agent in combination with the existing chemotherapeutic agent, gemcitabine, can be used to treat patients with pancreatic ductal adenocarcinoma.

DISCUSSION

6. Discussion

Pancreatic cancer is often referred to as the “silent killer“ due to the asymptomatic nature of the disease in the early stages and the extremely poor prognosis overall. Early detection of PDAC still remains a major challenge as it contributes to the dismal five-year survival rates. Excluding a small percentage of operable disease, there is no long-term effective chemotherapy. Treatment regimens available to PDAC patients have not changed over the past decade and although gemcitabine in combination with other chemotherapeutic drugs have brought about modest improvement in overall survival, therapeutic options are still limited. Thus any potential therapeutic target to treat PDAC patients is worth pursing. It was with this in mind I investigated the role of integrin αvβ6 in PDAC.

αvβ6 expression in PDAC was tested on two independent cohorts (n=118 and n=147) with 91% of patients positive for αvβ6 at varying levels (median score >1). Although this data is similar to previously reported expression levels of αvβ6 in PDAC, where 100% of cases were positive [201], this high expression level seems typical to PDAC. Published literature to date looking at αvβ6 expression have reported 54% of NSCLC and 58% of cervical cancer patients positive for αvβ6 expression and in about 30%-35% of breast cancer patients (data not published). High αvβ6 expression, comparable to PDAC, was also observed in head & neck cancers, where 80% of patients were positive for αvβ6 [277]. αvβ6 as previously mentioned is an epithelial cell specific integrin and is expressed only by the tumour tissue (e.g. breast, colon, lung, cervix, ovarian, head & neck and pancreas cancers) and is almost entirely absent in normal adult human tissue. There are very few molecules that are expressed almost exclusively in tumour tissue and together with the fact that 91% of PDAC patients are positive for αvβ6, makes it an attractive therapeutic target.

Integrin αvβ6 was hypothesised to be a poor prognostic marker in PDAC patients, consistent with the published literature in other cancers including colon [173], lung (NSCLC) [204], cervical [267], breast (data not published). However, analysis on two independent data sets provided convincing evidence that αvβ6 at the protein level was not a marker for prognosis in PDAC patients although bioinformatics studies revealed that at the mRNA level, αvβ6 was indeed a marker for poor prognosis. This contradictory result was not expected. Interestingly, previous studies conducted on

oral squamous cell carcinoma, another cancer where 80% of patients expressed αvβ6 [277] did not predict any significant prognostic outcome but showed exactly the same contradicting pattern of expression between the mRNA and protein levels. However, unpublished data from our laboratory, which used *in situ* hybridisation technique, showed higher expression of αvβ6 mRNA at the invasive front of oral squamous cell carcinoma compared with the core of the tumours, despite the protein level expression being high in both areas. Thus, while I do not have any data to provide an explanation for the difference observed between αvβ6 protein and mRNA expression in PDAC samples, it could be similar to the OSCC data. All of the tissue studies reported here were conducted on tissue microarrays and there was no way to identify if the sections tested for αvβ6 expression were from the leading invasive front of the tumour. Thus, in order to investigate whether *ITGB6* is also highest at the leading edge of PDAC, potentially offering an explanation for the discrepancy between protein and mRNA analyses, it would be necessary to examine whole sections of PDAC tissues. If resources are made available, this is a possibility worth investigating as a priority to test this hypothesis.

Follow up clinical data was available from both the data sets and further analysis based on expression levels of αvβ6 did not show any significant correlation between αvβ6 and any of the parameters tested in the Beatson data set. However, there was a significant negative correlation with tumour stage (AJCC) in PDAC patients observed in the Verona data set. Significantly higher αvβ6 expression levels were observed in patients with perineural invasion from the same data set. These results have to be interpreted with great care as the same parameters tested in the Beatson data set did not show any correlation. There could be a variety of possible reasons as to why patients from one group showed a correlation and not the other. Patient care, treatment regimens, and time of diagnosis could all play an important factor, while performing follow up analyses. It could also be down to a 'chance probability'' that patients in one data set showed a statistically significant correlation with αvβ6 expression in some of the parameters tested. However, there was a definite trend observed in the Beatson data set, where high αvβ6 expression levels were associated with increased T-stage, grade, lymph node positivity and lymph node ratio, although none of these achieved significance. The ideal situation would be to test αvβ6 expression on a larger cohort of PDAC patients from the same centre with the same follow up treatment and care before carrying out clinical analyses of this nature.

With the need for novel targeted treatments, many therapeutic drugs are currently being tested in pre-clinical models and a further 18 clinical trials are active for pancreatic cancer patients (source: clinicaltrials.gov.uk). Targeting specific molecules using antibodies or small molecule inhibitors to treat cancers has been investigated previously; for example, Trastuzumab (Herceptin) is currently used in the clinic to target the 30% of breast cancer patients that are HER2 positive (Genentech Inc, 2010). Blocking $\alpha v\beta 3$ using an antibody LM609 has been shown to significantly decrease breast cancer tumour growth in xenograft mouse models [276]. Ibritumomab (Zevalin) is currently in trial to treat follicular B cell non-Hodgkin's lymphoma (NCT01578707, Clinical trials.gov, 2012) patients who are unresponsive to rituximab (binds to CD20 antigen) alone. Ibritumomab along with a chelating agent tiuxetan, with radioactive $Indium^{111}$, binds to CD20 antigen present in mature B cells and cancer cells but not in B cells in the bone marrow, thereby killing the cells.

Current treatment options available to PDAC patients are restricted to gemcitabine alone, or a combination of gemcitabine with other chemotherapeutic drugs (e.g. FOLFIRINOX) for patients with locally advanced unresectable metastatic disease [218]. Although FOLFIRINOX together with gemcitabine improves overall survival significantly, it has been shown to increase toxicity in patients thus compromising quality of life. Targeted monoclonal antibody therapies, which can potentially cause less discomfort to patients, to treat PDAC have been trialled as a single agent or in combination with gemcitabine, such as cetuximab (a monoclonal antibody targeting EGFR) [221] and bevacizumab (a monoclonal antibody targeting VEGF) [222], although both failed to show any significant difference in overall survival. Erlotinib, a small molecule inhibitor targeting EGFR, showed a small but significant increase in the overall survival of PDAC patients [219] but is associated with side effects including toxicity due to its non-specific nature. Studies published by colleagues in our laboratory have shown in *in vitro* 3D models, that by modifying the stromal environment by treatment with all trans retinoic acid (ATRA), PDAC tumour growth can be inhibited through modulation of the wnt-β catenin pathway [91]. There is therefore an urgent need to continue developing new therapeutic agents that specifically target tumour cells or the surrounding stromal cells to treat pancreatic cancer patients.

Due to their ability to generate survival, migration, proliferation, invasion and induction of proteases, integrins have generally been associated with the promotion

of tumour growth. The β6 gene (ITGB6) was identified as one of the genes in a "gene signature" essential for survival of lung and pancreatic cancer cell lines that have mutated *KRAS* [207]. Due to its tumour specific expression, αvβ6 makes an ideal imaging target. In fact, it has been used to image breast cancer in a pre-clinical mouse model using a radiolabelled peptide (In^{111}-DTPA-A20FMDV2), specific to αvβ6, using a SPECT/CT scanner [278]. Data showed a 7-10 fold selective retention in αvβ6 expressing tumours versus αvβ6 negative tumours. In a separate study, BxPC3, a moderate to poorly differentiated αvβ6 positive cell line, was used to image αvβ6 in a subcutaneous xenograft model using a radiolabelled peptide (A20FMDV2) specific for αvβ6, [(18F)] FBA-A20FMDV2 [235]. It is possible that radio-imaging αvβ6 in PDAC could potentially be a non-invasive diagnostic tool for screening PDAC in humans. Although it might not become a reality in the near future due to the costs involved, a PET/CT scan with the αvβ6 targeted peptide for people in the age group most susceptible to develop PDAC could be used as a screening programme to try and diagnose pancreatic cancer at an earlier stage (PanIN 2 – PanIN 3) thus, potentially identifying individuals at risk destined to develop PDAC. Another observation worth commenting on but not discussed in this study, due to very limited tissue sample numbers, was the upregulation of expression of αvβ6 as the neoplastic cells progressed from PanIN1 (weak/negative) through to PDAC (strong). Similar observations were also noted in tissue sections obtained from a transgenic mouse model for PDAC.

In vitro analyses were performed on a set of αvβ6 positive and negative cell lines to further understand the functional role of αvβ6 in PDAC. In many other cancers αvβ6 has been shown to be involved with various tumour associated processes including proliferation, migration, invasion and survival [125, 207, 210]. These functional assays were tested on PDAC cell lines using the αvβ6 function blocking antibodies 264RAD and 53A.2 (both monoclonal antibodies). Targeting with these antibodies significantly decreased cell proliferation in a dose dependent manner in both of the αvβ6 positive cell lines tested, Panc04.03 and CFPac1 (Figure 36 and Figure 38). Specifically, further cell cycle analysis revealed a G2/M phase block in the Panc04.03 cell line and an increase in the sub-G1 phase, indicative of apoptosis, in the CFPac1 cell line (Figure 46). Time-lapse video of CFPac1 cells treated with αvβ6 function blocking antibody also confirmed that there were more dying/dead cells in the αvβ6 function blocking antibody treated wells compared to the control antibody treated wells and that the antibody did not cause complete detachment of cells from

the culture dish (data not shown). This suggests that anoikis may not be the primary mechanism of the anti-proliferative effects of the αvβ6 function-blocking antibodies.

In addition, αvβ6 function-blocking antibodies significantly reduced cell migration to fibronectin and LAP over a 16hr time period (Figure 53, Figure 55) and invasion over 72 hours in a panel of αvβ6 positive PDAC cell lines (Figure 57, Figure 58). In order to better understand the mechanism through which blocking αvβ6 brings about functional changes in cellular behaviour, it would be of interest to examine signalling pathways downstream of αvβ6. Very little is known about the pathways that are regulated by αvβ6 *in vitro*. Ahmed et al, have shown that ERK2 binds directly to the cytoplasmic tail of the β6 subunit in colon carcinoma cells [181]. Levels of phospho ERK were monitored in CFPac1 cell line, even though small changes were observed in the levels of ERK phosphorylation at the earlier time points, it was not observed in the later time points. This made the results difficult to interpret and no definite conclusions could be drawn from that experiment.

The PDAC microenvironment is highly fibrotic and αvβ6 could have an indirect role in regulating this through activating the tumour microenvironment via activation of TGFβ. It has been established that, like fibroblasts, TGFβ activates stellate cells into similar myofibroblast like cells. Since the activated stellate cells have been shown to be the principal source of desmoplastic stroma in PDAC, the possibility that αvβ6 could be a source of activated TGFβ must be considered. It would be interesting to monitor TGFβ activity in PDAC cell lines in response to blocking αvβ6 function. This hypothesis could be tested *in vitro* by co-culturing quiescent PS1 cells with αvβ6 positive and negative PDAC cell lines and observe if they become activated or not. It should also be noted that TGFβ can act as both a tumour suppressor and promoter and a recent study has shown that blocking TGFβ or αvβ6 in a murine model of PDAC actually promoted cancer growth. These results are contrary to most published literature linking αvβ6 and cancer. However, further scrutiny of the report brings into question the choice of the animal model used and also the timing when these studies were conducted in the experimental animals as discussed previously (Section 5.5)

Pre-clinical subcutaneous xenograft models were generated and validated against an orthotopic model to ensure that they were morphologically similar prior to performing αvβ6 targeted antibody mediated therapy experiments. Levels of collagen deposition

and tumour vascularity were used as markers to determine if the subcutaneous model could be used as a replacement to the orthotopic model (Figure 97). Unlike most subcutaneous models used for *in vivo* studies, the modified subcutaneous model used in this study had increased levels of collagen deposition that were comparable to those observed in the orthotopic model. The desmoplastic response observed was very similar to the human disease. Pancreatic cancer tumours are known to be hypo-vascularised and analysis of the modified subcutaneous tumours showed significantly lower number of blood vessels compared with the cancer cell alone model. The addition of stellate cells with cancer cells in both the orthotopic and subcutaneous models reduced numbers of blood vessels, suggesting that there is a dynamic interaction between the tumour cells and the stroma and that the increased desmoplasia might be the reason for the poor vasculature, much like in the human disease (Figure 98).

It was extremely encouraging that this modified subcutaneous model was morphologically relevant to the orthotopic model and in limited aspects comparable to the human disease but providing $\alpha v\beta 6$ directed therapy to a hypo-vascularised tumour was always a concern. Using agents to increase blood supply to the tumours might be a potential way to overcome this issue. The Tuveson group has already used IPI-926 (smoothened inhibitor) to target hedgehog signalling in the stromal cells to enhance drug delivery to the PDAC tumour. Although this particular drug was not successful in clinical trials, I feel it is still worth pursuing this and perhaps use other drugs, for example verapamil, which could be used to increase blood supply to the tumour to enhance drug delivery to the PDAC tumour.

This study did not use any agents to enhance blood supply to the tumour. The modified subcutaneous model (CFPac1/PS1) was used to examine the effect of blocking $\alpha v\beta 6$, either alone or in combination with gemcitabine. There was a significant difference in tumour volume when compared with the IgG control arm. This was in line with the recently published data using 264RAD antibody, where tumour growth of Detroit 562 OSCC cancer cell line and growth and metastasis of the 4T1 murine breast cancer cell line was significantly inhibited in an orthotopic xenograft mouse model [233]. However, in the current study, the gemcitabine single therapy arm out performed the 264RAD single therapy arm, though it should be noted that the 264RAD single agent was effective and slowed tumour growth. This could be down to using gemcitabine at 100mg/Kg, 10 times more than the dose of

the antibody at 10mg/Kg, it was perhaps not that surprising that this effect was observed. These data reflected results published on the use of cetuximab in human clinical trials as a single agent to treat PDAC, where gemcitabine out performed cetuximab and no significant difference in overall survival was observed. However the combination of both gemcitabine and 264RAD antibody, significantly inhibited CFPac1 tumour growth in comparison with both the gemcitabine and 264RAD single agent treatment arms, suggesting an additive effect (Figure 106). Tumour burden continued to fall even after 2 months post treatment and results indicate that tumour recurrence in the combination treatment therapy arm is slower compared with either of the single agent therapy arms (Figure 106). It is important to bear in mind that various other monoclonal antibodies (e.g. bevacizumab) used in combination with gemcitabine (5.8 months) have not yielded any significant gain in overall survival in PDAC patients when compared to gemcitabine alone (5.9 months).

Further analysis on tumour sections treated with 264RAD or control IgG antibody revealed that there was a significant up regulation of caspase 3 in the $\alpha v\beta 6$ function-blocking antibody treated tumours compared to the IgG control antibody treated tumours, indicative of cell death through apoptosis (Figure 104) This was in contrast to the regulation of caspase 3 in cell monolayer cultures treated with $\alpha v\beta 6$ function-blocking antibodies. It is possible that activation of caspase 3 is stronger *in vivo*. There was also a significant down regulation of Ki67, a proliferation marker, in the $\alpha v\beta 6$ function-blocking antibody treated tumours compared to the IgG control antibody treated tumours (Figure 103). Staining for phospho ERK revealed that the $\alpha v\beta 6$ function-blocking antibody treated tumours expressed significantly lower levels of phospho ERK compared to the IgG control antibody treated tumours. This was similar to the results reported in a recent study, where a significant reduction in the levels of Ki67 in 264RAD antibody treated Detroit 562 oral SCC tumours was observed compared with controls [233].

These data imply that blocking the function of $\alpha v\beta 6$ with a function-blocking antibody, 264RAD, results in significantly reduced tumour progression both by reducing proliferation of tumour cells in an ERK/MAPK pathway dependent manner and by increasing apoptosis in a caspase dependent manner. These results are extremely promising and it highlights the fact that by blocking $\alpha v\beta 6$ function in combination with existing chemotherapeutic drugs given to PDAC patients, such as gemcitabine, PDAC tumour progression may be inhibited in humans. These data reaffirm that

αvβ6 is a novel therapeutic target and that 264RAD can be used as a novel agent to treat pancreatic adenocarcinoma patients.

Future *in vivo* experiments could be modified to answer several interesting questions that arise as a result of this work.

1) Gemcitabine is a chemotherapeutic drug, which is a cytosine nucleotide analogue. It is non-specific and can kill normal dividing cells in the body too. In comparison with many platinum based drugs, gemcitabine has relatively milder side effects but it can still cause discomfort to patients. With the aim of reducing the doses of gemcitabine given to patients, the doses of gemcitabine administered in the pre-clinical model could be lowered from 100mg/Kg to perhaps 50mg/Kg or even 25mg/Kg when used in combination with 264RAD antibody. This would aim to reduce the off target effects of gemcitabine and study if differences in tumour progression are still observed.

2) A higher concentration of the αvβ6 function-blocking antibody, as used in the published literature [233], would also be worth considering, particularly if an additive effect is observed in the combination therapy treatment arm when combined with gemcitabine. Preliminary *in vitro* assays were performed where CFPac1 cells were treated with varying doses of gemcitabine combined with αvβ6 function blocking antibody at 10μg/ml to test if a decrease in cell proliferation can be observed with lower doses of gemcitabine (data not shown).

3) It is important to use other αvβ6-positive cell lines and possibly an αvβ6 positive cell line with an inducible stable knock down of β6, and compare results to the antibody-mediated therapy experiment. This has to be done in order to confirm that the effect seen by the treatment with αvβ6 function-blocking antibody is reproducible and not an effect observed only in this particular model.

4) Although never tested in this study, gemcitabine resistance is another key problem when it comes to treating patients with PDAC. Most tumours are sensitive to gemcitabine but rapidly acquire resistance to it, reducing treatment options to palliative care. Some patients acquire resistance much faster than others and there are very interesting studies looking at gemcitabine resistance in PDAC patients, even though all patients succumb to the disease regardless of sensitivity to gemcitabine [279, 280]. Bearing this is mind, another option would be to maintain gemcitabine doses at 100mg/Kg but stagger the number of doses over a longer period of time

whilst regularly treating with the αvβ6 function-blocking antibody. This might help overcome the problem of chemo-resistance to gemcitabine in PDAC tumours.

5) Another option is to treat the KPC mouse model for PDAC with the αvβ6 function-blocking antibody and observe if tumour progression can be arrested. β6 null mice were created many years ago and they do not show any apparent phenotypic changes [189]. They have been used to study the effect of radiation on pulmonary fibrosis [281]. KPC mice tumour tissues were stained for αvβ6 expression, both PanIN 3 and PDAC were positive for αvβ6. So another interesting proposition would be to breed β6 null mice with KPC mice with the aim of generating a β6 null KPC mice and compare it with the KPC model to study differences in tumour progression.

So in summary, αvβ6 is essential for growth in the PDAC cell lines tested in this study. αvβ6 plays an important role in regulating PDAC migration and invasion. Targeting αvβ6 using a function-blocking antibody supresses growth of PDAC xenograft tumours and when combined with gemcitabine, significantly improves therapy when compared with gemcitabine treatment alone in the modified subcutaneous xenograft model (CFPac1/PS1) used in this study. Bearing in mind that 91% of PDAC patients express αvβ6 at varying levels, it is hoped that these effects can be translated into humans and provide a significant beneficial effect in terms of quality of life and overall survival in the long run.

References

7. References

1. Hanahan, D. and R.A. Weinberg, *The hallmarks of cancer.* Cell, 2000. **100**(1): p. 57-70.
2. Hanahan, D. and R.A. Weinberg, *Hallmarks of cancer: the next generation.* Cell, 2011. **144**(5): p. 646-74.
3. Apte, M.V. and J.S. Wilson, *The Desmoplastic Reaction in Pancreatic Cancer: An Increasingly Recognised Foe.* Pancreatology, 2007. **7**(4): p. 378-379.
4. Mitjans, F., et al., *An anti-alpha v-integrin antibody that blocks integrin function inhibits the development of a human melanoma in nude mice.* J Cell Sci, 1995. **108 (Pt 8)**: p. 2825-38.
5. Sheppard, D., et al., *Complete amino acid sequence of a novel integrin beta subunit (beta 6) identified in epithelial cells using the polymerase chain reaction.* The Journal of biological chemistry, 1990. **265**(20): p. 11502-7.
6. Forman, D., et al., *Cancer prevalence in the UK: results from the EUROPREVAL study.* Ann Oncol, 2003. **14**(4): p. 648-54.
7. Hidalgo, M., *Pancreatic cancer.* N Engl J Med, 2010. **362**(17): p. 1605-17.
8. ; Available from: http://pathology.jhu.edu/pc/BasicOverview1.php.
9. Gittes, G.K., *Developmental biology of the pancreas: a comprehensive review.* Dev Biol, 2009. **326**(1): p. 4-35.
10. Klimstra, D.S., M.B. Pitman, and R.H. Hruban, *An algorithmic approach to the diagnosis of pancreatic neoplasms.* Arch Pathol Lab Med, 2009. **133**(3): p. 454-64.
11. Murtaugh, L.C. and S.D. Leach, *A case of mistaken identity? Nonductal origins of pancreatic "ductal" cancers.* Cancer Cell, 2007. **11**(3): p. 211-3.
12. Reya, T., et al., *Stem cells, cancer, and cancer stem cells.* Nature, 2001. **414**(6859): p. 105-11.
13. Lee, J.M., et al., *The epithelial-mesenchymal transition: new insights in signaling, development, and disease.* J Cell Biol, 2006. **172**(7): p. 973-81.
14. Li, C., et al., *Identification of pancreatic cancer stem cells.* Cancer Res, 2007. **67**(3): p. 1030-7.
15. Fellous, T.G., et al., *A methodological approach to tracing cell lineage in human epithelial tissues.* Stem Cells, 2009. **27**(6): p. 1410-20.
16. Hermann, P.C., et al., *Distinct populations of cancer stem cells determine tumor growth and metastatic activity in human pancreatic cancer.* Cell Stem Cell, 2007. **1**(3): p. 313-23.
17. Kong, B., et al., *From tissue turnover to the cell of origin for pancreatic cancer.* Nat Rev Gastroenterol Hepatol, 2011. **8**(8): p. 467-72.
18. Hariharan, D., A. Saied, and H.M. Kocher, *Analysis of mortality rates for pancreatic cancer across the world.* HPB (Oxford), 2008. **10**(1): p. 58-62.
19. Ghaneh, P., E. Costello, and J.P. Neoptolemos, *Biology and management of pancreatic cancer.* Gut, 2007. **56**(8): p. 1134-52.
20. Neoptolemos, J.P., et al., *A randomized trial of chemoradiotherapy and chemotherapy after resection of pancreatic cancer.* N Engl J Med, 2004. **350**(12): p. 1200-10.
21. Iodice, S., et al., *Tobacco and the risk of pancreatic cancer: a review and meta-analysis.* Langenbecks Arch Surg, 2008. **393**(4): p. 535-45.
22. Li, D., et al., *Pancreatic cancer.* Lancet, 2004. **363**(9414): p. 1049-57.
23. Hart, A.R., H. Kennedy, and I. Harvey, *Pancreatic cancer: a review of the evidence on causation.* Clin Gastroenterol Hepatol, 2008. **6**(3): p. 275-82.
24. Jiao, L., et al., *Alcohol use and risk of pancreatic cancer: the NIH-AARP Diet and Health Study.* Am J Epidemiol, 2009. **169**(9): p. 1043-51.

25. Chari, S.T., et al., *Probability of pancreatic cancer following diabetes: a population-based study.* Gastroenterology, 2005. **129**(2): p. 504-11.
26. Malka, D., et al., *Risk of pancreatic adenocarcinoma in chronic pancreatitis.* Gut, 2002. **51**(6): p. 849-52.
27. Shi, C., R.H. Hruban, and A.P. Klein, *Familial pancreatic cancer.* Arch Pathol Lab Med, 2009. **133**(3): p. 365-74.
28. Langer, P., et al., *Five years of prospective screening of high-risk individuals from families with familial pancreatic cancer.* Gut, 2009. **58**(10): p. 1410-8.
29. Wang, W., et al., *PancPRO: risk assessment for individuals with a family history of pancreatic cancer.* J Clin Oncol, 2007. **25**(11): p. 1417-22.
30. Maitra, A., et al., *Precursors to invasive pancreatic cancer.* Adv Anat Pathol, 2005. **12**(2): p. 81-91.
31. Hruban, R.H., A. Maitra, and M. Goggins, *Update on pancreatic intraepithelial neoplasia.* Int J Clin Exp Pathol, 2008. **1**(4): p. 306-16.
32. Hruban, R.H. and N.V. Adsay, *Molecular classification of neoplasms of the pancreas.* Hum Pathol, 2009. **40**(5): p. 612-23.
33. Wilentz, R.E., J. Albores-Saavedra, and R.H. Hruban, *Mucinous cystic neoplasms of the pancreas.* Semin Diagn Pathol, 2000. **17**(1): p. 31-42.
34. Hruban, R.H., et al., *Clinical importance of precursor lesions in the pancreas.* J Hepatobiliary Pancreat Surg, 2007. **14**(3): p. 255-63.
35. Maitra, A. and R.H. Hruban, *Pancreatic cancer.* Annu Rev Pathol, 2008. **3**: p. 157-88.
36. Winter, J.M., A. Maitra, and C.J. Yeo, *Genetics and pathology of pancreatic cancer.* HPB (Oxford), 2006. **8**(5): p. 324-36.
37. Wilentz, R.E. and R.H. Hruban, *Pathology of cancer of the pancreas.* Surg Oncol Clin N Am, 1998. **7**(1): p. 43-65.
38. Hansel, D.E., et al., *Expression of neuropilin-1 in high-grade dysplasia, invasive cancer, and metastases of the human gastrointestinal tract.* Am J Surg Pathol, 2004. **28**(3): p. 347-56.
39. Lohr, M., et al., *Frequency of K-ras mutations in pancreatic intraductal neoplasias associated with pancreatic ductal adenocarcinoma and chronic pancreatitis: a meta-analysis.* Neoplasia, 2005. **7**(1): p. 17-23.
40. Lohr, M., et al., *Immortalized bovine pancreatic duct cells become tumorigenic after transfection with mutant k-ras.* Virchows Arch, 2001. **438**(6): p. 581-90.
41. Borras, E., et al., *Clinical pharmacogenomic testing of KRAS, BRAF and EGFR mutations by high resolution melting analysis and ultra-deep pyrosequencing.* BMC Cancer, 2011. **11**: p. 406.
42. Bardeesy, N. and R.A. DePinho, *Pancreatic cancer biology and genetics.* Nat Rev Cancer, 2002. **2**(12): p. 897-909.
43. Hezel, A.F., et al., *Genetics and biology of pancreatic ductal adenocarcinoma.* Genes Dev, 2006. **20**(10): p. 1218-49.
44. Bertwistle, D. and C.J. Sherr, *Regulation of the Arf tumor suppressor in Emicro-Myc transgenic mice: longitudinal study of Myc-induced lymphomagenesis.* Blood, 2007. **109**(2): p. 792-4.
45. Maitra, A., et al., *Multicomponent analysis of the pancreatic adenocarcinoma progression model using a pancreatic intraepithelial neoplasia tissue microarray.* Mod Pathol, 2003. **16**(9): p. 902-12.
46. Serrano, M., et al., *Oncogenic ras provokes premature cell senescence associated with accumulation of p53 and p16INK4a.* Cell, 1997. **88**(5): p. 593-602.
47. Collado, M., et al., *Tumour biology: senescence in premalignant tumours.* Nature, 2005. **436**(7051): p. 642.
48. Scarpa, A., et al., *Pancreatic adenocarcinomas frequently show p53 gene mutations.* Am J Pathol, 1993. **142**(5): p. 1534-43.

49. Morton, J.P., et al., *Mutant p53 drives metastasis and overcomes growth arrest/senescence in pancreatic cancer.* Proc Natl Acad Sci U S A, 2010. **107**(1): p. 246-51.
50. Olive, K.P., et al., *Mutant p53 gain of function in two mouse models of Li-Fraumeni syndrome.* Cell, 2004. **119**(6): p. 847-60.
51. Munger, J.S., et al., *Latent transforming growth factor-beta: structural features and mechanisms of activation.* Kidney international, 1997. **51**(5): p. 1376-82.
52. Liu, F., *SMAD4/DPC4 and pancreatic cancer survival. Commentary re: M. Tascilar et al., The SMAD4 protein and prognosis of pancreatic ductal adenocarcinoma. Clin. Cancer Res., 7: 4115-4121, 2001.* Clin Cancer Res, 2001. **7**(12): p. 3853-6.
53. Massague, J., S.W. Blain, and R.S. Lo, *TGFbeta signaling in growth control, cancer, and heritable disorders.* Cell, 2000. **103**(2): p. 295-309.
54. Duda, D.G., et al., *Restoration of SMAD4 by gene therapy reverses the invasive phenotype in pancreatic adenocarcinoma cells.* Oncogene, 2003. **22**(44): p. 6857-64.
55. Hruban, R.H., et al., *Emerging molecular biology of pancreatic cancer.* Gastrointest Cancer Res, 2008. **2**(4 Suppl): p. S10-5.
56. Morris, J.P.t., S.C. Wang, and M. Hebrok, *KRAS, Hedgehog, Wnt and the twisted developmental biology of pancreatic ductal adenocarcinoma.* Nat Rev Cancer, 2010. **10**(10): p. 683-95.
57. Cunha, G.R., et al., *Role of the stromal microenvironment in carcinogenesis of the prostate.* Int J Cancer, 2003. **107**(1): p. 1-10.
58. Ohtani, H., *Stromal reaction in cancer tissue: pathophysiologic significance of the expression of matrix-degrading enzymes in relation to matrix turnover and immune/inflammatory reactions.* Pathol Int, 1998. **48**(1): p. 1-9.
59. Froeling, F.E., J.F. Marshall, and H.M. Kocher, *Pancreatic cancer organotypic cultures.* J Biotechnol, 2010. **148**(1): p. 16-23.
60. Mollenhauer, J., I. Roether, and H.F. Kern, *Distribution of extracellular matrix proteins in pancreatic ductal adenocarcinoma and its influence on tumor cell proliferation in vitro.* Pancreas, 1987. **2**(1): p. 14-24.
61. Imamura, T., et al., *Quantitative analysis of collagen and collagen subtypes I, III, and V in human pancreatic cancer, tumor-associated chronic pancreatitis, and alcoholic chronic pancreatitis.* Pancreas, 1995. **11**(4): p. 357-64.
62. Schafer, M. and S. Werner, *Cancer as an overhealing wound: an old hypothesis revisited.* Nat Rev Mol Cell Biol, 2008. **9**(8): p. 628-38.
63. Mueller, M.M., T. Werbowetski, and R.F. Del Maestro, *Soluble factors involved in glioma invasion.* Acta Neurochir (Wien), 2003. **145**(11): p. 999-1008.
64. Bergers, G. and L.E. Benjamin, *Tumorigenesis and the angiogenic switch.* Nat Rev Cancer, 2003. **3**(6): p. 401-10.
65. Paget, S., *The distribution of secondary growths in cancer of the breast. 1889.* Cancer Metastasis Rev, 1989. **8**(2): p. 98-101.
66. Fidler, I.J., *The pathogenesis of cancer metastasis: the 'seed and soil' hypothesis revisited.* Nat Rev Cancer, 2003. **3**(6): p. 453-8.
67. Tlsty, T.D. and P.W. Hein, *Know thy neighbor: stromal cells can contribute oncogenic signals.* Curr Opin Genet Dev, 2001. **11**(1): p. 54-9.
68. Beacham, D.A. and E. Cukierman, *Stromagenesis: the changing face of fibroblastic microenvironments during tumor progression.* Semin Cancer Biol, 2005. **15**(5): p. 329-41.
69. Mueller, M.M. and N.E. Fusenig, *Friends or foes - bipolar effects of the tumour stroma in cancer.* Nat Rev Cancer, 2004. **4**(11): p. 839-49.
70. Bhowmick, N.A., E.G. Neilson, and H.L. Moses, *Stromal fibroblasts in cancer initiation and progression.* Nature, 2004. **432**(7015): p. 332-7.

71. Lohr, M., et al., *Transforming growth factor-beta1 induces desmoplasia in an experimental model of human pancreatic carcinoma.* Cancer Res, 2001. **61**(2): p. 550-5.
72. Bhowmick, N.A., et al., *TGF-beta signaling in fibroblasts modulates the oncogenic potential of adjacent epithelia.* Science, 2004. **303**(5659): p. 848-51.
73. Shao, Z.M., M. Nguyen, and S.H. Barsky, *Human breast carcinoma desmoplasia is PDGF initiated.* Oncogene, 2000. **19**(38): p. 4337-45.
74. Ohuchida, K., et al., *Radiation to stromal fibroblasts increases invasiveness of pancreatic cancer cells through tumor-stromal interactions.* Cancer Res, 2004. **64**(9): p. 3215-22.
75. Watari, N., Y. Hotta, and Y. Mabuchi, *Morphological studies on a vitamin A-storing cell and its complex with macrophage observed in mouse pancreatic tissues following excess vitamin A administration.* Okajimas Folia Anat Jpn, 1982. **58**(4-6): p. 837-58.
76. Ikejiri, N., *The vitamin A-storing cells in the human and rat pancreas.* Kurume Med J, 1990. **37**(2): p. 67-81.
77. Apte, M.V., et al., *Periacinar stellate shaped cells in rat pancreas: identification, isolation, and culture.* Gut, 1998. **43**(1): p. 128-33.
78. Bachem, M.G., et al., *Identification, culture, and characterization of pancreatic stellate cells in rats and humans.* Gastroenterology, 1998. **115**(2): p. 421-32.
79. Buchholz, M., et al., *Transcriptome analysis of human hepatic and pancreatic stellate cells: organ-specific variations of a common transcriptional phenotype.* J Mol Med, 2005. **83**(10): p. 795-805.
80. Zhao, L. and A.D. Burt, *The diffuse stellate cell system.* J Mol Histol, 2007. **38**(1): p. 53-64.
81. Omary, M.B., et al., *The pancreatic stellate cell: a star on the rise in pancreatic diseases.* J Clin Invest, 2007. **117**(1): p. 50-9.
82. Bachem, M.G., et al., *Pancreatic carcinoma cells induce fibrosis by stimulating proliferation and matrix synthesis of stellate cells.* Gastroenterology, 2005. **128**(4): p. 907-21.
83. Hwang, R.F., et al., *Cancer-associated stromal fibroblasts promote pancreatic tumor progression.* Cancer Res, 2008. **68**(3): p. 918-26.
84. Vonlaufen, A., et al., *Pancreatic stellate cells: partners in crime with pancreatic cancer cells.* Cancer Res, 2008. **68**(7): p. 2085-93.
85. Bachem, M.G., et al., *Role of stellate cells in pancreatic fibrogenesis associated with acute and chronic pancreatitis.* J Gastroenterol Hepatol, 2006. **21 Suppl 3**: p. S92-6.
86. Apte, M.V., et al., *Desmoplastic reaction in pancreatic cancer: role of pancreatic stellate cells.* Pancreas, 2004. **29**(3): p. 179-87.
87. Phillips, P.A., et al., *Cell migration: a novel aspect of pancreatic stellate cell biology.* Gut, 2003. **52**(5): p. 677-82.
88. Ohnishi, N., et al., *Activin A is an autocrine activator of rat pancreatic stellate cells: potential therapeutic role of follistatin for pancreatic fibrosis.* Gut, 2003. **52**(10): p. 1487-93.
89. Masamune, A. and T. Shimosegawa, *Signal transduction in pancreatic stellate cells.* J Gastroenterol, 2009. **44**(4): p. 249-60.
90. Nystrom, M.L., et al., *Development of a quantitative method to analyse tumour cell invasion in organotypic culture.* J Pathol, 2005. **205**(4): p. 468-75.
91. Froeling, F.E., et al., *Retinoic acid-induced pancreatic stellate cell quiescence reduces paracrine Wnt-beta-catenin signaling to slow tumor progression.* Gastroenterology, 2011. **141**(4): p. 1486-97, 1497 e1-14.
92. Cespedes, M.V., et al., *Mouse models in oncogenesis and cancer therapy.* Clin Transl Oncol, 2006. **8**(5): p. 318-29.

93. Olive, K.P. and D.A. Tuveson, *The use of targeted mouse models for preclinical testing of novel cancer therapeutics.* Clin Cancer Res, 2006. **12**(18): p. 5277-87.
94. Cano, D.A., M. Hebrok, and M. Zenker, *Pancreatic development and disease.* Gastroenterology, 2007. **132**(2): p. 745-62.
95. Offield, M.F., et al., *PDX-1 is required for pancreatic outgrowth and differentiation of the rostral duodenum.* Development, 1996. **122**(3): p. 983-95.
96. Rajewsky, K., et al., *Conditional gene targeting.* J Clin Invest, 1996. **98**(3): p. 600-3.
97. Nagy, A., *Cre recombinase: the universal reagent for genome tailoring.* Genesis, 2000. **26**(2): p. 99-109.
98. Hingorani, S.R., et al., *Preinvasive and invasive ductal pancreatic cancer and its early detection in the mouse.* Cancer Cell, 2003. **4**(6): p. 437-50.
99. Aguirre, A.J., et al., *Activated Kras and Ink4a/Arf deficiency cooperate to produce metastatic pancreatic ductal adenocarcinoma.* Genes Dev, 2003. **17**(24): p. 3112-26.
100. Hingorani, S.R., et al., *Trp53R172H and KrasG12D cooperate to promote chromosomal instability and widely metastatic pancreatic ductal adenocarcinoma in mice.* Cancer Cell, 2005. **7**(5): p. 469-83.
101. Bardeesy, N., et al., *Both p16(Ink4a) and the p19(Arf)-p53 pathway constrain progression of pancreatic adenocarcinoma in the mouse.* Proc Natl Acad Sci U S A, 2006. **103**(15): p. 5947-52.
102. Tamkun, J.W., et al., *Structure of integrin, a glycoprotein involved in the transmembrane linkage between fibronectin and actin.* Cell, 1986. **46**(2): p. 271-82.
103. Hynes, R.O., *Integrins: bidirectional, allosteric signaling machines.* Cell, 2002. **110**(6): p. 673-87.
104. de Melker, A.A. and A. Sonnenberg, *Integrins: alternative splicing as a mechanism to regulate ligand binding and integrin signaling events.* BioEssays : news and reviews in molecular, cellular and developmental biology, 1999. **21**(6): p. 499-509.
105. Ruoslahti, E., *RGD and other recognition sequences for integrins.* Annual review of cell and developmental biology, 1996. **12**: p. 697-715.
106. Oldak, M., S. Smola-Hess, and R. Maksym, *Integrin beta4, keratinocytes and papillomavirus infection.* Int J Mol Med, 2006. **17**(2): p. 195-202.
107. Humphries, M.J., et al., *Integrin structure: heady advances in ligand binding, but activation still makes the knees wobble.* Trends Biochem Sci, 2003. **28**(6): p. 313-20.
108. Plow, E.F., et al., *Ligand binding to integrins.* The Journal of biological chemistry, 2000. **275**(29): p. 21785-8.
109. Xiong, J.P., et al., *Crystal structure of the extracellular segment of integrin alpha Vbeta3.* Science, 2001. **294**(5541): p. 339-45.
110. Takagi, J. and T.A. Springer, *Integrin activation and structural rearrangement.* Immunol Rev, 2002. **186**: p. 141-63.
111. Ylanne, J., et al., *Distinct functions of integrin alpha and beta subunit cytoplasmic domains in cell spreading and formation of focal adhesions.* J Cell Biol, 1993. **122**(1): p. 223-33.
112. Reszka, A.A., Y. Hayashi, and A.F. Horwitz, *Identification of amino acid sequences in the integrin beta 1 cytoplasmic domain implicated in cytoskeletal association.* J Cell Biol, 1992. **117**(6): p. 1321-30.
113. Otey, C.A., F.M. Pavalko, and K. Burridge, *An interaction between alpha-actinin and the beta 1 integrin subunit in vitro.* J Cell Biol, 1990. **111**(2): p. 721-9.

114. Coppolino, M., et al., *Inducible interaction of integrin alpha 2 beta 1 with calreticulin. Dependence on the activation state of the integrin.* The Journal of biological chemistry, 1995. **270**(39): p. 23132-8.
115. Michalak, M., et al., *Calreticulin.* Biochem J, 1992. **285 (Pt 3)**: p. 681-92.
116. Guo, W. and F.G. Giancotti, *Integrin signalling during tumour progression.* Nature reviews. Molecular cell biology, 2004. **5**(10): p. 816-26.
117. Pierschbacher, M.D. and E. Ruoslahti, *Cell attachment activity of fibronectin can be duplicated by small synthetic fragments of the molecule.* Nature, 1984. **309**(5963): p. 30-3.
118. Yamada, K.M., *Adhesive recognition sequences.* J Biol Chem, 1991. **266**(20): p. 12809-12.
119. Kilshaw, P.J., *Alpha E beta 7.* Mol Pathol, 1999. **52**(4): p. 203-7.
120. Spring, F.A., et al., *Intercellular adhesion molecule-4 binds alpha(4)beta(1) and alpha(V)-family integrins through novel integrin-binding mechanisms.* Blood, 2001. **98**(2): p. 458-66.
121. Miller, L.C., et al., *Role of the cytoplasmic domain of the beta-subunit of integrin alpha(v)beta6 in infection by foot-and-mouth disease virus.* J Virol, 2001. **75**(9): p. 4158-64.
122. Annes, J.P., D.B. Rifkin, and J.S. Munger, *The integrin alphaVbeta6 binds and activates latent TGFbeta3.* FEBS letters, 2002. **511**(1-3): p. 65-8.
123. Weinacker, A., et al., *Role of the integrin alpha v beta 6 in cell attachment to fibronectin. Heterologous expression of intact and secreted forms of the receptor.* J Biol Chem, 1994. **269**(9): p. 6940-8.
124. DiCara, D., et al., *Structure-function analysis of Arg-Gly-Asp helix motifs in alpha v beta 6 integrin ligands.* J Biol Chem, 2007. **282**(13): p. 9657-65.
125. Thomas, G.J., et al., *AlphaVbeta6 integrin promotes invasion of squamous carcinoma cells through up-regulation of matrix metalloproteinase-9.* Int J Cancer, 2001. **92**(5): p. 641-50.
126. Staatz, W.D., et al., *Identification of a tetrapeptide recognition sequence for the alpha 2 beta 1 integrin in collagen.* J Biol Chem, 1991. **266**(12): p. 7363-7.
127. Kuijpers, T.W., et al., *Freezing adhesion molecules in a state of high-avidity binding blocks eosinophil migration.* The Journal of experimental medicine, 1993. **178**(1): p. 279-84.
128. Takagi, J., et al., *Global conformational rearrangements in integrin extracellular domains in outside-in and inside-out signaling.* Cell, 2002. **110**(5): p. 599-11.
129. Frelinger, A.L., 3rd, et al., *Occupancy of an adhesive glycoprotein receptor modulates expression of an antigenic site involved in cell adhesion.* The Journal of biological chemistry, 1988. **263**(25): p. 12397-402.
130. Humphries, J.D., et al., *Dual functionality of the anti-beta1 integrin antibody, 12G10, exemplifies agonistic signalling from the ligand binding pocket of integrin adhesion receptors.* J Biol Chem, 2005. **280**(11): p. 10234-43.
131. Phillips, D.R., et al., *The platelet membrane glycoprotein IIb-IIIa complex.* Blood, 1988. **71**(4): p. 831-43.
132. Lampugnani, M.G., et al., *Role of manganese in MG-63 osteosarcoma cell attachment to fibrinogen and von Willebrand factor.* Lab Invest, 1991. **65**(1): p. 96-103.
133. Wilkins, J.A., et al., *Beta 1 integrin-mediated lymphocyte adherence to extracellular matrix is enhanced by phorbol ester treatment.* Eur J Immunol, 1991. **21**(2): p. 517-22.
134. Priddle, H., et al., *Disruption of the talin gene compromises focal adhesion assembly in undifferentiated but not differentiated embryonic stem cells.* J Cell Biol, 1998. **142**(4): p. 1121-33.

135. Martel, V., et al., *Conformation, localization, and integrin binding of talin depend on its interaction with phosphoinositides.* J Biol Chem, 2001. **276**(24): p. 21217-27.
136. Ruoslahti, E. and J.C. Reed, *Anchorage dependence, integrins, and apoptosis.* Cell, 1994. **77**(4): p. 477-8.
137. Frisch, S.M. and H. Francis, *Disruption of epithelial cell-matrix interactions induces apoptosis.* The Journal of cell biology, 1994. **124**(4): p. 619-26.
138. Tilghman, R.W., et al., *Focal adhesion kinase is required for the spatial organization of the leading edge in migrating cells.* J Cell Sci, 2005. **118**(Pt 12): p. 2613-23.
139. Cluzel, C., et al., *The mechanisms and dynamics of (alpha)v(beta)3 integrin clustering in living cells.* J Cell Biol, 2005. **171**(2): p. 383-92.
140. Trusolino, L., A. Bertotti, and P.M. Comoglio, *A signaling adapter function for alpha6beta4 integrin in the control of HGF-dependent invasive growth.* Cell, 2001. **107**(5): p. 643-54.
141. Liddington, R.C. and L.A. Bankston, *The structural basis of dynamic cell adhesion: heads, tails, and allostery.* Experimental cell research, 2000. **261**(1): p. 37-43.
142. Stewart, M. and N. Hogg, *Regulation of leukocyte integrin function: affinity vs. avidity.* Journal of cellular biochemistry, 1996. **61**(4): p. 554-61.
143. Hood, J.D. and D.A. Cheresh, *Role of integrins in cell invasion and migration.* Nat Rev Cancer, 2002. **2**(2): p. 91-100.
144. Shimaoka, M., J. Takagi, and T.A. Springer, *Conformational regulation of integrin structure and function.* Annual review of biophysics and biomolecular structure, 2002. **31**: p. 485-516.
145. Hughes, P.E., et al., *Suppression of integrin activation: a novel function of a Ras/Raf-initiated MAP kinase pathway.* Cell, 1997. **88**(4): p. 521-30.
146. O'Toole, T.E., et al., *Integrin cytoplasmic domains mediate inside-out signal transduction.* J Cell Biol, 1994. **124**(6): p. 1047-59.
147. Howe, A., et al., *Integrin signaling and cell growth control.* Current opinion in cell biology, 1998. **10**(2): p. 220-31.
148. Falcioni, R., et al., *Alpha 6 beta 4 and alpha 6 beta 1 integrins associate with ErbB-2 in human carcinoma cell lines.* Exp Cell Res, 1997. **236**(1): p. 76-85.
149. Schlaepfer, D.D., et al., *Integrin-mediated signal transduction linked to Ras pathway by GRB2 binding to focal adhesion kinase.* Nature, 1994. **372**(6508): p. 786-91.
150. Schlaepfer, D.D. and T. Hunter, *Focal adhesion kinase overexpression enhances ras-dependent integrin signaling to ERK2/mitogen-activated protein kinase through interactions with and activation of c-Src.* J Biol Chem, 1997. **272**(20): p. 13189-95.
151. Zhang, W., et al., *E-cadherin loss promotes the initiation of squamous cell carcinoma invasion through modulation of integrin-mediated adhesion.* J Cell Sci, 2006. **119**(Pt 2): p. 283-91.
152. Bergmeier, W. and R.O. Hynes, *Extracellular matrix proteins in hemostasis and thrombosis.* Cold Spring Harb Perspect Biol, 2012. **4**(2).
153. Klemke, M., et al., *High affinity interaction of integrin alpha4beta1 (VLA-4) and vascular cell adhesion molecule 1 (VCAM-1) enhances migration of human melanoma cells across activated endothelial cell layers.* J Cell Physiol, 2007. **212**(2): p. 368-74.
154. Ma, Z., et al., *p66Shc mediates anoikis through RhoA.* J Cell Biol, 2007. **179**(1): p. 23-31.
155. Vachon, P.H., *Integrin signaling, cell survival, and anoikis: distinctions, differences, and differentiation.* J Signal Transduct, 2011. **2011**: p. 738137.
156. Martin, S.S. and K. Vuori, *Regulation of Bcl-2 proteins during anoikis and amorphosis.* Biochim Biophys Acta, 2004. **1692**(2-3): p. 145-57.

157. Janes, S.M. and F.M. Watt, *Switch from alphavbeta5 to alphavbeta6 integrin expression protects squamous cell carcinomas from anoikis.* J Cell Biol, 2004. **166**(3): p. 419-31.
158. Stoker, M., et al., *Anchorage and growth regulation in normal and virus-transformed cells.* Int J Cancer, 1968. **3**(5): p. 683-93.
159. Roovers, K., et al., *Alpha5beta1 integrin controls cyclin D1 expression by sustaining mitogen-activated protein kinase activity in growth factor-treated cells.* Mol Biol Cell, 1999. **10**(10): p. 3197-204.
160. del Pozo, M.A., et al., *Adhesion to the extracellular matrix regulates the coupling of the small GTPase Rac to its effector PAK.* EMBO J, 2000. **19**(9): p. 2008-14.
161. Khwaja, A., et al., *Matrix adhesion and Ras transformation both activate a phosphoinositide 3-OH kinase and protein kinase B/Akt cellular survival pathway.* EMBO J, 1997. **16**(10): p. 2783-93.
162. Schwartz, M.A. and R.K. Assoian, *Integrins and cell proliferation: regulation of cyclin-dependent kinases via cytoplasmic signaling pathways.* J Cell Sci, 2001. **114**(Pt 14): p. 2553-60.
163. Hall, A., *Rho GTPases and the actin cytoskeleton.* Science, 1998. **279**(5350): p. 509-14.
164. van Leeuwen, R.L., et al., *Attachment, spreading and migration of melanoma cells on vitronectin. The role of alpha V beta 3 and alpha V beta 5 integrins.* Exp Dermatol, 1996. **5**(6): p. 308-15.
165. Potter, D.A., et al., *Calpain regulates actin remodeling during cell spreading.* J Cell Biol, 1998. **141**(3): p. 647-62.
166. Parri, M. and P. Chiarugi, *Rac and Rho GTPases in cancer cell motility control.* Cell Commun Signal, 2010. **8**: p. 23.
167. Yurchenco, P.D., P.S. Amenta, and B.L. Patton, *Basement membrane assembly, stability and activities observed through a developmental lens.* Matrix Biol, 2004. **22**(7): p. 521-38.
168. Liotta, L.A., et al., *Metastatic potential correlates with enzymatic degradation of basement membrane collagen.* Nature, 1980. **284**(5751): p. 67-8.
169. Klein, C.E., et al., *Integrin alpha 2 beta 1 is upregulated in fibroblasts and highly aggressive melanoma cells in three-dimensional collagen lattices and mediates the reorganization of collagen I fibrils.* J Cell Biol, 1991. **115**(5): p. 1427-36.
170. Bonkhoff, H., U. Stein, and K. Remberger, *Differential expression of alpha 6 and alpha 2 very late antigen integrins in the normal, hyperplastic, and neoplastic prostate: simultaneous demonstration of cell surface receptors and their extracellular ligands.* Hum Pathol, 1993. **24**(3): p. 243-8.
171. Matsuoka, T., et al., *Increased expression of alpha2beta1-integrin in the peritoneal dissemination of human gastric carcinoma.* Int J Mol Med, 2000. **5**(1): p. 21-5.
172. Zutter, M.M., G. Mazoujian, and S.A. Santoro, *Decreased expression of integrin adhesive protein receptors in adenocarcinoma of the breast.* Am J Pathol, 1990. **137**(4): p. 863-70.
173. Bates, R.C., et al., *Transcriptional activation of integrin beta6 during the epithelial-mesenchymal transition defines a novel prognostic indicator of aggressive colon carcinoma.* J Clin Invest, 2005. **115**(2): p. 339-47.
174. Seftor, R.E., et al., *Role of the alpha v beta 3 integrin in human melanoma cell invasion.* Proc Natl Acad Sci U S A, 1992. **89**(5): p. 1557-61.
175. Breuss, J.M., et al., *Expression of the beta 6 integrin subunit in development, neoplasia and tissue repair suggests a role in epithelial remodeling.* J Cell Sci, 1995. **108 (Pt 6)**: p. 2241-51.

176. Busk, M., R. Pytela, and D. Sheppard, *Characterization of the integrin alpha v beta 6 as a fibronectin-binding protein.* The Journal of biological chemistry, 1992. **267**(9): p. 5790-6.
177. Hynes, R.O., *Integrins: versatility, modulation, and signaling in cell adhesion.* Cell, 1992. **69**(1): p. 11-25.
178. Scott, K.A., et al., *TNF-alpha regulates epithelial expression of MMP-9 and integrin alphavbeta6 during tumour promotion. A role for TNF-alpha in keratinocyte migration?* Oncogene, 2004. **23**(41): p. 6954-66.
179. Bates, R.C. and A.M. Mercurio, *Tumor necrosis factor-alpha stimulates the epithelial-to-mesenchymal transition of human colonic organoids.* Molecular biology of the cell, 2003. **14**(5): p. 1790-800.
180. Jackson, T., et al., *Integrin alphavbeta8 functions as a receptor for foot-and-mouth disease virus: role of the beta-chain cytodomain in integrin-mediated infection.* Journal of virology, 2004. **78**(9): p. 4533-40.
181. Ahmed, N., et al., *Direct integrin alphavbeta6-ERK binding: implications for tumour growth.* Oncogene, 2002. **21**(9): p. 1370-80.
182. Giancotti, F.G. and E. Ruoslahti, *Integrin signaling.* Science, 1999. **285**(5430): p. 1028-32.
183. Gu, X., et al., *Integrin alpha(v)beta6-associated ERK2 mediates MMP-9 secretion in colon cancer cells.* Br J Cancer, 2002. **87**(3): p. 348-51.
184. Playford, M.P. and M.D. Schaller, *The interplay between Src and integrins in normal and tumor biology.* Oncogene, 2004. **23**(48): p. 7928-46.
185. Li, X., et al., *Alphavbeta6-Fyn signaling promotes oral cancer progression.* J Biol Chem, 2003. **278**(43): p. 41646-53.
186. Wary, K.K., et al., *A requirement for caveolin-1 and associated kinase Fyn in integrin signaling and anchorage-dependent cell growth.* Cell, 1998. **94**(5): p. 625-34.
187. Akhurst, R.J. and R. Derynck, *TGF-beta signaling in cancer--a double-edged sword.* Trends Cell Biol, 2001. **11**(11): p. S44-51.
188. Moustakas, A., et al., *Mechanisms of TGF-beta signaling in regulation of cell growth and differentiation.* Immunol Lett, 2002. **82**(1-2): p. 85-91.
189. Munger, J.S., et al., *The integrin alpha v beta 6 binds and activates latent TGF beta 1: a mechanism for regulating pulmonary inflammation and fibrosis.* Cell, 1999. **96**(3): p. 319-28.
190. Agrez, M., et al., *The alpha v beta 6 integrin promotes proliferation of colon carcinoma cells through a unique region of the beta 6 cytoplasmic domain.* J Cell Biol, 1994. **127**(2): p. 547-56.
191. Bierie, B., et al., *Transforming growth factor-beta regulates mammary carcinoma cell survival and interaction with the adjacent microenvironment.* Cancer Res, 2008. **68**(6): p. 1809-19.
192. Mao, J.H., et al., *Genetic variants of Tgfb1 act as context-dependent modifiers of mouse skin tumor susceptibility.* Proc Natl Acad Sci U S A, 2006. **103**(21): p. 8125-30.
193. Derynck, R., R.J. Akhurst, and A. Balmain, *TGF-beta signaling in tumor suppression and cancer progression.* Nat Genet, 2001. **29**(2): p. 117-29.
194. Massague, J., *A very private TGF-beta receptor embrace.* Mol Cell, 2008. **29**(2): p. 149-50.
195. Flavell, R.A., et al., *The polarization of immune cells in the tumour environment by TGFbeta.* Nat Rev Immunol, 2010. **10**(8): p. 554-67.
196. Thomas, G.J., M.L. Nystrom, and J.F. Marshall, *Alphavbeta6 integrin in wound healing and cancer of the oral cavity.* J Oral Pathol Med, 2006. **35**(1): p. 1-10.
197. Walker, R.A. and S.J. Dearing, *Transforming growth factor beta 1 in ductal carcinoma in situ and invasive carcinomas of the breast.* Eur J Cancer, 1992. **28**(2-3): p. 641-4.

198. Haapasalmi, K., et al., *Keratinocytes in human wounds express alpha v beta 6 integrin.* J Invest Dermatol, 1996. **106**(1): p. 42-8.
199. Clark, R.A., et al., *Re-epithelialization of normal human excisional wounds is associated with a switch from alpha v beta 5 to alpha v beta 6 integrins.* Br J Dermatol, 1996. **135**(1): p. 46-51.
200. Dvorak, H.F., *Tumors: wounds that do not heal. Similarities between tumor stroma generation and wound healing.* N Engl J Med, 1986. **315**(26): p. 1650-9.
201. Sipos, B., et al., *Immunohistochemical screening for beta6-integrin subunit expression in adenocarcinomas using a novel monoclonal antibody reveals strong up-regulation in pancreatic ductal adenocarcinomas in vivo and in vitro.* Histopathology, 2004. **45**(3): p. 226-36.
202. Jones, J., F.M. Watt, and P.M. Speight, *Changes in the expression of alpha v integrins in oral squamous cell carcinomas.* J Oral Pathol Med, 1997. **26**(2): p. 63-8.
203. Van Aarsen, L.A., et al., *Antibody-mediated blockade of integrin alpha v beta 6 inhibits tumor progression in vivo by a transforming growth factor-beta-regulated mechanism.* Cancer Res, 2008. **68**(2): p. 561-70.
204. Elayadi, A.N., et al., *A peptide selected by biopanning identifies the integrin alphavbeta6 as a prognostic biomarker for nonsmall cell lung cancer.* Cancer Res, 2007. **67**(12): p. 5889-95.
205. Kawashima, A., et al., *Expression of alphav integrin family in gastric carcinomas: increased alphavbeta6 is associated with lymph node metastasis.* Pathol Res Pract, 2003. **199**(2): p. 57-64.
206. Berry, M.G., et al., *Integrin beta1-mediated invasion of human breast cancer cells: an ex vivo assay for invasiveness.* Breast Cancer, 2003. **10**(3): p. 214-9.
207. Singh, A., et al., *A gene expression signature associated with "K-Ras addiction" reveals regulators of EMT and tumor cell survival.* Cancer Cell, 2009. **15**(6): p. 489-500.
208. Huang, X., et al., *The integrin alphavbeta6 is critical for keratinocyte migration on both its known ligand, fibronectin, and on vitronectin.* Journal of cell science, 1998. **111 (Pt 15)**: p. 2189-95.
209. Thomas, G.J., et al., *Expression of the alphavbeta6 integrin promotes migration and invasion in squamous carcinoma cells.* J Invest Dermatol, 2001. **117**(1): p. 67-73.
210. Thomas, G.J., et al., *alpha v beta 6 Integrin upregulates matrix metalloproteinase 9 and promotes migration of normal oral keratinocytes.* J Invest Dermatol, 2001. **116**(6): p. 898-904.
211. Hahm, K., et al., *Alphav beta6 integrin regulates renal fibrosis and inflammation in Alport mouse.* Am J Pathol, 2007. **170**(1): p. 110-25.
212. Hezel, A.F., et al., *TGF-beta and alphavbeta6 Integrin Act in a Common Pathway to Suppress Pancreatic Cancer Progression.* Cancer Res, 2012. **72**(18): p. 4840-5.
213. Ijichi, H., et al., *Aggressive pancreatic ductal adenocarcinoma in mice caused by pancreas-specific blockade of transforming growth factor-beta signaling in cooperation with active Kras expression.* Genes Dev, 2006. **20**(22): p. 3147-60.
214. Iqbal, N., et al., *A comparison of pancreaticoduodenectomy with pylorus preserving pancreaticoduodenectomy: a meta-analysis of 2822 patients.* Eur J Surg Oncol, 2008. **34**(11): p. 1237-45.
215. Glanemann, M., et al., *Surgical strategies for treatment of malignant pancreatic tumors: extended, standard or local surgery?* World J Surg Oncol, 2008. **6**: p. 123.

216. Huguet, F., et al., *Chemoradiotherapy in the management of locally advanced pancreatic carcinoma: a qualitative systematic review.* J Clin Oncol, 2009. **27**(13): p. 2269-77.
217. Heinemann, V., et al., *Meta-analysis of randomized trials: evaluation of benefit from gemcitabine-based combination chemotherapy applied in advanced pancreatic cancer.* BMC Cancer, 2008. **8**: p. 82.
218. Conroy, T., et al., *FOLFIRINOX versus gemcitabine for metastatic pancreatic cancer.* N Engl J Med, 2011. **364**(19): p. 1817-25.
219. Moore, M.J., et al., *Erlotinib plus gemcitabine compared with gemcitabine alone in patients with advanced pancreatic cancer: a phase III trial of the National Cancer Institute of Canada Clinical Trials Group.* J Clin Oncol, 2007. **25**(15): p. 1960-6.
220. Burris, H.A., 3rd, et al., *Improvements in survival and clinical benefit with gemcitabine as first-line therapy for patients with advanced pancreas cancer: a randomized trial.* J Clin Oncol, 1997. **15**(6): p. 2403-13.
221. Philip, P.A., et al., *Phase III study comparing gemcitabine plus cetuximab versus gemcitabine in patients with advanced pancreatic adenocarcinoma: Southwest Oncology Group-directed intergroup trial S0205.* J Clin Oncol, 2010. **28**(22): p. 3605-10.
222. Kindler, H.L., et al., *Gemcitabine plus bevacizumab compared with gemcitabine plus placebo in patients with advanced pancreatic cancer: phase III trial of the Cancer and Leukemia Group B (CALGB 80303).* J Clin Oncol, 2010. **28**(22): p. 3617-22.
223. Wong, H.H. and N.R. Lemoine, *Pancreatic cancer: molecular pathogenesis and new therapeutic targets.* Nat Rev Gastroenterol Hepatol, 2009. **6**(7): p. 412-22.
224. Chen, W.H., et al., *Human pancreatic adenocarcinoma: in vitro and in vivo morphology of a new tumor line established from ascites.* In Vitro, 1982. **18**(1): p. 24-34.
225. Tan, M.H., et al., *Characterization of a new primary human pancreatic tumor line.* Cancer Invest, 1986. **4**(1): p. 15-23.
226. Fogh, J., W.C. Wright, and J.D. Loveless, *Absence of HeLa cell contamination in 169 cell lines derived from human tumors.* J Natl Cancer Inst, 1977. **58**(2): p. 209-14.
227. Schoumacher, R.A., et al., *A cystic fibrosis pancreatic adenocarcinoma cell line.* Proc Natl Acad Sci U S A, 1990. **87**(10): p. 4012-6.
228. Morgan, R.T., et al., *Human cell line (COLO 357) of metastatic pancreatic adenocarcinoma.* Int J Cancer, 1980. **25**(5): p. 591-8.
229. Metzgar, R.S., et al., *Antigens of human pancreatic adenocarcinoma cells defined by murine monoclonal antibodies.* Cancer Res, 1982. **42**(2): p. 601-8.
230. Yunis, A.A., G.K. Arimura, and D.J. Russin, *Human pancreatic carcinoma (MIA PaCa-2) in continuous culture: sensitivity to asparaginase.* Int J Cancer, 1977. **19**(1): p. 128-35.
231. Jaffee, E.M., et al., *Development and characterization of a cytokine-secreting pancreatic adenocarcinoma vaccine from primary tumors for use in clinical trials.* Cancer J Sci Am, 1998. **4**(3): p. 194-203.
232. Lieber, M., et al., *Establishment of a continuous tumor-cell line (panc-1) from a human carcinoma of the exocrine pancreas.* Int J Cancer, 1975. **15**(5): p. 741-7.
233. Eberlein, C., et al., *A human monoclonal antibody 264RAD targeting alphavbeta6 integrin reduces tumour growth and metastasis, and modulates key biomarkers in vivo.* Oncogene, 2012.
234. Coughlan, L., et al., *In vivo retargeting of adenovirus type 5 to alphavbeta6 integrin results in reduced hepatotoxicity and improved tumor uptake following systemic delivery.* J Virol, 2009. **83**(13): p. 6416-28.

235. Hausner, S.H., et al., *Targeted in vivo imaging of integrin alphavbeta6 with an improved radiotracer and its relevance in a pancreatic tumor model.* Cancer Res, 2009. **69**(14): p. 5843-50.
236. Landen, C.N., et al., *Tumor-selective response to antibody-mediated targeting of alphavbeta3 integrin in ovarian cancer.* Neoplasia, 2008. **10**(11): p. 1259-67.
237. Wang, Y., et al., *Integrin subunits alpha5 and alpha6 regulate cell cycle by modulating the chk1 and Rb/E2F pathways to affect breast cancer metastasis.* Mol Cancer, 2011. **10**: p. 84.
238. Broker, L.E., F.A. Kruyt, and G. Giaccone, *Cell death independent of caspases: a review.* Clin Cancer Res, 2005. **11**(9): p. 3155-62.
239. Loeffler, M., et al., *Dominant cell death induction by extramitochondrially targeted apoptosis-inducing factor.* FASEB J, 2001. **15**(3): p. 758-67.
240. Bidere, N., et al., *Cathepsin D triggers Bax activation, resulting in selective apoptosis-inducing factor (AIF) relocation in T lymphocytes entering the early commitment phase to apoptosis.* J Biol Chem, 2003. **278**(33): p. 31401-11.
241. Susin, S.A., et al., *Two distinct pathways leading to nuclear apoptosis.* J Exp Med, 2000. **192**(4): p. 571-80.
242. Hood, J.D. and D.A. Cheresh, *Role of integrins in cell invasion and migration.* Nature reviews. Cancer, 2002. **2**(2): p. 91-100.
243. Bapat, A.A., et al., *Perineural invasion and associated pain in pancreatic cancer.* Nat Rev Cancer, 2011. **11**(10): p. 695-707.
244. Friess, H., et al., *Enhanced expression of transforming growth factor beta isoforms in pancreatic cancer correlates with decreased survival.* Gastroenterology, 1993. **105**(6): p. 1846-56.
245. Yoshida, S., et al., *Pancreatic stellate cells (PSCs) express cyclooxygenase-2 (COX-2) and pancreatic cancer stimulates COX-2 in PSCs.* Mol Cancer, 2005. **4**: p. 27.
246. Bu, X., C. Zhao, and X. Dai, *Involvement of COX-2/PGE(2) Pathway in the Upregulation of MMP-9 Expression in Pancreatic Cancer.* Gastroenterol Res Pract, 2011. **2011**: p. 214269.
247. Nystrom, M.L., et al., *Cyclooxygenase-2 inhibition suppresses alphavbeta6 integrin-dependent oral squamous carcinoma invasion.* Cancer Res, 2006. **66**(22): p. 10833-42.
248. Roletto, F., et al., *Basic fibroblast growth factor stimulates hepatocyte growth factor/scatter factor secretion by human mesenchymal cells.* J Cell Physiol, 1996. **166**(1): p. 105-11.
249. Gaggioli, C., et al., *Fibroblast-led collective invasion of carcinoma cells with differing roles for RhoGTPases in leading and following cells.* Nat Cell Biol, 2007. **9**(12): p. 1392-400.
250. Ramos, D.M., D. Dang, and S. Sadler, *The role of the integrin alpha v beta6 in regulating the epithelial to mesenchymal transition in oral cancer.* Anticancer Res, 2009. **29**(1): p. 125-30.
251. Chelala, C., et al., *Pancreatic Expression database: a generic model for the organization, integration and mining of complex cancer datasets.* BMC Genomics, 2007. **8**: p. 439.
252. Cutts, R.J., et al., *The Pancreatic Expression database: 2011 update.* Nucleic Acids Res, 2011. **39**(Database issue): p. D1023-8.
253. Thompson, C.C., et al., *Pancreatic cancer cells overexpress gelsolin family-capping proteins, which contribute to their cell motility.* Gut, 2007. **56**(1): p. 95-106.
254. Grzesiak, J.J. and M. Bouvet, *The alpha2beta1 integrin mediates the malignant phenotype on type I collagen in pancreatic cancer cell lines.* Br J Cancer, 2006. **94**(9): p. 1311-9.

255. Delany, A.M. and E. Canalis, *The metastasis-associated metalloproteinase stromelysin-3 is induced by transforming growth factor-beta in osteoblasts and fibroblasts.* Endocrinology, 2001. **142**(4): p. 1561-6.
256. Lai-Cheong, J.E., et al., *Loss-of-function FERMT1 mutations in kindler syndrome implicate a role for fermitin family homolog-1 in integrin activation.* Am J Pathol, 2009. **175**(4): p. 1431-41.
257. Landemaine, T., et al., *A six-gene signature predicting breast cancer lung metastasis.* Cancer Res, 2008. **68**(15): p. 6092-9.
258. Shou, J.Z., et al., *Overexpression of CDC25B and LAMC2 mRNA and protein in esophageal squamous cell carcinomas and premalignant lesions in subjects from a high-risk population in China.* Cancer Epidemiol Biomarkers Prev, 2008. **17**(6): p. 1424-35.
259. Collisson, E.A., et al., *Subtypes of pancreatic ductal adenocarcinoma and their differing responses to therapy.* Nat Med, 2011. **17**(4): p. 500-3.
260. Stratford, J.K., et al., *A six-gene signature predicts survival of patients with localized pancreatic ductal adenocarcinoma.* PLoS Med, 2010. **7**(7): p. e1000307.
261. Winter, C., et al., *Google goes cancer: improving outcome prediction for cancer patients by network-based ranking of marker genes.* PLoS Comput Biol, 2012. **8**(5): p. e1002511.
262. Zhang, G., et al., *DPEP1 inhibits tumor cell invasiveness, enhances chemosensitivity and predicts clinical outcome in pancreatic ductal adenocarcinoma.* PLoS One, 2012. **7**(2): p. e31507.
263. Biankin, A.V., et al., *Pancreatic cancer genomes reveal aberrations in axon guidance pathway genes.* Nature, 2012. **491**(7424): p. 399-405.
264. Riediger, H., et al., *The lymph node ratio is the strongest prognostic factor after resection of pancreatic cancer.* J Gastrointest Surg, 2009. **13**(7): p. 1337-44.
265. Buchs, N.C., et al., *Vascular invasion in pancreatic cancer: Imaging modalities, preoperative diagnosis and surgical management.* World J Gastroenterol, 2010. **16**(7): p. 818-31.
266. Camp, R.L., M. Dolled-Filhart, and D.L. Rimm, *X-tile: a new bio-informatics tool for biomarker assessment and outcome-based cut-point optimization.* Clin Cancer Res, 2004. **10**(21): p. 7252-9.
267. Hazelbag, S., et al., *Overexpression of the alpha v beta 6 integrin in cervical squamous cell carcinoma is a prognostic factor for decreased survival.* J Pathol, 2007. **212**(3): p. 316-24.
268. Marshall, J.F. and I.R. Hart, *The role of alpha v-integrins in tumour progression and metastasis.* Semin Cancer Biol, 1996. **7**(3): p. 129-38.
269. Olive, K.P., et al., *Inhibition of Hedgehog signaling enhances delivery of chemotherapy in a mouse model of pancreatic cancer.* Science, 2009. **324**(5933): p. 1457-61.
270. Phillips, P.A., et al., *Rat pancreatic stellate cells secrete matrix metalloproteinases: implications for extracellular matrix turnover.* Gut, 2003. **52**(2): p. 275-82.
271. Rueda Dominguez, A., et al., *Treatment of stage I and II Hodgkin's lymphoma with ABVD chemotherapy: results after 7 years of a prospective study.* Ann Oncol, 2004. **15**(12): p. 1798-804.
272. Muraoka-Cook, R.S., N. Dumont, and C.L. Arteaga, *Dual role of transforming growth factor beta in mammary tumorigenesis and metastatic progression.* Clin Cancer Res, 2005. **11**(2 Pt 2): p. 937s-43s.
273. Stover, D.G., B. Bierie, and H.L. Moses, *A delicate balance: TGF-beta and the tumor microenvironment.* J Cell Biochem, 2007. **101**(4): p. 851-61.

274. Stuelten, C.H., et al., *Transient tumor-fibroblast interactions increase tumor cell malignancy by a TGF-Beta mediated mechanism in a mouse xenograft model of breast cancer.* PLoS One, 2010. **5**(3): p. e9832.
275. de Caestecker, M.P., E. Piek, and A.B. Roberts, *Role of transforming growth factor-beta signaling in cancer.* J Natl Cancer Inst, 2000. **92**(17): p. 1388-402.
276. Brooks, P.C., et al., *Antiintegrin alpha v beta 3 blocks human breast cancer growth and angiogenesis in human skin.* J Clin Invest, 1995. **96**(4): p. 1815-22.
277. Moutasim, K.A., et al., *Betel-derived alkaloid up-regulates keratinocyte alphavbeta6 integrin expression and promotes oral submucous fibrosis.* J Pathol, 2011. **223**(3): p. 366-77.
278. Saha, A., et al., *High-resolution in vivo imaging of breast cancer by targeting the pro-invasive integrin alphavbeta6.* J Pathol, 2010. **222**(1): p. 52-63.
279. Kim, M.P. and G.E. Gallick, *Gemcitabine resistance in pancreatic cancer: picking the key players.* Clin Cancer Res, 2008. **14**(5): p. 1284-5.
280. Mori-Iwamoto, S., et al., *A proteomic profiling of gemcitabine resistance in pancreatic cancer cell lines.* Mol Med Report, 2008. **1**(3): p. 429-34.
281. Puthawala, K., et al., *Inhibition of integrin alpha(v)beta6, an activator of latent transforming growth factor-beta, prevents radiation-induced lung fibrosis.* Am J Respir Crit Care Med, 2008. **177**(1): p. 82-90.
282. Izeradjene, K., et al., *Kras(G12D) and Smad4/Dpc4 haploinsufficiency cooperate to induce mucinous cystic neoplasms and invasive adenocarcinoma of the pancreas.* Cancer Cell, 2007. **11**(3): p. 229-43.
283. Guerra, C., et al., *Chronic pancreatitis is essential for induction of pancreatic ductal adenocarcinoma by Kras oncogenes in adult mice.* Cancer Cell, 2007. **11**(3): p. 291-302.
284 Habbe, N., et al., *Spontaneous induction of murine pancreatic epithelial neoplasia (mPanIN) by acinar cell targeting of oncogeneic Kras in adult mice.* Proc. Natl. Acad. Sci. USA, 2008. **105**(48): p. 18913-8.
285 Heiser, P.W., et al., *Stabilization of beta-catenin induces pancreas tumour formation.* Gastroenterology, 2008. **135**(4): p. 1288-300.
286 Hamidi, S., et al., *Expression of alpha(v)beta6 integrin in oral leukoplakia.* Br. J. Cancer, 2000. **82**(8): p. 1433-40
287 Jones, J., et al., *Changes in the expression of alpha v integrins in oral squamous cell carcinomas.* J. Oral. Pathol. Med, 1997. **26**(2): p. 63-8.
288 Impola, U., et al., *Differential expression of Matrylisin 1 (MMP-7), 92kD gelatinase (MMP-9), and metalloelastase (MMP-12) in oral verrucous and squamous cell cancer.* J. Pathol, 2004. **202**(1): p. 14-22
289 Regezi, J.A., et al., *Tenascin and beta 6 integrin are overexpressed in floor of mouth in situ carcinomas and invasive squamous cell carcinomas.* Oral Oncol, 2002. **38**(4): p. 332-6.
290 Smythe, W.R., et al., *Loss of alpha-v integrin expression and recurrence in node negative lung carcinoma.* Ann. Thorac. Surg., 1997. **64**(4): p. 949-53.
291 Arihiro, K., et al., *Significance of alpha 9 beta 1 and alpha v beta 6 integrin expression in breast carcinoma.* Breast Cancer, 2000. **7**(1): p. 19-26.
292 Van Cutsem, E., et al., *Phase III trial of gemcitabine plus tipifarnib compared with gemcitabine plus placebo in advanced pancreatic cancer.* J. Clin. Oncol., 2004. **22**(8): p. 1430-8.